DIRECTORIO DEL CURSO ANALISIS DE RIESGO SISMICO 1983.

1. M. en C. Jorge Prince Alfaro
Investigador
Instituto de Ingeniería
Cubículo 211
U N A M
México, D.F.
548 11 35

2. Dr. Luis Esteva Maraboto (Coordinador)
Director
Instituto de Ingeniería
U N A M
México, D.F.
548 30 44

3. M. en I. Oswaldo Rubén Guerra Jiménez
Subdirector de Ingeniería de Proyectos
Comité Administrador del Programa Federal de Construcción de Escuelas
Vito Alessio Robles No. 380
Col. Florida
México,D.F.

4. Dr. Gustavo Ayala Milián
Investigador
Instituto de Ingeniería
UNAM
México,D.F.
550 52 15 Ext.3628

5. Dr. Juan Manuel Espíndola
Investigador
Instituto de Geofísica
U N A M
Circ. Exterior
México,D.F.
550 52 15 Ext.4358

6. M. en I. Sonia Ruiz Gómez
Investigadora de Tiempo Completo
Instituto de Ingeniería
UNAM
México,D.F.
550 52 15 Ext.3629

ANALISIS DE RIESGO SISMICO

TEMA	DIA	HORA	EXPOSITOR
Origen de los Temblores, Tectónica de Placas, Mecanismos Sísmicos, Predicción	26 Julio	17:00-18:30	Dr. Juan Manuel Espíndola
Instrumentos para registrar Temblores Magnitud e Intensidad	26 Julio	18:30-19:30	M. en C. Jorge Prince A.
Relaciones entre magnitud, intensidad y distancia y entre amplitud del movimiento del terreno y ordenadas espectrales	26 Julio	19:45-21:15	M. en I. Rubén Guerra
Conceptos fundamentales de la Teoría de probabilidades para análisis de riesgo sísmico	28 Julio	17:00-19:00	M. en I. Sonia E. Ruíz
Influencias de las condiciones locales en las características del movimiento sísmico	28 Julio	19:15-21:15	Dr. Gustavo Ayala
a) Modelos Teóricos			
b) Comparación entre observaciones y Teoría			
b) Criterios probabilísticos	2 Agosto	17:00-18:30	Dr. Luis Esteva
Sismicidad local y regional, Estimación Bayesiana	2 Agosto	18:30-21:00	Dr. Luis Esteva
Análisis de riesgo. Criterios para la obtención de espectros de diseño Aplicaciones	4 Agosto	17:00-21:00	Dr. Luis Esteva

EVALUACION DEL PERSONAL DOCENTE

(1)

CURSO: IX CURSO INTERNACIONAL DE ING. SISM. ANALISIS DE RIESGO SISMICO

FECHA: Del 20 de julio al 4 de agosto de 1986

CONFERENCISTA	DOMINIO DEL TEMA	EFICIENCIA EN EL USO DE AYUDAS AUDIOVISUALES	MANTENIMIENTO DEL INTERES.(COMUNICACION CON LOS ASISTENTES, AMENIDAD, FACILIDAD DE EXPRESION).	PUNTUALIDAD	
1. DR. OCTAVIO AYALA MILIAN					
2. DR. JUAN MANUEL ESPINOSA					
3. DR. LUIS ESTEVA MARAVILLA					
4. M. EN I. ROMULO E. OJEDA					
5. M. EN C. JORGE PRINCE ALTARO					
6. M. EN I. SONIA RUIZ					
7.					
8.					
9.					
ESCALA DE EVALUACION: 1 a 10					

EVALUACION DE LA ENSEÑANZA

(2)

SU EVALUACION SINCERA NOS AYUDARA A MEJORAR LOS PROGRAMAS POSTERIORES QUE DISEÑAREMOS PARA USTED.

TEMA	ORGANIZACION Y DESARROLLO DEL TEMA	GRADO DE PROFUNDIDAD LOGRADO EN EL TEMA	GRADO DE ACTUALIZACION LOGRADO EN EL TEMA	UTILIDAD PRACTICA DEL TEMA	
ORIGEN DE LOS TERREMOTOS. TECTONICA DE PLACAS. MECANISMOS SISMICOS. PREDICCION					
INSTRUMENTOS PARA REGISTRAR TERREMOTOS MAGNITUD E INTENSIDAD					
RELACIONES ENTRE MAGNITUD, INTENSIDAD Y DISTANCIA Y ENTRE AMPLITUD DEL MOVIMIENTO DEL TERRENO Y ORDENADAS ESPECTRALES					
CONCEPTOS FUNDAMENTALES DE LA TEORIA DE PROBABILIDADES PARA ANALISIS DE RIESGO SISMICO					
INFLUENCIAS DE LAS CONDICIONES LOCALES EN LAS CARACTERISTICAS DEL MOVIMIENTO SISMICO.					
SISMICIDAD LOCAL Y REGIONAL. ESTIMACION BAYESIANA					
ANALISIS DE RIESGO. CRITERIOS PARA LA OBTENCION DE ESPECTROS DE DISEÑO APLICACIONES					

ESCALA DE EVALUACION: 1 a 10

EVALUACION DEL CURSO

(3)

	CONCEPTO	EVALUACION
1.	APLICACION INMEDIATA DE LOS CONCEPTOS EXPUESTOS	
2.	CLARIDAD CON QUE SE EXPUSIERON LOS TEMAS	
3.	GRADO DE ACTUALIZACION LOGRADO CON EL CURSO	
4.	CUMPLIMIENTO DE LOS OBJETIVOS DEL CURSO	
5.	CONTINUIDAD EN LOS TEMAS DEL CURSO	
6.	CALIDAD DE LAS NOTAS DEL CURSO	
7.	GRADO DE MOTIVACION LOGRADO CON EL CURSO	

ESCALA DE EVALUACION DE 1 A 10

1. ¿Qué le pareció el ambiente en la División de Educación Continua?

MUY AGRADABLE	AGRADABLE	DESAGRADABLE

2. Medio de comunicación por el que se enteró del curso:

PERIODICO EXCELSIOR ANUNCIO TITULADO DI VISION DE EDUCACIÓN CONTINUA	PERIODICO NOVEDADES ANUNCIO TITULADO DI VISION DE EDUCACIÓN CONTINUA	FOLLETO DEL CURSO

CARTEL MENSUAL	RADIO UNIVERSIDAD	COMUNICACION CARTA, TELEFONO, VERBAL, ETC.

REVISTAS TECNICAS	FOLLETO ANUAL	CARTELERA UNAM "LOS UNIVERSITARIOS HOY"	GACETA UNAM

3. Medio de transporte utilizado para venir al Palacio de Minería:

AUTOMOVIL PARTICULAR	METRO	OTRO MEDIO

4. ¿Qué cambios haría usted en el programa para tratar de perfeccionar el curso?

_____

_____

_____

5. ¿Recomendaría el curso a otras personas?

SI	NO

6. ¿Qué cursos le gustaría que ofreciera la División de Educación Continua?

7. La coordinación académica fue:

EXCELENTE	BUENA	REGULAR	MALA

8. Si está interesado en tomar algún curso intensivo ¿Cuál es el horario más conveniente para usted?

LUNES A VIERNES DE 9 A 13 H. Y DE 14 A 18 H. (CON COMIDAS)	LUNES A VIERNES DE 17 A 21 H.	LUNES, MIERCOLES Y VIERNES DE 18 A 21 H.	MARTES Y JUEVES DE 18 A 21 H.

VIERNES DE 17 A 21 H. SABADOS DE 9 A 14 H.	VIERNES DE 17 A 21 H. SABADOS DE 9 A 13 Y DE 14 a 18 H.	O T R O

9. ¿Qué servicios adicionales desearía que tuviese la División de Educación Continua, para los asistentes?

10. Otras sugerencias:

IX CURSO INTERNACIONAL DE INGENIERIA SISMICA

ANALISIS DE RIESGO SISMICO

INSTRUMENTOS USADOS EN MEDICIONES SISMICAS

JORGE PRINCE ALFARO

4 - INSTRUMENTOS USADOS EN MEDICIONES SISMICAS

Por Jorge Prince Alfaro

4.1 Introducción

Para el estudio de fenómenos sísmicos ha sido necesario construir aparatos que registren los movimientos del terreno con una precisión que permita obtener información cuantitativa sobre los diversos aspectos del temblor. Los instrumentos que actualmente se usan para este fin pueden clasificarse en dos grupos: sismógrafos y acelerógrafos. Los primeros son de gran sensibilidad. Se emplean en estaciones sismológicas para estudiar, entre otras cosas, la propagación de las ondas sísmicas en el interior de la Tierra y en las capas superficiales; para determinar la dirección, distancia y profundidad a la que se ha originado el movimiento y para el estudio de temblores lejanos.

La alta sensibilidad de los sismógrafos impide obtener registros completos de temblores intensos, ya que no es posible registrar el movimiento a lo largo de toda la duración del temblor por salirse la línea del registro. Ello ha dado lugar al desarrollo de aparatos denominados acelerógrafos que se destinan a este objeto únicamente.

En este capítulo se presente en forma simplificada la teoría en que se basan ambos instrumentos, así como las características peculiares a cada uno. Se describen los tipos de sismógrafos y acelerógrafos más frecuenvemente empleados y se hace mención de algunos instrumentos de carácter auxiliar como los sismoscopios.

4.2 Generalidades

La principal dificultad que se encuentra al tratar de reproducir en una gráfica el movimiento del terreno durante un temblor, es la falta de una referencia fija con respecto a la cual se efectúen las mediciones. Para salvar este obstáculo se recurre a sistemas inerciales que hacen uso de la tendencia de los cuerpos a mantenerse en reposo.

El péndulo es el ejemplo clásico de sistemas de esta clase. La mayoría de los sismógrafos usados en la actualidad consiste esencialmente de algún tipo particular de péndulo.

Consideremos el sistema de la Fig. 4.1. Cuando el soporte experimenta el desplazamiento u, la masa m tenderá a permanecer en su sitio. Si el movimiento es muy rápido la masa permanecerá casi estacionaria, si es muy lento se limitará a seguir el movimiento u, para velocidades intermedias el péndulo se atrasará o adelantará con respecto al soporte. Si a este sistema se añade un medio para registrar la diferencia δ entre los movimientos de masa y soporte, se habrá completado un sismógrafo elemental como el que muestra esquemáticamente la Fig. 4.2.

En este estado el aparato adolece de graves defectos, ya que la masa seguirá en movimiento aún después de que el soporte se haya detenido, lo que complica innecesariamente la relación entre el registro de δ y el verdadero movimiento u del suelo.

Con objeto de evitar esta desventaja se introduce un elemento que se oponga parcialmente al movimiento del péndulo. Esta oposición, o amortiguamiento, puede ser proporcionada por un fluido viscoso, o mediante un freno magnético. En la Fig. 4.3 se representa por el amortiguador de constante c.

El amortiguamiento tiene además la función de eliminar rápidamente las oscilaciones que el péndulo trata de efectuar, con su período natural, durante la excitación. Las dos funciones mencionadas del amortiguamiento contribuyen a la fidelidad con que el registro de la diferencia δ representa el movimiento u del apoyo. Una tercera se trata más adelante.

Un sismógrafo o acelerógrafo común puede considerarse compuesto por las siguientes partes: a) sistema inercial; b) captador de movimiento relativo ; c) sistema para amplificar δ (pequeño en general) y d) sistema de registro, incluyendo marcas de tiempo. En los siguientes párrafos se hará referen-

cia a estos elementos componentes en el orden mencionado.

4.3 Sistema inercial. Ecuaciones básicas

Como se ha visto en capítulos anteriores, la respuesta del sistema de la Fig. 4.3 está definido por la ecuación

$$m\frac{d^2(\delta+u)}{dt^2}+c\frac{d\delta}{dt}+k\delta=0$$

que puede expresarse

$$m\ddot{\delta}+c\dot{\delta}+k\delta=-m\ddot{u} \qquad (4.1)$$

El signo negativo del segundo miembro indica que los sentidos positivos del desplazamiento u del terreno y del desplazamiento relativo δ se han tomado opuestos como se señala en la Fig. 4.3, de tal manera que a una u positiva corresponda una δ del mismo signo.

Supongamos que el movimiento u del soporte es senoidal,

$$u=u_0\cos\omega t \qquad (4.2)$$

En este caso la respuesta δ del instrumento, despreciando los términos transitorios, quedará definida por:

$$\delta=\delta_0\cos(\omega t-\theta) \qquad (4.3)$$

donde

$$\theta=\text{arc tan}\frac{\omega\, c/m}{k/m-\omega^2} \qquad (4.4)$$

y la solución de la ec. 4.1 puede expresarse

$$\frac{\delta_0}{u_0}=\frac{\omega^2}{\sqrt{(k/m-\omega^2)^2+\omega^2(c/m)^2}} \qquad (4.5)$$

Por otra parte, se tienen las siguientes relaciones, mencionadas en capítulos anteriores.

$$\omega_n^2 = k/m$$

$$c_c = 2\sqrt{k m}$$

y
$$\xi = c/c_c = c/2\sqrt{k m} \qquad (4.6)$$

donde

$\omega_n = 2\pi f = 2\pi/T$ = frecuencia circular natural\(seg^{-1})

k = constante del resorte (gr/cm)

m = masa (gr seg^2/cm)

c = coeficiente de amortiguamiento (gr seg/cm)

c_c = coeficiente de amortiguamiento crítico (gr seg/cm)

ξ = fracción del amortiguamiento crítico (adimensional)

Al sustituir estos valores en la ec. 4.5 la solución de la ec. 4.1 queda expresada en términos de ω/ω_n y de la fracción del amortiguamiento crítico ξ como sigue:

$$\delta_o/u_o = \frac{(\omega/\omega_n)^2}{\sqrt{[1-(\omega/\omega_n)^2]^2 + 4\xi^2(\omega/\omega_n)^2}} \qquad (4.7)$$

Esta ecuación puede escribirse en términos de la aceleración $\ddot{u}$ del apoyo sustituyendo $\ddot{u}_o = -\omega^2 u_o$; resulta

$$\delta_o \omega_n^2/\ddot{u}_o = -\frac{1}{\sqrt{[1-(\omega/\omega_n)^2]^2 + 4\xi^2(\omega/\omega_n)^2}} \qquad (4.8)$$

Efectuando las mismas sustituciones en la ec.4.4., tenemos

$$\theta = \text{ángulo de fase} = \frac{2\xi\,\omega/\omega_n}{1-(\omega/\omega_n)^2} \qquad (4.9)$$

la relación entre δ_o/u_o y ω/ω_n se muestra en la Fig. 4.4 para diversos valores de ξ . La Fig. 4.5 presenta las curvas correspondientes para valores absolutos de $\delta_o \omega_n^2/\ddot{u}_o$.

4.3.1 Características del sistema inercial en sismógrafos

Las Figs. 4.4 y 4.5 permiten determinar las caracterís- $\omega/\omega_n > 1$

ticas que se requieren en instrumentos destinados a medir, respectivamente, desplazamiento (sismógrafo) o aceleración (acelerógrafo), de acuerdo con la aplicación específica a que se destine el aparato.

Para lograr que el desplazamiento relativo δ represente fielmente el desplazamiento u del terreno es necesario que la relación δ_o/u_o sea constante para todos los valores de ω/ω_n. Como muestra la Fig. 4.4, esta solución ideal no es posible, y se presentan varias alternativas para la selección de las características más adecuadas del aparato.

Como primera solución se podría hacer que la relación $\ddot{u}_o/u_o$ fuera constante para el máximo intervalo posible de ω/ω_n. De acuerdo con la Fig. 4.4 esto se consigue con una fracción del amortiguamiento crítico aproximadamente igual a 0.7. Otra solución consistiría en diseñar el instrumento con un valor muy bajo de ω_n, de tal manera que para todos los valores de ω que se pretende medir, el cociente ω/ω_n fuera suficientemente grande, resultanto aproximadamente constante aún cuando el amortiguamiento fuese nulo. Sin embargo, éste se incluye para frenar la masa una vez que desaparece la excitación del soporte.

Cada una de estas soluciones ofrece ventajas y desventajas de orden práctico. Debe notarse que en cualquier caso se requiere que el valor de ω_n sea inferior a ω, es decir, que el valor del período natural T del instrumento sea grande en comparación con los períodos de las principales ondas sísmicas que se desea registrar. Ello se logra por medio de la combinación adecuada de una masa considerable con un resorte de constante baja.

Cuando condiciones especiales requieren énfasis en el registro de una frecuencia determinada, basta que ω/ω_n tenga un valor cercano a la unidad e introducir en el sismógrafo una fracción adecuada del amortiguamiento crítico dd acuerdo con lo que indica la Fig. 4.4.

La Fig. 4.6 reproduce la parte útil ($\omega/\omega_n > 1$) de la Fig.

4.4 a una escala lineal más conveniente. Todas las curvas de la Fig. 4.6 se apartan de la unidad menos de 5%. Para que un sismógrafo sin amortiguamiento distorsione la amplitud del movimiento en menos de 1% se requiere que $\omega/\omega_n \geq 10$. En cambio, con 65% del amortiguamiento crítico la distorsión será menor que 2% para valores de ω/ω_n ligeramente mayores que 1.5. Si se requiere una gran precisión la figura indica la conveniencia de emplear un valor de ξ igual a 0.70 y ω/ω_n deberá ser superior a 4.

4.3.2 Caracteristicas del sistema inercial en acelerógrafos

Para determinar las características esenciales de un acelerógrafo se sigue un procedimiento análogo mediante las Figs. 4.5 y 4.7.

En este caso deberá tenerse $\omega/\omega_n \ll 1$ para que $\bar{z}_0/\ddot{u}_0$ sea constante, o sea, el período T del instrumento debe ser corto con respecto a los períodos de las ondas sísmicas que se pretenda registrar. La fracción de amortiguamiento crítico más conveniente estará cercana a 0.7 de acuerdo con lo señalado por la Fig. 4.5. Debe notarse que las ordenadas a las curvas de la Fig. 4.5 no corresponden a valores de $\bar{z}_0/\ddot{u}_0$ sino a valores proporcionales a esta último expresión y la constante de proporcionalidad es $1/\omega_n$. Por tanto, el uso de la Fig. 4.5 es posible debido a que ω_n es constante en cada aparato. $\omega/\omega_n < 1$

La Fig. 4.7 presenta en detalle la parte de la Fig. 4.5 correspondiente a $\omega/\omega_n < 0.9$ en la que la distorsión de la amplitud registrada es menor que 5%. El valor $\xi = 0.7$ mencionado da un registro con un error menor que 1% si $\omega/\omega_n \leq 0.4$. Esta figura señala las diferentes combinaciones de error aceptable y porcentaje de amortiguamiento crítico, así como las limitaciones de ω/ω_n para cada posible combinación.

El valor relativamente pequeño del período natural T de los acelerógrafos se obtiene por medio de una masa reducida y

un resorte rígido. Por esta razón los aparatos para medir aceleración son más ligeros y menos voluminosos que los sismógrafos.

Para ambas clases de aparato hemos conseguido que S_o represente sin gran error el desplazamiento u_o y la aceleración $\ddot{u}_o$ del terreno, variando el amortiguamiento hasta que las relaciones S_o/u_o y $S_o/\ddot{u}_o$, respectivamente, resultan constantes en el intervalo útil de ω/ω_n. Debe notarse que u es en general pequeño y en consecuencia es necesario amplificar S antes de registrarlo. Este tópico se trata posteriormente.

4.3.3 Distorsión de fase

Las ecs. 4.2 y 4.3 señalan una diferencia en tiempo igual a θ/ω entre la ocurrencia y el registro del movimiento u. Se dice en este caso que u y S difieren en un ángulo de fase θ que está dado por la ec. 4.9

$$\theta = \text{arc tan} \frac{2\xi \omega/\omega_n}{1-(\omega/\omega_n)^2} \qquad (4.9)$$

Esta ec. se representa gráficamente en la Fig. 4.8.

Si el movimiento u no es senoidal, sino solamente periódico, el ángulo θ será diferente para cada una de las componentes armónicas ya que θ depende de ω/ω_n.

Para el caso de un sismógrafo sin amortiguamiento la zona $\omega/\omega_n > 1$ de la Fig. 4.8 indica que el ángulo de fase es igual a 180° para todo valor de ω/ω_n y no hay distorsión de fase entre S y u. En cambio, para valores de ξ cercanos a 0.7, adoptados como óptimos para evitar distorsión de amplitudes, siempre se introducen distorsiones de fase al resultar un valor diferente de θ para las diversas componentes armónicas del movimiento del terreno. Como indica la Fig. 4.8, este efecto es más notable para valores de ω/ω_n cercanos a la unidad.

En un acelerógrafo, un valor de ξ ligeramente superior a

0.70 elimina casi por completo la distorsión de fase de las componentes del movimiento. En la Fig. 4.8 se observa que para $\omega/\omega_n \leq 1$ y $\zeta = 0.707$ el ángulo de fase θ varía entre 0 y 90° en forma sensiblemente lineal con ω/ω_n, o sea, $\theta = \pi\omega/2\omega_n$ Por tanto la diferencia de fase expresada en unidades de tiempo es:

$$\theta/\omega = \pi/2\omega_n = \text{constante}$$

lo que indica que todas las componentes armónicas tendrán el mismo corrimiento de fase, y la distorsión en el registro es despreciable.

4.3.4 Extensión a movimiento no armónico

Durante la discusión anterior ha existido una falla de importancia: el movimiento del suelo en un sismo dista de ser senoidal. Sin embargo, un movimiento arbitrario puede representarse como la superposición de componentes senoidales definidas cada una completamente en cuanto a fase y amplitud, lo que constituye un espectro de Fourier que es una función continua de la frecuencia.

Por tanto al ocurrir un temblor, el sismógrafo o acelerógrafo modifica cada componente de acuerdo con lo ya establecido y mostrado en las Figs. 4.4 y 4.5 para movimiento senoidal del apoyo. El instrumento es entonces utilizable para la medición de movimientos no periódicos, pues el registro corresponde a la superposición de las diversas componentes, cada una modificada de acuerdo con las mismas figuras.

4.4 Sismógrafos. Sistemas de captación, amplificación y registro

Existen diversos métodos para captar, amplificar y registrar el movimiento relativo.

4.4.1 Sistemas mecánicos. El primero es mecánico. En sismógrafos antiguos se tiene una serie de palancas con un estilete en el extremo de la última. El estilete graba el movimiento sobre papel ahumado generalmente.

Este sistema no permite grandes amplificaciones; la fricción en la punta del estilete se transmite hacia la masa por lo que se requiere que esta sea considerable. En Europa se llegaron a construir instrumentos con masas de más de 20 ton. La del sismógrafo Wiechert que aún esta en uso en la estación sismológica de Tacubaya pesa 17 ton. Además, las dificultades de orden práctico para evitar juego o movimiento perdido entre las palancas, que a la vez deben ser resistentes y ligeras, han hecho caer en desuso este sistema, excepto en aparatos que no requieren amplificaciones considerables, como en acelerógrafos.

4.4.2 Amplificación óptica directa. Otros aparatos registran en papel fotográfico por el denominado método directo, que consiste en fijar al péndulo un espejo que refleja la luz de una fuente luminosa sobre papel fotográfico. Este método elimina la fricción y permite amplificaciones considerables. El sismógrafo Milne-Shaw aún en uso en muchas estaciones sismológicas emplea este sistema.

En 1922 Anderson y Wood desarrollaron un pequeño sismómetro de torsión que resultó más efectivo que los de gran masa y constituyó un gran avance. La masa de este sismómetro, aproximadamente un gramo, está colocada sobre un alambre muy fino sujeto a tensión que proporciona la fuerza de restitución de la masa, la cual se mueve en el campo de un imán produciéndose un amortiguamiento cercano al crítico, Fig. 4.9. El conjunto ocupa un volumen relativamente pequeño (10 x 10 x 40 cm.)

4.4.3 Sismógrafos electromagnéticos. Esta clase de sismógrafos usan el registro fotográfico indirecto, es decir, el movimiento de genera una señal eléctrica que se transmite a un medidor sensible (galvanómetro) en donde se transforma nuevamen-

te en movimiento. Este arreglo tiene la ventaja que el registro puede hacerse en un lugar relativamente apartado de las partes del sismógrafo sensibles al movimiento del terreno.

Los sismógrafos que pueden considerarse modernos son electromagnéticos. En vista de ello se discutirán brevemente sus sistemas de captación y registro.

Los sismógrafos llamados de bobina móvil miden la velocidad relativa $\dot{v}$ eléctricamente usando un captador cuyos elementos principales, bobina e imán, están fijos respectivamente a la masa del sistema sísmico y a la caja que sigue el movimiento u (Fig. 4.3). La fuerza electromotriz inducida en la bobina por el movimiento es proporcional a la velocidad relativa $\dot{v}$ y sirve para alimentar un galvanómetro. El registro se obtiene en papel fotográfico.

El sismógrafo llamado de reluctancia variable se debe a Benioff. Es otro tipo de sismógrafo electromagnético de diseño relativamente reciente (1930) que emplea galvanómetros para el registro. Tanto este tipo como el de bobina móvil permiten alcanzar amplificaciones superiores a 100,000.

Existen además sismógrafos en que la amplificación de la señal se efectúa electrónicamente y aquella esta limitada solamente por el nivel de "ruido de fondo" existente en el lugar. Este "ruido" es la representación gráfica en el sismograma de los pequeñísimos movimientos de la superficie terrestre que resultan de la actividaddel hombre (tráfico, operación de maquinaria, etc) y de causas naturales (viento, oleaje en las costas, etc.) Por tanto una estación sismológica pra registro con muy alta amplificación se sitúa lejos del mar, de lugares habitados y de vías de comunicación.

4.4.4 Tambores de registro. De los sismógrafos usados en la actualidad la mayoría registran sobre papel ahumado o fotográfico colocado sobre un tambor que gira lentamente y se traslada, trazando el sismograma en forma de espiral. La velocidad

de rotación es reducida; la del papel varía generalmente entre 8 y 60 mm/min. Mantener esta velocidad constante parece a primera vista un problema menor. Sin embargo, los tiempos en sismogramas de estaciones de primera clase se determinan con una precisión de al menos 0.1 seg. Esto exige gran calidad en las componentes del tambor de registro y su elemento motor, así como en el reloj que produce las marcas de tiempo. El reloj debe ser ajustado día a día en forma automática de preferencia. Según Byerly, "Precisión en el tiempo es el primer requisito esencial en una estación sismológica... un buen instrumento es casi inútil para cualquier propósito científico si no registra en un tambor de velocidad precisa, en el que el tiempo se marca con un buen reloj cuyo error se determina con exactitud diariamente."

Instrumentos de diseño avanzado, que incluyen sistemas ópticos de gran calidad, permiten registrar varias componentes en película fotográfica.

4.5 Instrumentación de una estación sismológica moderna

Como ejemplo de la instrumentación empleada en instalaciones sismológicas modernas, la Fig. 4.11 muestra esquemáticamente los componentes de una estación del "Sistema Sismográfico Mundial" que consistirá de 125 estaciones. En esta figura se emplea la denominación usual de "sismógrafo de período corto" cuando $T \leq 1$ seg y "de período largo" para $T > 1$ seg. La Fig. 4.12 corresponde a las curvas de respuesta de los sismógrafos mencionados.

4.6 Diversos tipos de sismógrafos

Los sismógrafos que se usan actualmente se clasifican según diversas características: valor del período natural, dirección del eje sensible, sistema de captación, de amplificación, de registro, etc. Los nombres de los más conocidos se relacionan principalmente con un tipo determinado de suspensión de la masa sísmica (Fig. 4.10)

Una de las escasas excepciones al uso de sistemas inerciales en sismógrafos es el sismógrafo de deformación, diseñado

por Benioff en 1932. Consiste de dos pedestales colocados a 18 ó 20 m entre sí, con un tubo metálico, fijo a uno de ellos, que se prolonga hasta corta distancia del otro pedestal. Un captador de reluctancia variable asociado a un galvanómetro registra las variaciones en la distancia entre el extremo de la barra y el pedestal. Así, este aparato mide la deformación del suelo entre las dos bases, al ser atravesado por las ondas sísmicas o con el terreno en reposo. El objeto principal de este instrumento es proporcionar información que eventualmente permita correlacionar las condiciones locales de deformación con la distribución de las deformación unitaria anterior y posterior a temblores intensos.

4.7 Acelerógrafos

Tanto los registros incompletos de temblores intensos de estaciones sismológicas, como los estudios que de ellos se derivan son, en general, de escasa utilidad para el proyectista de estructuras. En el campo de la ingeniería, la observación cuidadosa de los daños sufridos por las construcciones durante un temblor ha suministrado datos valiosos para el avance del diseño sísmico. Sin embargo, este tipo de estudio, por detallado que sea, carece de un factor fundamental: las características del movimiento que produjo tales daños.

Los aparatos construídos para el registro de sismos completos no forman parte actualmente del equipo usual de observatorios sismológicos. Son de creación relativamente reciente; en 1933 se registró el primer temblor intenso en California. En la actualidad existen cadenas de aparatos de este tipo en la costa oeste de Estados Unidos y en Japón.

En la ciudad de México se han instalado nueve. En la provincia no hay, a pesar de la gran actividad sísmica de los estados del sur del país.

La escasez de acelerógrafos en la República Mexicana, debida en gran parte a su alto costo, aunque lamentable no es

excepcional en países afectados con frecuencia por temblores. A pesar del tiempo transcurrido entre el registro satisfactorio de los primeros sismos intensos y de la importancia de conocer el temblor mismo, solo se cuenta a la fecha con unos cuantos registros que se utilizan una y otra vez en cálculos de todas clases. El sismo más fuerte registrado, (El Centro, California, Mayo 1940) alcanzó una aceleración de 0.33 t

Hasta la fecha en México se han registrado cuatro en la Alameda Central: diciembre 10, 1961; mayo 11 y 19, 1962 y noviembre 30, 1962.

Para el objeto que nos ocupa se ha encontrado más adecuado el empleo de acelerógrafos porque el cálculo de respuestas estructurales requiere el conocimiento de la aceleración del terreno como función del tiempo.

Dado que el proceso de integración es en sí más preciso que el de diferenciación, es más conveniente calcular velocidades y desplazamientos del terreno a partir de la aceleración, que seguir el procedimiento inverso.

Además de ser posible construirlos en forma más compacta y resistente y requerir menor amplificación, estos instrumentos presentan, con respecto a los simógrafos, ventajas derivadas de trabajar en el intervalo $\omega/\omega_n < 1$, por lo que son también sensibles a aceleraciones de ω nula, como la de la gravedad. Su calibración es entonces posible mediante el simple expediente de inclinarlos.

A diferencia de los simógrafos, que operan continuamente, los acelerógrafos cuentan con un arrancador que los pone en marcha al ocurrir el temblor. En unos aparatos este arrancador es sensible a movimientos horizontales y en otros a movimientos verticales del terreno. El arrancador es a su vez un sistema pendular (Fig. 4.3), que cierra un circuito (o lo abre), cuando el desplazamiento relativo δ alcanza un valor prefijado, ini-

ciándose el registro.

Puesto que es necesario que $\ddot{u}$ tenga un valor diferente de cero para que funcione el arrancador, se pierde la parte del registro correspondiente a la iniciación del sismo. Se ha construido un instrumento que lo evita. Registra la aceleración del suelo continuamente en cinta magnética. Si después de un cierto tiempo no ha temblado, borra y usa la misma cinta nuevamente. Cuando ocurre un temblor el aparato deja de borrar y en la cinta queda grabado el movimiento del terreno anterior a la suspendión del borrado con lo que se obtiene el registro completo del temblor.

El empleo de disparadores en acelerógrafos, permite elevar a 1 o 2 cm/seg la velocidad de registro, con un rollo de papel de longitud usual (30-50m). Esto facilita la lectura del acelerograma pues las ondas no aparecen tan juntas entre sí, como en los registros obtenidos en sismógrafos.

Otra característica peculiar a los acelerógrafos es que un dispositivo suspende el registro después de un cierto tiempo de haberse iniciado, o de haberse efectuado el último contacto del arrancador, y el ciclo completo puede repetirse varias veces automáticamente. En consecuencia no necesita la atención constante que requieren los sismógrafos.

Las características de los acelerógrafos más conocidos se representan en la Tabla 4.1. Las Figs. 4.13 y 4.14 muestran los acelerógrafos instalados hasta ahora en México: el SMAC de fabricación japonesa y el AR-240 de manufactura norteamericana, respectivamente.

4.8 Sismoscopios.

Existe una tercera clase de aparatos denominados sismoscopios, de uso exclusivo en ingeniería sísmica, cuyo funcionamiento está relacionado con respuestas estructurales y no con la deformación o el movimiento del terreno como en el caso de sismógrafos y acelerógrafos.

En el capítulo 3 se ha definido espectro como la gráfica que relaciona las características de estructuras de un grado de libertad, expresadas mediante el periodo T de la estructura, con la respuesta máxima que produce un determinado movimiento de la base.

Se ha visto también que los espectros se representan generalmente con los valores dd T como abscisas y las ordenadas corresponden a las respuestas que se calculan mediante una expresión matemática en que interviene la aceleración ü del terreno. Así, una vez que se ha obtenido un registro de ü mediante un acelerógrafo, es posible calcular las ordenadas correspondientes a cada valor de T para diferentes valores de ξ. Por tanto, si un sistema de un grado de libertad, con valores fijos de T y ξ se sujeta a la misma aceleración ü del terreno, su respuesta máxima coincide teóricamente con la calculada. El sistema físico que se usa con este objeto se denomina sismoscopio.

La utilidad de estos aparatos es limitada ya que solamente suministran un punto en un espectro. En cambio su costo es en términos generales de 1/100 del de un acelerógrafo lo que hace posible la instalación de un número considerable y usualmente a un acelerógrafo se asocian grupos de varios sismoscopios. En esta forma se verifican fácilmente los espectros calculados al obtenerse puntos del mismo espectro para valores convenientes de T y ξ.

El mayor número de sismoscopios instalados en la actualidad es del tipo denominado USCGS que se muestra en la Fig. 4.15. Consiste en un péndulo de suspensión unifilar y amortiguamiento magnético al que va unido un cristal de reloj, ahumado en su exterior. El registro se obtiene mediante una aguja que marca sobre el cristal al desplazarse éste con respecto a la base. Para este aparato se escogieron los valores de T = 0.75 seg. y ξ = 0.10.

En la Ref. 4.9.13 se describe un sismoscopio desarrollado en nuestro país que permite obtener varios puntos del espectro simultáneamente.

4.9 Referencias

4.9.1 Harris, C. M. y Crede, C. E., (editores) "Shock and Vibration Handbook". Vol. 1, McGraw-Hill. 1961.

4.9.2 Myklestad, N. O., "Fundamentals of Vibration Analysis", McGraw-Hill. 1956.

4.9.3 Richter, C. F., "Elementary Seismology". W. H. Freeman. 1958.

4.9.4 Carder, D. S., "The Seismograph and the Seismograph Station" U. S. Department of Commerce, U. S. Coast and Geodetic Survey. Washington D. C. Septiembre 1956.

4.9.5 Byerly, P., "Seismology" Prentice-Hall. 1942.

4.9.6 Eiby, G. A., "Earthquakes" Frederick Muller. London. 1957.

4.9.7 Hudson, D. E., "The measurement of ground motion of destructive earthquakes". Bull. Seismological Society of America. Vol. 53, No. 2. Febrero 1964.

4.9.8 The Geotechnical Corporation. "Instrumentation of the world-wide seismograph system, Model 10700". U. S. Coast and Geodetic Survey. Washington D. C. Abril 1962.

4.9.10 The Geotechnical Corporation. "Information Bulletin No. 2, Wichita Mountains Seismological Observatory". Enero 1963.

4.9.11 Gudzin, M. G. y Holle, E. G. "Seismological observatories", Proc. IRE. Vol.50 No. 11. Noviembre 1962.

4.9.12 Halverson, H. T. "The strong-motion seismograph". Proc. American Geophysical Union Meeting. Boulder, Colorado. Diciembre 1963.

4.9.13 Prince, J. "Un nuevo sismoscopio." Rev. Ingeniería. Enero 1963.

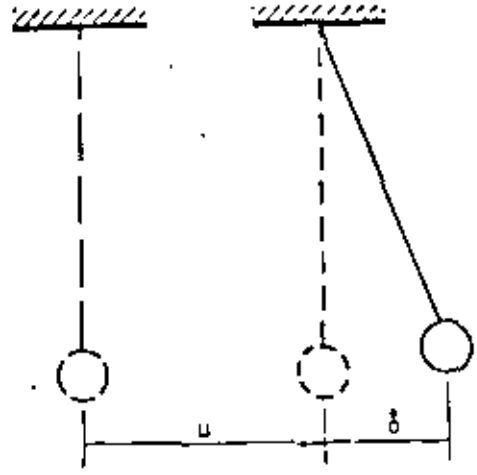

FIG.4.1

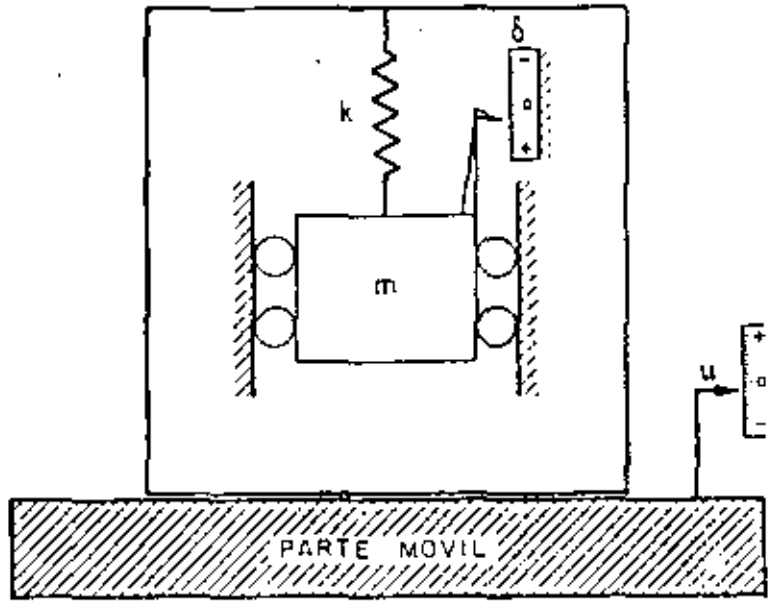

FIG. 4.2

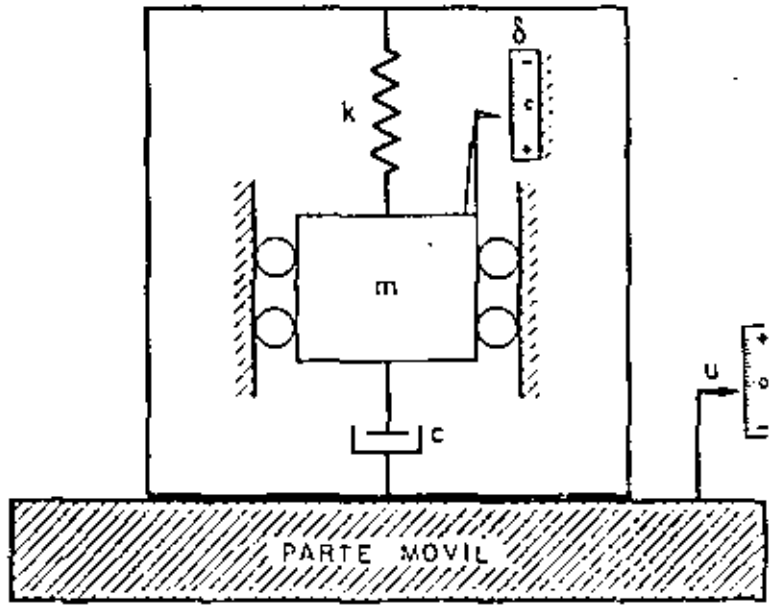

FIG. 4.3

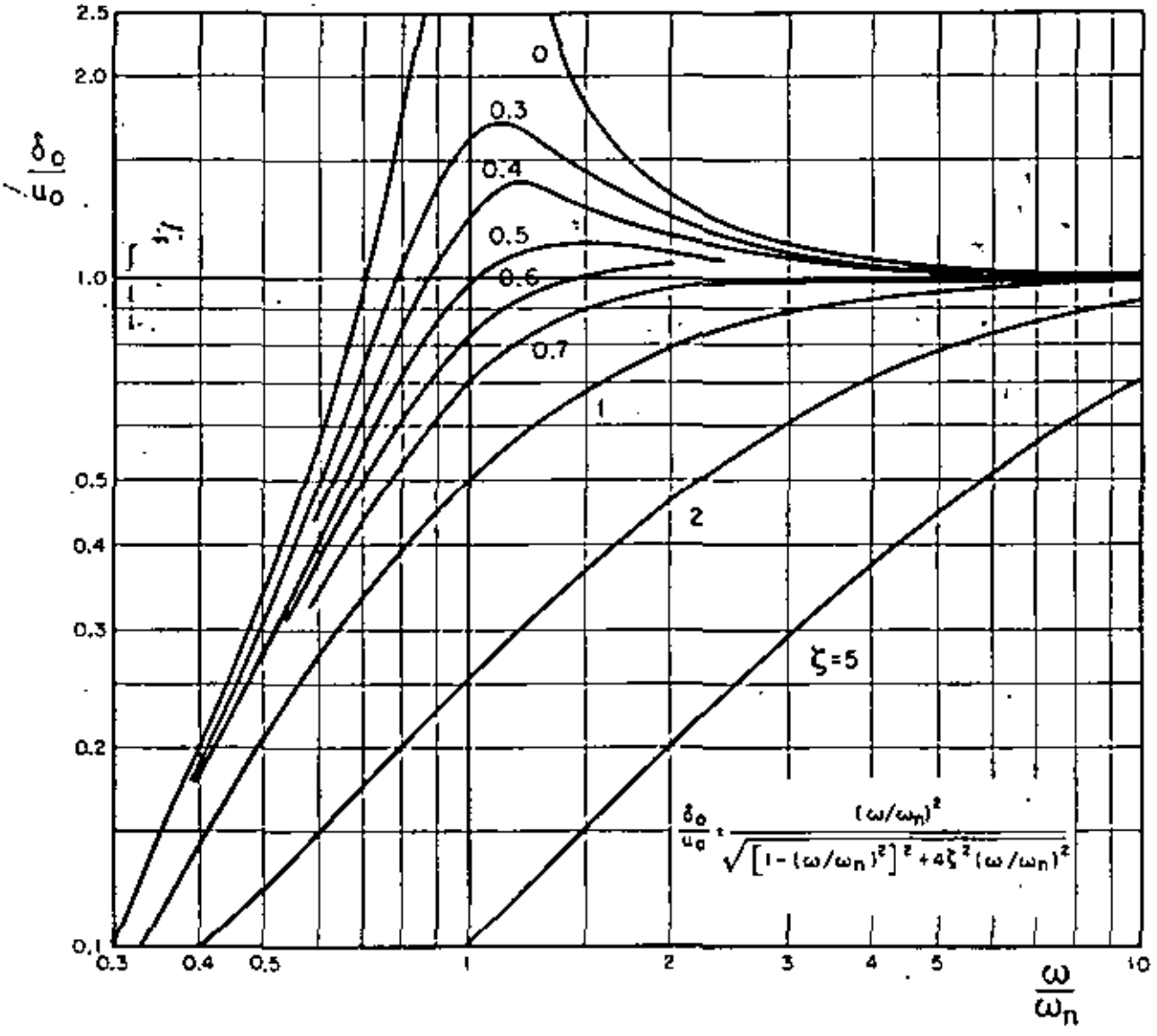

FIG. 4.4

$\omega/\omega_n > 1$

$T/T_n < 1$

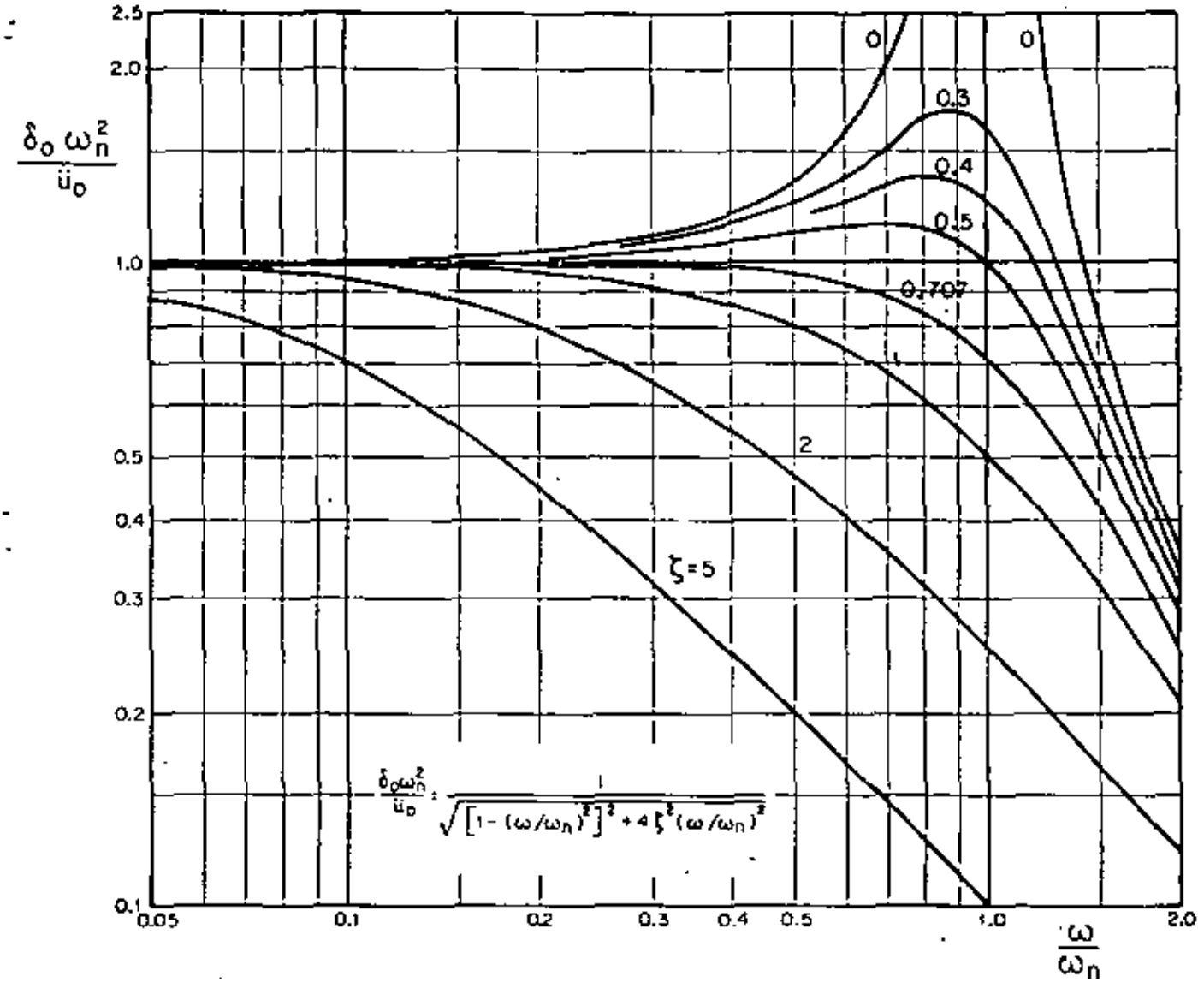

FIG. 4.5

$\omega/\omega_n < 1$

$T/T_n > 1$

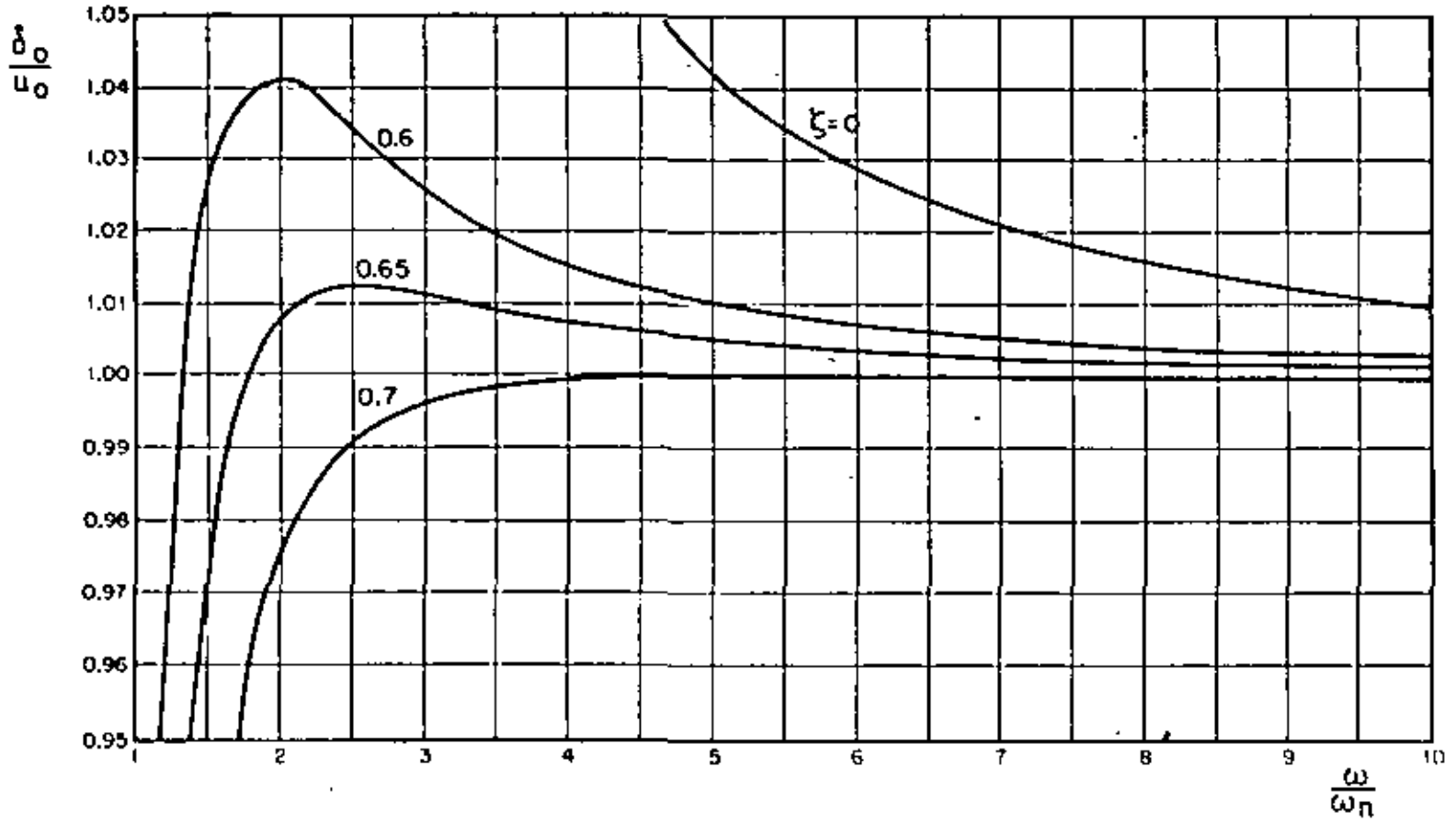
$\frac{\delta_o}{u_o}$
1.05
1.04
1.03
1.02
1.01
1.00
0.99
0.98
0.97
0.96
0.95
0.6
0.65
0.7
ζ=0
1
2
3
4
5
6
7
8
9
10
$\frac{\omega}{\omega_n}$

FIG. 4.6

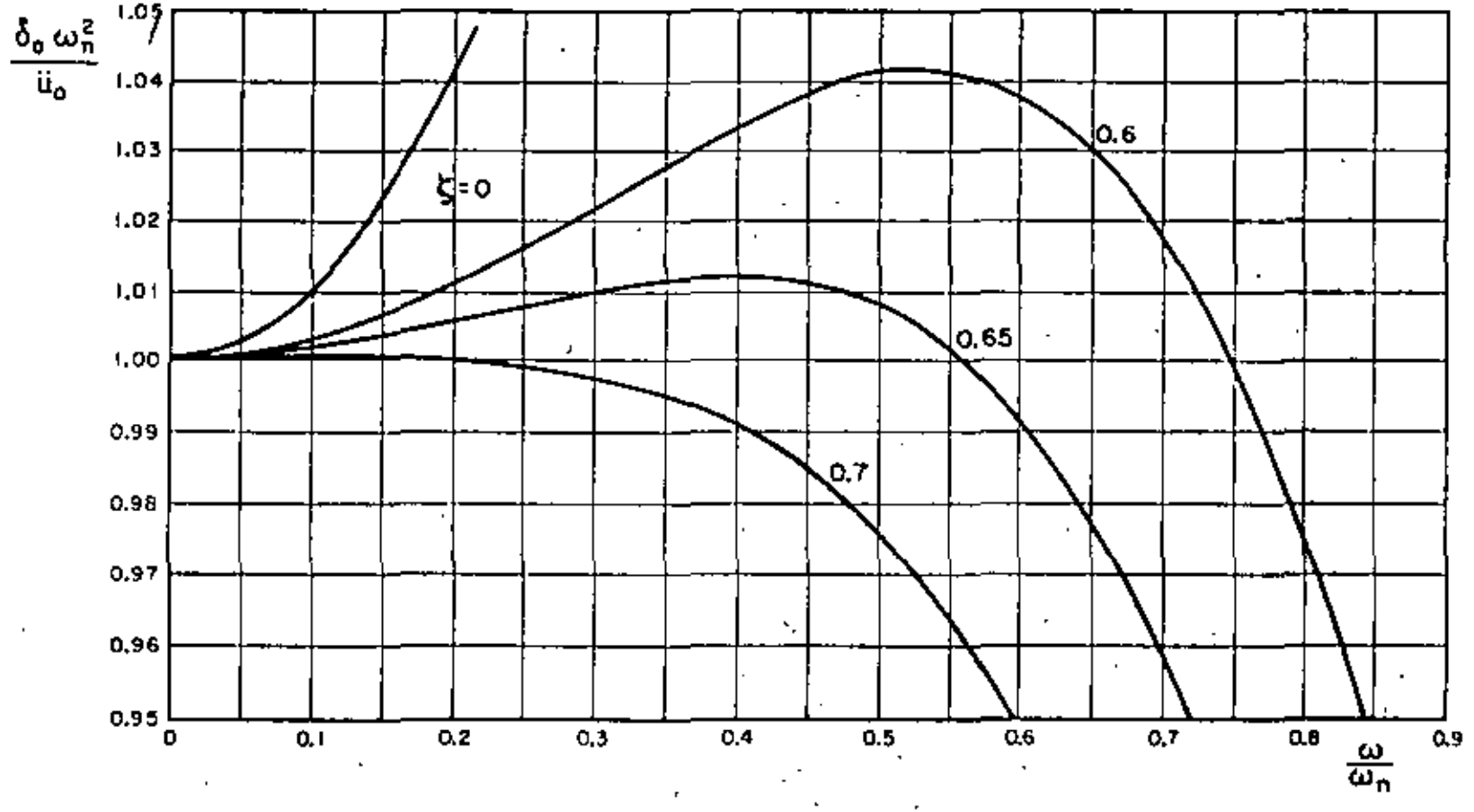
$\frac{\delta_0 \omega_n^2}{\ddot{u}_0}$
1.05
1.04
1.03
1.02
1.01
1.00
0.99
0.98
0.97
0.96
0.95
0
0.1
0.2
0.3
0.4
0.5
0.6
0.7
0.8
0.9
$\frac{\omega}{\omega_n}$
ζ = 0
0.6
0.65
0.7

FIG. 4.7

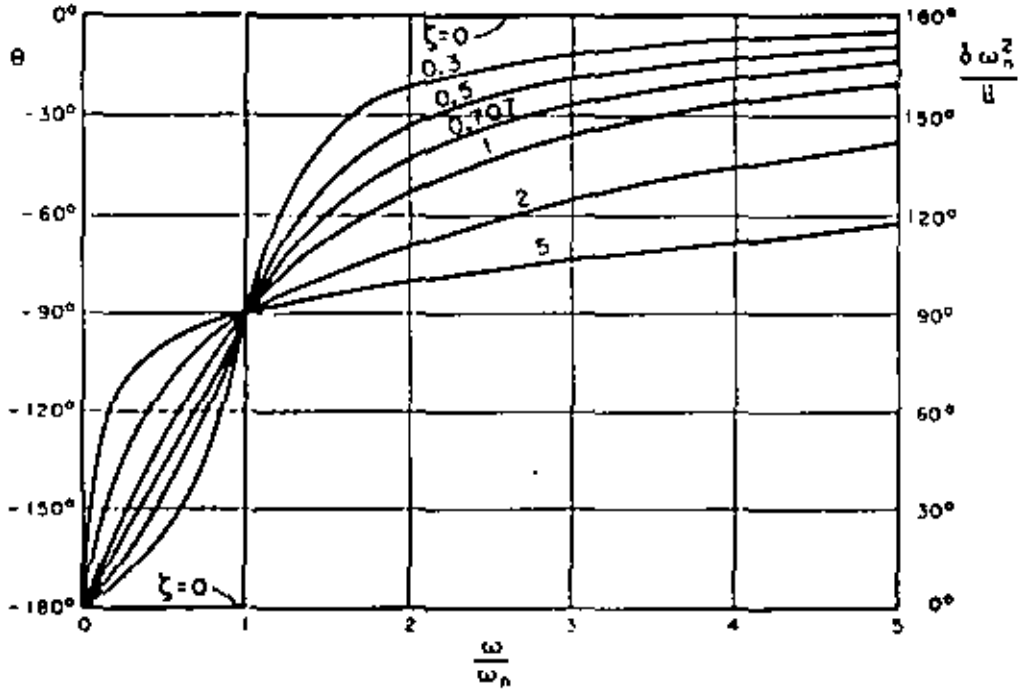
θ
0°
-30°
-60°
-90°
-120°
-150°
-180°
ζ=0
0.3
0.5
0.707
1
2
5
ζ=0
160°
150°
120°
90°
60°
30°
0°
δ ω_n² / u
0
1
2
3
4
5
ω / ω_n

FIG. 4.8

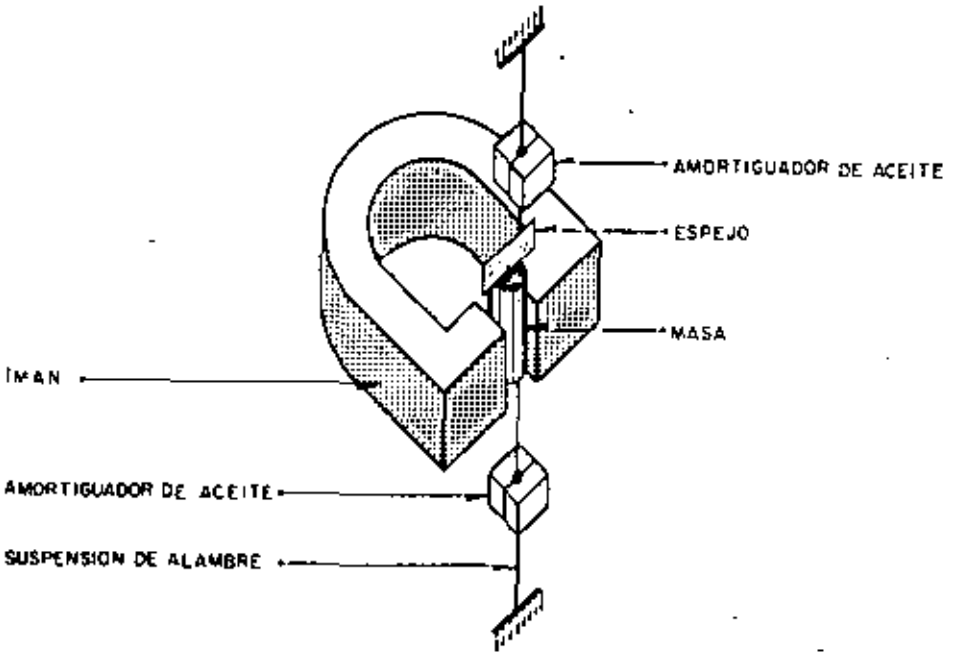
AMORTIGUADOR DE ACEITE
ESPEJO
MASA
IMAN
AMORTIGUADOR DE ACEITE
SUSPENSION DE ALAMBRE

FIG. 4.9

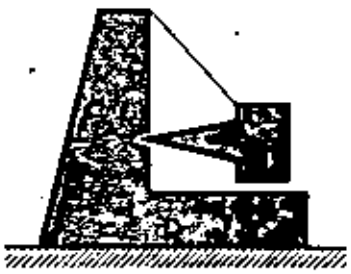

MILNE
(Horizontal)

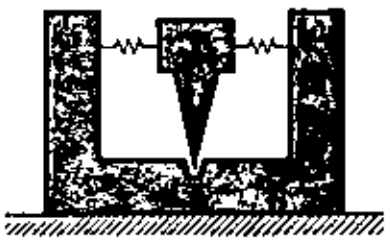

WIECHERT

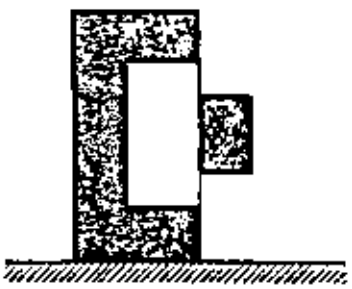

WOOD - ANDERSON

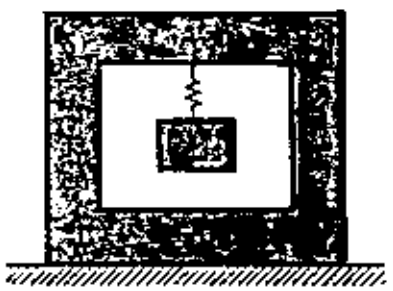

BENIOFF

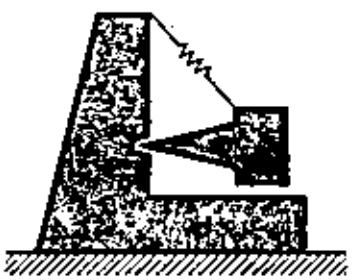

PRESS - EWING
(Vertical)

FIG. 4.10

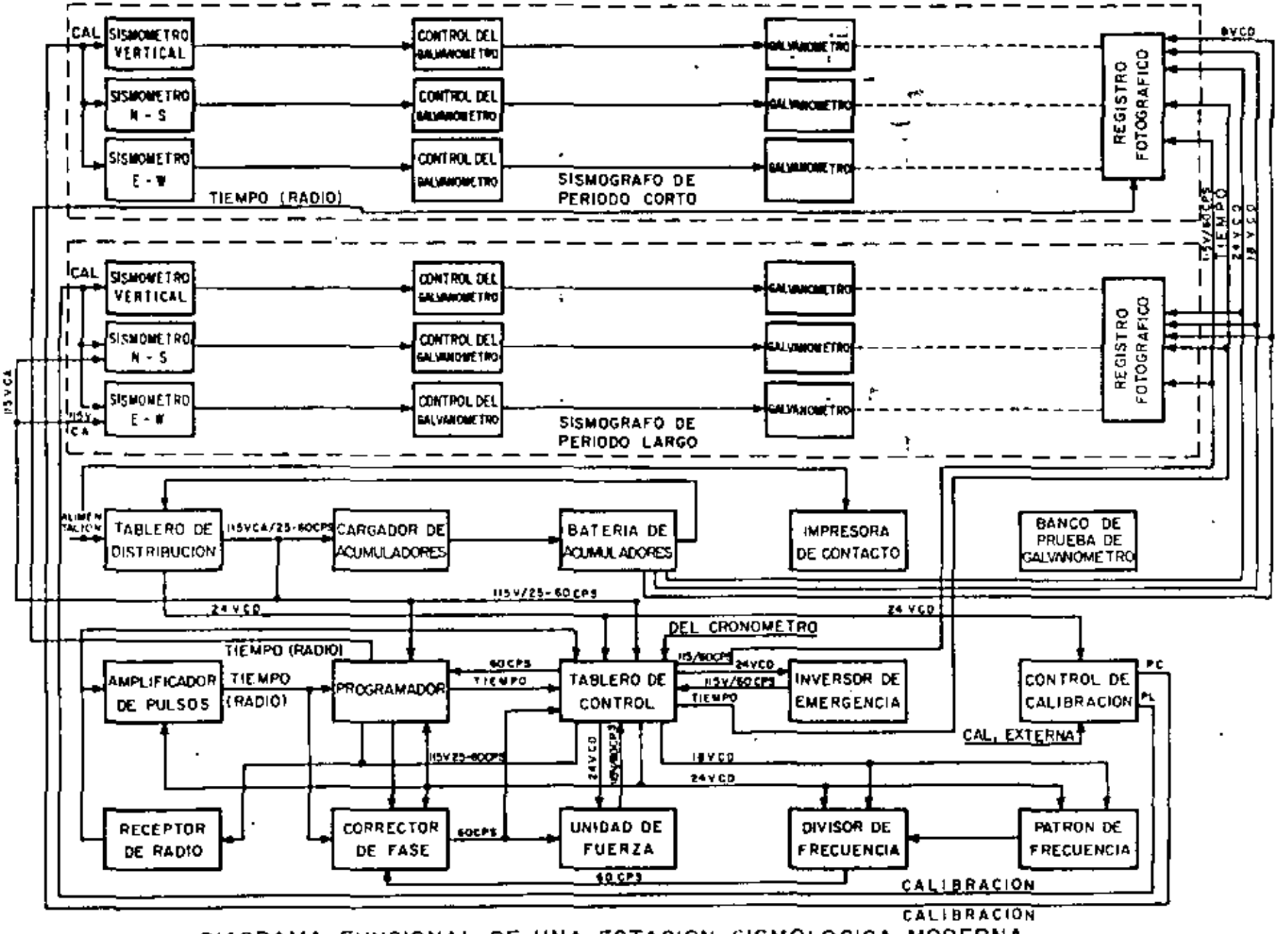

DIAGRAMA FUNCIONAL DE UNA ESTACION SISMOLOGICA MODERNA

FIG. 4.11

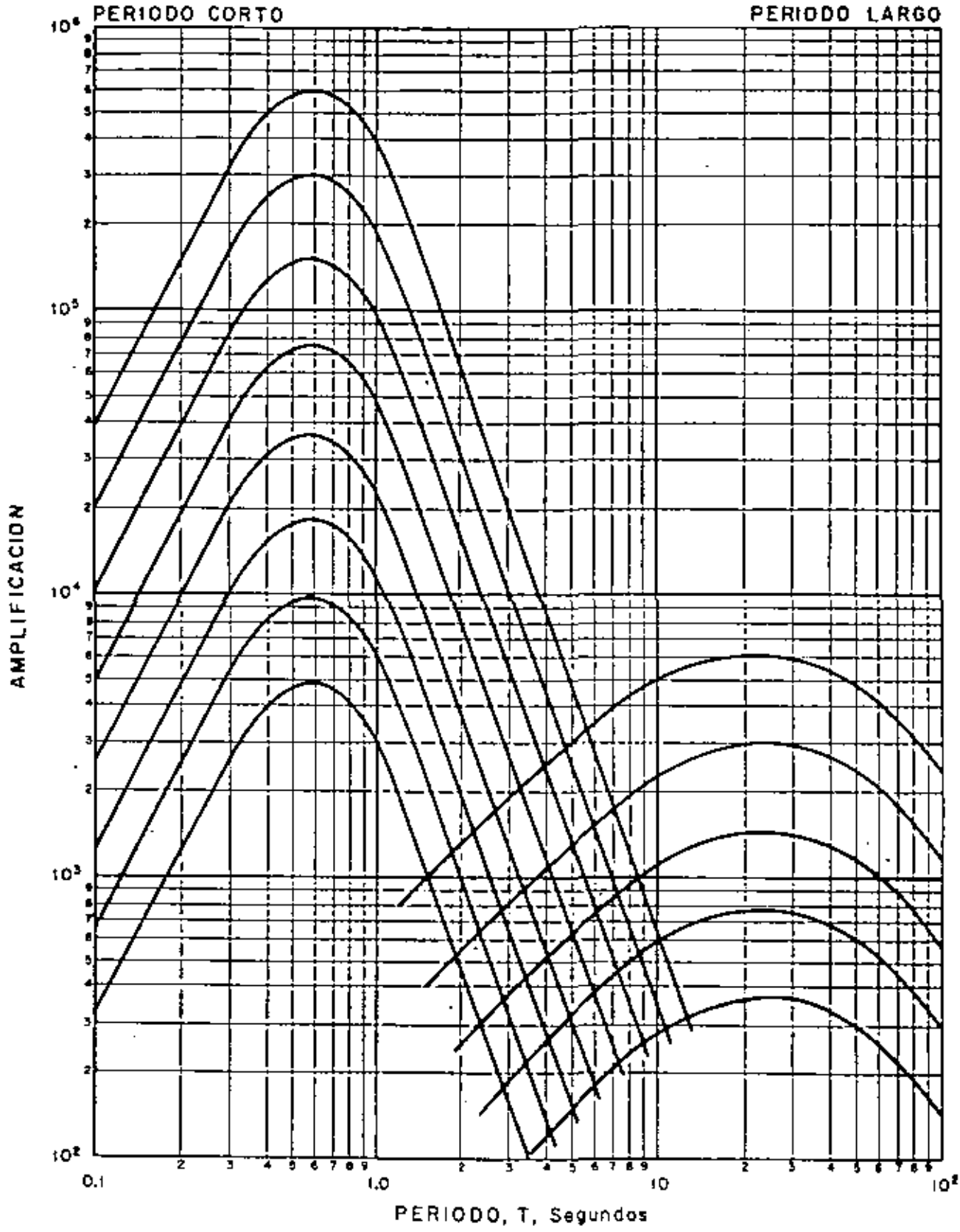
PERIODO CORTO
PERIODO LARGO
AMPLIFICACION
10^6
10^5
10^4
10^3
10^2
0.1
1.0
10
10^2
PERIODO, T, Segundos

FIG. 4.12

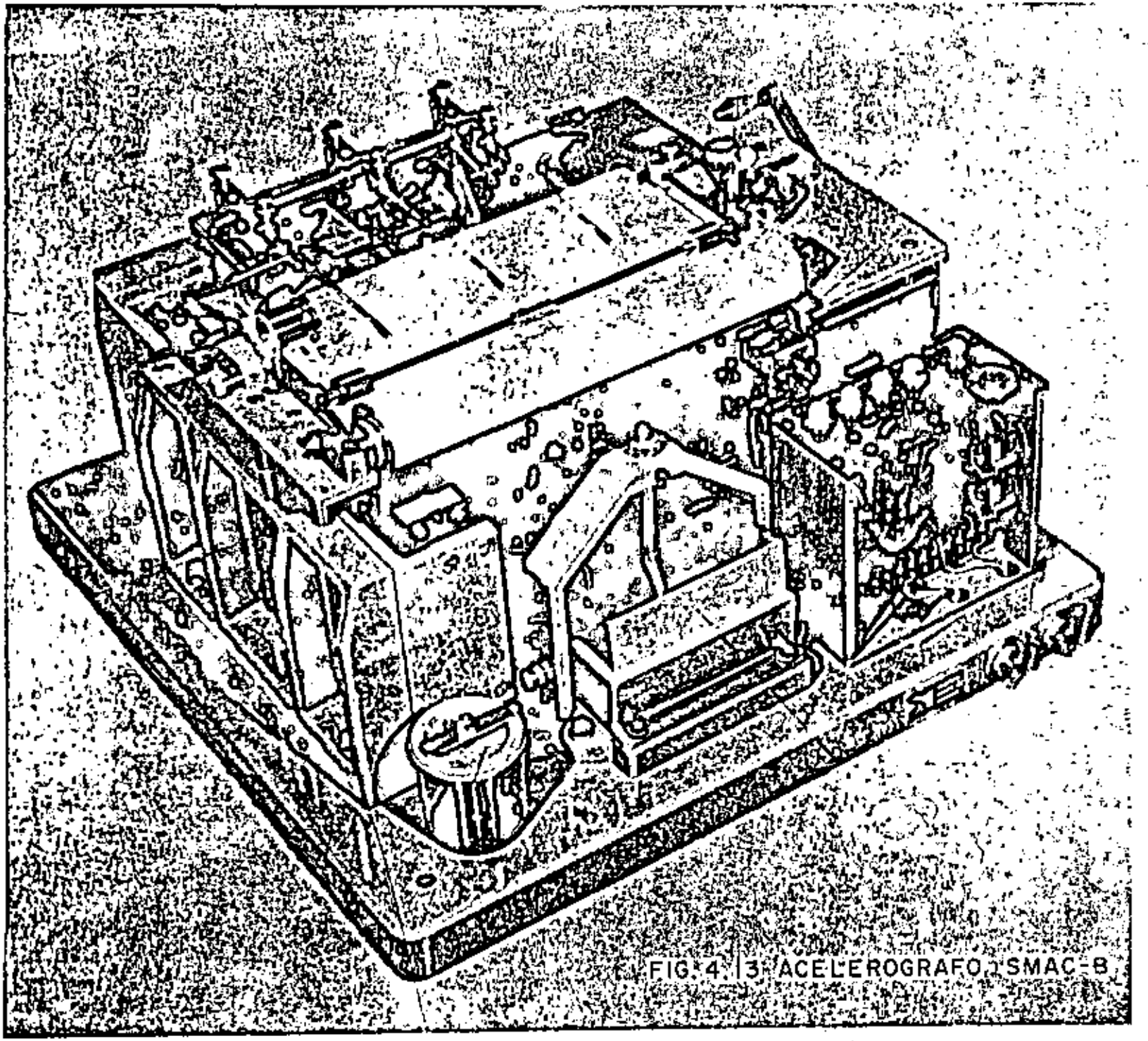

FIG. 4.13 ACELEROGRAFO SMAC-B

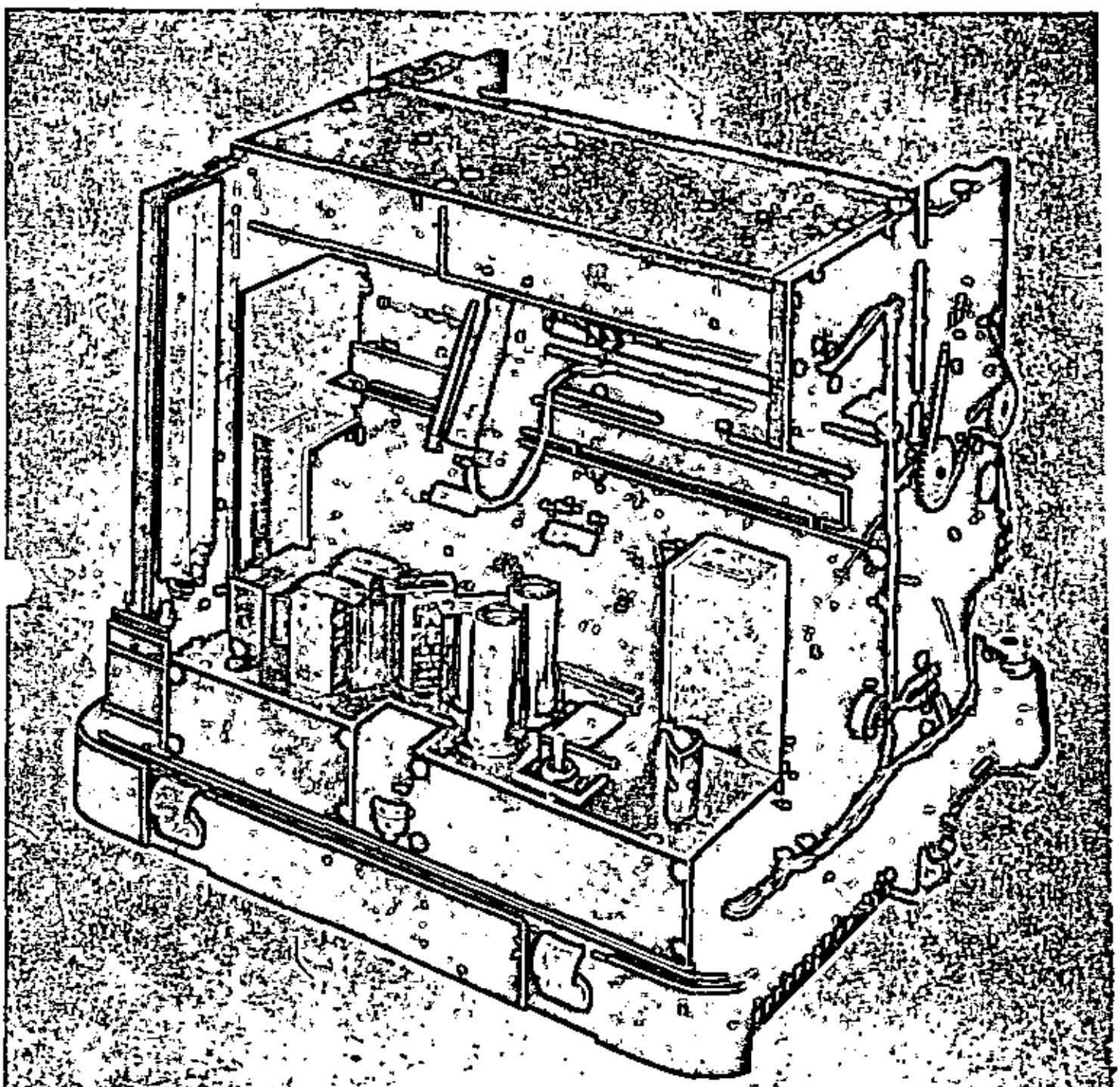

FIG. 4.14 ACELEROGRAFO AR-240

(Foto cortesía de United Electrodynamics Inc.)

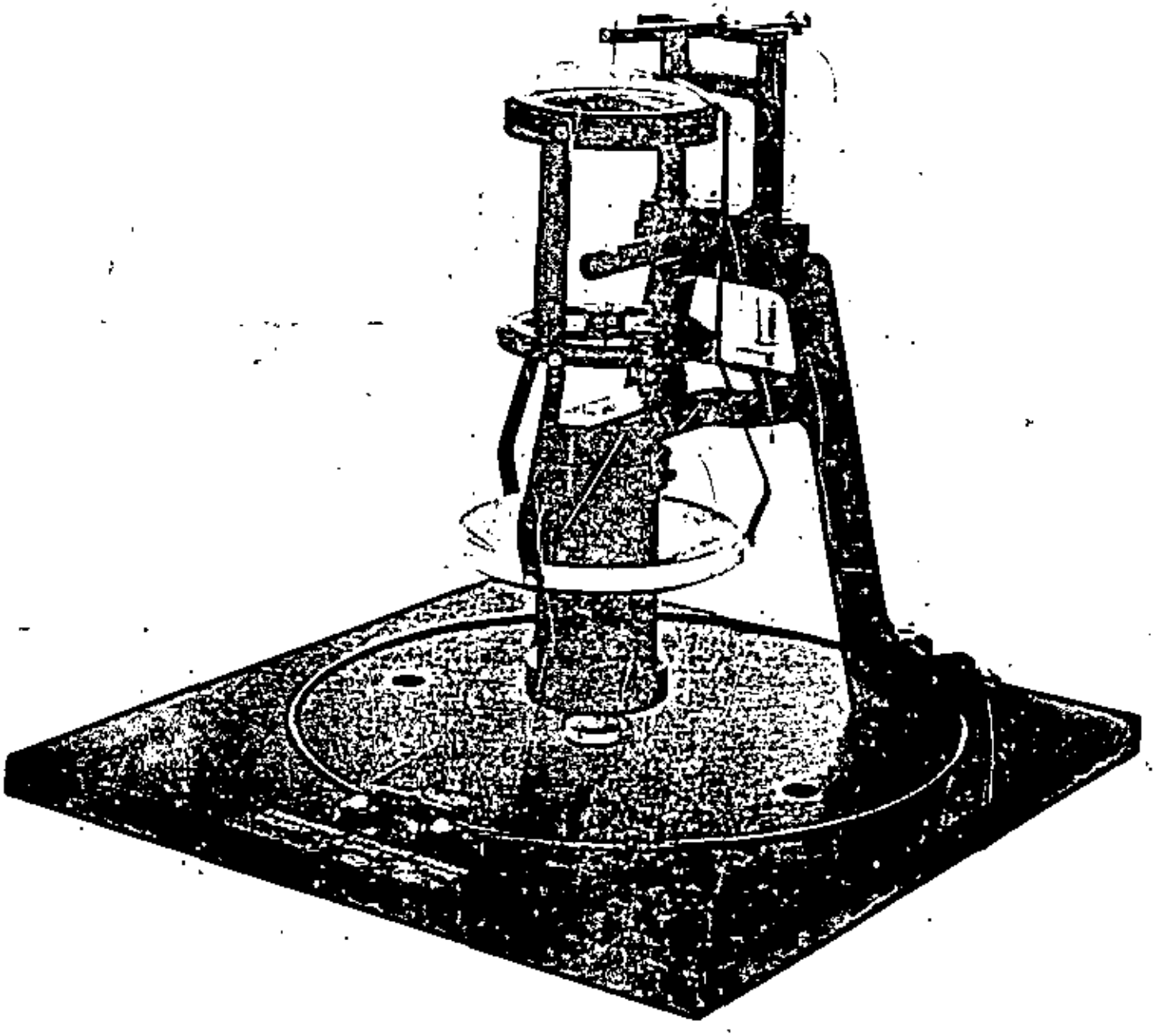

FIG. 4.15 SISMOSCOPIO WILMOT

(Foto cortesía de United Electrodynamics Inc.)

TABLA 4.1

CARACTERISTICAS DE ALGUNOS ACELEROGRAFOS

	USC&GS Estándar*	USC&GS Mark II *	AKASHI SMAC B/B2	HOSAKA DC-3*	UED AR - 240 *
Componentes	2 horiz., 1 vert.	2 horiz., 1 vert.	2 horiz., 1 vert.	2 horiz., 1 vert.	2 horiz., 1 vert.
Período natural (seg)	0.001-0.15 Ajust.	0.03-0.10 Ajust.	0.10/0.14	0.10	0.055-0.065
Amortiguamiento (% del crit.)	60 (magnético)	65 (electromagnético)	100 (pistón de aire)	100 (pistón de aceite)	55-65 (Aj.) (electro magnético).
Sensibilidad (gals/mm)	5-17 (Ajustable)	5-17 (Ajustable)	25/12.5	25	20-12.9 (Ajustable)
Intervalo de trabajo (gals)	1 a 1000	10 a 1000	10 a 1000/6 a 500	25 a 1000	10 a 1000
Registro	papel fot. a 1 cm/seg	película 70 mm a 1 cm/seg	papel encerado a 1 cm/seg	papel ahumado a 1 cm/seg	papel fot. a 2 cm/seg
Trazas registradas	3 fijas, 3 de acel., 2 de tiempo en extremos papel.	3 fijas, 3 de acel., 2 de tiempo en extremos película	3 de aceleración, 1 tiempo	3 de aceleración, 1 tiempo	3 fijas, 3 acel., 2 de tiempo en extremos papel.
Sistema motor	motor c.d.	motor sincrónico	mecánico de cuerda	motor c. d.	motor c. d.
Sistema para calibración	no	si	no	no	si
Arrancador eléctrico	péndulo sensible a movimiento horizontal	péndulo sensible a movimiento horizontal	péndulo sensible a movimiento vertical	péndulo sensible a movimiento vertical	péndulo sensible a mov. horizontal
período (seg)	1.0	0.6	0.3	0.3	1.0 aprox.
amortiguamiento (% crit.)	30 (aceite)	50 (electromagnético)	30 (aceite)	---	100 magnético
sensibilidad (gals)	---	10	10/5	10	6
Número ciclos de registro	5	hasta agotarse película	5	3	hasta agotarse papel
Tiempo de registro	1½ min	hasta 1-20 seg después del último contacto	3 min	3 min	hasta 7 seg. después del último contacto
Marcas de tiempo por segundo	2	5	1/5	5, 2, 6 1	2
Fuente de alimentación	Batería 12v con cargador a la línea	Batería 24v con cargador a la línea	8 pilas secas de 1.5 v	4 pilas secas de 1.5 v	Batería 12 v con cargador a la línea
Dimensiones (cm)	33 x 50 x 112	25 x 35 x 53	38x53x53 (incl. pilas)	40x60x78 (incl. pilas)	35x40x40
Peso (aprox. sin batería, kg)	61	28	100	200	28
Fabricante (diseño de)	(USC&GS) no comercial	(USC&GS) no comercial	Akashi Seisakusho Ltd. Tokio	Hosaka Shindo Keiki Mfg.Co. Tokio	United Electro-Dynamics Inc, Pasadena
Precio aproximado en fábrica (pesos)	---	---	50,000	50,000	50,000

*Datos cortesía de United ElectroDynamics, Inc.

DIVISION DE EDUCACION CONTINUA
FACULTAD DE INGENIERIA U.N.A.M.

IX CURSO INTERNACIONAL DE INGENIERIA SISMICA

ANALISIS DE RIESGO SISMICO

CONCEPTOS FUNDAMENTALES DE LA TEORIA DE PROBABILIDADES PARA ANALISIS DE RIESGO SISMICO

M.EN I. SONIA E. RUIZ

JULIO, 1983

CONCEPTOS FUNDAMENTALES DE LA TEORIA DE PROBABILIDADES PARA ANALISIS DE RIESGO SISMICO

INTRODUCCION

La teoría de Probabilidades es una herramienta muy útil para evaluar el riesgo sísmico.

Dado que la naturaleza de los temblores no es de tipo determinístico, el problma debe tratarse mediante modelos probabilístico. Por ejemplo, existen grandes incertidumbres respecto a las coordenadas del foco, magnitd del evento, tiempo de ocurrencia, relaciones magnitud-intensidad, etc.

No es posible decir con certeza cuando ocurrirá un temblor, pero sí podemos decir qué tan probable es que ocurra. El tiempo de ocurrencia de los sismos de diferentes características originados en una determinada fuente puede expresarse mediante un *proceso estocástico*, que es una descripción matemática de la forma en que varía con el tiempo la ocurrencia de ciertos eventos.

Para formular un modelo de sismicidad y estimar sus parámetros sería deseable contar con un número suficiente de registros de movimientos sísmicos fuentes, de las características de su fuente y de su ubicación, sin embargo esta información es muy escasa por lo que tiene que hacer uso de técnicas estadísticas más refinadas (por ejemplo el teorema de Bayes).

Enseguida se presenta un repaso de los conceptos fundamentales de la teoría de Probabilidades para la mejor comprensión del análisis de riesgo sísmico.

NOCIONES DE TEORIA DE PROBABILIDADES

AXIOMAS FUNDAMENTALES

AXIOMA 1.- La probabilidad de un evento A se encuentra 0 y 1

$$0 \leq P(A) \leq 1$$

AXIOMA 2.- La probabilidad de la unión de dos eventos mutuamente exclusivos es igual a la suma de sus probabilidades

$$P(A \cup B) = P(A) + P(B)$$

Si estos no son mutuamente exclusivos, entonces

$$P(A \cup B) = P(A) + P(B) - P(A \cap B)$$

PROBABILIDAD CONDICIONAL

La probabilidad de que ocurra un evento A, dado que conocemos el resultado de un evento B es igual a

$$P(A|B) = \frac{P(A \cap B)}{P(B)} \qquad (1)$$

De donde

$$P(A \cap B) = P(A|B)\,P(B)$$

Generalizando,

$$P(A \cap B \cap C \ldots \cap N) = P(A|B \cap C \ldots)\,P(B|C \cap \ldots) \ldots P(N)$$

Si los eventos son independientes entre sí, entonces

$$P(A \cap B \cap C \ldots \cap N) = P(A)\,P(B)\,P(C) \ldots P(N)$$

TEOREMA DE PROBABILIDADES TOTALES.

Dado un conjunto de eventos mutuamente exclusivos y colectivamente exhaustivos, B_1, B_2.... B_n, es posible siempre expresar la probabilidad P(A) de otro evento A como sigue

$$P(A) = P(A \cap B_1) + P(A \cap B_2) + \ldots = \sum_{i=1}^{n} P(A \cap B_i)$$

Entonces

$$P(A) = \sum_{i=1}^{n} P(A|B_i) P(B_i) \qquad (2)$$

TEOREMA DE BAYES

La probabilidad condicional de A_j dado que ha ocurrido el evento B es

$$P(A_j|B) = \frac{P(A_j \cap B)}{P(B)} = \frac{P(B \cap A_j)}{P(B)} \qquad (3)$$

Por lo visto en las definiciones anteriores es posible llegar a lo siguiente

$$P(A_j|B) = \frac{P(B|A_j)\ P(A_j)}{\sum_{i=1}^{n} P(B|A_i) P(A_i)} \qquad (4)$$

Generalmente a la probabilidad resultante se le llama "*a posteriori*" y a la probabilidad $P(A_j)$ se le llama "*a priori*"

DISTRIBUCION DE PROBABILIDAD DE LAS VARIABLES ALEATORIAS

El comportamiento de una variable aleatoria se describe a través de leyes probabilísticas representadas mediante funciones de distribución de probabilidad.

En el caso de variables aleatorias discretas estas leyes se repre

sentan mediante FUNCIONES DE MASA DE PROBABILIDAD, en el caso de variables continuas se utilizan las FUNCIONES DE DENSIDAD DE PROBABILIDAD. Cuando se tratan varias variables a la vez el comportamiento lo determinan leyes de probabilidad CONJUNTAS.

DISTRIBUCION DE PROBABILIDAD MARGINAL

El comportamiento de una (o varias) variable(s) aleatoria(s) se puede obtener a partir de una distribución conjunta, integrando sobre todos los valores de las variables cuyo comportamiento no interesa. La función que representa a este comportamiento es la distribución de probabilidad MARGINAL. Por ejemplo sean X y Y variables aleatorias continuas, con densidad de probabilidades $f_{x,y}(x, y)$; entonces la función de probabilidad marginal de x es igual a

$$f_x(x) = \int_{-\infty}^{\infty} f_{x,y}(x,y)\, dy \qquad (5)$$

Generalizando

$$f_{x_1,x_2}(x_1,x_2) = \iiint\cdots\int_{D} f_{x_1,x_2,x_3\ldots x_n}(x_1,x_2,x_3\ldots x_n)\, dx\, dx\, dx_3\ldots dx_n$$

DISTRIBUCION DE PROBABILIDAD CONDICIONAL

Si en una función de distribución de probabilidad conjunta algunas variables adquieren valores fijos la función de distribución de probabilidad normalizada resultante representa a la distribución CONDICIONAL. Sean X y Y variables aleatorias continuas y $f_{x,y}(x, y)$ su función de distribución; si Y adquiere el valor y_o, entonces la función de probabilidad condicional de X es igual a

$$f_{x|y}(x,y_o) = \frac{f_{x,y}(x,y_o)}{f_y(y_o)} \qquad (6)$$

En donde

$$f_y(y_o) = \int_{-\infty}^{\infty} f_{x,y}(x,y_o)\, dx$$

Generalizando,

$$f_{x_1|x_2,x_3}(x_1,x_2,x_3) = \frac{f_{x_1,x_2,x_3}(x_1,x_2,x_3)}{f_{x_2,x_3}(x_2,x_3)}$$

MOMENTOS DE UNA VARIABLE ALEATORIA

Media ó valor esperado de una variable continua X

$$m_x = E(x) = \int_{-\infty}^{\infty} x\, f_x(x)\, dx \qquad (7)$$

Variancia de una variable continua X

$$\sigma_x^2 = var(x) = \int_{-\infty}^{\infty} (x - m_x)^2 f_x(x) dx = E[x^2] - E^2[x] \qquad (8)$$

Desviación estandard de una variable continua X

$$\sigma_x = \sqrt{\sigma_x^2} = \left[\int_{-\infty}^{\infty} (x - m_x)^2 f_x(x) dx \right]^{1/2} \qquad (9)$$

PROPIEDADES DE LA ESPERANZA. Sean a, b, c constantes

$$E[cX] = c\,E[X]$$

$$E[a + bX] = a + b\,E[X]$$

$$cov[X,Y] = E[(X - m_x)(Y - m_y)] = E[XY] - E[X]E[Y]$$

ESPERANZA DE UN PRODUCTO DE VARIABLES

$$E[XY] = cov[X,Y] + E[X]E[Y]$$

FUNCIONES DE MASA DE PROBABILIDAD:

BINOMINAL Y DE POISSON

Enseguida se tratan dos distribuciones de variables aleatorias discretas ; discontinua de orden finito la BINOMIAL y de orden infinito la de POISSON

DISTRIBUCION BINOMINAL

Se aplica a experimentos de Bernoulli (acepta únicamente dos posibles resultados: éxito y fracaso).

Sea

p = probabilidad de obtener éxito

q = 1 - p = probabilidad de obtener fracaso

La probabilidad de obtener x éxtito al realizar n veces el experimento de Bernoulli es

$$\underbrace{p \cdot p \cdot p \cdot p}_{x} \cdot \underbrace{q \cdot q \cdot q \cdots q}_{n-x} = p^x q^{n-x}$$

Aquí se supuso que los x éxitos ocurren al principio. El número total de formas en que pueden presentarse los x éxitos es igual a las permutaciones de n objetos formados por dos grupos: uno de x objetos iguales y otro de n-x objetos iguales o sea igual a

$$\frac{n!}{x!(n-x)!}$$

o sea que la probabilidad buscada es la siguiente

$$P(x) = \frac{n!}{x!(n-x)!}\, p^x q^{n-x} \qquad (*)$$

La variable aleatoria x es un número entero entre cero y n

Su media es igual a

$$m_x = \sum_{x=0}^{n} x\, P(x) = np$$

Su variancia es

$$\sigma_x^2 = \sum_{x=0}^{n} x^2 P(x) = npq$$

Su desviación estándard

$$\sigma_x = \sqrt{npq}$$

La representación gráfica de P(x) para n = 6 y p = 0.5 es como sigue

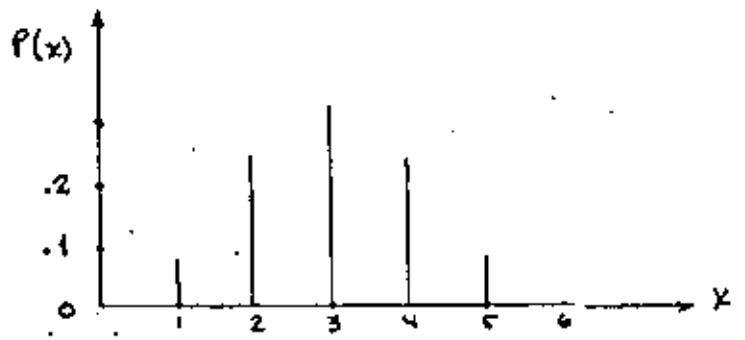

DISTRIBUCION DE POISSON

Si se considera que en la distribución binominal n tiende a infinito mientras que la probabilidad p de éxito tiende a cero, entonces la ec.(10) se convierte en

$$P(x) = \frac{\nu^x}{x!} e^{-\nu}, \quad x = 0,1,2,3\ldots,\infty \qquad (11)$$

Esta distribución de probabilidad se llama de POISSON de parámetro ν

Su media está dada por

$$m_x = \sum_{x=0}^{\infty} x\, P(x) = \nu$$

Su variancia es igual a

$$\sigma_x^2 = \sum_{x=0}^{\infty} x^2 P(x) = \nu$$

Su desviación estándard

$$\sigma_x = \sqrt{\nu}$$

La distribución de Poisson de parámetros $\nu = np$ se aproxima a la binomial siempre que $n > 50$ y $np < 5$.

En las siguientes figuras se ilustra la variación de la forma de las distribuciones con el parámetro ν:

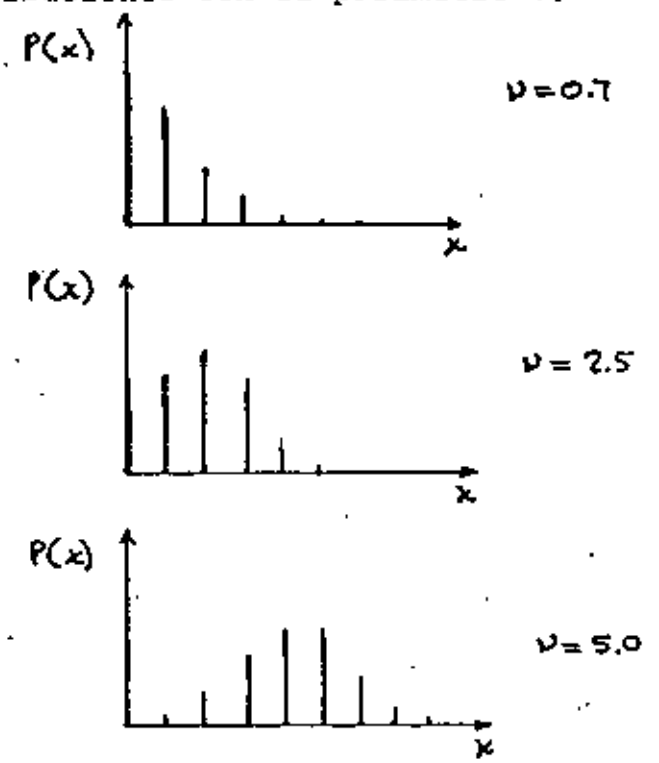

PROCESO DE POISSON

Este proceso representa el número de eventos que ocurre en un tiempo t cuando dicho número tiene distribución de Poisson; es decir,

$$P(n) = \frac{(\lambda t)^n e^{-\lambda t}}{n!}$$

Ilustrando esto gráficamente:

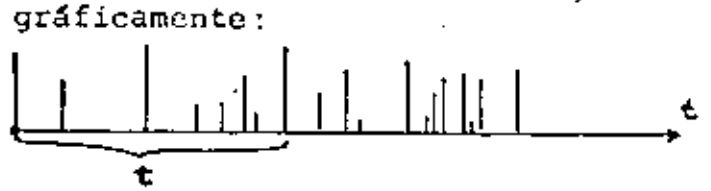

En un proceso de Poisson, la media de su distribución (de Poisson) es $m_n = \lambda t$. Al parámetro λ se le llama tasa media de ocurrencia del proceso.

Un proceso de Poisson debe satisfacer las siguientes hipótesis:

1. ESTACIONARIEDAD

La probabilidad de un evento en un intervalo corto de tiempo $(t, t + \Delta t)$ es aproximadamente $\lambda(\Delta t)$ para cualquier t.

2. NO MULTIPLICIDAD

La probabilidad de 2 o más eventos en un intervalo corto de tiempo es despreciable comparado con $\lambda(\Delta t)$

3. INDEPENDENCIA

El número de eventos en cualquier intervalo de tiempo es independiente de el número en cualquier otro intervalo de tiempo.

EJEMPLO

Mediante un estudio estadístico sobre la ocurrencia de sismos en cierta región se estimó que un temblor con una magnitud igual a 6 o mayor tiene un periodo de recurrencia de 100 años. Calcular las probabilidades de que en los próximos 10, 50 y 100 años no ocurra ningún sismo en dicha región cuya magnitud exceda a 6, suponiendo que la ocurrencia de los sismos se puede modelar mediante un proceso estocástico de Poisson.

$$\lambda = \frac{1}{100} = .01$$

$$P(n) = \frac{(.01t)^n e^{-.01t}}{n!}$$

Para, t = 10 años

$$P(10) = \frac{(.01 \times 10)^0 e^{-.01 \times 10}}{0!} = .905$$

Para t = 50 años

$$P(50) = \frac{(.01 \times 50)^{0} e^{-.01 \times 50}}{0!} = .607$$

Para t = 100 años

$$P(100) = \frac{(.01 \times 100)^{0} e^{-.01 \times 100}}{0!} = .368$$

Las probabilidades de que ocurra al menos un sismo con magnitud mayor que 6 son

$$P(n \geq 1) = 1 - .905 = .095$$

$$P(n \geq 1) = 1 - .607 = .393$$

$$P(n \geq 1) = 1 - .368 = .632$$

FUNCIONES DE DENSIDAD DE PROBABILIDAD:

NORMAL Y LOGNORMAL

DISTRIBUCION NORMAL

Una de las más importantes funciones dentro de la teoría de Probabilidades es la NORMAL O GAUSSIANA. Esta es aplicable a variables aleatorias continuas dentro del dominio de los números reales.

La función de densidad de probabilidad está dada por

$$f_x(x) = \frac{1}{\sqrt{2\pi}\,\sigma_x} e^{-\frac{(x-m_x)^2}{2\sigma_x^2}}, \quad -\infty < x < \infty \qquad (13)$$

en donde

m_x = media

σ_x^2 = variancia

Al examinar esta expresión se deduce que es una función simétrica con respecto a un eje vertical que pasa por m_x, que es asintótica al eje de las abscisas para valores que tiendan a $\pm\infty$, y, que su valor máximo corresponde a m_x. En la siguiente figura se presenta su representación cuando su media permanece constante igual a m_x y su desviación estándar (σ_x) varía

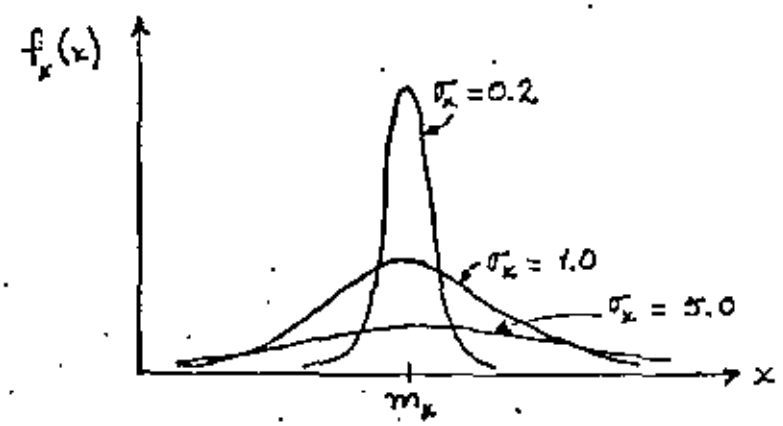

DISTRIBUCION LOGNORMAL

La distribución LOGARITMICO-NORMAL O LOGNORMAL se presenta en el caso de que el logaritmo natural de una variable aleatoria tenga distribución normal. Es decir, si la variable X tiene una función de densidad dada por la ec 13, y si $X = \ln Y$, entonces la función de densidad de Y resulta lognormal y está dada por

$$f_y(y) = \frac{1}{y\,\sigma_x\sqrt{2\pi}} \exp\left[-\frac{1}{2}\left(\frac{\ln y - m_x}{\sigma_x}\right)^2\right], \quad y \geq 0 \qquad (14)$$

La siguiente figura muestra la gráfica de una distribución logarítmico-normal con $m_x = 0$ y $\sigma_x = 1$.. Esta es de forma asimétrica positiva

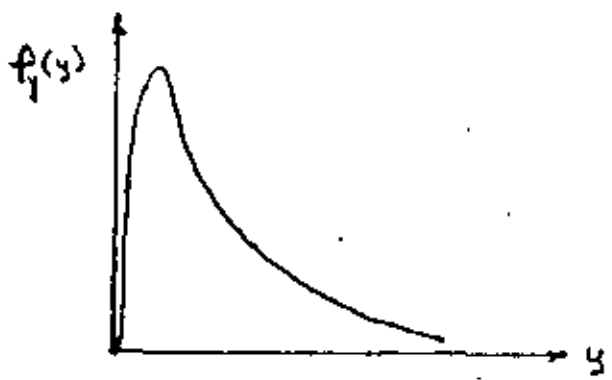

Su media está dada por

$$m_y = \int_0^\infty y\, f(y)\, dy = \exp(m_x + \sigma_x^2/2)$$

Su varianza es igual a

$$\sigma_y^2 = \exp(2m_x + \sigma_x^2) \cdot (\exp \sigma_x^2 - 1)$$

ANALISIS DE REGRESION

Una incógnita importante que debe despejarse en el análisis de regresión es la FORMA GENERAL DE LA EXPRESION MATEMATICA que se piensa puede explicar el comportamiento de cierto fenómeno. Un procedimiento gráfico puede resolver este problema. Dibujando los valores observados de la variable independiente X con los correspondientes valores observados de la variable dependiente y en un sistema de coordenadas rectangulares, se obtiene un conjunto de puntos conocidos como DIAGRAMA DE DISPERSION

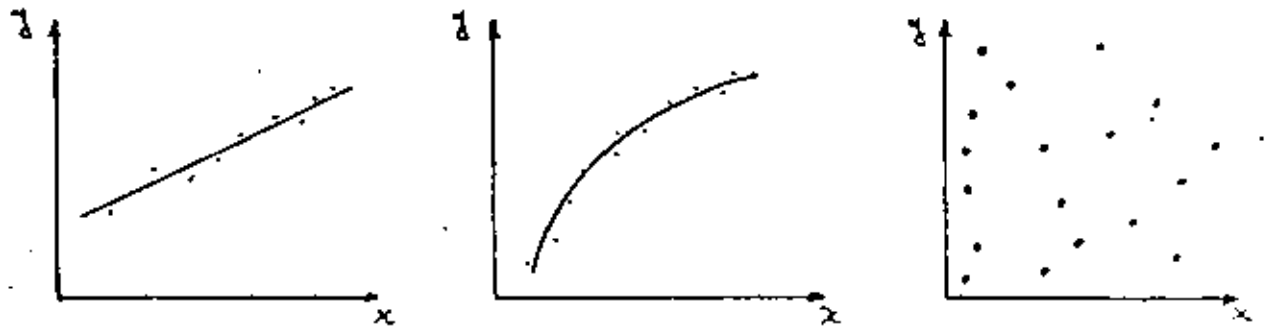

a) Relación lineal b) Relación no lineal c) No existe Relación

La CURVA DE REGRESION es aquella a la cual tienden a aproximarse los puntos del diagrama de dispersión. La ecuación de la curva de regresión es la ECUACION DE REGRESION.

En el caso de regresión lineal se tiene una ecuación de regresión de la forma

$$y = a_0 + a_1 x$$

con dos parámetros por determinar a_0 y a_1

Existen diferentes métodos para determinar estos parámetros aquí se estudiará el método de MINIMOS CUADRADOS

METODO DE MINIMOS CUADRADOS

Se llama DESVIACION, ERROR O RESIDUO a la diferencia de ordenadas

de un punto muestral y de la curva de regresión correspondiente a una misma abscisa

$$d_1 = y_1 - y_1'$$

$$y_1' = a_0 + a_1 x_1'$$

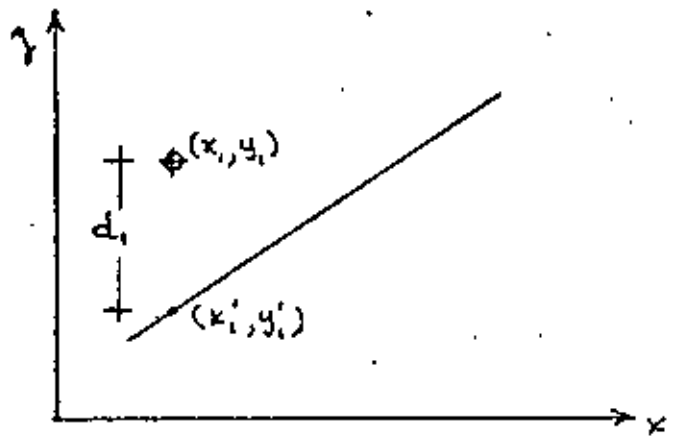

El método de los mínimos cuadrados establece que de todas las curvas de regresión que se pueden ajustar al conjunto de puntos muestrales dados la MEJOR es aquella que tenga la propiedad de que la suma de los cuadrados de sus residuos sea mínima

$$\min \sum_{i=1}^{n} d_i^2$$

Aplicando este criterio para el caso de una recta

$$\min \Sigma d_i^2 = \min \Sigma \left[y_i - (a_0 + a_1 x_i) \right]^2$$

Para encontrar el mínimo se aplica la condición necesaria conocida para que una función tenga un punto extremo, es decir, se iguala a cero las primeras derivadas parciales de la función con respecto a cada una de sus variables.

El resultado de esto conduce a un sistema de ecuaciones simultáneas cuya solución es el valor de los parámetros a_0 y a_1.

REGRESION NO LINEAL

Para resolver el caso de regresión no lineal, generalmente conviene MAPEAR los puntos muestrales a un sistema de referencia en donde sí se aproximen a una recta, mediante ecuaciones de TRANSFORMACION

$$x = x(u,v)$$
$$y = y(u,v)$$

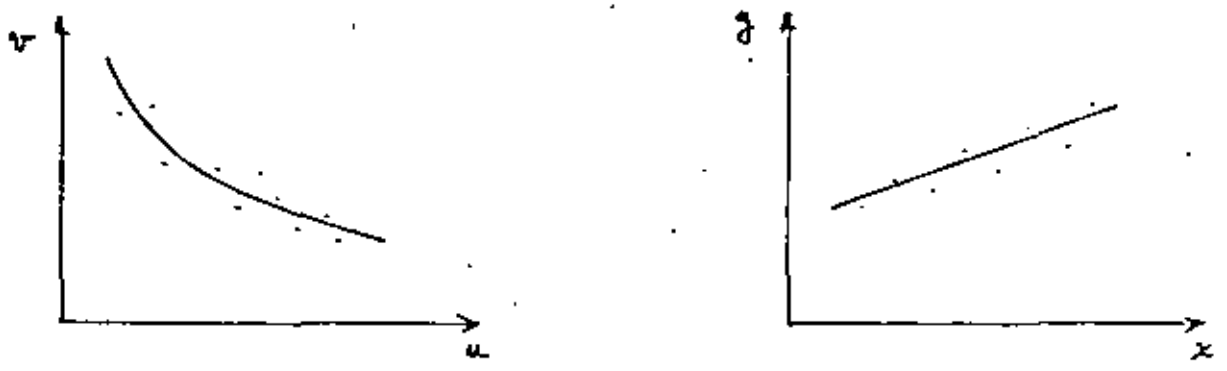

Los sistemas de transformación que se usan con mayor frecuencia con los SEMILOGARITMICOS Y LOS LOGARITMICOS

Por ejemplo una transformación SEMILOGARITMICA es como sigue:

$$x = u$$
$$y = \log v$$

En el sistema x-y el diagrama de dispersión de los puntos mapeados (x_i, y_i) corresponde a una recta cuya ecuación es $y = a_o + a_1 x$, en el sistema uv la ecuación correspondiente es

$$\log v = a_o + a_1 u$$
$$v = 10^{a_o + a_1 u}$$
$$= (10^{a_o})(10^{a_1})^u$$
$$= a\, b^u$$

En donde

$$a = 10^{a_o}$$
$$b = 10^{a_1}$$

Ejemplo. Sea $a_0 = 0$, $a_1 = 1$

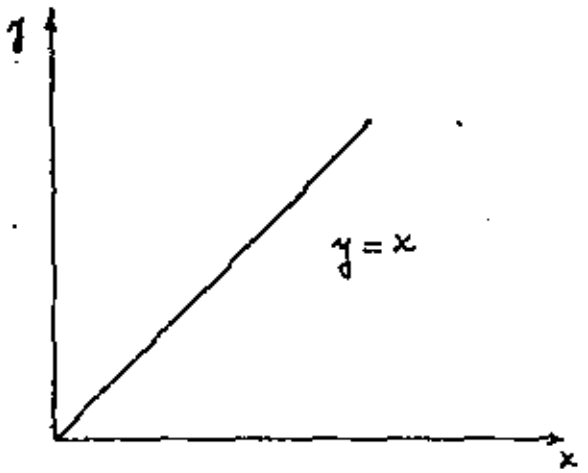

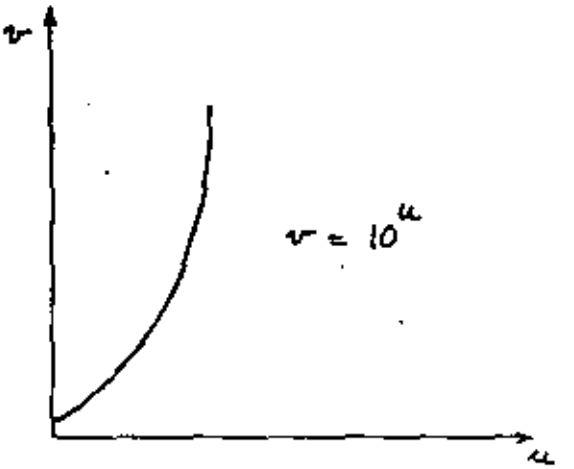

IX CURSOS INTERNACIONAL DE INGENIERIA SISMICA

ANALISIS DE RIESGO SISMICO

VALUACION DE LA SISMICIDAD COMO PROCESO ESTOCASTICO.

M.EN I.O.RUBEN GUERRA J.

JULIO, 1983

2. Valuación de la sismicidad como proceso estocástico

2.1 Introducción

El término sismicidad será usado en este escrito para designar el proceso de generación de sismos en una zona, sus correspondientes magnitudes y las intensidades que producen en los sitios vecinos. Dicho proceso debe describirse cuantitativamente, de manera que su uso permita tomar decisiones racionales.

La intensidad sísmica de un temblor en un sitio indica la capacidad destructiva de dicho temblor en el sitio en cuestión; depende de la cantidad de energía liberada en la fuente sísmica, del mecanismo de liberación de energía, de la distancia entre el sitio y la fuente, de las propiedades del material a lo largo de la trayectoria recorrida por las ondas sísmicas y de las condiciones locales del sitio que interesa. La cantidad de energía liberada se mide por la magnitud (Richter, 1958). Dada la gran dificultad de conocer y manejar todas las variables mencionadas, es necesario expresar a la intensidad sísmica en función de parámetros suficientemente simples, de

modo que sean manejables en forma práctica y permitan tomar decisiones de ingeniería.

Con frecuencia se mantiene que el riesgo sísmico debería expresarse en términos de la máxima intensidad que puede ser producida en el sitio por posibles temblores generados en la vecindad. Sin embargo, las obras de ingeniería no siempre pueden diseñarse para la peor condición posible. Un procedimiento más adecuado consiste en tomar decisiones basadas en estudios costo-beneficio. En consecuencia resulta conveniente expresar a la sismicidad en términos de intensidades y periodos de recurrencia correspondientes, entendiéndose como periodo de recurrencia el tiempo que en promedio tarda en ocurrir una intensidad mayor o igual que un valor dado.

En las aplicaciones de ingeniería, conviene expresar las intensidades sísmicas en términos de aceleración y velocidad máximas del terreno en suelos de características medias. Conociendo las propiedades mecánicas del suelo local, pueden transformarse las intensidades para cualquier tipo de terreno mediante el empleo de factores de amplificación. Las virtudes y limitaciones de los criterios para tomar en cuenta la influencia de las condiciones locales han sido presentados en un trabajo reciente (Ruiz, 1976).

En vista de que no es posible de acuerdo con los conocimientos actuales describir el proceso de generación de temblores en una cierta zona de manera determinística, la sismicidad deberá tratarse como un fenómeno aleatorio que depende del tiempo, esto es, como un proceso estocástico.

Este capítulo trata un criterio para valuar el riesgo sísmico, basado en el empleo de

la información proveniente tanto de registros instrumentales como de la información sobre las características geotectónicas de la corteza terrestre; consiste en identificar las fuentes potenciales de actividad sísmica cercanos al sitio, formular modelos matemáticos del proceso de generación de temblores en cada fuente, obtener la contribución de cada fuente al riesgo sísmico en el sitio en estudio e integrar las contribuciones de las diversas fuentes.

2.2 Respuesta espectral

La respuesta sísmica de estructuras lineales se puede estimar con buena precisión mediante superposición modal, siempre que se cuente con los espectros de respuesta (gráficas que muestran la relación entre respuesta máxima ante un temblor dado de sistemas de un grado de libertad y sus frecuencias naturales). Por lo tanto, es natural formular la valuación del riesgo sísmico y los criterios de diseño ingenieril en términos de ordenadas espectrales.

La aceleración y el desplazamiento máximos del terreno son buenos indicadores de las ordenadas de los espectros de respuesta correspondientes a frecuencias muy bajas y muy altas, respectivamente. A su vez, la velocidad máxima del terreno se correlaciona con las ordenadas espectrales correspondientes a frecuencias intermedias, aunque esta correlación es menos precisa que las anteriores. En consecuencia, el espectro de respuesta predicho para una magnitud M y distancia focal R dados, se obtiene usualmente en dos pasos, que consisten en estimar inicialmente la aceleración y velocidad máximas del terreno y posteriormente usando estos valores se predicen las ordenadas del espectro de respuesta.

El segundo paso de este proceso puede representarse por la operación $y_s = \alpha y_g$, en donde y_s es la ordenada del espectro de respuesta para una frecuencia y una fracción de amortiguamiento dadas, y_g es un valor (tal como aceleración o velocidad máximas del terreno) que puede ser tomado directamente del registro de un temblor dado. El valor de $\alpha = y_s/y_g$ es aleatorio. A su vez, para una magnitud y distancia focal y_g presenta incertidumbres, es decir, también es aleatorio; por lo tanto, y_s es aleatorio y su media y desviación estándar dependen de y_g y de α, así como del coeficiente de correlación entre ellas. Como se menciona posteriormente, y_g solo puede predecirse con un cierto grado de incertidumbre. El coeficiente de variación de y_s dados M y R puede ser menor que el de y_g solo si α y y_g están negativamente correlacionados, lo que ocurre con frecuencia; es decir, que en un rango de frecuencias intermedias los valores esperados de ordenadas espectrales para fracciones dadas de amortiguamiento pueden ser predichos en términos de magnitud y distancia focal con una incertidumbre menor o igual a la asociada a velocidades máximas predichas en el terreno. Para rangos de frecuencias muy cortos o muy largos las amplitudes máximas del movimiento del terreno se acercan a las ordenadas espectrales correspondientes y el margen de error tiende a ser el mismo en ambas.

2.3 Leyes de atenuación de la intensidad

Para valuar la contribución de fuentes sísmicas potenciales al riesgo sísmico en un sitio, se utilizan expresiones de atenuación de la intensidad, que relacionan a dicha variable con magnitud y distancia entre el sitio y la fuente. Dependiendo de las aplicaciones requeridas, la intensidad característica predicha puede expresarse de diferentes maneras, ya sea subjetivamente, como es el caso de intensidad Mercalli modi-

ficado; o bien una medida cuantitativa del movimiento del terreno o una combinación de estas.

Como se mencionó en la introducción de éste capítulo, la intensidad depende de varios parámetros, algunos de los cuales son difíciles de cuantificar; es por ello que suele estimarse en suelos con características de terreno firme o roca; para los fines que aquí se persiguen conviene tratarla en términos de velocidad y aceleración máximas del terreno. Cuando las isosistas (líneas que encierran sitios de igual intensidad) de un evento dado se trazan basados únicamente en intensidades observadas en sitios de condiciones homogeneas tales como terreno firme o suelo rocoso, presentan geometría gruesamente elíptica y la orientación de sus ejes está altamente correlacionada con la geología local o regional. Sin embargo, en muchas áreas del mundo, debido al insuficiente conocimiento de las características geotectónicas y a la limitada información en relación con el volumen donde la energía se libera en la fuente, la intensidad se predice en términos de expresiones simples que dependen únicamente de la magnitud y distancia entre el sitio y el foco instrumental.

Esteva y Villaverde (1973), basándose en aceleraciones reportadas por Hudson et al (1972, 1973), obtienen las siguientes expresiones para aceleración y velocidad máximas del terreno.

$$a/g = 5600\, e^{0.8M}/(R+40)^2 \qquad (2.1)$$

$$V = 32\, e^{M}/(R+25)^{1.7} \qquad (2.2)$$

en donde a es la aceleración máxima del terreno en cm/seg^2, g es la aceleración de la gravedad en cm/seg^2, R es la distancia entre el sitio en estudio y el foco ins-

trumental, M la magnitud Richter y V la velocidad máxima del terreno en cm/seg. La distribución de probabilidades del logaritmo natural del cociente de la intensidad observada entre la predicha es normal, con desviación stándard de 0.64 para aceleraciones y para velocidades de 0.74 (Esteva y Villaverde, 1973).

Las ecs 2.1 y 2.2 son productos de una función de R por una función de M. Esta forma es aceptable cuando las dimensiones de la fuente liberadora de energía son pequeñas comparadas con R, e inadecuada para fuentes sísmicas de dimensiones del orden de R.

La dependencia de la ecuación de error (distribución de probabilidades del cociente entre intensidades observadas y predichas) con respecto a M y R no ha sido analizada. Dado que las estimaciones de riesgo sísmico son muy sensibles a las expresiones de atenuación en el rango de cortas distancias focales y grandes magnitudes sísmicas, es necesario efectuar estudios más detallados para obtener la forma y los parámetros de expresiones que operen adecuadamente en cortas distancias, así como para valuar la influencia de R y M en la ecuación de error.

2.4 Proceso de generación de temblores

Diversas expresiones han sido propuestas para describir el proceso de generación de temblores en una fuente dada. Una de las más usadas es la debida a Gutemberg y Richter (1954); relaciona las magnitudes sísmicas con la frecuencia media de excedencia (ec 2.3)

$$\lambda = \alpha e^{-\beta M} \qquad (2.3)$$

En esta ecuación λ es el número medio de temblores con magnitud mayor que M, que ocurren en un volumen unitario en la unidad de tiempo, siendo α y β parámetros que dependen de las coordenadas del volumen unitario en estudio.

El parámetro α varía ampliamente de un sitio a otro, y β se encuentra dentro de un rango relativamente pequeño; esto puede apreciarse en el mapa de epifocos de la figura 2.1, y en la figura 2.2 que presenta las gráficas de las expresiones del tipo de la ec 2.3 obtenidas para varias macrozonas sísmicas de la tierra. La ec 2.3 implica una distribución de energía liberada por evento sísmico similar a la observada en experimentos de laboratorio consistentes en microfracturación de especímenes de diversos tipos de roca sujetos a esfuerzos gradualmente crecientes de compresión ó de deformaciones por flexión (Mogi, 1962; Scholz, 1968). El valor de β determinado en laboratorio es del mismo orden del que proviene de eventos sísmicos y se ha demostrado que depende de la heterogeneidad de los especímenes y de su habilidad para fluir localmente.

En la figura 2.2 se observa que para magnitudes muy altas la frecuencia predicha por la ec 2.3 es mayor que la que indican los catálogos de sismos. Rosenblueth (1969) demostró que β no puede ser menor que 3.46, pues de lo contrario la cantidad de energía liberada por unidad de tiempo sería infinito. Sin embargo, los valores estimados de β de la figura 2.2 son todos menores que 3.46, pero la evidencia estadística indica que para valores muy altos de M la curva logarítmica debe tener pendiente más pronunciada.

En vista de las objeciones mencionados, Esteva (1976) propone la expresión 2.4 para

representar la relación magnitud-recurrencia; dicho modelo se adopta en este trabajo.

$$\lambda = \lambda_L \, G^*(M) \qquad \text{para } M_L \leq M_u$$

$$\lambda = \lambda_L \qquad M < M_L \tag{2.4}$$

$$\lambda = 0 \qquad M > M_u$$

Aquí, M_L es la menor magnitud que contribuye significativamente al riesgo sísmico, M_u es la magnitud máxima posible cuyo foco puede encontrarse en el volumen unitario en estudio, y $G^*(M)$ es la distribución de probabilidades acumulada complementaria de magnitudes de eventos sísmicos tales que $M \geq M_L$. La forma de $G^*(M)$ adoptado en este trabajo se expresa en la ecuación siguiente,

$$G^*(M) = A_o + A_1 e^{-\beta M} - A_2 e^{-(\beta - \beta_1)M} \tag{2.5}$$

en donde

$$A_o = A \, \beta_1 \, e^{-\beta(M_u - M_L)}$$

$$A_1 = A \, (\beta - \beta_1) \, e^{\beta M_L}$$

$$A_2 = A \, \beta e^{-\beta_1 M_u + \beta M_L}$$

$$A = \left[\beta \left\{ 1 - e^{-\beta_1 (M_u - M_L)} \right\} - \beta_1 \left\{ 1 - e^{-\beta (M_u - M_L)} \right\} \right]^{-1}$$

Los parámetros de la ecs 2.5 hasta ahora no han sido estimados para ningún sitio en el país; ello requiere un estudio más amplio que el que se realiza en este trabajo.

2.5 Modelo estocástico de la sismicidad

Como se menciona en 2.1, las decisiones ingenieriles relacionadas con construccio-

nes en áreas sísmicas no deben basarse únicamente en la intensidad máxima posible en el sitio, sino en las probabilidades de excedencia de intensidades dadas en lapsos. Por ello es necesario expresar a la sismicidad en términos de la distribución de probabilidades de la intensidad máxima que puede ocurrir en el sitio durante lapsos dados.

Estas probabilidades dependen de lo siguiente:

a) Relaciones frecuencia-magnitud para volúmenes pequeños de la corteza terrestre.

b) Funciones de correlación estadística del proceso de generación de temblores en el tiempo y en el espacio.

Diversos investigadores han desarrollado modelos para describir la ocurrencia de temblores; muchos de ellos se basan en métodos clásicos de series temporales. Uno de los primeros procedimientos propuestos consiste en construir histogramas de tiempos de espera entre eventos sísmicos (Knopoff, 1964; Aki, 1963). Por razones prácticas, es frecuente adoptar la hipótesis de que la distribución de dichos tiempos de espera se representa adecuadamente mediante un proceso de Poisson. Se suele suponer, además, que la magnitud de cada evento es estocásticamente independiente de la historia previa, lo cual a su vez implica que la magnitud de cada sismo es la misma. Para una zona dada, el modelo de Poisson indica que la probabilidad de que ocurran N temblores con magnitud mayor que M en el intervalo de tiempo (0, t) es igual a

$$P_N = \left\{ (\nu_M t)^N \exp(-\nu_M t) \right\} / N! \qquad (2.6)$$

en donde ν_M es el número medio de temblores con magnitud mayor que M que ocurren en la zona en estudio en la unidad de tiempo. Si se toma N igual a cero en la ec 2.6, se obtiene que la distribución de probabilidades de la magnitud máxima durante el intervalo de tiempo t es igual a, $\exp(-\nu_M t)$. Si ν_M está dado por la ec 2.3, se obtiene la distribución de probabilidades extrema tipo I.

Es evidente que el modelo de Poisson presenta algunos inconvenientes, por ejemplo la implicación de que la distribución de probabilidades del tiempo de espera entre un evento y otro no se ve modificada por el tiempo transcurrido a partir del último evento, siendo que el estudio de la naturaleza del fenómeno físico sugiere que la energía de deformación se acumula gradualmente antes de liberarse súbitamente; esto implica que el valor esperado del tiempo de espera para el próximo evento debe decrecer a medida que el tiempo transcurre (Esteva, 1975). Los datos estadísticos muestran que la hipótesis de Poisson puede ser aceptable cuando se trata de sismos fuertes al estudiar una zona amplia de la corteza terrestre (Ben Menahen, 1960), lo que implica escasez de correlación entre la sismicidad de diferentes regiones; sin embargo, cuando se consideran volúmenes pequeños de la corteza terrestre, del orden de los que contribuyen significativamente al riesgo sísmico en un sitio, los datos contradicen frecuentemente el modelo de Poisson en vista del agrupamiento de temblores en el tiempo: el número observado de eventos sísmicos en lapsos cortos inmediatos a la ocurrencia de un sismo moderado o grande es significativamente mayor que el predicho por este modelo, debido a las réplicas. Dicho modelo también presenta incogruencias respecto al espacio (Tsuboi, 1958; Gajardo y Lomnitz, 1960), dada la sistemática correlación existente entre fuentes sísmicas y accidentes geológicos.

A pesar de los inconvenientes mencionados, debido a su simplicidad, el modelo de Poisson proveé una herramienta aceptable para la formulación de algunas decisiones de diseño sísmico, particularmente en el caso de que éste sea sensible solo a eventos con magnitudes que posean periodos de recurrencia muy grandes.

Esteva (1975) postula un modelo de sismicidad basado en procesos estocásticos del tipo de renovación los lapsos entre la ocurrencia de temblores sucesivos con magnitud mayor que un valor dado son variables aleatorias mutuamente independientes. Sea T cualquiera de dichos lapsos. Se supondrá que su densidad de probabilidades es de tipo gamma:

$$f_T(t) = \frac{\nu_M}{(k-1)!}(\nu_M t)^{k-1} \exp(-\nu_M t) \qquad (2.7)$$

en donde, ν_M y k son dos números positivos y a! indica el factorial de a. Se adopta esta familia de distribuciones debido a que puede representar una gran variedad de condiciones si se escogen adecuadamente los parámetros ν_M y k (Raiffa y Schlaifer, 1969); ν_M y k están relacionados con los primeros dos momentos de la densidad de probabilidades de T:

$$k = 1/V^2(t), \qquad \nu_M = k/E(t) \qquad (2.8)$$

en donde E significa esperanza y V coeficiente de variación.

La densidad de probabilidades del tiempo de espera T_1, del origen a la ocurrencia del primer evento, difiere de la ec 2.7, dado que el lapso transcurrido a partir del evento inmediato anterior es usualmente desconocido. Su distribución coincide con la del tiempo de supervivencia en un proceso de renovación para un valor arbitrario de t que tiende a infinito. Se demuestra (Parzen, 1962) que la correspondiente densidad

de probabilidad es

$$f_{T_1}(t) = \frac{1}{E(T)} \left\{1 - F_T(t)\right\} \qquad (2.9)$$

en donde $F_T(t)$ es la función de distribución (acumulada) del tiempo entre dos eventos sucesivos.

Este modelo es congruente con las conclusiones de Kelleher etal (1973) consistentes en la teoría de activación periódica de fuentes sísmicas. Dicha teoría es parcialmente probada por los resultados de análisis cualitativos de migración de actividad sísmica a través de algunas estructuras geológicas. Por ejemplo, en la costa sur de México, que es una de las regiones más activas en el mundo, se generan temblores superficiales de altas magnitudes probablemente por la interacción entre la masa continental y la placa oceánica subductiva de Cocos. Los datos sismológicos muestran tramos de actividad sísmica significativa durante el presente siglo, así como "Lagunas sísmicas", o zonas de muy baja actividad, y no se dispone de suficiente información previa. En estas "lagunas", la estimación de riesgo sísmico basada únicamente en intensidades observadas es baja; sin embargo, no existe evidencia de diferencias significativas en la estructura geológica de estas regiones respecto al resto de la costa, salvo algunas fallas geológicas transversales que dividen la formación continental en bloques. Basándose en consideraciones geofísicas podría asignarse un riesgo sísmico igual en todo el área. Con base en datos de sismicidad, Kelleher etal concluyen que la actividad migra de uno a otro tramo, de manera que los temblores fuertes tienden a ocurrir en las lagunas sísmicas.

En otras regiones se han observado fenómenos similares (Allen, 1969).

2.6 Empleo de diferentes tipos de información en la valuación de riesgo sísmico

Solo en casos excepcionales las relaciones magnitud-recurrencia para pequeños volúmenes de corteza terrestre y funciones de correlación del proceso de generación de temblores pueden definirse exclusivamente por análisis estadísticos basados en datos instrumentales. En muchos casos dicha información es insuficiente para este propósito y no siempre refleja la evidencia geológica. Debido a esto y a su relación con la sismicidad los márgenes de incertidumbre obtenidos resultan altos. Es por ello que conviene usar información de diferente naturaleza, analizar su incertidumbre y obtener conclusiones que sean congruentes con todas las piezas de información. Esteva (1970) propone un criterio probabilístico congruente con lo expuesto. Dicho criterio toma en cuenta los datos geotectónicos y los modelos conceptuales del proceso físico en cuestión: se formula un grupo de hipótesis alternativas sobre la función en estudio (magnitud-recurrencia, tiempo, y correlación espacial); a cada una de dichas hipótesis se asigna una probabilidad inicial; se introduce la información estadístico a fin de juzgar la bondad de las hipótesis hechas, con lo que se obtiene una distribución posterior de probabilidad. La información estadística contribuye a modificar la distribución de probabilidades de las hipótesis, dependiendo de su cantidad disponible y del grado de incertidumbre implícito en la distribución inicial de probabilidades. Es decir, si la evidencia geológica proporciona un grado de confianza suficiente para una hipótesis particular o un rango de hipótesis, la información estadística no modificará significativamente a las probabilidades iniciales. Si por lo contrario, se dispone de amplia y confiable información, ésta prácticamente determina la forma y los parámetros del modelo matemático seleccionado para representar la sismicidad.

El conocimiento de la estructura geológica puede usarse para formular la distribución inicial de probabilidades de la sismicidad. La distribución de probabilidades inicial de los parámetros del proceso de generación de temblores para volúmenes relativamente pequeños de la corteza terrestre que contribuye significativamente al riesgo sísmico de un sitio puede ser asignada por comparación con la sismicidad observada en amplias zonas de características geotectónicas similares o con zonas donde la cantidad y confiabilidad de la información estadística disponible proveé estimaciones aceptables de la relación frecuencia magnitud.

La estadística bayesiana proveé un procedimiento para inferencia probabilística, tal que toma en cuenta las probabilidades apriori asignadas a un grupo de modelos hipotéticos de fenómenos físicos dados, así como los datos estadísticos de eventos relacionados con dicho fenómeno. A diferencia de los métodos convencionales de inferencia estadística, los métodos bayesianos dan peso a medidas de probabilidad obtenidas de ejemplos o de otras fuentes; número, coordenadas y magnitud de temblores observados en lapsos dados sirven para afinar la validez probable de cada uno de los modelos alternativos de sismicidad que pueden postularse con base en la evidencia geológica, según se detalla a continuación.

Sea H_i, $i = 1, 2, \ldots n$, un grupo de hipótesis mutuamente exclusivas inherentes con un fenómeno dado que se conoce inperfectamente y sea A la evidencia observada en relación con dicho fenómeno. Antes de observar la evidencia A, se asignó una probabilidad inicial $p(H_i)$ a cada hipótesis. Si $p(A|H_i)$ es la probabilidad de que ocurra A en caso de que la hipótesis H_i fuese cierta, el teorema de Bayes (Raiffa y Schlaifer, 1968) establece que

$$p(H_i \mid A) = p(H_i) \frac{P(A \mid H_i)}{\sum_i p(H_i)\, p(A \mid H_i)} \qquad (2.10)$$

El primer miembro en esta ecuación es la probabilidad (posterior) de que la hipótesis H_i sea cierta, dada la evidencia observada A. En la valuación de riesgo sísmico, el teorema de Bayes puede ser usado para proveer distribuciones posteriores de probabilidad de $\lambda(M)$ y de su variación respecto a la profundidad en un área dada, así como la correspondiente a los parámetros que definen la forma de $\lambda(M)$, o sea, de la distribución de probabilidades condicional dada la ocurrencia de algún temblor. Para los propósitos de este trabajo, $\lambda(M)$ se toma como el producto de una función de tasa $\lambda_L = \lambda(M_L)$ por una función de forma $G^*(M,B)$, igual a la distribución de probabilidades condicional complementaria de magnitudes sísmicas mayores o iguales a M_L, en donde M_L es la magnitud menor del grupo de datos usado en la estimación, y B es el vector de parámetros (inciertos) $B_1, B_2, \ldots, B_r$, que definen la forma de $\lambda(M)$. Por ejemplo, si $\lambda(M)$ se toma de la ec 2.4, B es un vector de tres elementos: β, β_1 y M_u. La distribución de probabilidades inicial de la sismicidad se expresa en este caso mediante la densidad de probabilidades conjunta de λ_L y B: $F'(\lambda_L, B)$. La evidencia observada A puede ser expresada por las magnitudes de todos los temblores generados en una fuente dada durante un lapso dado. Por ejemplo, suponiendo que se observan N temblores en el lapso t y que sus magnitudes fueron $m_1, m_2, \ldots m_N$, la expresión de Boyes toma la forma

$$F''(\lambda_L, B \mid m_1, m_2, \ldots m_N;t) = F'(\lambda_L, B) \frac{p(m_1, m_2 \ldots m_N;t \mid \lambda_L, B)}{\iint p(m_1, m_2 \ldots m_N;t \mid l,b)\, F'(l,b)\, dl\, db} \qquad (2.11)$$

en donde $f''(\cdot)$ es la densidad de probabilidades posterior, l y b son variables mudas que pueden tomar todos los valores posibles de λ_L y B respectivamente.

La estimación de λ_L usualmente puede ser formulada de manera independiente para cada uno de los parámetros. La evidencia observada es entonces representada por N_L, el número de temblores con magnitud mayor que M_L que ocurren en el lapso t, y se obtiene la siguiente expresión como primer paso en la estimación de $\lambda(M)$

$$f''(\lambda_L \mid N_L;t) = f'(\lambda_L) \frac{p(N_L;t \mid \lambda_L)}{p(N_L;t \mid l)\, f'(l)\, dl} \qquad (2.12)$$

En el caso mas general consistirá en la determinación de la función conjunto de probabilidades bayesiana posterior de sus componentes, tomando las frecuencias relativas de magnitudes observadas como evidencia estadística. Entonces, si b_i, $i = 1, 2, \ldots, r$ son los valores adoptados para las componentes del vector B, y el evento A significa la ocurrencia de N temblores con magnitudes, $m_1, m_2, \ldots m_N$, la expresión 2.10 se convierte en

$$f''_B(b_1, b_2, \ldots, b_r \mid A) = \frac{f'_B(b_1, b_2, \ldots b_r)\, P(A \mid b_1, b_2, \ldots, b_r)}{\iiint \cdots \int f'_B(U_1, U_2, \ldots U_r)\, P(A \mid U_1, U_2, \ldots U_r) d_{u1}, d_{u2}, \ldots d_{ur}} \qquad (2.13)$$

en donde $P(A \mid U_1, U_2, \ldots, U_r)$ es proporcional a $\prod_{i=1}^{N} g(m_i \mid U_1, U_2, \ldots U_r)$

y $g(m) = -\frac{\partial G^*(m)}{\partial m}$.

En general no es posible obtener soluciones cerradas de la ec (2.13). Sin embargo

es posible estimar los primeros y segundos momentos de f'' mediante aproximaciones de primer orden (Benjamin and Cornell, 1970; Rosenblueth, 1975). Entonces el valor posterior de la esperanza de B_i está dado por $\int u f''_{B_i}(U)\, dU$, en donde $f''_{B_i}(U_i) = \int\int \cdots \int f'_B(U_1, U_2, \ldots U_r)\, dU_1\, dU_2 \ldots dU_n$ y la integral múltiple es de orden r-1.

Es decir

$$E''(B_i) = \frac{E'_B\{B_i\, P(A \mid B_1, B_2, \ldots B_r)\}}{E'_B\{P(A \mid B_1, B_2, \ldots B_r)\}} \tag{2.14}$$

en donde E' y E'' significan esperanza inicial y posterior respectivamente, y el subíndice B indica que la esperanza es tomada respecto a todos los componentes de B.

Y la esperanza de $\lambda(M)$

$$E''(\lambda(M)) = E''(\lambda_1)\, E''(G^*(M;B)) = E''(\lambda_1)\, \frac{E'_B(G^*(M;B)P(A \mid B_1, B_2, \ldots B_r))}{E'(P(A \mid B_1, B_2, \ldots B_r))} \tag{2.15}$$

En algunos casos solo se requiere la esperanza posterior de $\lambda(M)$ para describir la sismicidad. Sin embargo frecuentemente es necesario conocer su incertidumbre. Por ejemplo, se ha obtenido la probabilidad de excedencia de una magnitud dada en lapsos dados como la esperanza de las probabilidades correspondientes dadas todas las hipótesis alternativas relacionadas con $\lambda(M)$. En particular, es de interés la probabilidad marginal de que no ocurran eventos en el intervalo t.

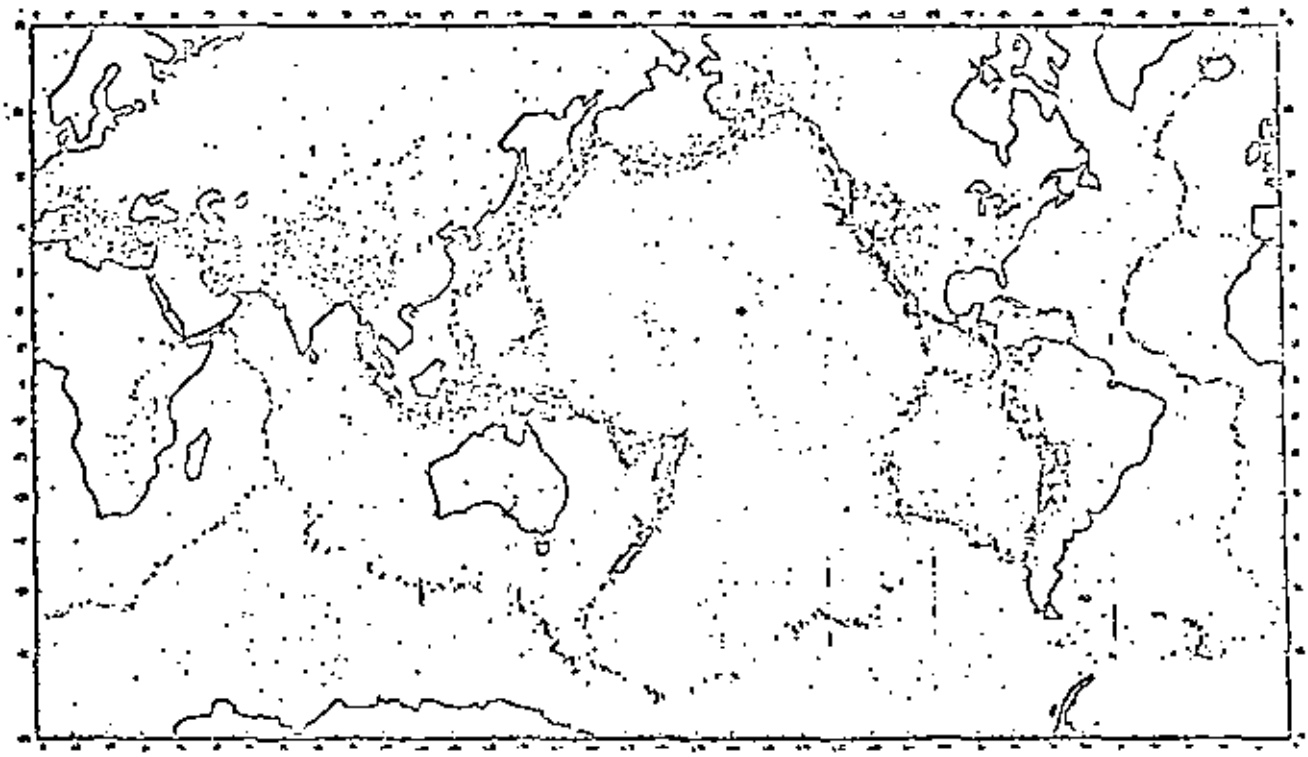

Fig 2.1 Mapa de epifocos en el lapso 1961-1967
(Newmark y Rosenblueth, 1976)

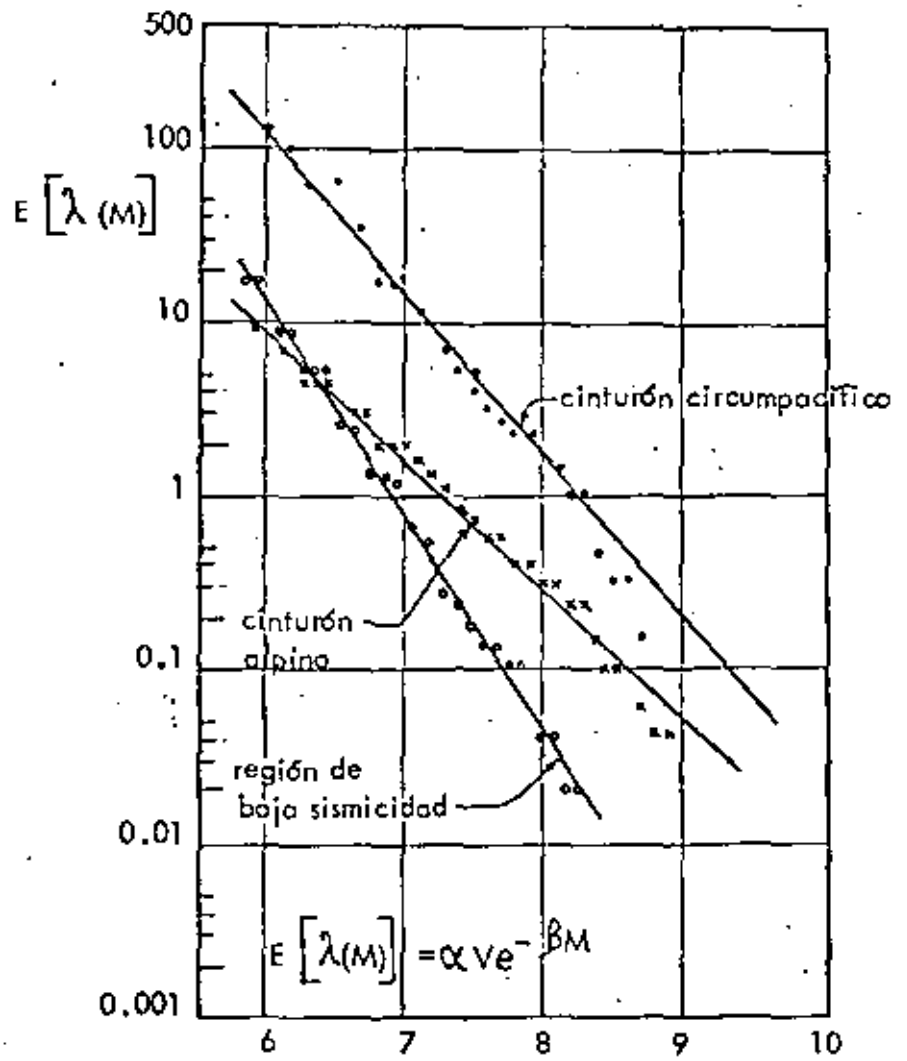

Región	β
región de baja sismicidad	2.16
cinturón alpino	1.70
cinturón circumpacífico	2.88

Fig 2.2 Sismicidad de las macrozonas

(Esteva, 1968)

IX CURSO INTERNACIONAL DE INGENIERIA SISMICA

ANALISIS DE RIESGO SISMICO

RIESGO SISMICO Y DECISIONES DE DISEÑO SISMICO

DR. LUIS ESTEVA

SEISMIC RISK AND SEISMIC DESIGN DECISIONS

by

Luis Esteva

I. INTRODUCTION

Earthquake resistant design aims at obtaining an optimum balance between expected benefits and costs of structures built in seismic areas. Once the overall dimensions of a project and its main architectural and functional features are defined, the expected benefits per unit time may be estimated for any time period during which the construction is assumed to be in operation. The cost term includes initial and maintenance costs as well as costs due to damage or failure of the whole system or of portions of it.

Qualitatively, attainment of the above goals implies review of each possible alternative design in regard to its capacity to provide adequate safety against collapse during exceptionally intense earthquakes, and protection against material loss during motions of an intensity that occurs at the site with relatively short return periods. Design recommendations for some particular structures establish two corresponding levels of intensity, which are often designated as the largest possible and the largest probable intensities, respectively. However, it will be shown that these two intensities cannot be taken as independent of the characteristics of the particular structure being designed and of the possible consequences of its failure.

The notion of designing for a double level of excitation under prescribed performance conditions for each of them applies directly to systems that may be assumed to have only two significant failure modes, provided failure in one of the modes takes place consistently at lower intensities than in the other. In complex systems, where each component may fail at a different intensity,* drastic assumptions have to be made

---

* Throughout this paper, the term intensity is used to designate any parameter of the ground motion at a site that may be significant in the estimation of structural response. Hence, the term may apply to quantities so different as modified Mercalli intensity, peak ground velocity, or spectral response for a given period and damping.

the latter case the damage undergone by a structure of known characteristics may be directly related to the maximum amplitude of structural response. For a given motion, this maximum amplitude may in turn be obtained from the ordinate of the response spectrum of the motion, when the characteristics (natural period, damping, load-deformation curve) of the structure are taken into account.

In seismic design it does not suffice to compute the structural response to a given motion: it is necessary to predict its statistical distribution for the earthquakes that may occur in the future. The uncertainty in this prediction stems from two main sources, respectively associated to the maximum intensity to be expected during a given time period, and to the peak value of the structural response for a given intensity.

From the foregoing it is concluded that any rational formulation of earthquake resistant design decisions must give explicit attention to the following points:

a) Statistical prediction of structural responses to earthquakes defined by one or several simple parameters. These parameters may include direct instrumental data, such as peak ground acceleration, velocity or displacement; subjective data, such as intensity in the modified Mercalli scale, or even such indirect data as magnitude and distance to the hypocenter.

b) Uncertainties associated to the properties of actual structures: mass, stiffness, damping, strength, deterioration.

c) Statistical prediction of the parameters mentioned in (a). This is based on the stock of information that will be designated as <u>seismicity</u> in this paper.

The degree of uncertainty associated with the description of seismicity is usually much greater than that related to the two other groups of parameters. This means that in many practical problems the properties of a structure as well as its response to an earthquake of

a given intensity, may be treated as deterministic quantities, while the stochastic nature of the maximum intensity has to be explicitly recognized.

This paper presents a simple model of the optimization process implicit in the selection of design earthquakes. Then it deals with the manners in which seismic risk may be defined and with the ways in which the available seismological information may be assimilated and then reported in a form that suits better the needs of the engineer. Finally, a discussion is presented of the difficulties that may arise in the evaluation of seismic risk in areas where statistical data are scanty, and of the methods that have been developed for dealing with such cases.

II. EARTHQUAKE RESISTANT DESIGN DECISIONS

2.1 Stochastic Process Model of Seismicity. Seismic design decisions consider initial costs of structures, the benefits that may be obtained while they are in operation, and the costs of damage caused by earthquakes. The last term depends on the seismic history that will take place at the site after the construction of the structure is initiated. Since the seismic history is greatly uncertain, it will be treated as a stochastic process.

The occurrence of earthquakes whose intensity at a site is greater than a given value will be represented by a homogeneous Poisson process.[2] It has been shown[5] that the number of earthquakes that generate in a given zone of the earth's crust and that have magnitudes in excess of a given value is not strictly a Poisson process, even when fore- and aftershocks are discarded, and even when only magnitudes above six are considered. The same conclusion may be thought to apply, perhaps in a weaker manner, to the process of interest to us. However, the hypothesis will be retained on the grounds of its simplicity, and of the facts that it is probably more adequate for the highest intensities, and

that seismic design decisions are usually more sensitive to the mean number of events than to their distribution in time.

Let $N_y(t)$ designate the number of earthquakes that may produce an intensity greater than y at a given site, during time interval t. Let $\nu(y)$ represent the expected value of $N_y(t)$ per unit time. From the assumption of Poisson process, the probability mass function[3] of $N_y(t)$ is

$$P_r\{N_y(t) = n\} = \frac{e^{-\nu(y)t}(\nu(y)t)^n}{n!}, \qquad (1)$$

The distribution of the waiting time between successive events will be exponential, and its expected value, known as the return period, will be equal to $[\nu(y)]^{-1}$.

2.2 Utilities in Seismic Design Decisions. Utilities in engineering decisions are made up of initial costs, benefits, and costs of damage or failure. In seismic design problems, at least the last two terms correspond to contributions that are to be generated in the future. The scale of values of most decision makers is such that they are more sensitive to utilities that may be obtained in the near future than to those that may arise long time after the decision is made. In order to be able to compare utilities that may be obtained at different instants, they have to be actualized, that is, converted from their nominal value to a value that the decision maker would take as equivalent if it were obtained at the moment of making the decision. If a certain amount of money C_o is invested at a compound interest rate γ, and if capitalization is assumed to take place in a continuous manner with time, the sum of initial capital plus interests at time t, C_t, will be equal to $C_o e^{\gamma t}$. Conversely, a certain nominal utility $u(t)$ produced at instant t will have an actualized value, or equivalent value at instant 0, equal to $u(t)e^{-\gamma t}$. From the standpoint of the decision maker, γ would be chosen so as to account for the nominal interest rate plus the decrease in the real value of money.

In seismic design problems the decision maker is frequently faced with the possible outcome of events whose utility cannot be easily put in terms of money, either because it involves values that cannot be expressed in monetary units, or because the problem is not linear in them. The basic problem here is that of developing a utility scale that consistently reflects the preferences of the decision maker. Some methods have been suggested to help in the attainment of the required consistency,[4] but perhaps the formulation of utility scales has still to rely greatly on a comparison with those that have been implicitly and intuitively considered in other facets of human activity.

It will be assumed in the following that it is possible to assign a utility value to every given form of structural behavior. At the moment, the attention will be focused on the case where the behavior may be described by means of a two-state model (fails, does not fail). The cost of failure will be taken as D_o. If the structure is assumed to possess a deterministically defined strength, y_s, expressed in the same units as the earthquake intensity, its probability of failure during time interval t will be equal to the probability that at least one motion of intensity greater than y_s occurs during that time interval. According to Eq. (1), this probability equals

$$P_f(t|y_s) = 1 - e^{-\nu(y_s)t} \qquad (2)$$

The event whose probability is given by Eq. (2) is equivalent to the event that the waiting time to the occurrence of failure is shorter than t. Hence, Eq. (2) provides also the value of the cumulative distribution function of the time to failure; when it is differentiated with respect to t it yields the corresponding probability density function:

$$\text{Pr[failure occurs during time interval } t,t+dt] = \nu(y_s)e^{-\nu(y_s)t}\,dt \qquad (3)$$

In many design decisions it is convenient to assume that a new structure, identical to the original, will be built every time that a

failure takes place. In this case, the significant information is included in $\nu(y_s)$, the mean number of failures per unit time. The expected cost of the damage that may occur during time interval t, t + dt will thus be equal to $D_0\nu(y_s)dt$, its actualized value will be $D_0\nu(y_s)e^{-\gamma t}dt$, and the expected actualized cost of all the failures that may occur since the original structure is built may be obtained as the corresponding integral:

$$E[D] = \int_0^\infty D_0\nu(y_s)e^{-\gamma t}\,dt = \frac{D_0\nu(y_s)}{\gamma} \tag{4}$$

The expected actualized benefits that derive from the use of a structure may be expressed as:

$$E[B] = \int_0^\infty b(t)L(t)e^{-\gamma t}\,dt \tag{5}$$

where b(t) is the expected value of benefits per unit time, and L(t) is the probability that the structure will be in operation at time t. If the model that assumes reconstruction after each failure is adopted, if the expected cost of benefits per unit time is constant, and if the benefits that are not obtained while the structure is being reconstructed are included in D_0, the nominal cost of failure, Eq.(5) leads to the following:

$$E[B] = \frac{b}{\gamma} \tag{6}$$

Expressions of utility terms for different reconstruction or reinvestment policies may be derived in similar manner.

2.3 Formulation of the Decision Problem. It will be assumed that decisions will be made in accordance with the criterion of maximum expected utility. Expected utility will be taken as the algebraic sum of the expected values of all actualized benefits and costs:

$$E[U] = E[B] - E[C] - E[D] \qquad (7)$$

In this equation, E[B] and E[D] are computed taking into account the concepts of section 2.2. The same ideas apply to E[C], the expected actualized initial cost. This must include the cost of construction, as well as of design and studies. In many cases the corresponding expenditures are made during a short, practically deterministic period of time, so that actualization is irrelevant.

2.4 Selection of Optimum Design Intensity in Simple Systems. Consider a simple structure that is rebuilt after each failure. If the utility terms of Eqs. (4) and (6) are substituted into Eq. (7), the following expression is obtained:

$$E[U] = \frac{b}{\gamma} - C - \frac{\nu(y_s)}{\gamma} D_o \qquad (8)$$

here, the expected initial cost has been substituted with a deterministic estimate of that variable.

Differentiating Eq. (8), and equating to zero leads to:

$$\frac{dC}{dy_s} = -\frac{D_o}{\gamma} \frac{d\nu(y_s)}{dy_s} \qquad (9)$$

Solution of this equation for y_s will lead to the optimum value of the required structural strength. It is clear from this example that the design intensity does depend not only on the seismicity parameters, but also on the rate of cost increase with respect to design intensity and on the nominal cost of failure.

Example. Assume a situation to which Eq. (9) applies. Assume also that the initial cost is related to the design intensity as follows:

$$C = A_o + A_1 y_s^n \qquad (10)$$

and that the return periods that correspond to given intensities may be obtained from the following equation:

$$1/T_y = \nu(y) = Ky^{-r} \qquad (11)$$

In Eq. (10), A_0 is the cost that the structure would have if it were not designed to resist earthquakes. From Eqs. (9), (10) and (11), one obtains:

$$nA_1 y_s^{n-1} = \frac{rKD_0}{\gamma} y_s^{-r-1}$$

and hence,

$$y_s = \left[\frac{rKD_0}{n\gamma A_1}\right]^{\frac{1}{r+n}} \qquad (12)$$

The value of the design intensity was computed by means of Eq. (12) for the cases listed in Table 1. In that Table y_s is assumed to be measured in terms of the peak ground acceleration expressed as a fraction of gravity. Seismicity of station 1 may be considered as low, while that at station 2 is very high. Structures 1 and 2 differ only in the relative importance of the consequences of their failure. Table 2 shows the results obtained by applying Eq. (12). It is clear that the design intensity grows with the seismicity and with the consequences of failure. According to Eq. (12) it should decrease with increasing A, which is a measure of the rate of increase of initial cost with respect to design intensity.

The last line of Table 2 shows that structures built in areas of high seismicity have to be designed for motions having shorter return periods than those corresponding to the design intensities that must be adopted in areas of lower seismicity. Also, the fact that the last two columns show very short return periods points out the possible situation in which the optimum solution might be not to build the structure at the selected site.

2.5 Systems Designed for Two Levels of Excitation. Consider a two-component system, as shown in Fig. 1, that is made up of a main structural frame (subsystem 1) and a collection of non-structural elements (subsystem 2). Subsystem 1 will be designed to resist intensity y_1 without failure. For any given intensity, the excitation acting on subsystem 2 depends on the properties of subsystem 1. Under some conditions (for instance when subsystem 1 is assumed to be linear and its period and damping are fixed) the action on subsystem 2 may be taken as depending only on the intensity. If this assumption is kept, it is possible to define an intensity y_2 at which subsystem 2 fails. The problem now is how to determine y_1 and y_2 considered as the design variables.

Failure of subsystem 2 gives place to damage D_2, which is assumed to include direct material losses, costs of repair, or costs of stopping operation of an industrial or power plant. Damage D_1 is produced by collapse of the main structural frame. The cost of each subsystem may be related to its design strength as follows:

$$C_1 = A_{01} + A_{11} y_1^{n_1}, \quad C_2 = A_{02} + A_{12} y_2^{n_2} \tag{13}$$

The expected utility of the system would be

$$E[U] = \frac{b}{r} - (A_{01} + A_{02}) - (A_{11} y_1^{n_1} - A_{12} y_2^{n_2}) - \frac{D_1 v(y_1)}{r} - \frac{D_2}{r}[v(y_2) - v(y_1)] \tag{14}$$

Differentiation with respect to each design intensity leads to a system of uncoupled equations:

$$n_1 A_{11} y_1^{n_1 - 1} + \frac{D_1 - D_2}{r} \frac{dv(y_1)}{dy} = 0 \tag{15}$$

$$n_2 A_{12} y_2^{n_2 - 1} + \frac{D_2}{r} \frac{dv(y_2)}{dy} = 0 \tag{16}$$

If the return periods are supposed to be given by Eq. (11), the following design intensities are obtained,

$$y_1 = \left[\frac{r}{n_1}\,\frac{(D_1 - D_2)K}{\nu A_{11}}\right]^{\frac{1}{n_1 + r}} \tag{17}$$

$$y_2 = \left[\frac{r}{n_2}\,\frac{D_2 K}{\nu A_{12}}\right]^{\frac{1}{n_2 + r}} \tag{18}$$

where y_2 must not be taken greater than y_1.

2.6 Additional Comments on the Selection of Design Parameters. The equations derived in the former examples may be easily generalized to be applied to cases when several non-structural subsystems are attached to the main frame, provided the response of every subsystem is independent of the design parameters of the structure, and provided also that collapse of the latter does not occur prematurely before failure of any non-structural subsystem. For deterministic structures this condition is easily satisfied if the restriction $y_2 \leq y_1$ is enforced. For systems having uncertain properties, it is usually the case that the consequences of damage D_1 are much greater than those associated with any other possible level of damage. Hence, the nominal design intensity for subsystem 1 is much greater than that for any other subsystem, the probability of premature collapse will be very small, and equations similar to (17) and (18) will apply.

More general models of system behavior may be considered, to account for interaction between the various components, for the possibility of multiple levels of damage on each component, and for the random nature of their mechanical properties.[1]

III. REGIONAL AND LOCAL SEISMICITY

3.1 Definitions. Local seismicity may be defined in terms of the mean value of the amount of energy dissipated per unit volume and per unit time and of the proportion in which that energy is divided among earthquakes of different magnitudes. This simplified description is sufficient once it is assured that the number of earthquakes whose magnitude exceeds a given value may be represented by a Poisson process and that occurrence of earthquakes in any two volumes of the earth's crust are independent processes.

Regional seismicity may be defined at a site in terms of the return periods that correspond to given intensities. Different parameters associated with the ground motion are contemplated in this paper as possible measures of intensity. Correspondingly, various possible representations of regional seismicity are feasible. Since different kinds of structures may be sensitive to different parameters of the ground motion (for instance, rigid structures are sensitive to peak ground acceleration, while structures having moderate natural periods are more sensitive to peak ground velocity), some of the representations of regional seismicity may be not alternate, but complementary, pieces of information.

3.2 Evaluation of Seismic Risk. Seismic design decisions were formulated above under the assumption that it is possible to predict statistically the values of the ground motion parameters that are relevant to structural behavior. Spectral ordinates that correspond to different periods, damping values and yield levels, are the most significant among those parameters. Only in exceptional cases do the available instrumental data suffice to quantitatively describe ground motions at the site. Hence, the statistical prediction of spectral ordinates cannot be exclusively based on the analysis of response spectra computed from local records, and other sources of data have to be used.

For many locations, statistical information is not available even with regard to relatively rough data, such as subjectively based intensities or as peak ground accelerations during earthquakes which occurred during time periods of at least several tens of years.

Regional seismicity may be inferred from data of local seismicity, provided they are available or may be estimated for the regions of the earth's crust near the station of interest. If this procedure is adopted, use has to be made of frequency-magnitude expressions as well as of correlations between spectral ordinates and maximum absolute values of ground acceleration, velocity, and displacement, and also between these and earthquake magnitude and focal distance.

The attention will now be turned to the generation of regional seismicity models when local seismicity estimates are assured to be available, while the problems related to evaluation of local seismicity will be deferred to the last section of the paper.

3.3 Local Seismicity. Figure 2 shows the earth divided into three areas according to their general seismic characteristics: the Circum-Pacific Belt, the Alpine Belt, and the less active area. Figures 3-5 show mean annual numbers of earthquakes occurring in each region. The plotted data were obtained from Reference 6, which reports coordinates, focal depth, and magnitude, of the largest shocks which occurred since the beginning of the century. According to the authors, the collection is complete for all the motions with magnitude greater than 5.9 occurring from 1932 to 1934, for $M \geq 7.0$ in the interval 1918 - 1952, and for $M > 7.75$ in the interval 1904 - 1918. The empirical equations adjusted correspond to the form previously suggested by Gutenberg and Richter:[6,7]

$$\nu(M) = \alpha e^{-\beta M} \qquad (19)$$

This equation may be objected to on the grounds that it predicts too large frequencies for magnitudes greater than 8. Besides, according to Richter's relation between magnitude and energy, Eq. (19) leads to infinite amounts of energy liberated per unit time by seismic activity if β is not greater than 1.5 log 10 = 3.45, while empirical data justify β values smaller than 3. Figure 3 shows the bad fit of Eq. (19) to the data for $M \geq 8$. Even if an expression of this type were valid for the Circum-Pacific Belt, for instance, it would not be true for a smaller region contained in it, because the addition of terms similar to the second member of Eq. (19) does not give place to a function of the same form, unless β is the same in all additive terms. Despite these objections, the equation will be used to express local seismicity of the small volumes of the earth's crust that may contribute significantly to the regional seismicity at a site. It will be shown later that even when dealing with intensities that correspond to very long return periods the greatest contribution to the seismic risk comes from the probability of having moderate shocks occurring at short distances. Hence, even major variations in the ordinates of the magnitude-frequency curve lead to relatively unimportant changes in the intensity-frequency curve.

Some empirical expressions suggested to represent the frequency of earthquakes of different magnitudes in California assign a null value to the probability of occurrence of earthquakes with magnitudes in excess of a certain upper bound. There has been some argument in regard to the value of such an upper bound in given areas. The fact is that it seems to be larger than what is required to produce catastrophic effects, and that most seismic design decisions are not particularly sensitive to it.

3.4 Correlations between Earthquake Properties. The scope of this paper will be limited to earthquakes of moderate duration (several dozen seconds) recorded on soils of intermediate properties, when focal distances are shorter than 600 km. The accelerograms of such motions are rather chaotic and justify the development of

theoretical studies treating earthquakes as stochastic processes. As a result of such studies, it has been possible to establish correlations between the amplitude of ground motion (maximum absolute values of ground acceleration, velocity or displacement) and the expected ordinates of the response spectra, as well as the probability distribution of maximum spectral ordinates divided by the expectation of their undamped values.[P] This matter is treated in another paper in this seminar.[9]

Prediction of spectral ordinates by the method suggested in the previous paragraphs requires knowledge of maximum absolute values of ground acceleration, velocity and displacement, or their computation, in terms of magnitude and focal distance.* Eqs. 20 and 21 serve that purpose for peak ground acceleration and velocity, respectively.**

$$\ddot{s} = 1230\, e^{0.8M}\, (R + 25)^{-2} \tag{20}$$

$$v = 15\, e^{M}\, (R + 0.17\, e^{0.59M})^{-1.7} \tag{21}$$

Here, accelerations and velocities are expressed in cm/sec.^{2} and cm/sec., respectively, M is the earthquake magnitude, and R is the hypocentral distance in kilometers.

Figures 6 and 7 show the data from which Eqs. (20) and (21) were derived. The data were obtained mainly from Refs. 10 and 11. In the derivation of Eq. (21) the additional condition was imposed that v tends to 300 cm/sec. when R approaches zero, regardless of the magnitude value. The great dispersion displayed in these figures may be attributed to the large number of variables that affect the data: local

---

* These are not the only significant quantities. A more refined study might decrease the dispersion in the correlations, at the expense of considerably wider analysis of statistical data.

** Eqs. (20) and (21) as well as Figs. 6 - 9, constitute improved versions of the material recently presented in Ref. 13.

ground conditions, nature of geologic formations crossed by seismic waves, shock mechanism, and many others. In particular, the variability due to the nature of local ground properties has been partly eliminated by restricting the scope of these studies to sites with intermediate soil comparable to a stiff clay or a compact conglomerate.* Even so the dispersion is significant, and hence it becomes necessary to allow for it in the evaluation of seismic risk.

Observed and computed values of a and v (maximum ground acceleration and velocity) were analyzed, and their ratios represented on normal probability paper following Gumbel's method[12] (Figs. 8 and 9). Distributions composed of segments of the log normal family were adjusted to each set of data, in order to facilitate further computations. Standard deviations of $\ln (a/a_c)$ and $\ln (v/v_c)$ were found to be 1.2 and 0.84, respectively. Here, subscript c stands for computed and ln means natural logarithm.

3.5 Predicted Distribution of Intensities at a Site. Starting from the knowledge of local seismicity of the various neighboring earthquake sources, the distribution of intensities at a station can be predicted using Eqs. (20) or (21) or similar expressions. If no allowance is made for the dispersion in these correlations, the model arrived at will correspond to computed intensities, while proper account of the uncertainties involved will lead to the predicted distribution of actual intensities.

Let $N_c(y,t)$ and $N(y,t)$ be the numbers of earthquakes occurring during time interval t, and having computed and actual intensities, respectively, greater than y at the site of interest. Let ν_c and ν be the corresponding mean numbers per unit time. Suppose a number of sources near the station are identified, and their local seismicities are described by $\lambda(M)$. These are functions of position, and represent the

*This is still a very crude manner of restricting the analysis to a certain type of soil, but it had to be adopted in view of the lack of better descriptions of local ground conditions.

mean number of earthquakes, occurring per unit time and per unit volume, whose magnitude is greater than M. Let M(y,R) be the magnitude that gives place to computed intensity y at distance R. If earthquake occurrence at any elementary source may be represented by a Poisson process independent from the corresponding processes developing at all other sources, then $N_c(y,t)$ will be represented by a Poisson process. Its mean rate of occurrence is given by the following equation:

$$\nu_c(y) = \int_V \lambda(M(y,R))\, dv . \qquad (22)$$

This integral must be evaluated over all the potential sources of seismic risk at the station. If $\lambda(M)$ is assumed to be constant, regardless of position, and if it is taken as proportional to $e^{-\beta M}$ (see Eq. (19)), then $\nu_c(y)$ adopts the following form:

$$\boxed{\nu_c(y) = K_c y^{-r}} \qquad (23)$$

This form may provide an approximate representation of other frequent cases.

Reference 15 contains a set of graphs with the value of the integral in Eq. (22), under several assumptions, concerning the shape and location of the seismic sources with respect to the station of interest.

3.6 Uncertainty in Magnitude-Intensity-Distance Correlations. Figures 8 and 9 contain the implicit assumption that the distribution of Y/Y_c (actual and computed intensities) does not depend on Y_c. Hence, for any event of the process $N_c(\cdot,t)$ it is possible to compute the probability that $Y \geq y$, and $\nu(y)$ may be computed from $\nu_c(y)$ as follows:

$$\nu(y) = \int_0^\infty -\frac{d}{d\eta}\, \nu_c(\eta)\, P[Y > y \mid Y_c > \eta]\, d\eta \qquad (24)$$

Derivation of this equation is based on the property that whenever each event of a Poisson process is such that it may give place to a new

event with probability p, then the process of the new events will also be of the Poisson type, its mean rate of occurrence being that of the original process multiplied by p. The probability term in the integral of Eq. (24) is computed from the distributions in Figs. 8 and 9. If G(·) is used to designate the cumulative distribution function of Y/Y_c, and if Eq. (23) is adopted to represent ν_c, Eq. (25) is obtained for ν:

$$\nu(y) = \nu_c(y) r \int_0^\infty z^{-r-1}[1-G(1/z)]dz \qquad (25)$$

Alternatively, the ratio y/y_c of actual to computed intensities having equal return periods may be obtained.

$$y/y_c = (r \int_0^\infty z^{-r-1}[1-G(1/z)]dz)^{1/r} \qquad (26)$$

Under the present assumption this ratio depends strongly on r, but not on either y or y_c. It is presented in Figs. 10 and 11 for the cases of maximum ground acceleration and velocity, respectively. Further application of Eqs. (25) and (26) are possible for computing ν for excitations expressed in a different manner, such as by means of spectral ordinates, provided their distributions may be expressed in terms of the amplitude of the ground motion.[14]

Example. Suppose that evaluation of seismic risk is required for the site shown in Fig. 12.* The situation is hypothetical, but the numbers used were based on a study of an actual site made by a practicing seismologist. It is assumed to be located in rock, at distances of 140 km and 59 km, respectively, from two vertical faults. These are the only significant sources of seismicity in the vicinity of the site. Focal depths are 20 km and 50 km for motions generating at faults 1 and 2, respectively. Local seismicity of each source is defined in terms of a value of $\nu(4.5)$, the mean annual number of earthquakes with magnitudes greater than 4.5 generated along the whole fault. Frequency-

* This example was worked out by Professor C. Allin Cornell

magnitude curves were assumed to be of the form of Eq. (19), but subjected to the additional condition that $\nu(M)$ be null for $M \geq 7.25$ and for $M \geq 6.75$ at faults 1 and 2, respectively. In other words, in the seismologist's judgement history, fault lengths, and experience suggest that no greater magnitude can be generated by these faults. Values of all the parameters defining local seismicity are shown in Fig. 12. Total seismicity along each fault was assumed to be uniformly distributed throughout. Hence, a value of $\lambda(M)$, expressed in terms of unit length of fault, was obtained for each source. Eq. (22) was then applied separately to each fault, in order to obtain its contribution to seismic risk at the site. In practice available curves reduce this calculation to a simple table of slide rule calculations.[15,17] The results are shown in Fig. 13. Broken lines represent the separate contribution of each fault to seismic risk in terms of computed intensities (peak ground accelerations or velocities). The full line represents the total effect. Clearly, more than 90 percent of the total risk comes from the contribution of fault 1, although the influence of the larger, more active (but more distant) fault 2 is somewhat larger in the case of velocity than acceleration.

Figure 13 was prepared under the assumption that magnitudes, focal distances and intensities may be related in a deterministic manner. As explained before, the net result of taking into account the dispersion in the correlations between these variables is that the computed intensities that correspond to a given return period have to be multiplied by a factor greater than 1, in order to obtain the actual values that correspond to the same return period. The corrective factors shown on Figs. 10 and 11 would not exactly apply to the problem being considered, because they start from the assumption that y_c may be expressed as Ky^{-r}, which is not the present case. However, if approximate values of an equivalent r are adopted, corrective factors y/y_c of 4 and 2 are obtained for acceleration and velocity, respectively. This means, for instance, that peak ground acceleration that corresponds to a return period of 50 years should be taken equal to 0.025 g (taken from Fig. 13) multiplied by 4, that is, 0.10 g.

IV. UNCERTAINTY IN SEISMICITY MODELS

4.1 Nature and Extent of Information Used in the Derivation of Seismicity Models. Strong motion records constitute the most desirable source of information in the studies of seismic risk for engineering design decisions. In the absence of such data, use of subjective intensities, or of even more indirect quantities, such as magnitude and focal distance, may be considered acceptable substitutes. Evaluation of local seismicity still offers serious difficulties: seismic risk at a site is in practice obtained from the frequency, magnitude, and focal coordinates of earthquakes that may originate in regions of relatively small dimensions, of the order of 600 to 800 km in diameter, but statistical data often do not suffice to evaluate local seismicity throughout such regions. It would not be sound to make seismic design decisions only or mainly on the basis of statistical data when this information is as scanty as it is in many areas of moderate or low seismicity, or as it is when the analysis is concerned with shocks of exceptionally high magnitudes. This comment applies particularly strongly to the situation where attempts are made to predict for a given zone the magnitude that would correspond to a return period of several thousand years (which is likely to be the recommended value for a nuclear reactor, for instance) from only the data recorded in the same area for a period of at most several centuries. Use has to be made of every available piece of information, regardless of how incomplete it may be. Engineering judgement has played, and will continue to play, even in the frame of modern analytical formulations of design, an important role in interpreting data other than statistical, or in extending or adapting to the region of interest the conclusions derived from other, better studied, regions of similar geotectonic properties. Formal manipulation of information of different nature, including statistical data, is accomplished through the use of Bayesian statistics, as described below.

Sources of significant information may be grouped as follows:
a) Related to local seismicity. Some are of geophysical nature, such as geotectonic features, studies of regional strain and of energy available for sudden release; others are of statistical nature, such as mag-

nitude, focal coordinates, and energy released by earthquakes in different regions of the earth. They are to be complemented by conclusions derived from similarity with other physical phenomena and by qualitative descriptions of earthquake history over long time periods.

b) Related to regional seismicity. These include all information on frequency and intensity at a site. The latter variable may be expressed in subjective or nearly qualitative terms, such as the modified Mercalli scale, or it may include more quantitative descriptions, ranging from simple measures of earthquake intensity, such as peak ground accelerations and velocities, to spectral ordinates or detailed strong motion records. (See, for example, the paper at this seminar by Professor Aries.)

4.2 Bayes' Theorem. Suppose a decision maker had formulated a collection of hypotheses that he would consider as alternate representations of an imperfectly known phenomenon. Suppose further that he had used any information or intuitive idea he might have about that phenomenon, in order to assign to each hypothesis a probability of being true. This probability distribution would express his degree of belief in the various alternative hypotheses. If he makes some experiment that will allow him to observe a new outcome of the phenomenon, he should be willing to study how the new piece of evidence should modify his previous belief. He may accomplish this through use of Bayes' theorem.

Let H_i, $i = 1, \ldots, n$ be a set of mutually exclusive hypotheses, $P(H_i)$ their associated initial or a priori probabilities of being true, and A an event that may occur in combination with any one of the n hypotheses. Let $P(A|H_i)$ be the conditional probability of occurrence of A in case H_i were true. From the fundamental law of conditional probability, the following equation is obtained.

$$P(H_i|A) = \frac{P(H_i)P(A|H_i)}{P(A)} = \frac{P(H_i)P(A|H_i)}{\sum_j P(H_j)P(A|H_j)} \qquad (27)$$

This is the analytical expression of Bayes' theorem. In it, $P(H_i|A)$ is a modified, or posterior, probability of hypothesis H_i being true, once event A (statistical observation) is known to have occurred.

Severe criticism has been made of the use of Bayes' theorem, on the grounds of the apparent arbitrariness involved in choosing the prior distribution. A careful study of the methods used in classical statistics will show that they contain concealed assumptions equivalent to arbitrary prior distributions. It must be understood that Bayes' theorem is not merely a substitute for statistical data. On the contrary; its use gives explicit recognition to the role played by engineering judgement in design decisions, but goes farther and asks the engineer to meditate on the extent to which his judgement and factual evidence agree or are in conflict, and on how the comparison of both sources of information should set the basis for making decisions. The fact is that every decision we make, either in engineering or in any other rational discipline, is arrived at after an implicit, perhaps approximate, Bayesian formulation for assimilating subjective concepts and factual evidence . A priori subjective information is far less arbitrary then it may seem at first sight if proper judgement is applied in extrapolating to the case of interest the results of similar, better-studied phenomena.

4.3 Bayesian Statistics in the Prediction of Seismicity. The set of alternative hypotheses to which Bayes' theorem is applied may be described in several manners, according to the information that was available to the decision maker when formulating his initial distributions, and to the type of statistical information that he may be obtaining. In most cases, prior knowledge is more easily expressed in terms of local seismicity. Algebraic manipulations will convert this information into the initial distribution of $v_c(y)$ or $v(y)$.

A discussion is made in Refs. 13 and 14 of the various concepts available at present for basing initial distribution of local seismicity parameters. Most of the efforts to interpret geotectonic data and to express them quantitatively in earthquake risk terms are in an embryonic stage. Accordingly, Refs. 13 and 14 use geotectonic information only for the purpose of dividing the earth's crust into regions, without introducing prior distributions of local seismicity parameters on the

basis of this information alone. The essence of the procedure for that effect stands on the estimation of the seismicity of narrow zones from that of similar, but wider zones, for which statistical data permit a direct evaluation.

As applied to the establishment of the initial distribution of $\lambda_x(M)$ for subzone x in Fig. 2, the procedure would include the following steps (treated in detail in Refs. 13 and 14).

a) An estimate of the order of magnitude of $\lambda_x(M)$ for the mentioned zone would be given by $\lambda(M)$, the average value of the same parameter for the Circum-Pacific Belt, within which the former zone is located. The average properties of the Circum-Pacific Belt are not deterministically known, although uncertainty in the corresponding parameters would be clearly smaller than that in $\lambda_x(M)$.

b) The expected value of $\lambda_x(M)$ associated with its initial distribution may be taken as equal to the expected value of $\lambda(M)$. The initial coefficient of variation of $\lambda_x(M)$ must account for the uncertainties in both $\lambda(M)$ and $\lambda_x(M)/\lambda(M)$. The coefficient of variation of this quotient is a measure of the non-uniformity in the seismicity properties of regions that belong to the Circum-Pacific Belt. It is a function of the ratio of the volumes of the zone of interest and of the Circum-Pacific Belt, and has been estimated for different values of this ratio and of M.[13,14]

Suppose that the initial distributions of local seismicity of the regions close to a station have been proposed. The corresponding initial distributions of $\lambda_c(y)$ and $\lambda(y)$ may be estimated (at least the initial expectations and coefficient. variation of those parameters) after application of Eqs. (20), (21), (22), and (24). Application of Bayes' theorem to obtain a posterior distribution of the seismicity parameters will be explained in the next paragraph, assuming that quantitative intensity data are recorded. If not intensities, but only magnitudes have been recorded, computed intensities may be obtained by application of Eqs (20) and (21), and the next paragraph also applies if in all cases the word intensity is substituted with computed intensity.[16]

Let $N(y_1,y_2,t)$ be the number of earthquakes with intensities in the interval (y_1,y_2) that have occurred during time period t at a given station. This number will be assumed to be a Poisson process with mean $\nu(y_1,y_2)$ per unit time, and independent of the corresponding processes in any other intensity intervals. Hence, $N(y,t) = N(y,\infty,t)$ the number of earthquakes exceeding a given intensity during the specified time interval, will also be a Poisson process with expected value $\nu(y)t$.

Assume that $\nu(y)$ may be expressed as a function of known form and unknown parameters, $\nu = \nu_y(Z_1,\ldots,Z_m)$. Let $f(z_1,\ldots,z_m)$ be the a priori m-dimensional joint probability density function of the parameters, and A the event that during time interval t, $n_1, \ldots, n_k$ earthquakes have occurred with intensities in the intervals $(y_0,y_1)\ldots,(y_{k-1},y_k)$, respectively. Then, if $\Delta_i\nu = \nu_{y_i} - \nu_{y_{i-1}}$, the probability of A, given the hypothesis $(Z_j=z_j, j=1,\ldots,n)$ is obtained as follows:

$$P(A|z_1,\ldots,z_n) = \prod_{i=1}^{k}\left[e^{-\Delta_i\nu t}\frac{(\Delta_i\nu t)^{n_i}}{n_i!}\right] \tag{28}$$

Hence, the posterior distribution of the parameters would be

$$f(z_1,\ldots,z_n|A) = Kf(z_1,\ldots,z_n)\prod_{i=1}^{k}\left[e^{-\Delta_i\nu t}\frac{(\Delta_i\nu t)^{n_i}}{n_i!}\right] \tag{29}$$

where K is a normalizing constant.

4.4 Design Decisions with Uncertain Seismicity Parameters. If $\nu(y)$ is now assumed to be equal to Ky^{-r}, where K and r are defined by their joint probability density function, the expected values of the cost of failure would now have to account for uncertainty in K and r. The result is that Eq. (8) would turn to the following:

$$U = \frac{b}{\lambda} - A_0 - A_1 y^n - \frac{D}{r}\int\int Ky^{-r} f(K,r)\,dK\,dr \tag{30}$$

Solving of this equation for y leads to the optimum value of the design intensity.

Example. After performing studies of local and regional seismicity, a designer ends up with two alternate assumptions to represent $\nu(y)$ at a site. Since to him both assumptions are considered to be equally likely, their corresponding probabilities of being true are taken as 0.5. Both hypotheses take $\nu = Ky^{-r}$, with the following values of the parameters for each of them.

$$K_1 = 10^{-6}, \qquad r_1 = 2$$
$$K_2 = 10^{-3}, \qquad r_2 = 2.5$$

The expected utility may be written:

$$U = \frac{b}{\gamma} - A_0 - A_1 y^n - \frac{D}{\gamma}\left[K_1 y^{-r_1} p_1 + K_2 y^{-r_2} p_2\right]$$

When this equation is differentiated and the derivative set equal to zero, one obtains:

$$\frac{nA_1}{D} y^n = r_1 K_1 p_1 y^{-r_1} + r_2 K_2 p_2 y^{-r_2}$$

which was numerically solved to obtain $y = 0.55$. This is the optimum design intensity.

V. CONCLUSIONS

The occurrence of earthquake motions at a site is a stochastic process. Seismic design decisions should be based on studies that compare initial costs of a structure, its expected actualized benefits, and its expected actualized costs of failure. Consequently, it is unreasonable in most cases to establish design intensities at a site without previous consideration of both the seismicity parameters and the consequences of each possible manner of structural behavior.

The distribution of intensities at a site has in many cases to be estimated from the local seismicity parameters. These in turn may be evaluated through the use of statistical data on frequency, magnitudes and focal coordinates of shocks, or through the use of more indirect forms of information. Wide margins of uncertainty may characterize the form and the parameters of the stochastic process model that is used to represent seismicity. Hence, point estimates of these parameters may not suffice for an adequate formulation of design decisions. Consideration has to be made of all possible alternative hypotheses and their corresponding consequences. This is accomplished through the use of Bayesian statistics.

TABLE 1

EXAMPLE OF SELECTION OF DESIGN INTENSITY. PROBLEM VARIABLES

a) SEISMICITY

	Station 1	Station 2
K	10^{-4}	10^{-2}
r	2	2
Intensity for $\nu = 1$	0.01	0.1
$\nu(0.1)$	0.01	1

b) PARAMETERS OF STRUCTURE

	Structure 1	Structure 2
A_1/A_o	2	2
n	2	2
D/A_o	2	20
D/A_1	1	10

TABLE 2

COMPARISON OF DESIGN INTENSITIES

Station	1	1	2	2
Structure	1	2	1	2
y_s	0.177	0.316	0.565	1
$\nu(y_s)$	0.0032	0.001	0.032	0.01
$T(y_s)$	320	1000	32	100

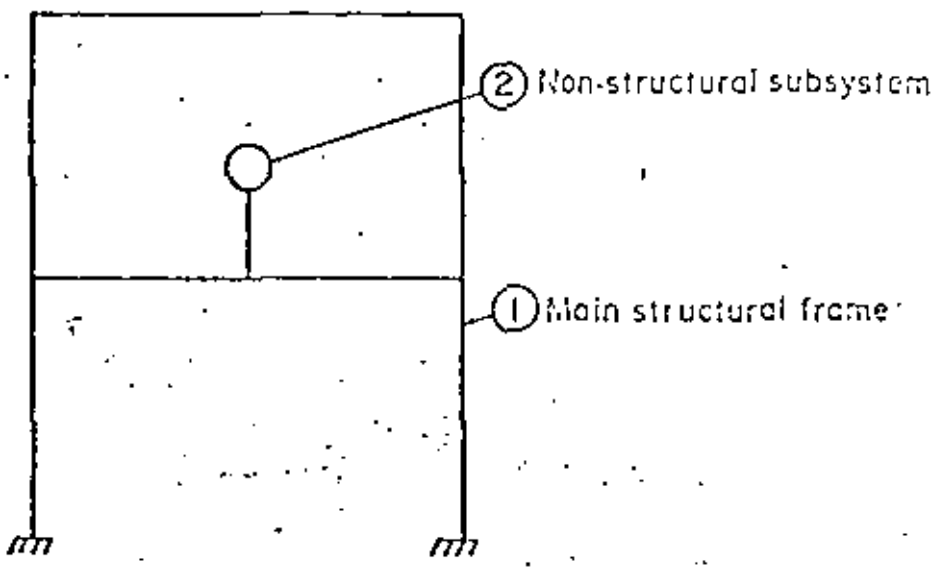

Fig.1 Two-component structural system

(See "Seismicity of the Earth and Associated Phenomena," by B. Gutenberg and C. F. Richter, Princeton University Press, Princeton, New Jersey; Published more recently by Stechert & Haffner, New York City, 1965).

FIGURE 2

$\nu(3)$ = Valor esperado de ...
producir ... magnitud mayor que ... por ...
dad de tiempo

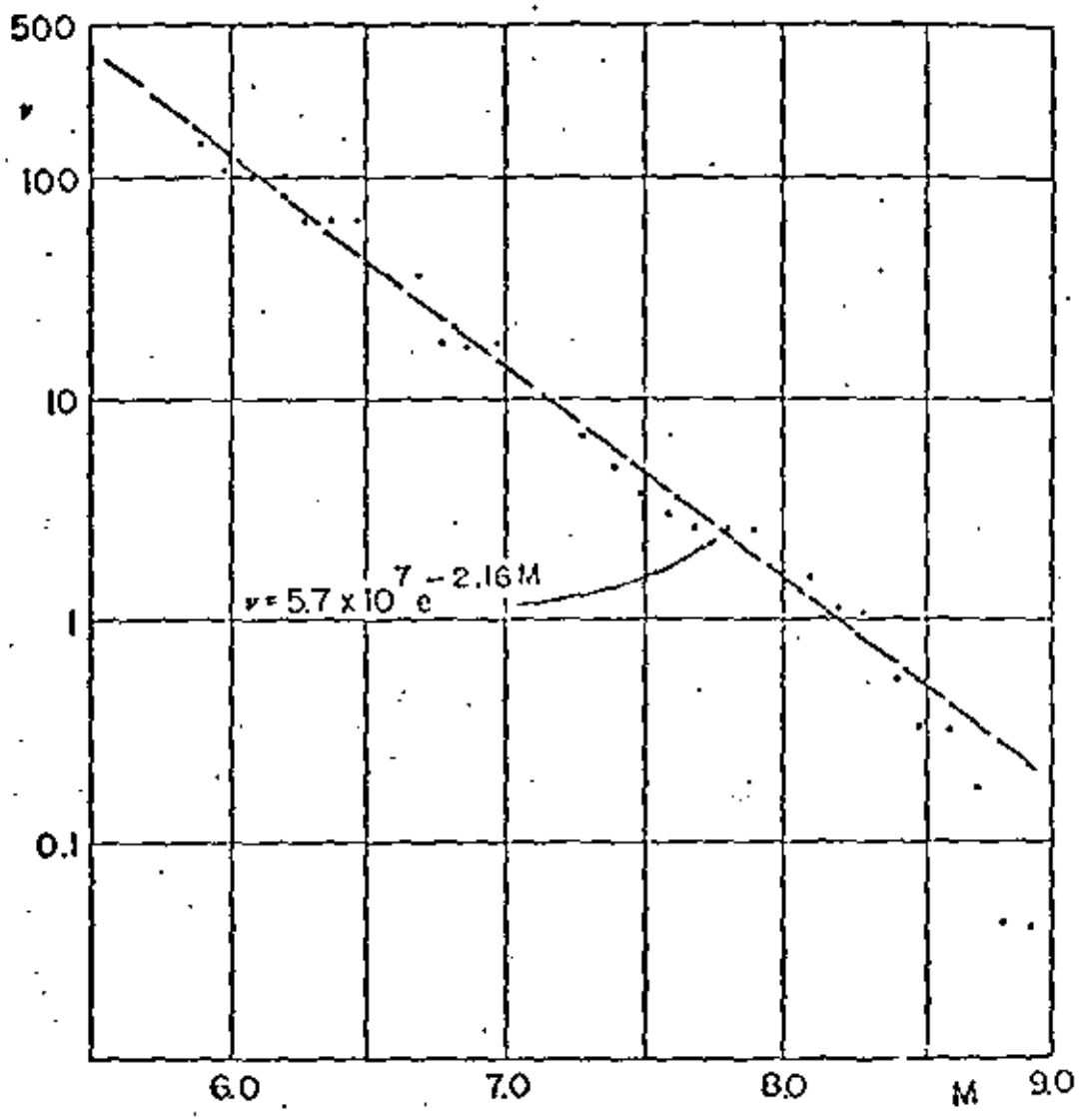

Fig. 3 Mean number of earthquakes with magnitude higher than M. Circumpacific Belt

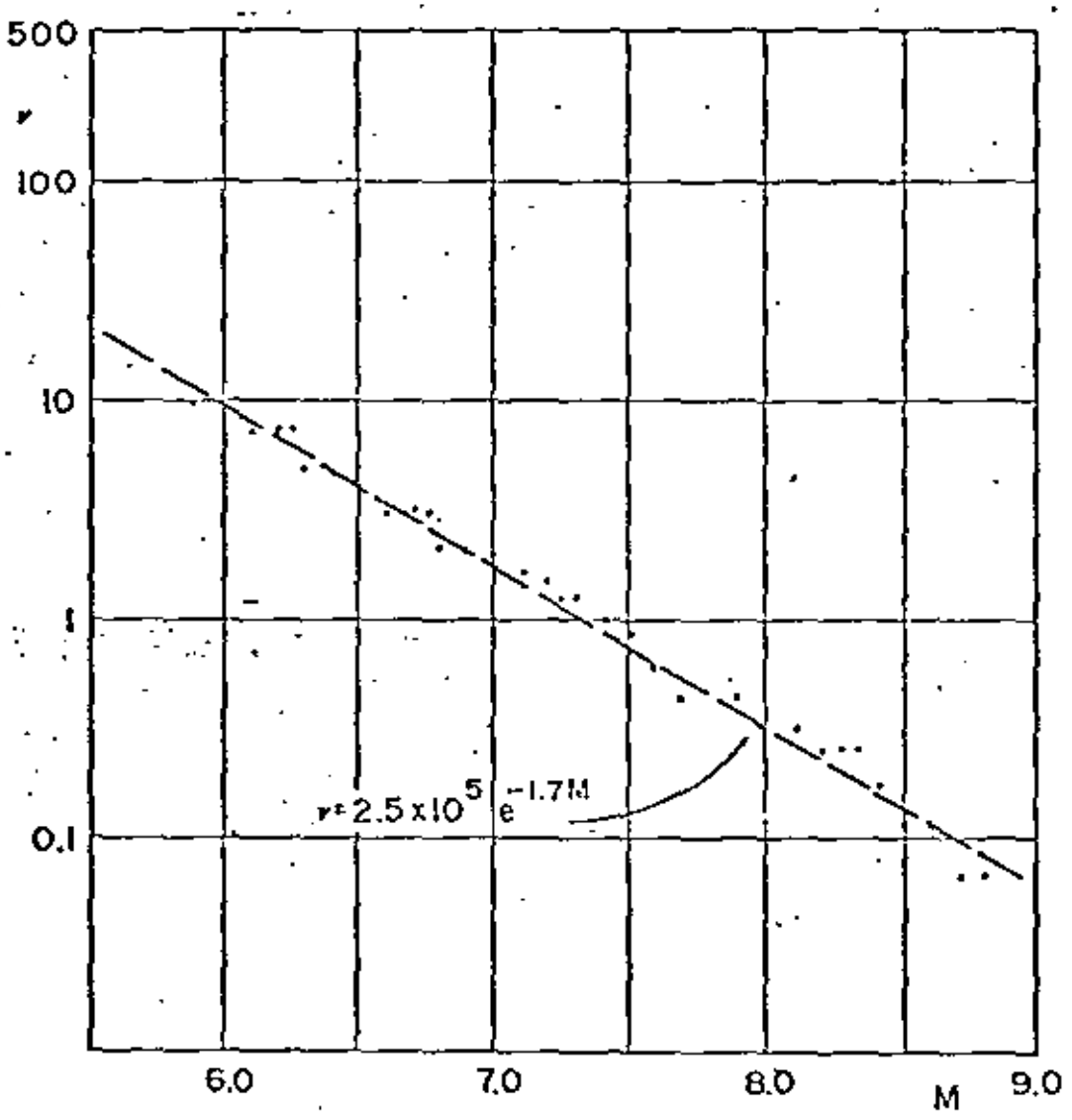

Fig.4 Mean number of earthquakes with magnitude higher than M. Alpine Belt

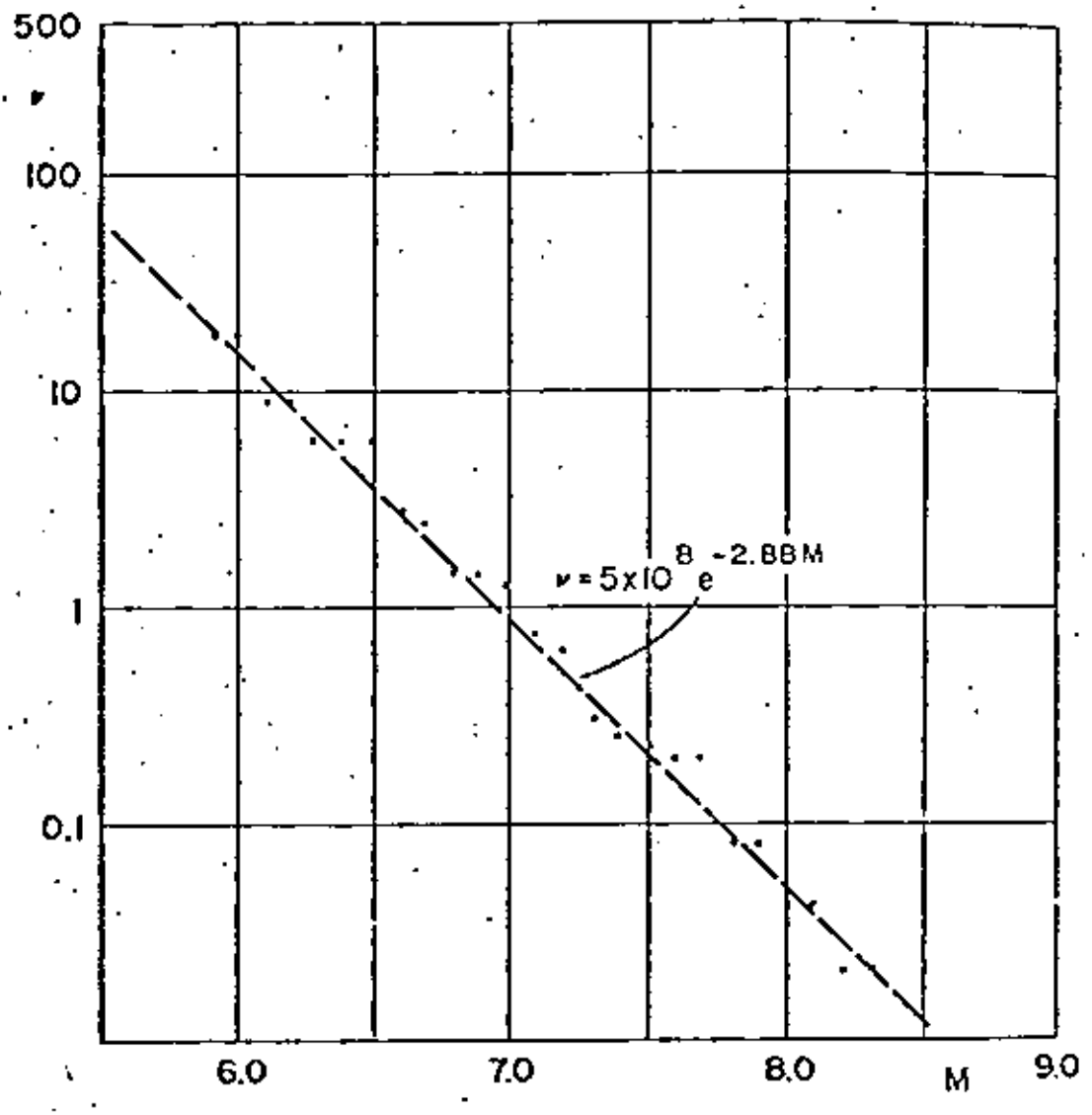

Fig.5 Mean number of earthquakes with magnitude higher than M. Low seismicity zone.

a = acceleration

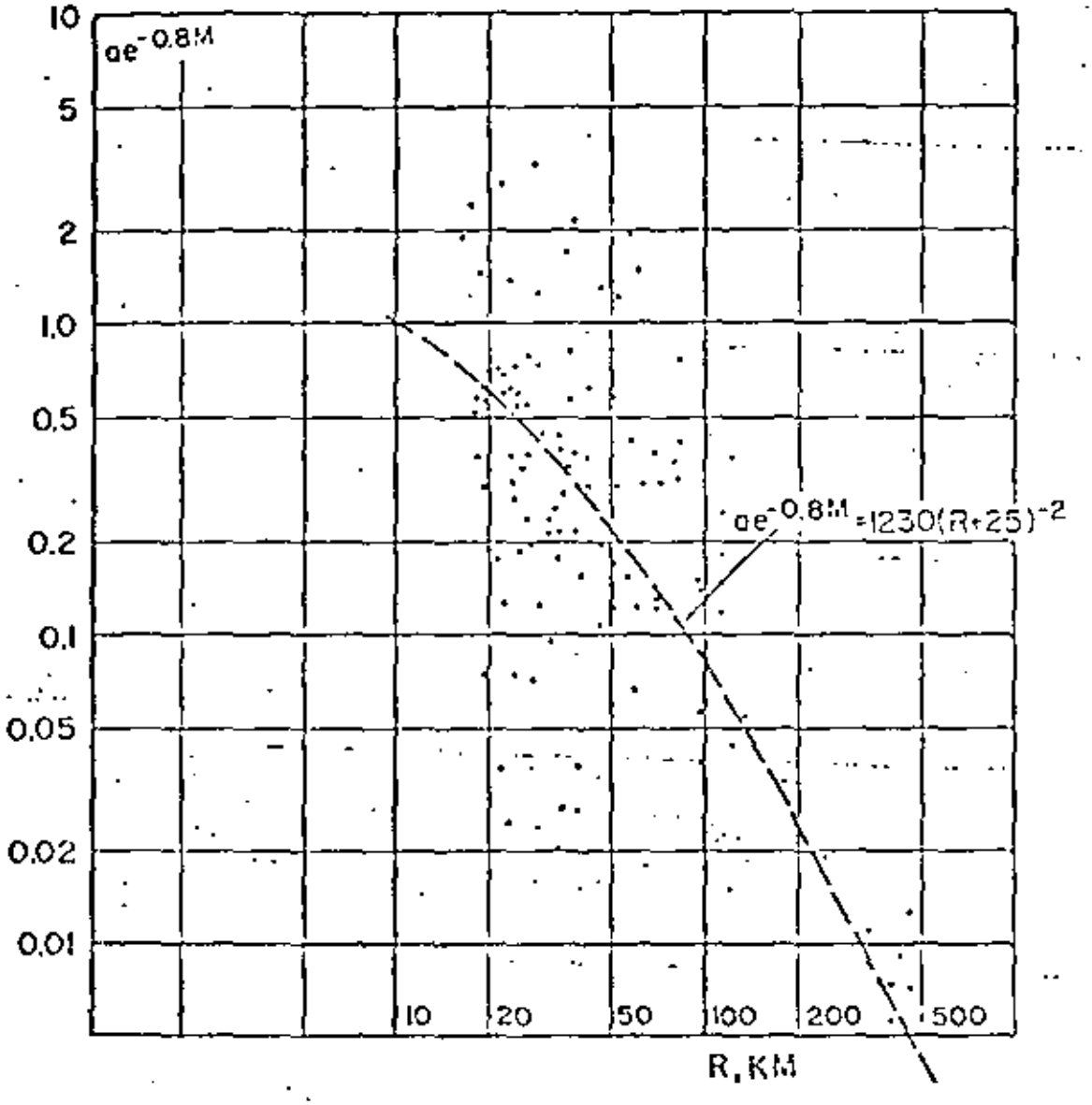

Fig.6 Peak ground acceleration in terms of magnitude and hypocentral distance.

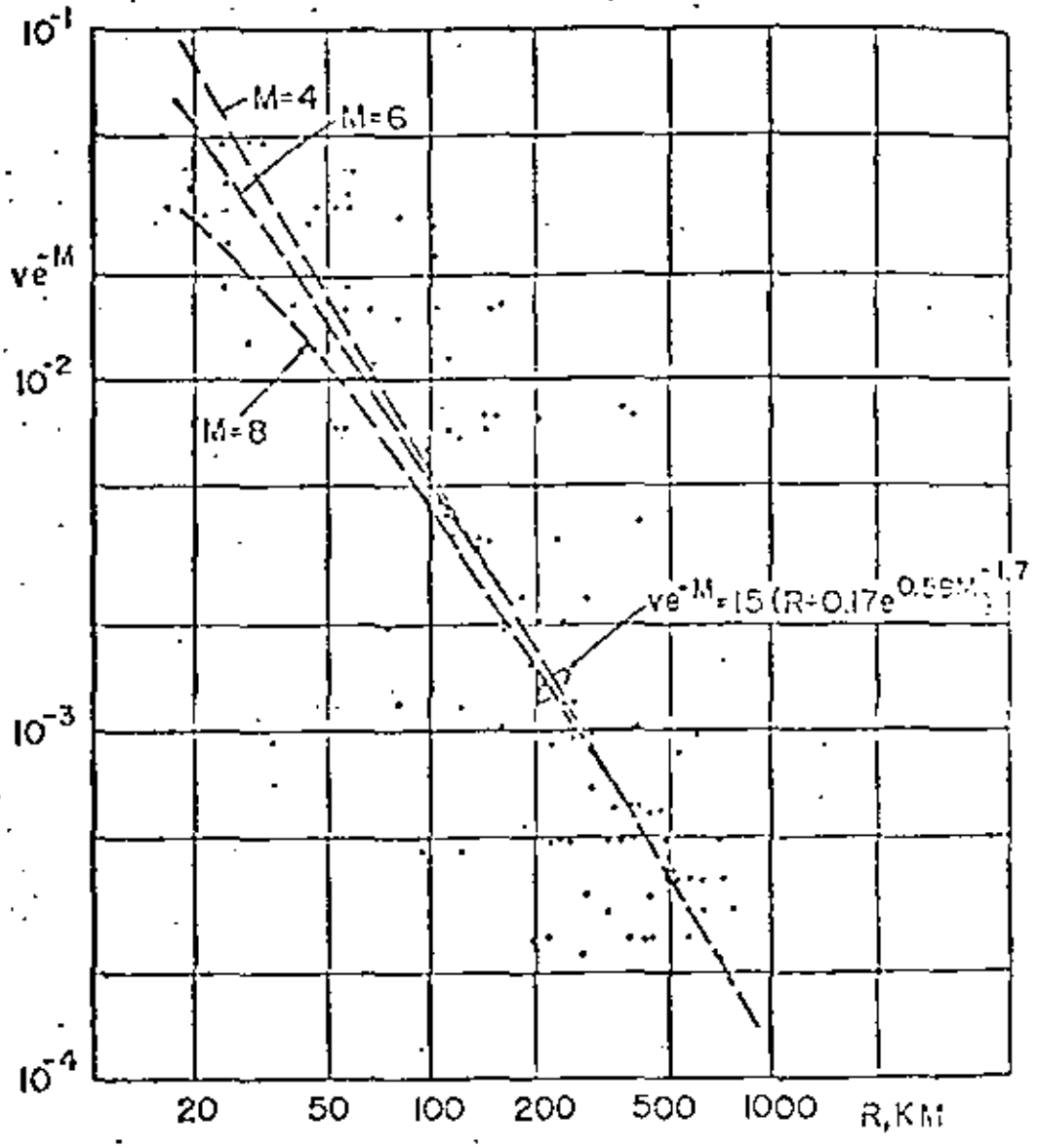

Fig.7 Peak ground velocity in terms of magnitude and hypocentral distance.

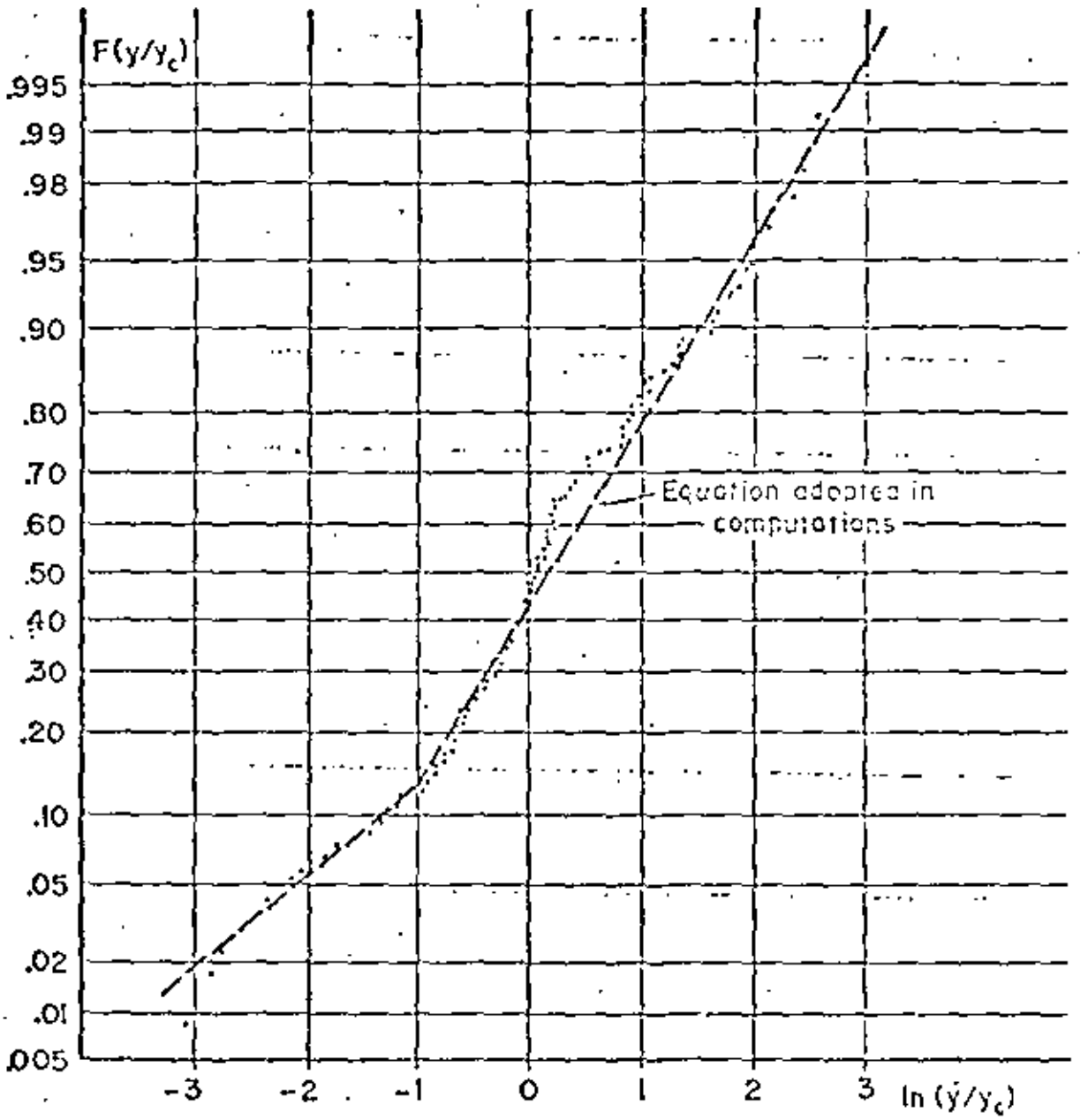

Fig.8 Distribution of actual /computed peak ground accelerations

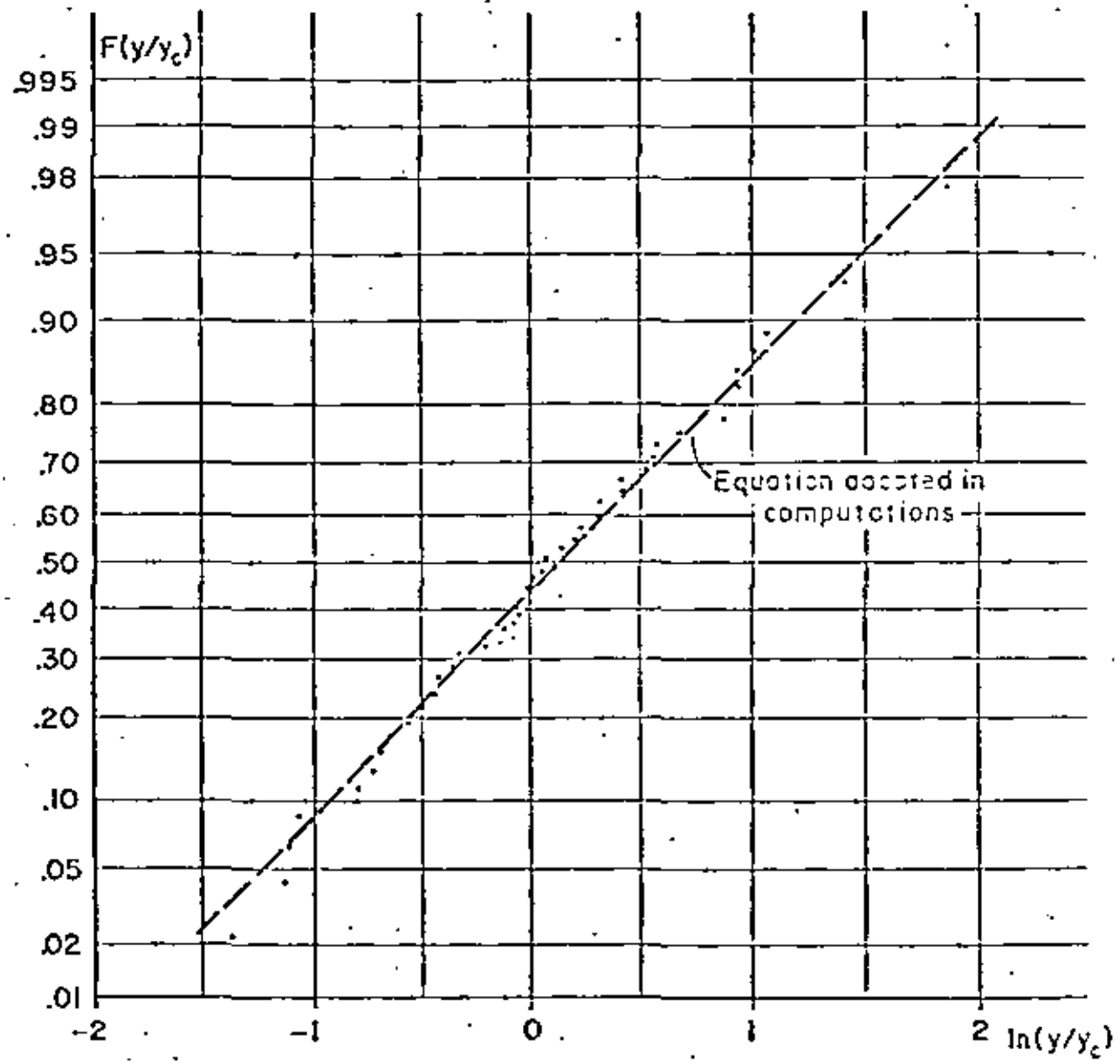

Fig.9 Distribution of actual/computed peak ground velocities

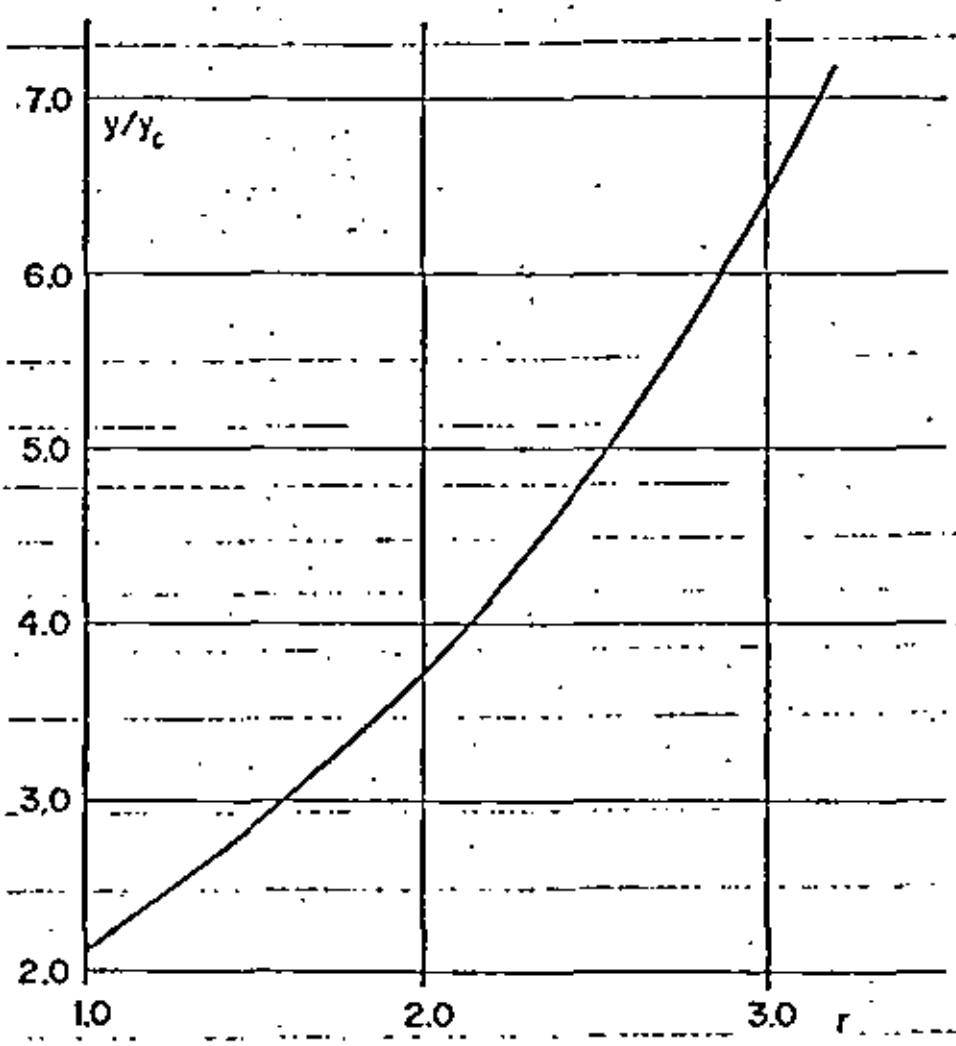

Fig. 10 Ratio of actual to computed peak ground accelerations having equal return period.

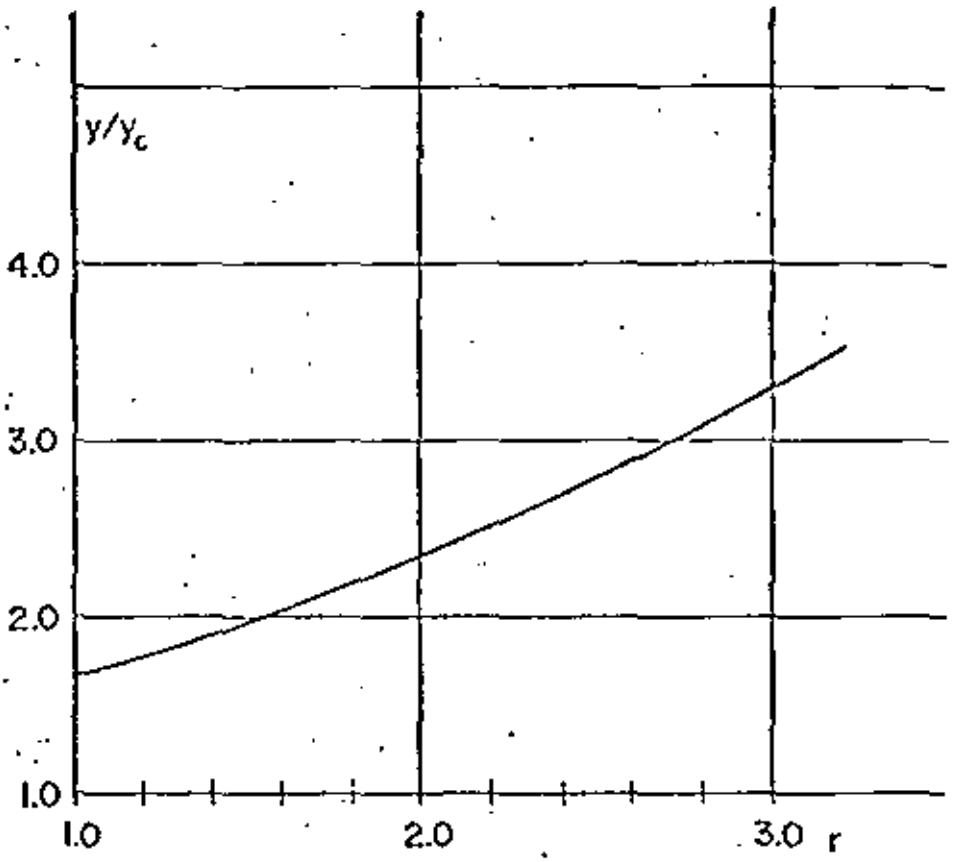

Fig.11 Ratio of actual to computed peak ground velocities having equal return period.

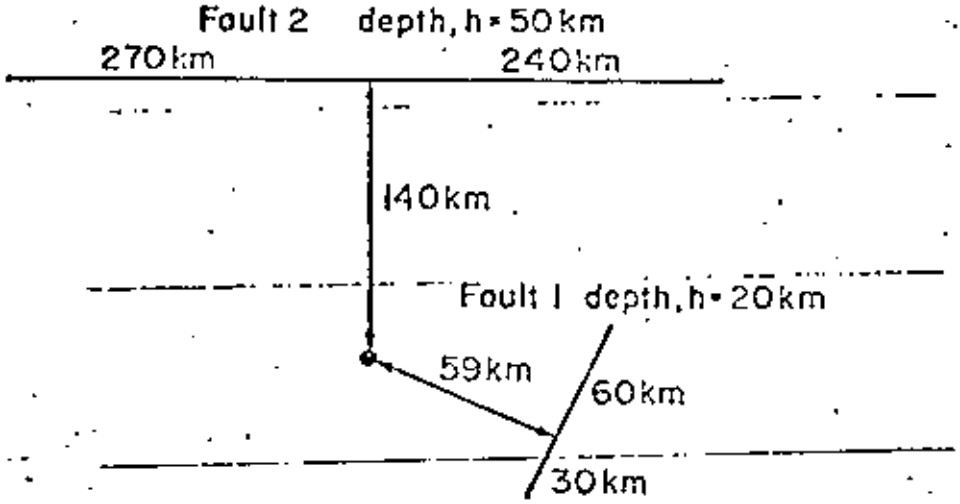

Local seismicity parameters:

$$\nu(M) = \nu(4.5)e^{-\beta(M-4.5)} \quad , M \leq M_1$$

$$\nu(M) = 0 \quad , M > M_1$$

	Fault 1	Fault 2
$\nu(4.5)$	0.35	1.2
β	1.72	1.63
M_1	7.25	8.75

Fig.12 Local seismicity parameters

IX CURSO INTERNACIONAL DE INGENIERIA SISMICA

ANALISIS DE RIESGO SISMICO

S I S M I C I D A D

DR. LUIS ESTEVA

Chapter 6

SEISMICITY

LUIS ESTEVA

Instituto de Ingeniería, Universidad Nacional Autónoma de México, Mexico

6.1 ON SEISMICITY MODELS

Rational formulation of engineering decisions in seismic areas requires quantitative descriptions of seismicity. These descriptions should conform with their intended applications: in some instances, simultaneous intensities during each earthquake have to be predicted at several locations, while in others it suffices to make independent evaluations of the probable effects of earthquakes at each of those locations.

The second model is adequate for the selection of design parameters of individual components of a regional system (the structures in a region or country) when no significant interaction exists between response or damage of several such individual components, or between any of them and the system as a whole. In other words, it applies when the damage — or negative utility — inflicted upon the system by an earthquake can be taken simply as the addition of the losses in the individual components.

The linearity between monetary values and utilities implied in the second model is not always applicable. Such is the case, for instance, when a significant portion of the national wealth or of the production system is concentrated in a relatively narrow area, or when failure of life-line components may disrupt emergency and relief actions just after an earthquake. Evaluation of risk for the whole regional system has then to be based on seismicity models of the first type, that is, models that predict simultaneous intensities at several locations during each event; for the purpose of decision making, nonlinearity between monetary values and utilities can be accounted for by means of adequate scale transformations. These models are also of interest to insurance companies, when the probability distribution of the maximum loss in a given region during a given time interval is to be estimated.

Whatever the category to which a seismic risk problem belongs, it requires the prediction of probability distributions of certain ground motion characteristics (such as peak ground acceleration or velocity, spectral density, response or Fourier spectra, duration) at a given site during a single shock or of maximum values of some of those characteristics in earthquakes occurring during given time intervals. When the reference interval tends to infinity, the probability distribution of the maximum value of a given characteristic ap-

proaches that of its maximum *possible* value. Because different systems or subsystems are sensitive to different ground motion characteristics, the term *intensity characteristic* will be used throughout this chapter to mean a particular parameter or set of parameters of an earthquake motion, in terms of which the response is to be predicted. Thus, when dealing with the failure probability of a structure, intensity can be alternatively measured — with different degrees of correlation with structural response — by the ordinate of the response spectrum for the corresponding period and damping, the peak ground acceleration, or the peak ground velocity.

In general, local instrumental information does not suffice for estimating the probability distributions of maximum intensity characteristics, and use has to be made of data on subjective measures of intensities of past earthquakes, of models of *local seismicity*, and of expressions relating characteristics with magnitude and site-to-source distance. Models of local seismicity consist, at least, of expressions relating magnitudes of earthquakes generated in given volumes of the earth's crust with their return periods. More often than not, a more detailed description of local seismicity is required, including estimates of the maximum magnitude that can be generated in these volumes, as well as probabilistic (stochastic process) models of the possible histories of seismic events (defined by magnitudes and coordinates).

This chapter deals with the various steps to be followed in the evaluation of seismic risk at sites where information other than direct instrumental records of intensities has to be used: identifying potential sources of activity near the site, formulating mathematical models of local seismicity for each source, obtaining the contribution of each source to seismic risk at the site and adding up contributions of the various sources and combining information obtained from local seismicity of sources near the site with data on instrumental or subjective intensities observed at the site.

The foregoing steps consider use of information stemming from sources of different nature. Quantitative values derived therefrom are ordinarily tied to wide uncertainty margins. Hence they demand probabilistic evaluation, even though they cannot always be interpreted in terms of relative frequencies of outcomes of given experiments. Thus, geologists talk of the maximum magnitude that can be generated in a given area, assessed by looking at the dimensions of the geological accidents and by extrapolating the observations of other regions which available evidence allows to brand as similar to the one of interest; the estimates produced are obviously uncertain, and the degree of uncertainty should be expressed together with the most probable value. Following nearly parallel lines, some geophysicists estimate the energy that can be liberated by a single shock in a given area by making quantitative assumptions about source dimensions, dislocation amplitude and stress drop, consistent with tectonic models of the region and, again, with comparisons with areas of similar tectonic characteristics.

Uncertainties attached to estimates of the type just described are in gen-

eral extremely large: some studies relating fault rupture area, stress drop, and magnitude (Brune, 1968) show that, considering not unusually high stress drops, it does not take very large source dimensions to get magnitudes 8.0 and greater, and those studies are practically restricted to the simplest types of fault displacement. It is not clear, therefore, that realistic bounds can always be assigned to potential magnitudes in given areas or that, when this is feasible, those bounds are sufficiently low, so that designing structures to withstand the corresponding intensities is economically sound, particularly when occurrence of those intensities is not very likely in the near future. Because uncertainties in maximum feasible magnitudes and in other parameters defining magnitude-recurrence laws can be as significant as their mean values when trying to make rational seismic design decisions, those uncertainties have to be explicitly recognized and accounted for by means of adequate probabilistic criteria. A corollary is that geophysically based estimates of seismicity parameters should be accompanied with corresponding uncertainty measures.

Seismic risk estimates are often based only on statistical information (observed magnitudes and hypocentral coordinates). When this is done, a wealth of relevant geophysical information is neglected, while the probabilistic prediction of the future is made to rely on a sample that is often small and of little value, particularly if the sampling period is short as compared with the desirable return period of the events capable of severely damaging a given system.

The criterion advocated here intends to unify the foregoing approaches and rationally to assimilate the corresponding pieces of information. Its philosophy consists in using the geological, geophysical, and all other available non-statistical evidence for producing a set of alternate assumptions concerning a mathematical (stochastic process) model of seismicity in a given source area. An initial probability distribution is assigned to the set of hypotheses, and the statistical information is then used to improve that probability assignment. The criterion is based on application of *Bayes theorem*, also called the *theorem of the probabilities of hypotheses*. Since estimates of risk depend largely on conceptual models of the geophysical processes involved, and these are known with different degrees of uncertainty in different zones of the earth's crust, those estimates will be derived from stochastic process models with uncertain forms or parameters. The degree to which these uncertainties can be reduced depends on the limitations of the state of the art of geophysical sciences and on the effort that can be put into compilation and interpretation of geophysical and statistical information. This is an economical problem that should be handled, formally or informally, by the criteria of decision making under uncertainty.

6.2 INTENSITY ATTENUATION

Available criteria for the evaluation of the contribution of potential seismic sources to the risk at a site make use of *intensity attenuation* expressions that relate intensity characteristics with magnitude and distance from site to source. Depending on the application envisaged, the intensity characteristic to be predicted can be expressed in a number of manners, ranging from a subjective index, such as the *Modified Mercalli intensity*, to a combination of one or more quantitative measures of ground shaking (see Chapter 1).

A number of expressions for attenuation of various intensity characteristics with distance have been developed, but there is little agreement among most of them (Ambraseys, 1973). This is due in part to discrepancies in the definitions of some parameters, in the ranges of values analyzed, in the actual wave propagation properties of the geological formations lying between source and site, in the dominating shock mechanisms, and in the forms of the analytical expressions adopted a priori.

Most intensity-attenuation studies concern the prediction of earthquake characteristics on rock or firm ground, and assume that these characteristics, properly modified in terms of frequency-dependent soil amplification factors, should constitute the basis for estimating their counterparts on soft ground. Observations about the influence of soil properties on earthquake damage support the assumption of a strong correlation between type of local ground and intensity in a given shock. Attempts to analytically predict the characteristics of motions on soil given those on firm ground or on bedrock have not been too successful, however (Crouse, 1973; Hudson and Udwadia, 1973; Salt, 1974), with the exception of some peculiar cases, like Mexico City (Herrera et al., 1965), where local conditions favor the fulfillment of the assumptions implied by usual analytical models. The following paragraphs concentrate on prediction on intensities on firm ground; the influence of local soil is discussed in Chapter 4.

6.2.1 Intensity attenuation on firm ground

When isoseismals (lines joining sites showing equal intensity) of a given shock are based only on intensities observed on homogeneous ground conditions, such as *firm ground* (compact soils) or bedrock, they are roughly elliptical and the orientations of the corresponding axes are often correlated with local or regional geological trends (Figs. 6.1–6.3). In some regions — for instance near major faults in the western United States — those trends are well defined and the correlations are clear enough as to permit prediction of intensity in the near and far fields in terms of magnitude and distance to the generating fault or to the centroid of the energy liberating volume. In other regions, such as the eastern United States and most of Mexico, isoseismals seem to elongate systematically in a direction that is a function of the epi-

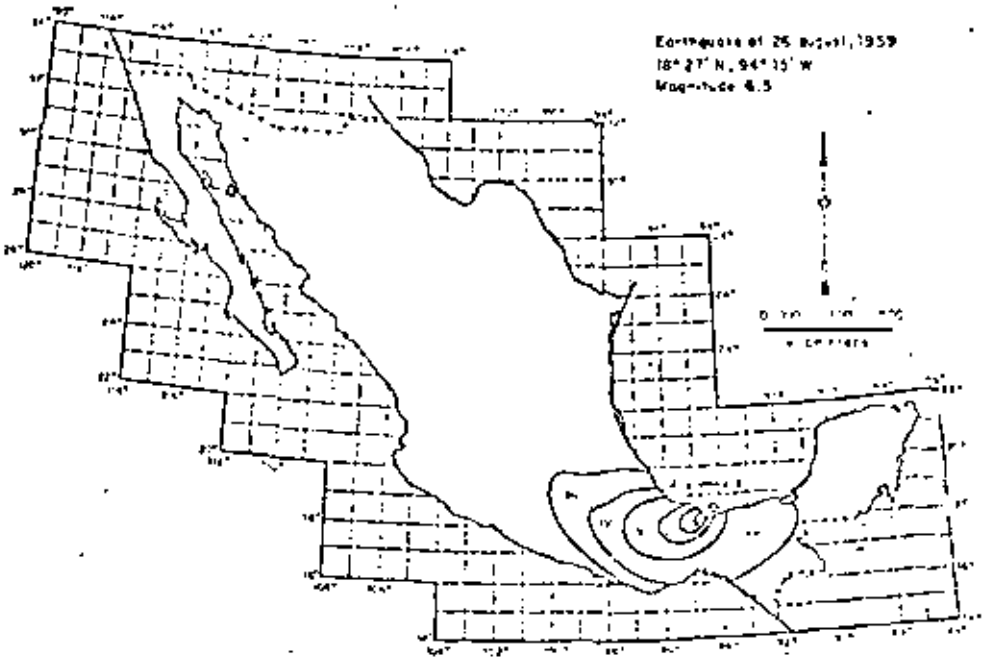

Fig. 6.1. Isoseismals of an earthquake in Mexico. (After Figueroa, 1963.)

central coordinates (Bollinger, 1973; Figueroa, 1963). In that case, intensity should be expressed as a function of magnitude and coordinates of source and site. For most areas in the world, intensity has to be predicted in terms of simple — and cruder — expressions that depend only on magnitude and distance from site to instrumental hypocenter. This stems from inadequate knowledge of geotectonic conditions and from limited information concerning the volume where energy is liberated in each shock.

A comparison of the rates of attenuation of intensities on firm ground for shocks on western and eastern North America has disclosed systematic differences between those rates (Milne and Davenport, 1969). This is the source of a basic, but often unavoidable, weakness of most intensity-attenuation expressions, because they are based on heterogeneous data, recorded in different zones, and the very nature of their applications implies that the less is known about possible systematic deviations in a given zone, as a consequence of the meagerness of local information, the greater weight is given to predictions with respect to observations.

6.2.1.1 Modified Mercalli intensities

An analysis of the Modified Mercalli intensities on firm ground reported for earthquakes occurring in Mexico in the last few decades leads to the fol-

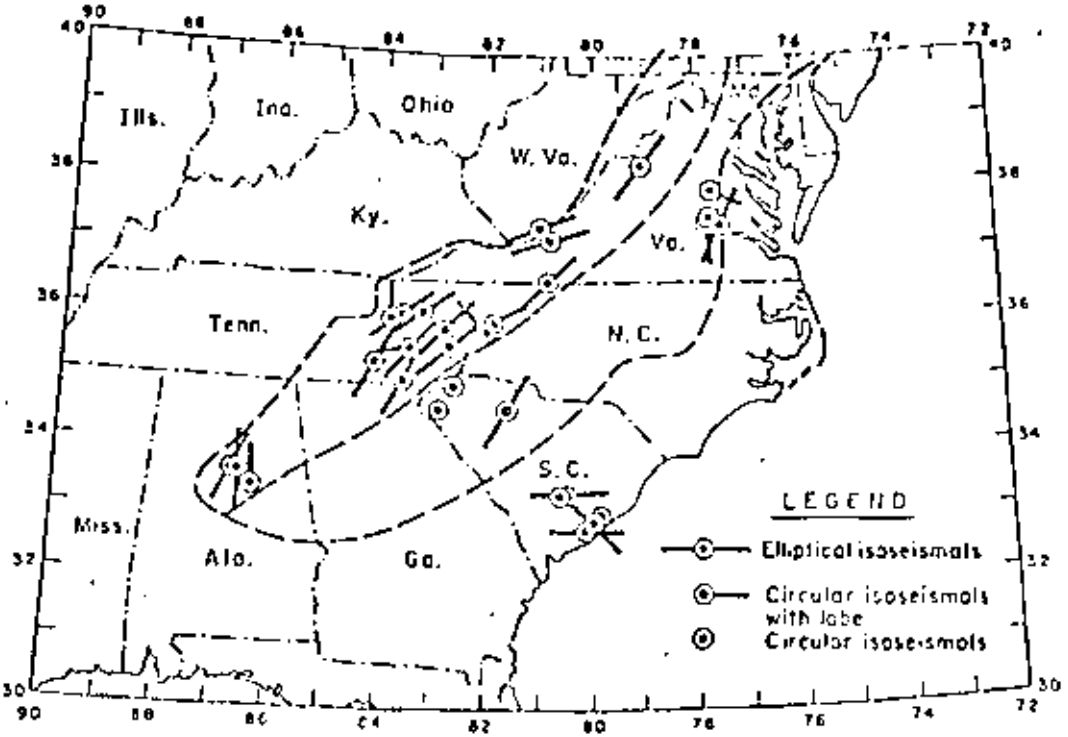

Fig. 6.2. Elongation of isoseismals in the southeastern United States. (After Bollinger, 1973.)

lowing expression relating magnitude M, hypocentral distance R (in kilometers) and intensity I (Esteva, 1968):

$$I = 1.45\,M - 5.7\log_{10} R + 7.9 \qquad (6.1)$$

The prediction error, defined as the difference between observed and computed intensity, is roughly normally distributed, with a standard deviation of 2.04, which means that there is a probability of 68% that an observed intensity is more than one degree greater or smaller than its predicted value.

6.2.1.2 Peak ground accelerations and velocities

A few of the available expressions will be described. Their comparison will show how cautiously a designer intending to use them should proceed.

Housner studied the attenuation of peak ground accelerations in several regions of the United States and presented his results graphically (1969) in terms of fault length (in turn a function of magnitude), shapes of isoseismals and areas experiencing intensities greater than given values (Fig. 6.4 and 6.5).

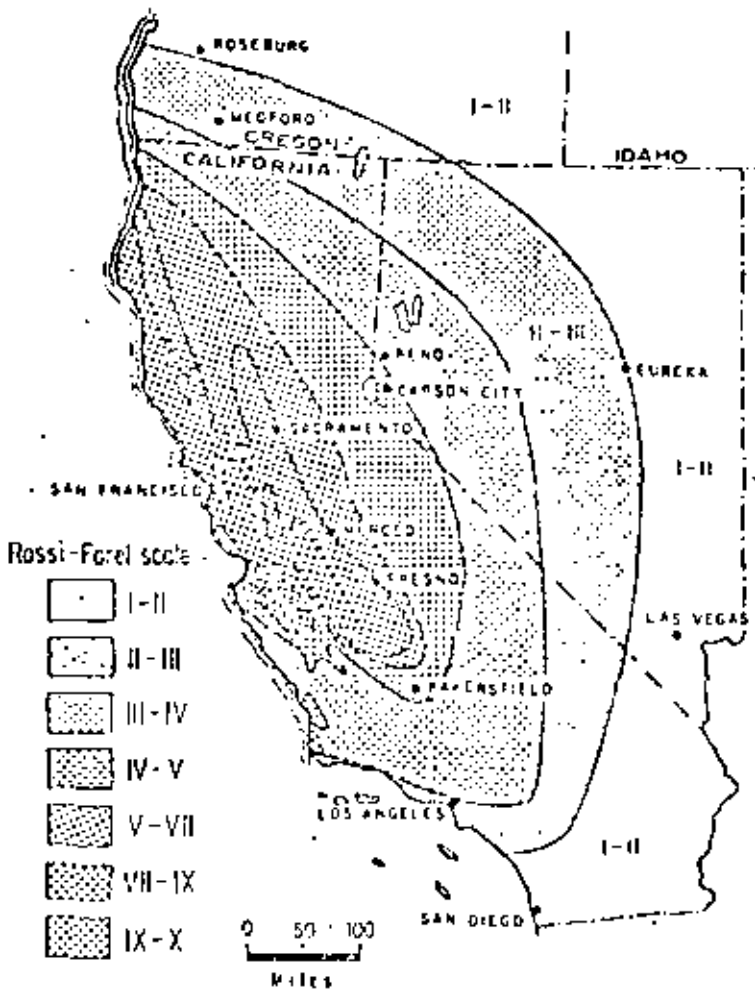

Fig. 6.3. Isoseismals in California. (After Bolt, 1970.)

He showed that intensities attenuate faster with distance on the west coast than in the rest of the country. This comparison is in agreement with Milne and Davenport (1969), who performed a similar analysis for Canada. From observations of strong earthquakes in California and in British Columbia, they developed the following expression for a, the peak ground acceleration, as a fraction of gravity:

$$a/g = 0.0069\, e^{1.03M}/(1.1\, e^{1.03M} + R^2) \qquad (6.2)$$

Here, R is epicentral distance in kilometers. The acceleration varies roughly as $e^{1.03M}R^{-2}$ for large R, and as $e^{0.54M}$ where R approaches zero. This reflects to some extent the fact that energy is released not at a single point but from a finite volume. A later study by Davenport (1972) led him

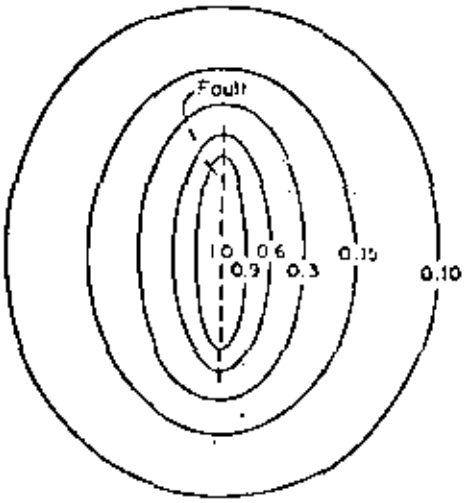

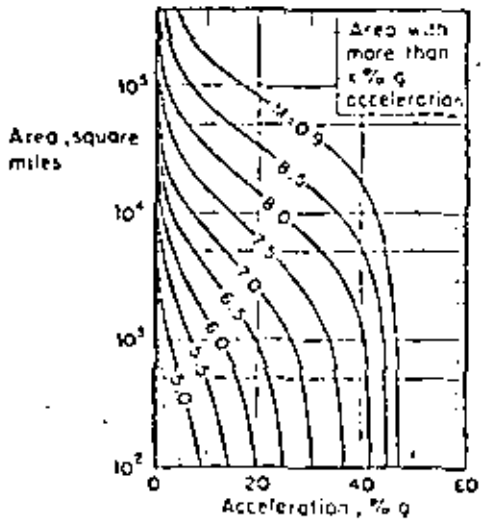

Fig. 6.4. Idealized contour lines of intensity of ground shaking. (After Housner, 1969.)

Fig. 6.5. Area in square miles experiencing shaking of x %g or greater for shocks of different magnitudes. (After Housner, 1969.)

to propose the expression:

$$a/g = 0.279\, e^{0.8M}/R^{1.64} \tag{6.3}$$

The statistical error of this equation was studied by fitting a lognormal probability distribution to the ratios of observed to computed accelerations. A standard deviation of 0.71 was found in the natural logarithms of those ratios.

Esteva and Villaverde (1973), on the basis of accelerations reported by Hudson (1971, 1972a,b), derived expressions for peak ground accelerations and velocities, as follows:

$$a/g = 5.7\, e^{0.8M}/(R + 40)^2 \tag{6.4}$$

$$v = 32\, e^{M}/(R + 25)^{1.7} \tag{6.5}$$

Here v is peak ground velocity in cm/sec and the other symbols mean the same as above. The standard deviation of the natural logarithm of the ratio of observed to predicted intensity is 0.64 for accelerations and 0.74 for velocities. If judged by this parameter, eqs. 6.3 and 6.4 seem equally reliable. However, as shown by Fig. 6.6, their mean values differ significantly in some ranges.

With the exception of eq. 6.2, all the foregoing attenuation expressions are products of a function of R and a function of M. This form, which is acceptable when the dimensions of the energy-liberating source are small com-

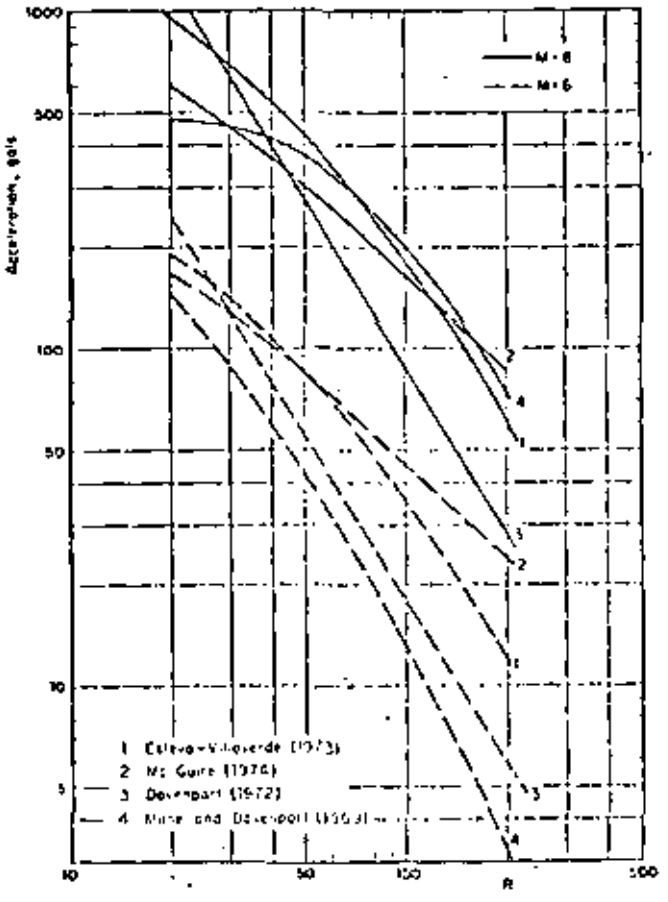

Fig. 6.6. Comparison of several attenuation expressions.

pared with R, is inadequate when dealing with earthquake sources whose dimensions are of the order of moderate hypocentral distances, and often greater than them. Although equation errors (probability distributions of the ratio of observed to predicted intensities) have been evaluated by Davenport (1972) and Esteva and Villaverde (1973), their dependence on M and R has not been analyzed. Because seismic risk estimates are very sensitive to the attenuation expressions in the range of large magnitudes and short distances, more detailed studies should be undertaken, aiming at improving those expressions in the mentioned range, and at evaluating the influence of M and R on equation error. Information on strong-motion records will probably be scanty for those studies, and hence they will have to be largely based on analytical or physical models of the generation and propagation of seismic waves. Although significant progress has been lately attained in this direction (Trifunac, 1973) the results from such models have hardly influenced the

practice of seismic risk estimation because they have remained either unknown to or imperfectly appreciated by engineers in charge of the corresponding decisions.

6.2.1.3 Response spectra

Peak ground acceleration and displacement are fairly good indicators of the response of structures possessing respectively very high and very small natural frequencies. Peak velocity is correlated with the response of intermediate-period systems, but the correlation is less precise than that tying the former parameters; hence, it is natural to formulate seismic risk evaluation and engineering design criteria in terms of spectral ordinates.

Response spectrum prediction for given magnitude and hypocentral or site-to-fault distance usually entails a two-step process, according to which peak ground acceleration, velocity and displacement are initially estimated and then used as reference values for prediction of the ordinates of the response spectrum. Let the second step in the process be represented by the operation $y_s = \alpha y_g$, where y_s is an ordinate of the response spectrum for a given natural period and damping ratio, and y_g is a parameter (such as peak ground acceleration or velocity) that can be directly obtained from the time-history record of a given shock regardless of the dynamic properties of the systems whose response is to be predicted. For given M and R, y_g is random and so is y_s; $f y_g = \alpha$; the mean and standard deviation of y_s depend on those of y_g and α and on the coefficient of correlation of the latter variables. As shown above, y_g can only be predicted within wide uncertainty limits, often wider than those tied to y_s (Esteva and Villaverde, 1973). The coefficient of variation of y_s given M and R can be smaller than that of y_g only if α and y_g are negatively correlated, which is often the case; the greater the deviation of an observed value of y_g with respect to its expectation for given M and R, the lower is likely to be α. In other words, it seems that in the intermediate range of natural periods the expected values of spectral ordinates for given damping ratios can be predicted directly in terms of magnitude and focal distance with narrower (or at most equal) margins of uncertainty than those tied to predicted peak ground velocities. For the ranges of very short or very long natural periods, peak amplitudes of ground motion and spectral ordinates approach each other and their standard errors are therefore nearly equal.

McGuire (1974) has derived attenuation expressions for the conditional values (given M and R) of the mean and of various percentiles of the probability distributions of the ordinates of the response spectra for given natural periods and damping ratios. Those expressions have the same form as eqs. 6.4 and 6.5, but their parameters show that the rates of attenuation of spectral ordinates differ significantly from those of peak ground accelerations or velocities. For instance, McGuire finds that peak ground velocity attenuates in proportion to $(R + 25)^{-1.20}$, while the mean of the pseudovelocity for a

TABLE 6.1

McGuire's attenuation expressions $y = b_1\, 10^{b_2 M}(R + 25)^{-b_3}$

y	b_1	b_2	b_3	$V(y)$ = coeff. of var. of y
a gals	472.3	0.278	1.301	0.518
v cm/sec	5.61	0.401	1.202	0.696
d cm	0.393	0.434	0.885	0.683
Undamped spectral pseudovelocities				
T = 0.1 sec	11.0	0.278	1.346	0.911
0.5	3.05	0.391	1.091	0.636
1.0	0.631	0.378	0.619	0.768
2.0	0.0768	0.469	0.419	0.989
5.0	0.0831	0.561	0.897	1.344
5% damped spectral pseudovelocities				
T = 0.1 sec	10.09	0.233	1.341	0.651
0.5	5.74	0.356	1.197	0.591
1.0	0.432	0.309	0.701	0.703
2.0	0.122	0.466	0.675	0.911
5.0	0.0706	0.557	0.938	1.193

natural period of 1 sec and a damping ratio of 2% attenuates in proportion to $(R + 25)^{-0.59}$. These results stem from the way that frequency content changes with R and lead to the conclusion that the ratio of spectral velocity should be taken as a function of M and R.

Table 6.1 summarizes McGuire's attenuation expressions and their coefficients of variation for ordinates of the pseudovelocity spectra and for peak ground acceleration, velocity and displacement. Similar expressions were derived by Esteva and Villaverde (1973), but they are intended to predict only the maxima of the expected acceleration and velocity spectra, regardless of the periods associated with those maxima. No analysis has been performed of the relative validity of McGuire's and Esteva and Villaverde's expressions for various ranges of M and R.

6.3 LOCAL SEISMICITY

The term *local seismicity* will be used here to designate the degree of seismic activity in a given volume of the earth's crust; it can be quantitatively described according to various criteria, each providing a different amount of information. Most usual criteria are based on upper bounds to the magnitudes of earthquakes that can originate in a given seismic source, on the

amount of energy liberated by shocks per unit volume and per unit time or on more detailed statistical descriptions of the process.

6.3.1 Magnitude-recurrence expressions

Gutenberg and Richter (1954) obtained expressions relating earthquake magnitudes with their rates of occurrence for several zones of the earth. Their results can be put in the form:

$$\lambda = \alpha e^{-\beta M} \tag{6.6}$$

where λ is the mean number of earthquakes per unit volume and per unit time having magnitude greater than M and α and β are zone-dependent constants; α varies widely from point to point, as evidenced by the map of epicenters shown in Fig. 6.7, while β remains within a relatively narrow range, as shown in Fig. 6.8. Equation 6.6 implies a distribution of the energy liberated per shock which is very similar to that observed in the process of microfracturing of laboratory specimens of several types of rock subjected to gradually increasing compressive or bending strain (Mogi, 1962; Scholz, 1968). The values of β determined in the laboratory are of the same order as those obtained from seismic events, and have been shown to depend on the heterogeneity of the specimens and on their ability to yield locally. Thus, in heterogeneous specimens made of brittle materials many small shocks precede a major fracture, while in homogeneous or plastic materials the number of small shocks is relatively small. These cases correspond to large and small β-values, respectively. No general relationship is known to the writer between β and geotectonic features of seismic provinces: complexity of crustal structure and of stress gradients precludes extrapolation of laboratory results; and statistical records for relatively small zones of the earth are not, as a rule, adequate for establishing local values of β. Figure 6.8 shows that for very high magnitudes the observed frequency of events is lower than predicted by eq. 6.6. In addition, Rosenblueth (1969) has shown that β cannot be smaller than 3.46, since that would imply an infinite amount of energy liberated per unit time. However, Fig. 6.8 shows that the values of β which result from fitting expressions of the form 6.6 to observed data are smaller than 3.46; hence, for very high values of M (above 7, approximately) the curve should bend down, in accordance with statistical evidence.

Expressions alternative to eq. 6.6 have been proposed, attempting to represent more adequately the observed magnitude-recurrence data (Rosenblueth, 1964; Merz and Cornell, 1973). Most of these expressions also fail to recognize the existence of an upper bound to the magnitude that can be generated in a given source. Although no precise estimates of this upper bound can yet be obtained, recognition of its existence and of its dependence on the geotectonic characteristics of the source is inescapable. Indeed, the prac-

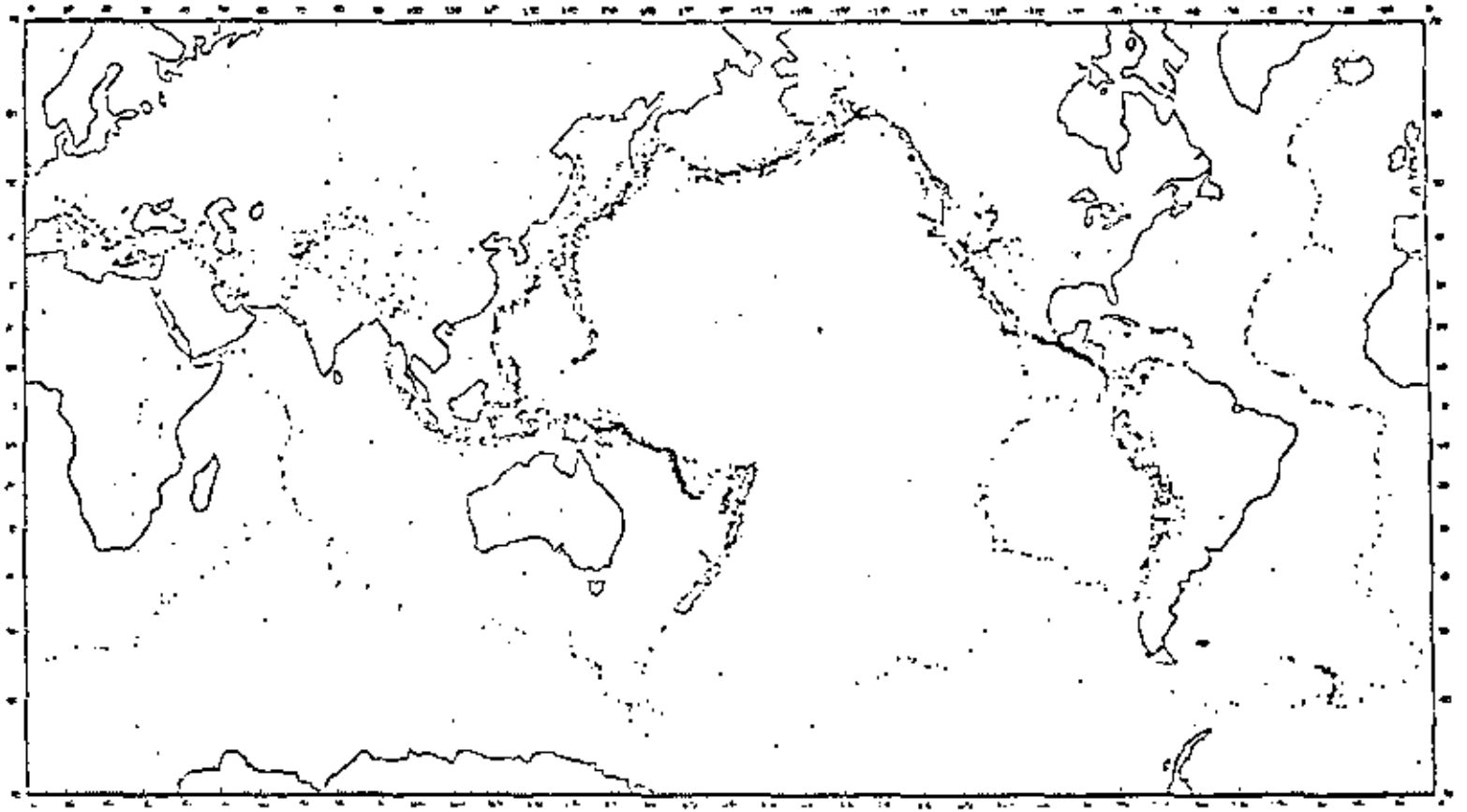

Fig. 6.7. Map showing epicenters for the interval 1961—1967. (After Newmark and Rosenblueth, 1971.)

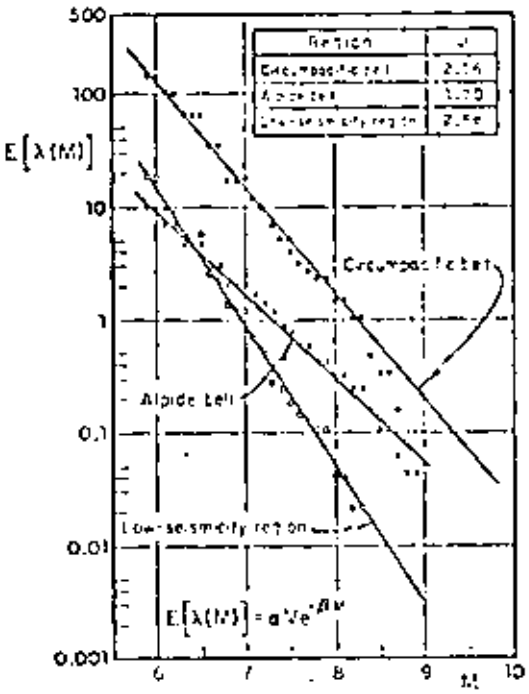

Fig. 6.8. Seismicity of macrozones. (After Esteva, 1968.)

tice of seismic zoning in the Soviet Union has been based on this concept (Gzovsky, 1962; Ananiin et al., 1968) and in many countries design spectra for very important structures, such as nuclear reactors or large dams, are usually derived from the assumption of a maximum credible intensity at a site; that intensity is ordinarily obtained by taking the maximum of the intensities that result at the site when at each of the potential sources an earthquake with magnitude equal to the maximum feasible value for that source is generated at the most unfavourable location within the same source. When this criterion is applied no attention is usually paid to the uncertainty in the maximum feasible magnitude nor to the probability that an earthquake with that magnitude will occur during a given time period. The need to formulate seismic-risk-related decisions that account both for upper bounds to magnitudes and for their probabilities of occurrence suggests adoption of magnitude recurrence expressions of the form:

$$\begin{aligned} \lambda &= \lambda_L G^*(M) && \text{for } M_L \leq M \leq M_U \\ &= \lambda_L && \text{for } M < M_L \\ &= 0 && \text{for } M > M_U \end{aligned} \qquad (6.7)$$

where M_L = lowest magnitude whose contribution to risk is significant, M_U

= maximum feasible magnitude, and $G^*(M)$ = complementary cumulative probability distribution of magnitudes every time that an event ($M \geq M_L$) occurs. A particular form of $G^*(M)$ that lends itself to analytical derivations is:

$$G^*(M) = A_0 + A_1 \exp(-\beta M) - A_2 \exp[-(\beta - \beta_1)M] \tag{6.8}$$

where:

$$A_0 = A\beta_1 \exp[-\beta(M_U - M_L)]$$

$$A_1 = A(\beta - \beta_1) \exp(\beta M_L)$$

$$A_2 = A_3 \exp(-\beta_1 M_U + \beta M_L)$$

$$A = [\beta(1 - \exp[-\beta_1(M_U - M_L)]) - \beta_1 (1 - \exp[-\beta(M_U - M_L)])]^{-1}$$

As M tends to M_L from above, eq. 6.7 approaches eq. 6.6. Adoption of adequate values of M_U and β_1 permits satisfying two additional conditions: the maximum feasible magnitude and the rate of variation of λ in its vicinity. When $\beta_1 \to \infty$, eq. 6.8 tends to an expression proposed by Cornell and Vanmarcke (1969).

Yegulalp and Kuo (1974) have applied the theory of extreme-values to estimating the probabilities that given magnitudes are exceeded in given time intervals. They assume those probabilities to fit an extreme type-III distribution given by:

$$F_{M_{max}}(M|t) = \exp[-C(M_U - M)^K t] \quad \text{for } M \leq M_U$$

$$= 0 \quad \text{for } M > M_U \tag{6.9}$$

Here $F_{M_{max}}(M|t)$ indicates the probability that the maximum magnitude observed in t years is smaller than M, M_U has the same meaning as above, and C and K are zone-dependent parameters. This distribution is consistent with the assumption that earthquakes with magnitudes greater than M take place in accordance with a Poisson process with mean rate λ equal to $C(M_U - M)^K$. Equation 6.9 produces magnitude recurrence curves that fit closely the statistical data on which they are based for magnitudes above 5.2 and return periods from 1 to 50 years, even though the values of M_U that result from pure statistical analysis are not reliable measures of the upper bound to magnitudes, since in many cases they turn out inadmissibly high.

For low magnitudes, only a fraction of the number of shocks that take place is detected. As a consequence, λ-values based on statistical information lie below those computed according to eqs. 6.6 and 6.8 for M smaller than about 5.5. In addition, Fig. 6.9, taken from Yegulalp and Kuo (1974), shows that the numbers of detected shocks fit the extreme type III in eq. 6.9 better than the extreme type-I distribution implied by eq. 6.6, coupled with the assumption of Poisson distribution of the number of events. It is not

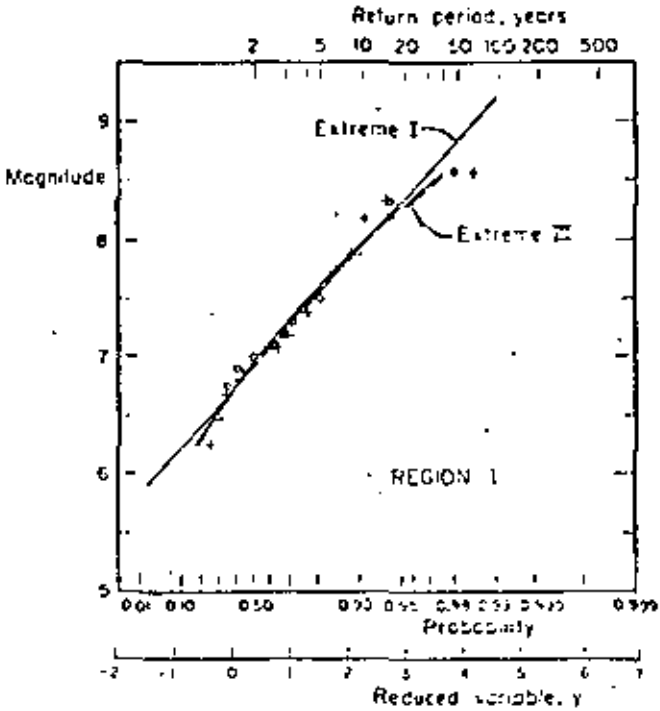

Fig. 6.9. Magnitude statistics in the Aleutian Islands region. (After Yegulalp and Kuo, 1974.)

clear what portion of the deviation from the extreme type-I distribution is due to the low values of the detectability levels and what portion comes from differences between the actual form of variation of λ with M and that given by eq. 6.6. The problem deserves attention because estimates of expected losses due to nonstructural damage may be sensitive to the values of λ for small magnitudes (say below 5.5) and because the evaluation of the level of seismic activity in a region is often made to depend on the recorded numbers of small magnitude shocks and on assumed detectability levels, i.e. of ratios of numbers of detected and occurred earthquakes (Kaila and Narain 1971; Kaila et al., 1972, 1974).

None of the expressions for λ presented in this chapter possess the desirable property that its applicability over a number of non-overlapping regions of the earth's crust implies the validity of an expression of the same form over the addition of those regions, unless some restrictions are imposed on the parameters of each λ. For instance, the addition of expressions like 6.6 gives place to an expression of the same form only if β is the same for all terms in the sum. Similar objections can be made to eq. 6.8. In what follows these forms will be preserved, however, as their accuracy is consistent with

the amount of available information and their adoption offers significant advantages in the evaluation of regional seismicity, as shown later.

6.3.2 Variation with depth

Depth of prevailing seismic activity in a region depends on its tectonic structure. For instance, most of the activity in the western coast of the United States and Canada consists of shocks with hypocentral depths in the range of 20–30 km. In other areas, such as the southern coast of Mexico, seismic events can be grouped into two ensembles: one of small shallow shocks and one of earthquakes with magnitudes comprised in a wide range, and with depths whose mean value increases with distance from the shoreline (Fig. 6.10). Figure 6.11 shows the depth distribution of earthquakes with magnitude above 5.9 for the whole circum-Pacific belt.

6.3.3 Stochastic models of earthquake occurrence

Mean exceedance rates of given magnitudes are expected averages during long time intervals. For decision-making purposes the times of earthquake occurrence are also significant. At present those times can only be predicted within a probabilistic context.

Let t_i ($i = 1, \ldots, n$) be the unknown times of occurrence of earthquakes generated in a given volume of the earth's crust during a given time interval, and let M_i be the corresponding magnitudes. For the moment it will be assumed that the risk is uniformly distributed throughout the given volume, and hence no attention will be paid to the focal coordinates of each shock.

Classical methods of time-series analysis have been applied by different researchers attempting to devise analytical models for random earthquake sequences. The following approaches are often found in the literature:

(a) Plotting of histograms of waiting times between shocks (Knopoff, 1964; Aki, 1963).

(b) Evaluation of Poisson's index of dispersion, that is of the ratio of the sample variance of the number of shocks to its expected value (Vere-Jones, 1970; Shlien and Toksöz, 1970). This index equals unity for Poisson processes, is smaller for nearly periodic sequences, and is greater than one when events tend to cluster.

(c) Determination of autocovariance functions, that is, of functions representing the covariance of the numbers of events observed in given time intervals, expressed in terms of the time elapsed between those intervals (Vere-Jones, 1970; Shlien and Toksöz, 1970). The autocovariance function of a Poisson process is a Dirac delta function. This feature is characteristic for the Poisson model since it does not hold for any other stochastic process.

(d) The hazard function $h(t)$, defined so that $h(t)\,dt$ is the conditional probability that an event will take place in the interval $(t, t + dt)$ given that

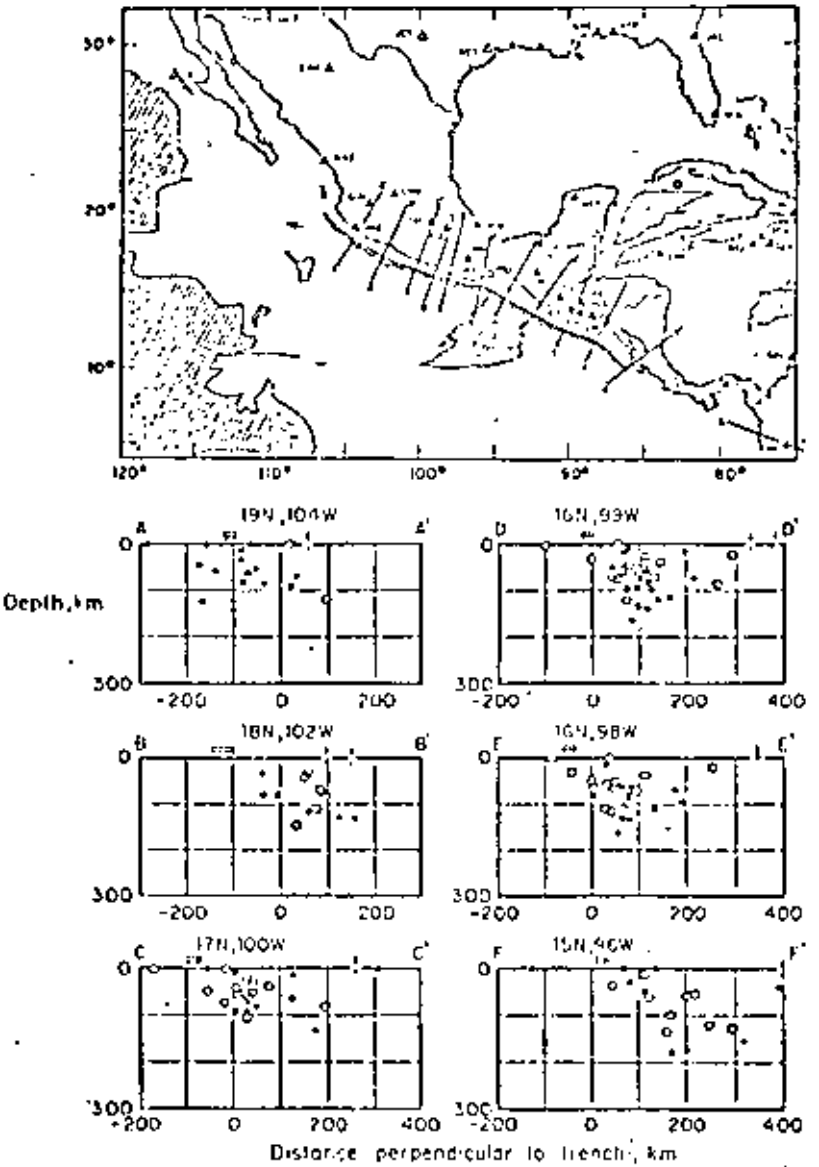

Fig. 6.10. Earthquake hypocenters projected onto a series of vertical sections through Mexico (After Molnar and Sykes, 1969.)

no events have occurred before t. If $F(t)$ is the cumulative probability distribution of the time between events:

$$h(t) = f(t)/[1 - F(t)] \tag{6.10}$$

where $f(t) = \partial F(t)/\partial t$.

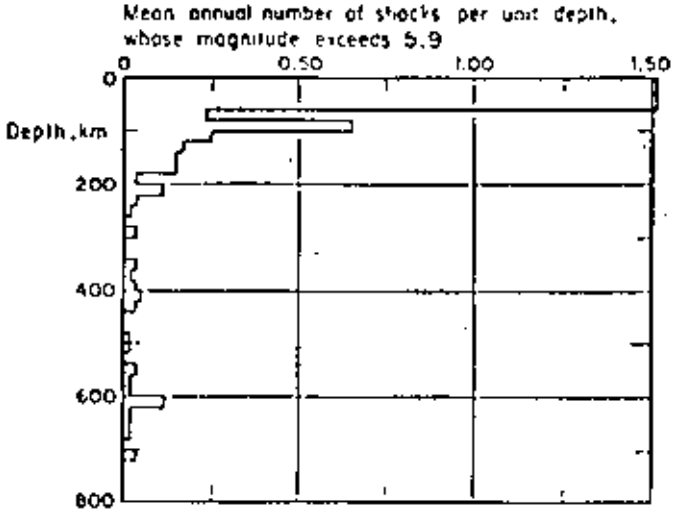

Fig. 6.11. Variation of seismicity with depth. Circum-Pacific Belt. (After Newmark and Rosenblueth, 1971.)

For the Poisson model, $h(t)$ is a constant equal to the mean rate of the process.

6.3.3.1 Poisson model

Most commonly applied stochastic models of seismicity assume that the events of earthquake occurrence constitute a Poisson process and that the M_i's are independent and identically distributed. This assumption implies that the probability of having N earthquakes with magnitude exceeding M during time interval $(0, t)$ equals:

$$p_N = [\exp(-\nu_M t)(\nu_M t)^N]/N! \qquad (6.11)$$

where ν_M is the mean rate of exceedance of magnitude M in the given volume. If N is taken equal to zero in eq. 6.11, one obtains that the probability distribution of the maximum magnitude during time interval t is equal to $\exp(-\nu_M t)$. If ν_M is given by eq. 6.6, the extreme type-I distribution is obtained.

Some weaknesses of this model become evident in the light of statistical information and of an analysis of the physical processes involved: the Poisson assumption implies that the distribution of the waiting time to the next event is not modified by the knowledge of the time elapsed since the last one, while physical models of gradually accumulated and suddenly released energy call for a more general renewal process such that, unlike what happens in the Poisson process, the expected time to the next event decreases as time goes on (Esteva, 1974). Statistical data show that the Poisson assump-

tion may be acceptable when dealing with large shocks throughout the world (Ben-Menahem, 1960), implying lack of correlation between seismicities of different regions; however, when considering small volumes of the earth, of the order of those that can significantly contribute to seismic risk at a site, data often contradict Poisson's model, usually because of clustering of earthquakes in time: the observed numbers of short intervals between events are significantly higher than predicted by the exponential distribution, and values of Poisson's index of dispersion are well above unity (Figs. 6.12 and 6.13). In some instances, however, deviations in the opposite direction have been observed: waiting times tend to be more nearly periodic, Poisson's index of dispersion is smaller than one, and the process can be represented by a renewal model. This condition has been reported, for instance, in the southern coast of Mexico (Esteva, 1971), and in the Kamchatka and Pamir—Hindu Kush regions (Gaisky, 1966 and 1967). The models under discussion also fail to account for clustering in space (Tsuboi, 1958; Gajardo and Lomnitz, 1960), for the evolution of seismicity with time, and for the systematic shifting of active sources along geologic accidents (Allen, Chapter 3 of this book). On account of its simplicity, however, the Poisson process model provides a valuable tool for the formulation of some seismic-risk-related decisions, particularly of those that are sensitive only to magnitudes of events having very long return periods.

6.3.3.2 Trigger models

Statistical analysis of waiting times between earthquakes does not favor the adoption of the Poisson model or of other forms of renewal processes, such as those that assume that waiting times are mutually independent with lognormal or gamma-distributions (Shlien and Toksöz, 1970). Alternative models have been developed, most of them of the 'trigger type' (Vere-Jones, 1970), i.e. the overall process of earthquake generation is considered as the superposition of a number of time series, each having a different origin, where the origin times are the events of a Poisson process. In general, let N be the number of events that take place during time interval $(0, t)$, τ_m = origin time of the mth series, $W_m(t, \tau_m)$ the corresponding number of events up to instant t, and n_t the random number of time series initiated in the interval $(0, t)$. The total number of events that occur before instant t is then:

$$N = \sum_{m}^{n_t} W_m(t, \tau_m) \qquad (6.12)$$

If origin times are distributed according to a homogeneous Poisson process with mean rate ν, and all W_m's are identically distributed stochastic processes with respect to $(t - \tau_m)$, it can be shown (Parzen, 1962) that the mean and variance of N can be obtained from:

$$E(N) = \nu \int_0^t E[W(t, \tau)]\mathrm{d}\tau \qquad (6.13)$$

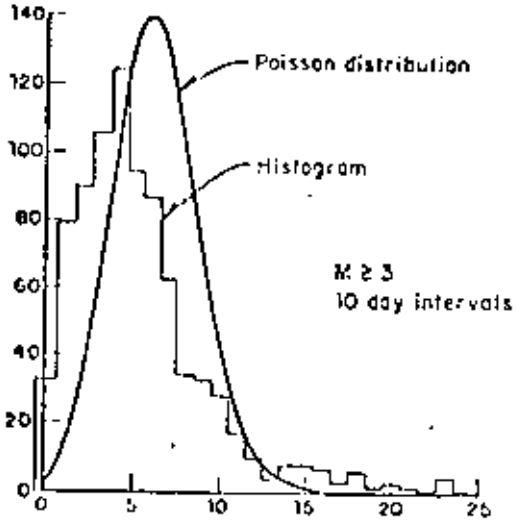

a) Including swarms

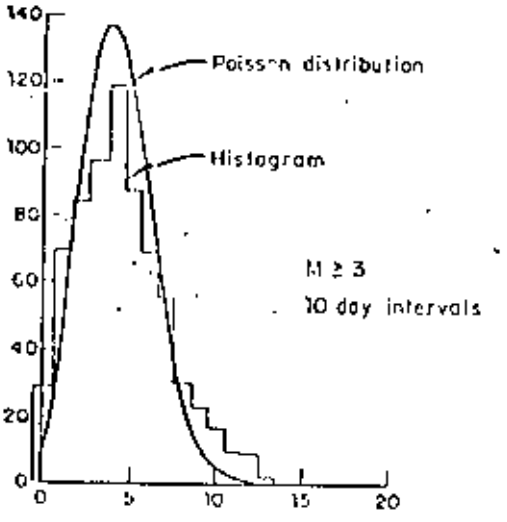

b) Eliminating swarms

Fig. 6.12. Evaluation of Poisson process assumption. (After Knopoff, 1964.)

$$\text{var}\,(N) = \nu \int_0^t E[W^2(t, \tau)]\,d\tau \tag{6.14}$$

Parzen (1962) gives also an expression for the probability generating function $\psi_N(Z; t)$ of the distribution of N in terms of $\psi_W(Z; t, \tau)$, the generat-

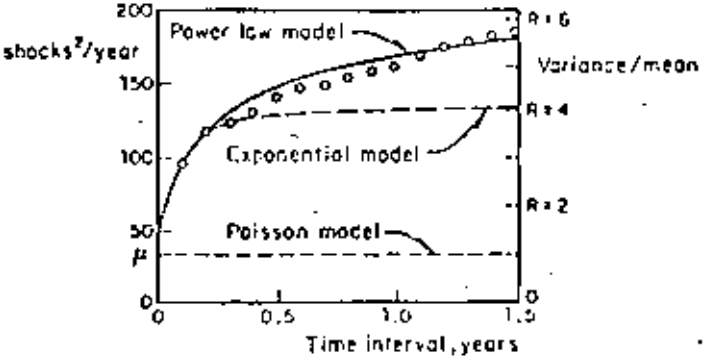

Fig. 6.13. Variance–time curve for New Zealand shallow shocks. (After Vere-Jones, 1966.)

ing function of each of the component processes:

$$\psi_N(Z; t) = \exp\left[-\nu t + \nu \int_0^t \psi_W(Z; t, \tau)d\tau\right] \tag{6.15}$$

where:

$$\psi_W(Z; t, \tau) = \sum_{n=0}^{\infty} Z^n \, P\{W(t, \tau) = n\} \tag{6.16}$$

and the probability mass function of N can be obtained from $\psi_N(Z; t)$ by recalling that:

$$\psi_N(Z; t) = \sum_{n=0}^{\infty} Z^n P\{N = n\}$$

expanding ψ_N in power series of Z, and taking $P\{N = n\}$ equal to the coefficient of Z^n in that expansion. For instance, if it is of interest to compute $P\{N = 0\}$, expansion of $\psi_N(Z; t)$ in a Taylor's series with respect to $Z = 0$ leads to:

$$\psi_N(Z; t) = \psi_N(0; t) + Z\psi'_N(0; t) + \frac{Z^2}{2!}\psi''_N(0; t) + \ldots \tag{6.17}$$

where the prime signifies derivative with respect to Z. From the definition of ψ_N, $P\{N = 0\} = \psi_N(0; t)$.

Because the component processes of 'trigger'-type time series appear overlapped in sample histories, their analytical representation usually entails study of a number of alternative models, estimation of their parameters, and comparison of model and sample properties — often second-order properties (Cox and Lewis, 1966).

Vere-Jones models. Applicability of some general 'trigger' models to rep-

resent local seismicity processes was discussed in a comprehensive paper by Vere-Jones (1970), who calibrated them mainly against records of seismic activity in New Zealand. In addition to simple and compound Poisson processes (Parzen, 1962), he considered Neyman-Scott and Bartlett-Lewis models, both of which assume that earthquakes occur in clusters and that the number of events in each cluster is stocastically independent of its origin time. In the Neyman-Scott model, the process of clusters is assumed stationary and Poisson, and each cluster is defined by p_N, the probability mass function of its number of events, and $A(t)$, the cumulative distribution function of the time of an event corresponding to a given cluster, measured from the cluster origin. The Bartlett-Lewis model is a special case of the former, where each cluster is a renewal process that ends after a finite number of renewals. In these models the conditional probability of an event taking place during the interval $(t, t + dt)$, given that the cluster consists of N shocks, is equal to $N\lambda(t)dt$, where $\lambda(t) = \partial A(t)/\partial t$.

Because clusters overlap in time they cannot easily be identified and separated. Estimation of process parameters is accomplished by assuming different sets of those parameters and evaluating the corresponding goodness of fit with observed data.

Various alternative forms of Neyman-Scott's model were compared by Vere-Jones with observed data on the basis of first- and second-order statistics: hazard functions, interval distributions (in the form of power spectra) and variance time curves. The statistical record comprises about one thousand New Zealand earthquakes with magnitudes greater than 4.5, recorded from 1912 to 1961. Figures 6.13–6.15 show results of the analysis for shallow New Zealand shocks as well as the comparison of observed data with sev-

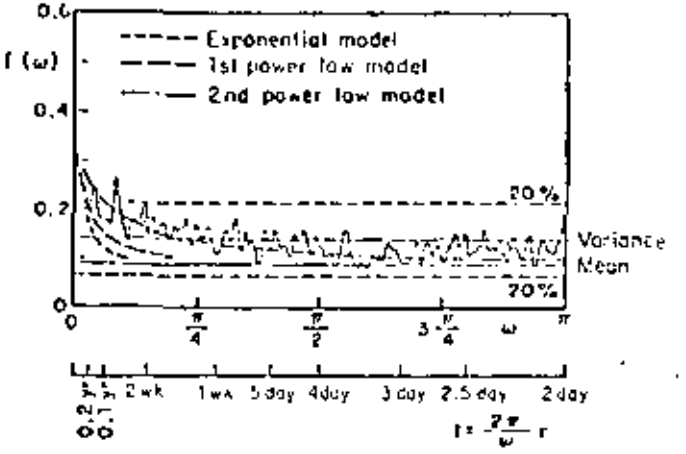

Fig. 6.14. Smoothed periodogram for New Zealand shallow shocks. (After Vere-Jones, 1966.)

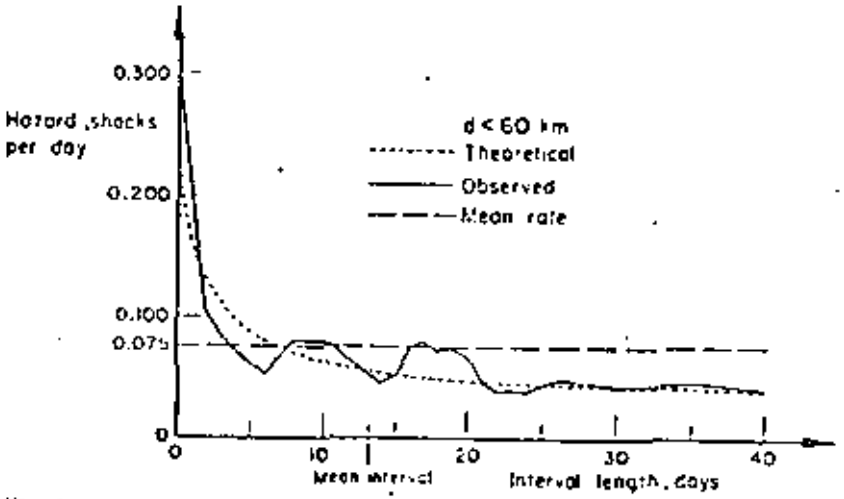

Fig. 6.15. Hazard function for New Zealand shallow shocks. (After Vere-Jones, 1970.)

eral alternative models. The process of cluster origins is Poisson in all cases, but the distributions of cluster sizes (N) and of times of events within clusters differ among the various instances: in the Poisson model no clustering takes place (the distribution of N is a Dirac delta function centered at $N = 1$) while in the exponential and in the power-law models the distribution of N is extremely skewed towards $N = 1$, and $A(t)$ is taken respectively as $1 - e^{-\lambda t}$

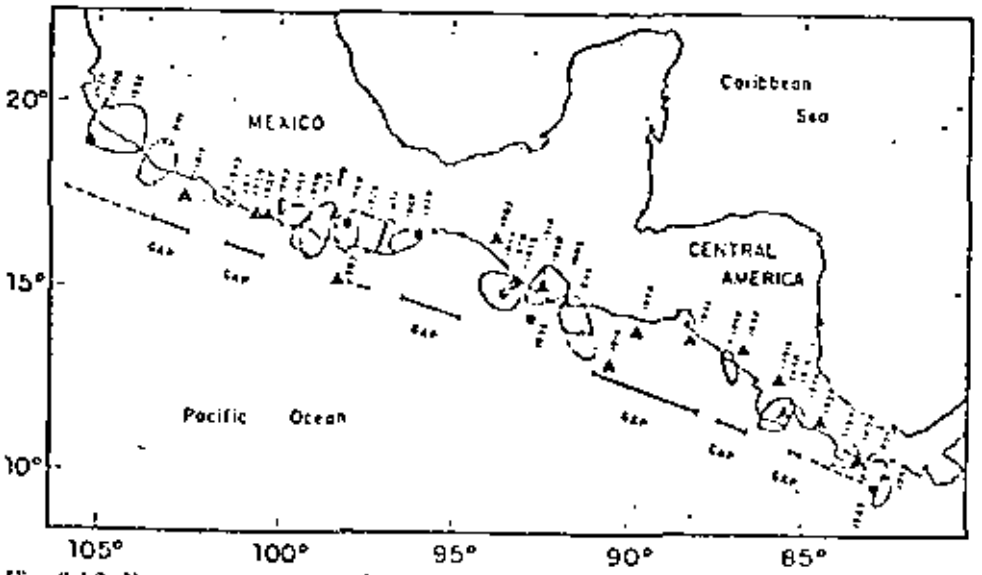

Fig. 6.16. Rupture zones and epicenters of large shallow Middle American earthquakes of this century. (After Kelleher et al., 1973.)

and $1 - [c/(c + t)]^{\delta}$ for $t \geq 0$, and as zero for $t < 0$, where λ, c, and δ are positive parameters. In Figs. 6.13—6.15, $\delta = 0.25$, $c = 2.3$ days, and $\lambda = 0.061$ shocks/day. The significance of clustering is evidenced by the high value of Poisson's dispersion index in Fig. 6.13, while no significant periodicity can be inferred from Fig. 6.14. Both figures show that the power-law model provides the best fit to the statistics of the samples. A similar analysis for New Zealand's deep shocks shows much less clustering: Poisson's dispersion index equals 2, and the hazard function is nearly constant with time.

Still, data reported by Gaisky (1967) have hazard functions that suggest models where the cluster origins as well as the clusters themselves may be represented by renewal processes. Mean return periods are of the order of several months, and hence these processes do not correspond, at least in the time scale, to the process of alternate periods of activity and quiescense of some geological structures cited by Kelleher et al. (1973), which have led to the concept of 'temporal seismic gaps', discussed below.

Simplified trigger models. Shlien and Toksöz (1970) proposed a simple particular case of the Neyman-Scott process; they lumped together all earthquakes taking place during non-overlapping time intervals of a given length and defined them as clusters for which $\lambda(t)$ was a Dirac delta function. Working with one-day intervals, they assumed the number of events per cluster to be distributed in accordance with the discrete Pareto law and applied a maximum-likelihood criterion to the information consisting of 35 000 earthquakes reported by the USCGS from January 1971 to August 1968. The model proposed represents reasonably well both the distribution of the number of earthquakes in one-day intervals and the dispersion index. However, owing to the assumption that no cluster lasts more than one day, the model fails to represent the autocorrelation function of the daily numbers of shocks for small time lags. The degree of clustering is shown to be a regional function, and to diminish with the magnitude threshold value and with the focal depth.

Aftershock sequences. The trigger processes described have been branded as reasonable representations of regional seismic activity, even when aftershock sequences and earthquake swarms are suppressed from statistical records, however arbitrary that suppression may be. The most significant instances of clustering are related, however, to aftershock sequences which often follow shallow shocks and only rarely intermediate and deep events. Persistence of large numbers of aftershocks for a few days or weeks has propitiated the detailed statistical analysis of those sequences since last century. Omori (1894) pointed out the decay in the mean rate of aftershock occurrence with t, the time elapsed since the main shock; he expressed that rate as inversely proportional to $t + q$, where q is an empirical constant. Utsu (1961) proposed a more general expression, proportional to $(t + c)^{-\zeta}$ where ζ is a constant; Utsu's proposal is consistent with the power-law expression for $\lambda(t)$ presented above.

Lomnitz and Hax (1966) proposed a clustering model to represent aftershock sequences; it is a modified version of Neyman and Scott's model, where the process of cluster origins is non-homogeneous Poisson with mean rate decaying in accordance with Omori's law, the number of events in each cluster has a Poisson distribution, and $M(t)$ is exponential. All the results and methods of analysis described by Vere-Jones (1970) for the stationary process of cluster origins can be applied to the nonstationary case through a transformation of the time scale. Fitting of paramrters to four aftershock sequences was accomplished through use of the second-order information of the sample defined on a transformed time scale. By applying this criterion to earthquake sets having magnitudes above different threshold values it was noticed that the degree of clustering decreases as the threshold value increases.

The magnitude of the main shock influences the number of aftershocks and the distribution of their magnitudes and, although the rate of activity decreases with time, the distribution of magnitudes remains stable throughout each sequence (Lomnitz, 1966; Utsu, 1962; Drakopoulos, 1971). Equation 6.6 represents fairly well the distribution of magnitudes observed in most aftershock sequences. Values of β range from 0.9 to 3.9 and decrease as the depth increases. Since values of β for regular (main) earthquakes are usually estimated from relatively small numbers of shocks generated throughout crust volumes much wider than those active during aftershock sequences, no relation has been established among β-values for series of both types of events. The parameters of Utsu's expression for the decay of aftershock activity with time have been estimated for several sequences, for instance those following the Aleutian earthquake of March 9, 1957, the Central Alaska earthquake of April 7, 1958, and the Southeastern Alaska earthquake of July 10, 1958 (Utsu, 1962); with magnitudes equal to 8.3, 7.3, and 7.9, respectively; c (in days) was 0.37, 0.40, and 0.03, while ζ was 1.05, 1.05 and 1.13, respectively. The relationship of the total number of aftershocks whose magnitude exceeds a given value with the magnitude of the main shock was studied by Drakopoulos (1971) for 140 aftershock sequences in Greece from 1912 to 1968. His results can be expressed by $N(M) = A \exp(-\beta M)$, where $N(M)$ is the total number of aftershocks with magnitude greater than M, and A is a function of M_0, the magnitude of the main shock:

$$A = \exp(3.62\,\beta + 1.1 M_0 - 3.46) \qquad (6.18)$$

Formulation of stochastic process models for given earthquake sequences is feasible once this relationship and the activity decay law are available for the source of interest. For seismic-risk estimation at a given site the spatial distribution of aftershocks may be as significant as the distribution of magnitudes and the time variation of activity, particularly for sources of relatively large dimensions.

6.3.3.3 Renewal process models

The trigger models described are based on information about earthquakes with magnitudes above relatively low thresholds recorded during time intervals of at most ten years. The degrees of clustering observed and the distributions of times between clusters cannot be extrapolated to higher magnitude thresholds and longer time intervals without further study.

Available information shows beyond doubt that significant clustering is the rule, at least when dealing with shallow shocks. However, there is considerable ground for discussion on the nature of the process of cluster origins during intervals of the order of one century or longer. While lack of statistical data hinders the formulation of seismicity models valid over long time intervals, qualitative consideration of the physical processes of earthquake generation may point to models which at least are consistent with the state of knowledge of geophysical sciences. Thus, if strain energy stored in a region grows in a more or less systematic manner, the hazard function should grow with the time elapsed since the last event, and not remain constant as the Poisson assumption implies. The concept of a growing hazard function is consistent with the conclusions of Kelleher et al. (1973) concerning the theory of periodic activation of *seismic gaps*. This theory is partially supported by results of nearly qualitative analysis of the migration of seismic activity along a number of geological structures. An instance is provided by the southern coast of Mexico, one of the most active regions in the world. Large shallow shocks are generated probably by the interaction of the continental mass and the subductive oceanic Cocos plate that underthrusts it and by compressive or flexural failure of the latter (Chapter 2). Seismological data show significant gaps of activity along the coast during the present century and not much is known about previous history (Fig. 6.16). Along these gaps, seismic-risk estimates based solely on observed intensities are quite low, although no significant difference is evident in the geological structure of these regions with respect to the rest of the coast, save some transverse faults which divide the continental formation into several blocks. Without looking at the statistical records a geophysicist would assign equal risk throughout the area. On the basis of seismicity data, Kelleher et al. have concluded that activity migrates along the region, in such a manner that large earthquakes tend to occur at seismic gaps, thus implying that the hazard function grows with time since the last earthquake. Similar phenomena have been observed in other regions; of particular interest is the North Anatolian fault where activity has shifted systematically along it from east to west during the last forty years (Allen, 1969).

Conclusions relative to activation of seismic gaps are controversial because the observation periods have not exceeded one cycle of each process. Nevertheless, those conclusions point to the formulation of stochastic models of seismicity that reflect plausible features of the geophysical processes.

These considerations suggest the use of renewal-process models to rep-

resent sequences of individual shocks or of clusters. Such models are characterized because times between events are independent and identically distributed. The Poisson process is a particular renewal model for which the distribution of the waiting time is exponential. Wider generality is achieved, without much loss of mathematical tractability, if inter-event times are supposed to be distributed in accordance with a gamma function:

$$f_T(t) = \frac{\nu}{(k-1)!}(\nu t)^{k-1}\, e^{-\nu t} \qquad (6.19)$$

which becomes the exponential distribution when $k = 1$. If $k < 1$, short intervals are more frequent and the coefficient of variation is greater than in the Poisson model; if $k > 1$, the reverse is true. Shlien and Toksöz (1970) found that gamma models were unable to represent the sequences of individual shocks they analyzed; but these authors handled time intervals at least an order of magnitude shorter than those referred to in this section.

On the basis of hazard function estimated from sequences of small shocks in the Hindu-Kush, Vere-Jones (1970) deduces the validity of 'branching renewal process' models, in which the intervals between cluster centers, as well as those between cluster members, constitute renewal processes.

Owing to the scarcity of statistical information, reliable comparisons between alternate models will have to rest partially on simulation of the process of storage and liberation of strain energy (Burridge and Knopoff, 1967; Veneziano and Cornell, 1973).

6.3.4 Influence of the seismicity model on seismic risk

Nominal values of investments made at a given instant increase with time when placing them at compound interest rates, i.e. when capitalizing them. Their real value — and not only the nominal one — will also grow, provided the interest rate overshadows inflation. Conversely, for the purpose of making design decisions, nominal values of expected utilities and costs inflicted upon in the future have to be converted into present or actualized values, which can be directly compared with initial expenditures. Descriptions of seismic risk at a site are insufficient for that purpose unless the probability distributions of the times of occurrence of different intensities — or magnitudes at neighbouring sources — are stipulated: this entails more than simple magnitude-recurrence graphs or even than maximum feasible magnitude estimates.

Immediately after the occurrence of a large earthquake, seismic risk is abnormally high due to aftershock activity and to the probability that damage inflicted by the main shock may have weakened natural or man-made structures if emergency measures are not taken in time. When aftershock activity has ceased and damaged systems have been repaired, a normal risk level is attained, which depends on the probability-density functions of the waiting times to the ensuing damaging earthquakes.

For the purpose of illustration, let it be assumed that a fixed and deterministically known damage D_0 occurs whenever a magnitude above a given value is generated at a given source. If $f(t)$ is the probability-density function of the waiting time to the occurrence of the damaging event, and if the risk level is sufficiently low that only the first failure is of concern, the expected value of the actualized cost of damage is (see Chapter 9):

$$\bar{D} = D_0 \int_0^{\infty} e^{-\gamma t} f(t) dt \qquad (6.20)$$

where γ is the discount (or compound interest) coefficient and the overbar denotes expectation. If the process is Poisson with mean rate ν, then $f(t)$ is exponential and $D \simeq D_0\ \nu/\gamma$; however, if damaging events take place in clusters and most of the damage produced by each cluster corresponds to its first event, the computation of D should make use of the mean rate ν corresponding to the clusters, instead of that applicable to individual events. Table 6.II shows a comparison of seismic risk determined under the alternative assumptions of a Poisson and a gamma model ($k = 2$), both with the same mean return period, k/ν (Esteva, 1974). Three descriptions of risk are presented as functions of the time t_0 elapsed since the last damaging event: T_1, the expected time to the next event, measured from instant t_0; the expected value of the present cost of failure computed from eq. 6.20, and the hazard function (or mean failure rate). Since clustering is neglected, risk of aftershock occurrence must be either included in D_0 or superimposed on that displayed in the table.

This table shows very significant differences among risk levels for both processes. At small values of t_0, risk is lower for the gamma process, but it

TABLE 6.II

Comparison of Poisson and gamma processes

$t_0\ \nu/k$	$T_1\ \nu/k$	Poisson process, $k = 1$		$h k/\nu$	$T_1\ \nu/k$	Gamma process, $k = 2$		$h k/\nu$
		D/D_0				D/D_0		
		$\gamma k/\nu = 10$	$\gamma k/\nu = 100$			$\gamma k/\nu = 10$	$\gamma k/\nu = 100$	
0					1.0	0.0278	0.0001	0
0.1					0.92	0.0511	0.0036	0.367
0.2					0.86	0.0675	0.0059	0.667
0.5					0.75	0.0973	0.0100	1.333
1	1.0	0.0909	0.0099	1.0	0.67	0.120	0.0132	2.000
2					0.60	0.139	0.0158	2.667
5					0.54	0.151	0.0179	3.333
10					0.52	0.160	0.0187	3.633
					0.50	0.167	0.0196	4.000

grows with time, until it outrides that for the Poisson process, which remains constant. The differences shown clearly affect engineering decisions.

6.4 ASSESSMENT OF LOCAL SEISMICITY

Only exceptionally can magnitude-recurrence relations for small volumes of the earth's crust and statistical correlation functions of the process of earthquake generation be derived exclusively from statistical analysis of recorded shocks. In most cases this information is too limited for that purpose and it does not always reflect geological evidence. Since the latter, as well as its connection with seismicity, is beset with wide uncertainty margins, information of different nature has to be evaluated, its uncertainty analyzed, and conclusions reached consistent with all pieces of information. A probabilistic criterion that accomplishes this is presented here: on the basis of geotectonic data and of conceptual models of the physical processes involved, a set of alternate assumptions can be made concerning the functions in question (magnitude recurrence, time, and space correlation) and an initial probability distribution assigned thereto; statistical information is used to judge the likelihood of each assumption, and a posterior probability distribution is obtained. How statistical information contibutes to the posterior probabilities of the alternate assumptions depends on the extent of that information and on the degree of uncertainty implied by the initial probabilities. Thus, if geological evidence supports confidence in a particular assumption or range of assumptions, statistical information should not greatly modify the initial probabilities. If, on the other hand, a long and reliable statistical record is available, it practically determines the form and parameters of the mathematical model selected to represent local seismicity.

6.4.1 Bayesian estimation of seismicity

Bayesian statistics provide a framework for probabilistic inference that accounts for prior probabilities assigned to a set of alternate hypothetical models of a given phenomenon as well as for statistical samples of events related to that phenomenon. Unlike conventional methods of statistical inference, Bayesian methods give weight to probability measures obtained from samples or from other sources; numbers, coordinates and magnitudes of earthquakes observed in given time intervals serve to ascertain the probable validity of each of the alternative models of local seismicity that can be postulated on the grounds of geological evidence. Any criterion intended to weigh information of different nature and different degrees of uncertainty should lead to probabilistic conclusions consistent with the degree of confidence attached to each source of information. This is accomplished by Bayesian methods.

Let H_i ($i = 1, ..., n$) be a comprehensive set of mutually exclusive assumptions concerning a given, imperfectly known phenomenon and let A be the observed outcome of such a phenomenon. Before observing outcome A we assign an initial probability $P(H_i)$ to each hypothesis. If $P(A|H_i)$ is the probability of A in case hypothesis H_i is true, then Bayes' theorem (Raiffa and Schlaifer, 1968) states that:

$$P(H_i|A) = P(H_i)\frac{P(A|H_i)}{\Sigma_j P(H_j)P(A|H_j)} \tag{6.21}$$

The first member in this equation is the (posterior) probability that assumption H_i is true, given the observed outcome A.

In the evaluation of seismic risk, Bayes' theorem can be used to improve initial estimates of $\lambda(M)$ and its variation with depth in a given area as well as those of the parameters that define the shape of $\lambda(M)$ or, equivalently, the conditional distribution of magnitudes given the occurrence of an earthquake. For that purpose, take $\lambda(M)$ as the product of a rate function $\lambda_L = \lambda(M_L)$ by a shape function $G^*(M,B)$, equal to the conditional complementary distribution of magnitudes given the occurrence of an earthquake with $M \geq M_L$; where M_L is the magnitude threshold of the set of statistical data used in the estimation, and B is the vector of (uncertain) parameters $B_1, ..., B_r$ that define the shape of $\lambda(M)$. For instance, if $\lambda(M)$ is taken as given by eq. 6.8; B is a vector of three elements equal respectively to β, β_1, and M_U; if eq. 6.9 is adopted, B is defined by h and M_U.

The initial distribution of seismicity is in this case expressed by the initial joint probability density function of λ_L and B: $f'(\lambda_L, B)$. The observed outcome A can be expressed by the magnitudes of all earthquakes generated in a given source during a given time interval. For instance, suppose that N earthquakes were observed during time interval t and that their magnitudes were $m_1, m_2, ..., m_N$. Bayes' expression takes the form:

$$f''(\lambda_L, B|m_1, ..., m_N; t) = f'(\lambda_L, B)\frac{P[m_1, m_2, ..., m_N; t|\lambda_L, B]}{\iint P[m_1, m_2, ..., m_N; t|l, b]f'(l,b)\mathrm{d}l\mathrm{d}b} \tag{6.22}$$

where $f''(.)$ is the posterior probability density function, and l and b are dummy variables that stand for all values that may be taken by λ_L and B, respectively. Estimation of λ_L can usually be formulated independently of that of the other parameters. The observed fact is then expressed by N_L, the number of earthquakes with magnitude above M_L during time t, and the following expression is obtained, as a first step in the estimation of $\lambda(M)$:

$$f''(\lambda_L|N_L; t) = f'(\lambda_L)\frac{P(N_L; t|\lambda_L)}{\int P(N_L; t|l)f'(l)\mathrm{d}l} \tag{6.23}$$

6.4.1.1 Initial probabilities of hypothetical models

Where statistical information is scarce, seismicity estimates will be very

sensitive to initial probabilities assigned to alternative hypothetical models; the opinions of geologists and geophysicists about probable models, about the parameters of these models, and the corresponding margins of uncertainty should be adequately interpreted and expressed in terms of a function f', as required by equations similar to 6.22 and 6.23. Ideally, these opinions should be based on the formulation of potential earthquake sources and on their comparison with possibly similar geotectonic structures. This is usually done by geologists, more qualitatively than quantitatively, when they estimate M_E. Initial estimates of λ_L are seldom made, despite the significance of this parameter for the design of moderately important structures (see Chapter 9).

Analysis of geological information must consider local details as well as general structure and evolution. In some areas it is clear that all potential earthquake sources can be identified by surface faults, and their displacements in recent geological times measured. When mean displacements per unit time can be estimated, the order of magnitude of creep and of energy liberated by shocks and hence of the recurrence intervals of given magnitudes can be established (Wallace, 1970; Davies and Brune, 1971), the corresponding uncertainty evaluated, and an initial probability distribution assigned. The fact that magnitude-recurrence relations are only weakly correlated with the size of recent displacements is reflected in large uncertainties (Petrushevsky, 1966).

Application of the criterion described in the foregoing paragraph can be unfeasible or inadequate in many problems, as in areas where the abundance of faults of different sizes, ages, and activity, and the insufficient accuracy with which focal coordinates are determined preclude a differentiation of all sources. Regional seismicity may then be evaluated under the assumption that at least part of the seismic activity is distributed in a given volume rather than concentrated in faults of different importance. The same situation would be faced when dealing with active zones where there is no surface evidence of motions. Hence, consideration of the overall behavior of complex geological structures is often more significant than the study of local details.

Not much work has been done in the analysis of the overall behavior of large geological structures with respect to the energy that can be expected to be liberated per unit volume and per unit time in given portions of those structures. Important research and applications should be expected, however, since, as a result of the contribution of plate-tectonics theory to the understanding of large-scale tectonic processes, the numerical values of some of the variables correlated with energy liberation are being determined, and can be used at least to obtain orders of magnitude of expected activity along plate boundaries. Far less well understood are the occurrence of shocks in apparently inactive regions of continental shields and the behavior of complex continental blocks or regions of intense folding, but even there some

progress is expected in the study of accumulation of stresses in the crust.

Knowledge of the geological structure can serve to formulate initial probability distributions of seismicity even when quantitative use of geophysical information seems beyond reach. Initial probability distributions of local seismicity parameters λ_L, B in the small volumes of the earth's crust that contribute significantly to seismic risk at a site, can be assigned by comparison with the average seismicity observed in wider areas of similar tectonic characteristics, or where the extent and completeness of statistical information warrant reliable estimates of magnitude-recurrence curves (Esteva, 1969). In this manner we can, for instance, use the information about the average distribution of the depths of earthquakes of different magnitudes throughout a seismic province to estimate the corresponding distribution in an area of that province, where activity has been low during the observation interval, even though there might be no apparent geophysical reason to account for the difference. Similarly, the expected value and coefficient of variation of λ_L in a given area of moderate or low seismicity (as a continental shield) can be obtained from the statistics of the motions originated at all the supposedly stable or aseismic regions in the world.

The significance of initial probabilities in seismic risk estimates, against the weight given to purely statistical information, becomes evident in the example of Fig. 6.16: if Kelleher's theory about activation of seismic gaps is true, risk is greater at the gaps than anywhere else along the coast; if Poisson models are deemed representative of the process of energy liberation, the extent of statistical information is enough to substantiate the hypothesis of reduced risk at gaps. Because both models are still controversial, and represent at most two extreme positions concerning the properties of the actual process, risk estimates will necessarily reflect subjective opinions.

6.4.1.2 Significance of statistical information

Estimation of λ_L. Application of eq. 6.23 to estimate λ_L independently of other parameters will be first discussed, because it is a relatively simple problem and because λ_L is usually more uncertain than M_U and much more so than β.

A model as defined by eq. 6.19 will be assumed to apply. If the possible assumptions concerning the values of λ_L constitute a continuous interval, the initial probabilities of the alternative hypotheses can be expressed in terms of a probability-density function of λ_L. If, in addition, a certain assumption is made concerning the form of this probability-density function, only the initial values of $E(\lambda_L)$ and $V(\lambda_L)$ have to be assumed. It is advantageous to assign to $\nu = k/E(T)$ a gamma distribution. Then, if ρ and μ are the parameters of this initial distribution of ν, if k is assumed to be known, and if the observed outcome is expressed as the time t_n elapsed during $n+1$ consecutive events (earthquakes with magnitude $\geq M_L$), application of eq. 6.23 leads to the conclusion that the posterior probability function of ν is

also gamma, now with parameters $\rho + nk$ and $\mu + t_n$. The initial and the posterior expected values of ν are respectively equal to ρ/μ, and to $(\rho + nk)/(\mu + t_n)$. When initial uncertainty about ν is small, ρ and μ will be large and the initial and the posterior expected values of ν will not differ greatly. On the other hand, if only statistical information were deemed significant, ρ and μ should be given very small values in the initial distribution, and $E(\nu)$, and hence λ_L, will be practically defined by n, k, and t_n. This means that the initial estimates of geologists should not only include expected or most probable values of the different parameters, but also statements about ranges of possible values and degrees of confidence attached to each.

In the case studied above only a portion of the statistical information was used. In most cases, especially if seismic activity has been low during the observation interval, significant information is provided by the durations of the intervals elapsed from the initiation of observations to the first of the $n + 1$ events considered, and from the last of these events until the end of the observation period. Here, application of eq. 6.23 leads to expressions slightly more complicated than those obtained when only information about t_n is used.

The particular case when the statistical record reports no events during *at least* an interval $(0, t_0)$ comes up frequently in practical problems. The probability-density function of the time T_1 from t_0 to the occurrence of the first event must account for the corresponding shifting of the time axis. Furthermore, if the time of occurrence of the last event before the origin is unknown, the distribution of the waiting time from $t = 0$ to the first event coincides with that of the *excess life* in a renewal process at an arbitrary value of t that approaches infinity (Parzen, 1962). For the particular case when the waiting times constitute a gamma process, T_1 is measured from $t = 0$, T is the waiting time between consecutive events, and it is known that $T_1 \geq t_0$, the conditional density function of $\tau_1 = (T_1 - t_0)/E(T)$ is given by eq. 6.24 (Esteva, 1974), where $u_0 = t_0/E(T)$:

$$f_{\tau_1}(u|T_1 \geq t_0) = \frac{\sum_{m=1}^{k} \frac{k}{(m-1)!} [k(u+u_0)]^{m-1}}{\sum_{m=1}^{k} \sum_{n=1}^{m} \frac{1}{(n-1)!} (ku_0)^{n-1}} e^{-ku} \qquad (6.24)$$

Consider now the implications of Bayesian analysis when applied to one of the seismic gaps in Fig. 6.16, under the conditions implicit in eq. 6.24. An initial set of assumptions and corresponding probabilities was adopted as described in the following. From previous studies referring to all the southern coast of Mexico, local seismicity in the gap area (measured in terms of λ for $M \geq 6.5$) was represented by a gamma process with $k = 2$. An initial

probability density function for ν was adopted such that the expected value of $\lambda(6.5)$ for the region coincided with its average throughout the complete seismic province. Two values of ρ were considered: 2 and 10, which correspond to coefficients of variation of 0.71 and 0.32, respectively. Values in Table 6.II were obtained for the ratio of the final to the initial expected values of ν, in terms of u_0.

The last two columns in the table contain the ratios of the computed values of $E''(T_1)$ and $E'(T)$ when ν is taken as equal respectively to its initial or to its posterior expected value. This table shows that, for $\rho = 10$, that is, when uncertainty attached to the geologically based assumptions is low, the expected value of the time to the next event keeps decreasing, in accordance with the conclusions of Kelleher et al. (1973). However, as time goes on and no events occur, the statistical evidence leads to a reduction in the estimated risk, which shows in the increased conditional expected values of T_1. For $\rho = 2$, the geological evidence is less significant and risk estimates decrease at a faster rate.

6.4.1.3 Bayesian estimation of jointly distributed parameters

In the general case, estimation of B will consist in the determination of the posterior Bayesian joint probability function of its components, taking as statistical evidence the relative frequencies of observed magnitudes. Thus, if event A is described as the occurrence of N shocks, with magnitudes $m_1, \ldots, m_N$, and b_i ($i = 1, \ldots, r$) are values that may be adopted by the components of vector B being estimated, eq. 6.21 becomes:

$$f''_B(b_1, \ldots, b_r|A) = \frac{f'_B(b_1, \ldots, b_r)P(A|b_1, \ldots, b_r)}{\int \ldots \int f'_B(u_1, \ldots, u_r)P(A|u_1, \ldots, u_r)\mathrm{d}u_1, \ldots, \mathrm{d}u_r} \qquad (6.25)$$

where $P(A|u_1, \ldots, u_r)$ is proportional to:

$$\prod_{i=1}^{N} g(m_i|u_1, \ldots, u_r)$$

and $g(m) = -\partial G^*(m)/\partial m$.

Closed-form solutions for f'' as given by eq. 6.25 are not feasible in general. For the purpose of evaluating risk, however, estimates of the posterior first and second moments of f'' can be obtained from eq. 6.25, making use of available first-order approximations (Benjamin and Cornell, 1970; Rosenblueth, 1975). Thus, the posterior expected value of B_i is given by $\int f''_{B_i}(u)\, u\, \mathrm{d}u$, where $f''_{B_i}(u_i) = \int \ldots \int f''_B(u_1, \ldots, u_r)\, \mathrm{d}u_1, \ldots, \mathrm{d}u_n$ and the multiple integral is of order $r - 1$, because it is not extended to the dominion of B_i. Hence:

$$E''(B_i) = \frac{E'_B[B_i P(A|B_1, \ldots, B_r)]}{E'_B[P(A|B_1, \ldots, B_r)]} \qquad (6.26)$$

TABLE 6.III

Bayesian estimates of seismicity in one seismic gap

$u_0 = t_0/E'(T)$	$E''(\nu)/E'(\nu)$		$E''(T_1 \mid T_1 > t_0)/E'(T)$	
	$\rho = 2$	$\rho = 10$	$\rho = 2$	$\rho = 10$
0	1.0	1.0	0.75	0.75
0.1	0.95	0.99	0.76	0.74
0.5	0.75	0.94	0.91	0.71
1	0.58	0.87	1.14	0.73
5	0.20	0.54	3.11	1.05
10	0.11	0.36	5.47	1.55
20	0.06	0.22	10.50	2.48

where E' and E'' stand for initial and posterior expectation, and subscript B means that expectation is taken with respect to all the components of B. Likewise, the following *posterior moments* can be obtained:

Covariance of B_i and B_j

$$\mathrm{Cov}''(B_i, B_j) = \frac{E'_B[B_i B_j P(A|B_1, \ldots, B_r)]}{E'_B[P(A|B_1, \ldots, B_r)]} - E''(B_i)E''(B_j) \tag{6.27}$$

Expected value of $\lambda(M)$

$$E''[\lambda(M)] = E''(\lambda_1)E''[G^*(M; B)]$$
$$= E''(\lambda_1)\frac{E'_B[G^*(M; B)P(A|B_1, \ldots, B_r)]}{E'_B[P(A|B_1, \ldots, B_r)]} \tag{6.28}$$

Marginal distributions. The posterior expectation of $\lambda(M)$ is in some cases all that is required to describe seismicity for decision-making purposes. Often, however, uncertainty in $\lambda(M)$ must also be acounted for. For instance, the probability of exceedance of a given magnitude during a given time interval has to be obtained as the expectation of the corresponding probabilities over all alternative hypotheses concerning $\lambda(M)$. In this manner it can be shown that, if the occurrence of earthquakes is a Poisson process and the Bayesian distribution of λ_L is gamma with mean $\bar{\lambda}_L$ and coefficient of variation V_L, the marginal distribution of the number of earthquakes is negative binomial with mean $\bar{\lambda}_L$. In particular, the marginal probability of zero events during time interval t — equivalently, the complementary distribution function of the waiting time between events — is equal to $(1 + t/t^*)^{-r^*}$, where $r^* = V_L^{-2}$ and $t^* = r^*/\bar{\lambda}_L$. The marginal probability-density function of the waiting time, that should be substituted in eq. 6.20, is $\bar{\lambda}_L(1 + t/t^*)^{-r^*-1}$, which tends to the exponential probability function as r^* and t^* tend to infinity (and $V_L \to 0$) while their ratio remains equal to $\bar{\lambda}_L$.

Bayesian uncertainty tied to the joint distribution of all seismicity parameters (λ_L, B_1, ..., B_r) can be included in the computation of the probability of occurrence of a given event Z by taking the expectation of that probability with respect to all parameters:

$$P(Z) = E_{\lambda_L, B}[P(Z); \lambda_L, B_1, ..., B_r)] \tag{6.29}$$

When the joint distribution of λ_L, B stems from Bayesian analysis of an initial distribution and an observed event, A, this equation adopts the form:

$$P''(Z) = \frac{E'_{\lambda_L, B}[P(Z|\lambda_L, B)P(A|\lambda_L, B)]}{E'_{\lambda_L, B}[P(A|\lambda_L, B)]} \tag{6.30}$$

where $'$ and $''$ stand for initial and posterior, respectively.

Spatial variability. Figure 6.17 shows a map of geotectonic provinces of Mexico, according to F. Mooser. Each province is characterized by the large-scale features of its tectonic structure, but significant local perturbations to the overall patterns can be identified. Take for instance zone 1, whose seismotectonic features were described above, and are schematically shown in Fig. 6.18 (Singh, 1975): the Pacific plate underthrusts the continental block and is thought to break into several blocks, separated by faults transverse to the coast, that dip at different angles. The continental mass is also

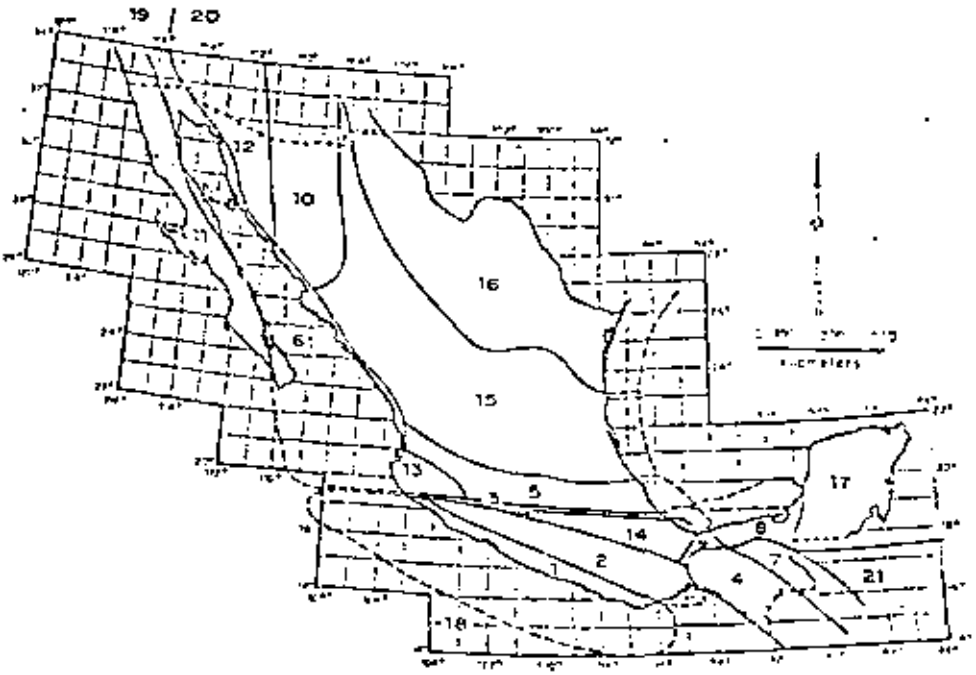

Fig. 6.17. Seismotectonic provinces of Mexico. (After F. Mooser.)

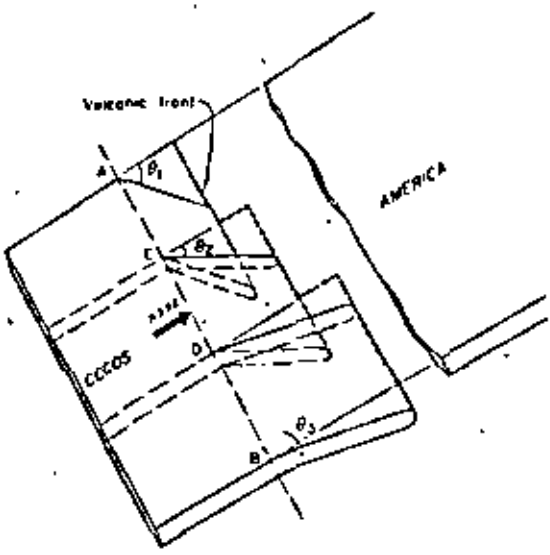

$\theta_1 > \theta_2 > \theta_3$

Fig. 6.16. Schematic drawing of the segmenting of Cocos plate as it subducts below American plate. (After Singh, 1974.)

made up of several large blocks. Seismic activity at the underthrusting plate or at its interface with the continental mass is characterized by magnitudes that may reach very high values and by the increase of mean hypocentral depth with distance from the coast; small and moderate shallow shocks are generated at the blocks themselves. Variability of statistical data along the whole tectonic system was discussed above and is apparent in Fig. 6.10. Bayesian estimation of local seismicity averaged throughout the system is a matter of applying eq. 6.21 or any of its special forms (eqs. 6.22 and 6.23), taking as statistical evidence the information corresponding to the whole system. However, seismic risk estimates are sensitive to values of local seismicity averaged over much smaller volumes of the earth's crust; hence the need to develop criteria for probabilistic inference of possible patterns of space variability of seismicity along tectonically homogeneous zones.

On the basis of seismotectonic information, the system under consideration can first be subdivided into the underthrusting plate and the subsystem of shallow sources; each subsystem can then be separately analyzed. Take for instance the underthrusting plate and subdivide it into s sufficiently small equal-volume subzones. Let ν_L be the rate of exceedance of magnitude M_L throughout the main system, ν_{L_i} the corresponding rate at each subzone, and define p_i as ν_{L_i}/ν_L, with p_i independent of ν_L (p_i is equal to the probability that an earthquake known to have been generated in the overall system originated at subzone i). Initial information about possible space variability of

ν_{L_i} can be expressed in terms of an initial probability distribution of p_i and of the correlation among p_i and p_j for any i and j. Because $\Sigma\nu_{L_i} = \nu_L$, one obtains $\Sigma p_i = 1$. This imposes two restrictions on the initial joint probability distribution of the p_i's: $E'(p_i) = 1$, $\text{var}'\ \Sigma p_i = 0$. If all p_i's are assigned equal expectations and all pairs $p_i, p_j, i \neq j$ are assumed to possess the same correlation coefficient $\rho_{ij} = \rho'$, the restrictions mentioned lead to $E'(p_i) = 1/s$ and $\rho' = -1/(s-1)$. Posterior values of $E(p_i)$ and ρ_{ij} are obtained according to the same principles that led to eqs. 6.25–6.28. Statistical evidence is in this case described by N, the total number of earthquakes generated in the system, and n_i $(i = 1, \ldots, s)$ the corresponding numbers for the subzones. Given the p_i's, the probability of this event is the multinomial distribution:

$$P[A|p_1, \ldots, p_s] = \frac{N!}{n_1!, \ldots, n_s!}\, p_1^{n_1} \ldots p_s^{n_s} \tag{6.31}$$

If the correlation coefficients among seismicities of the various subzones can be neglected, each p_i can be separately estimated. Because p_i has to be comprised between 0 and 1, it is natural to assign it a beta initial probability distribution, defined by its parameters n_i' and N_i', such that $E'(p_i) = n_i'/N_i'$ and $\text{var}'(p_i) = n_i'(N_i' - n_i')/[N_i'^2(N_i' + 1)]$ (Raiffa and Schlaifer, 1968). The parameters of the posterior distribution will be:

$$n_i'' = n_i' + n_i,\ N_i'' = N_i' + N$$

Take for instance a zone whose prior distribution of λ_L is assumed gamma with expected value λ_L' and coefficient of variation V_L'. Suppose that, on the basis of geological evidence and of the dimensions involved, it is decided to subdivide the zone into four subzones of equal dimensions; a-priori considerations lead to the assignment of expected values and coefficients of variation of p_i for those subzones, say $E'(p_i) = 0.25$, $V'(p_i) = 0.25$ $(i = 1, \ldots, 4)$. From previous considerations for $s = 4$ take $\rho_{ij}' = -1/3$ for $i \neq j$. Suppose now that, during a given time interval t, ten earthquakes were observed in the zone, of which 0, 1, 3, and 6 occurred respectively in each subzone. If the Poisson process model is adopted, λ_L' and V_L' can be expressed in terms of a fictitious number of events $n' = V_L'^{-2}$ occurred during a fictitious time interval $t' = n'/\bar{\lambda}_L'$; after observing n earthquakes during an interval t, the Bayesian mean and coefficient of variation of λ_L will be $\bar{\lambda}_L'' = (n' + n)/(t' + t)$, $V_L'' = (n' + n)^{-1/2}$ (Esteva, 1968). Hence:

$$\bar{\lambda}_L'' = (V_L'^{-2} + 10)/(V_L'^{-2}\bar{\lambda}_L'^{-1} + t), \qquad V_L'' = (V_L'^{-2} + 10)^{-1/2}$$

Local deviations of seismicity in each subzone with respect to the average λ_L can be analyzed in terms of p_i $(i = 1, \ldots, 4)$; Bayesian analysis of the proportion in which the ten earthquakes were distributed among the subzones proceeds according to:

$$E''(p_i|A) = \frac{E'[p_i P(A|p_i, \ldots, p_4)]}{E'[P(A|p_1, \ldots, p_4)]} \tag{6.32}$$

The expectations that appear in this equation have to be computed with respect to the initial joint distribution of the p_i's. In practice, adequate approximations are required. For instance, Benjamin and Cornells' (1970) first-order approximation leads to $E''(p_1) = 0.226$, $E''(p_4) = 0.294$.

If correlation among subzone seismicities is neglected, and statistical information of each subzone is independently analyzed, when the p_i's are assigned beta probability-density functions with means and coefficients of variation as defined above, one obtains $E''(p_1) = 0.206$, $E''(p_4) = 0.311$, which are not very different from those formerly obtained; however, when $E'(p_i) = 0.25$ and $V'(p_i) = 0.5$, the first criterion leads to $E''(p_1) = 0.206$, $E''(p_4) = 0.314$, while the second produces 0.131 and 0.416, respectively. Part of the difference may be due to neglect of ρ'_{ij}, but probably a significant part stems from inaccuracies of the first-order approximation to the expectations that appear in eq. 6.32; alternate approximations are therefore desirable.

Incomplete data. Statistical information is known to be fairly reliable only for magnitudes above threshold values that depend on the region considered, its level of activity, and the quality of local and nearby seismic instrumentation. Even incomplete statistical records may be significant when evaluating some seismicity parameters; their use has to be accompanied by estimates of detectability values, that is, of ratios of the numbers of events recorded to total numbers of events in given ranges (Esteva, 1970; Kaila and Narain, 1971).

6.5 REGIONAL SEISMICITY

The final goal of local seismicity assessment is the estimation of regional seismicity, that is, of probability distributions of intensities at given sites, and of probabilistic correlations among them. These functions are obtained by integrating the contributions of local seismicities of nearby sources, and hence their estimates reflect Bayesian uncertainties tied to those seismicities. In the following, regional seismicity will be expressed in terms of mean rates of exceedance of given intensities; more detailed probabilistic descriptions would entail adoption of specific hypotheses concerning space and time correlations of earthquake generation.

6.5.1 Intensity-recurrence curves

The case when uncertainty in seismicity parameters is neglected will be discussed first. Consider an elementary seismic source with volume dV and local seismicity $\lambda(M)$ per unit volume, distant R from a site S, where intensity-recurrence functions are to be estimated. Every time that a magnitude M shock is generated at that source, the intensity at S equals:

$$Y = \epsilon Y_p = \epsilon b_1 \exp(b_2 M) g(R) \tag{6.33}$$

(see eqs. 6.4 and 6.5), where ϵ is a random factor and Y and Y_p stand for actual and predicted intensities, b_1 and b_2 are given constants, and $g(R)$ is a function of hypocentral distance. The probability that an earthquake originating at the source will have an intensity greater than y is equal to the probability that $\epsilon Y_p > y$. If Y_p is expressed in terms of M and randomness in ϵ is accounted for, one obtains:

$$\nu(y) = \int_{a_U}^{a_L} \nu_p(y/u) f_\epsilon(u) du \tag{6.34}$$

where ν and ν_p are respectively mean rates at which actual and predicted intensities exceed given values, $a_U = y/y_U$, $a_L = y/y_L$, y_U, and y_L are the predicted intensities that correspond to M_U and M_L, and f_ϵ the probability-density function of ϵ. If eq. 6.33 is assumed to hold:

$$\nu_p(y) = K_0 + K_1 y^{-r_1} - K_2 y^{-r_2} \tag{6.35}$$

where:

$$K_i = \int [b_1 g(R)]^{r_i} A_i \lambda_{1_i} dV \quad (i = 0, 1, 2) \tag{6.36}$$

$$r_0 = 0, \quad r_1 = \beta/b_2, \quad r_2 = (\beta - \beta_1)/b_2 \tag{6.37}$$

Substitution of eq. 6.35 into 6.34, coupled with the assumption that $\ln \epsilon$ is normally distributed with mean m and standard deviation σ leads to:

$$\nu(y) = c_0 K_0 + c_1 K_1 y^{-r_1} - c_2 K_2 y^{-r_2} \tag{6.38}$$

where:

$$c_i = \exp(Q_i) \left[\phi\left(\frac{\ln a_L - u_i}{\sigma}\right) - \phi\left(\frac{\ln a_U - u_i}{\sigma}\right) \right] \tag{6.39}$$

ϕ is the standard normal cumulative distribution function, $Q_i = 1/2\ \sigma^2 r_i^2 + m r_i$, and $u_i = m + \sigma^2 r_i$. Similar expressions have been presented by Merz and Cornell (1973) for the special case of eq. 6.8 when $\beta_1 \to \infty$ and for a quadratic form of the relation between magnitude and logarithm of exceedance rate. Closed-form solutions in terms of incomplete gamma functions are obtained when magnitudes are assumed to possess extreme type-III distributions (eq. 6.9).

Intensity-recurrence curves at given sites are obtained by integration of the contributions of all significant sources. Uncertainties in local seismicities can be handled by describing regional seismicity in terms of means and variances of $\nu(y)$ and estimating these moments from eq. 6.34 and suitable first- and second-moment approximations. Influence of these uncertainties in design decisions has been discussed by Rosenblueth (in preparation).

6.5.2 Seismic probability maps

When intensity-recurrence functions are determined for a number of sites with uniform local ground conditions the results are conveniently represented by sets of seismic probability maps, each map showing contours of intensities that correspond to a given return period. For instance, Figs. 6.19 and 6.20 show peak ground velocities and accelerations that correspond to 100 years return period on firm ground in Mexico. These maps form part of a set that was obtained through application of the criteria described in this chapter. Because the ratio of peak ground accelerations and velocities does not remain constant throughout a region, the corresponding design spectra will not only vary in scale but also in shape (frequency content); in other words, seismic risk will usually have to be expressed in terms of at least the values of two parameters (for instance, as in this case, peak ground accelerations and velocities that correspond to various risk levels (return periods)).

6.5.3 Microzoning

Implicit in the above criteria for evaluation of regional seismicity is the adoption of intensity attenuation expressions valid on firm ground. Scatter of actual intensities with respect to predicted values was ascribed to differences in source mechanisms, propagation paths, and local site conditions; at least the latter group of variables can introduce systematic deviations in the

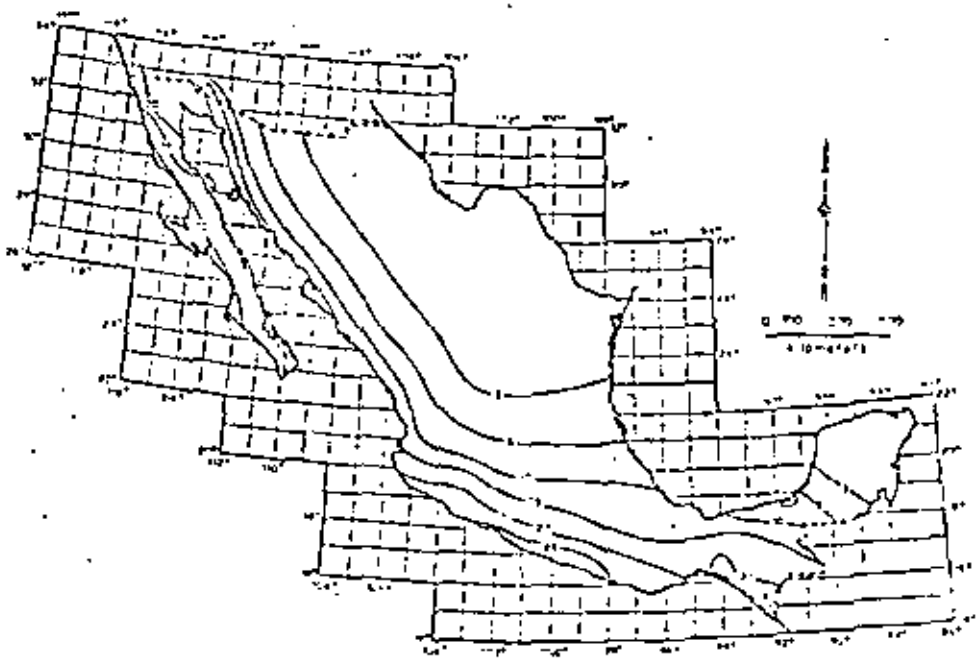

Fig. 6.19. Peak ground velocities with return period of 100 years (cm/sec).

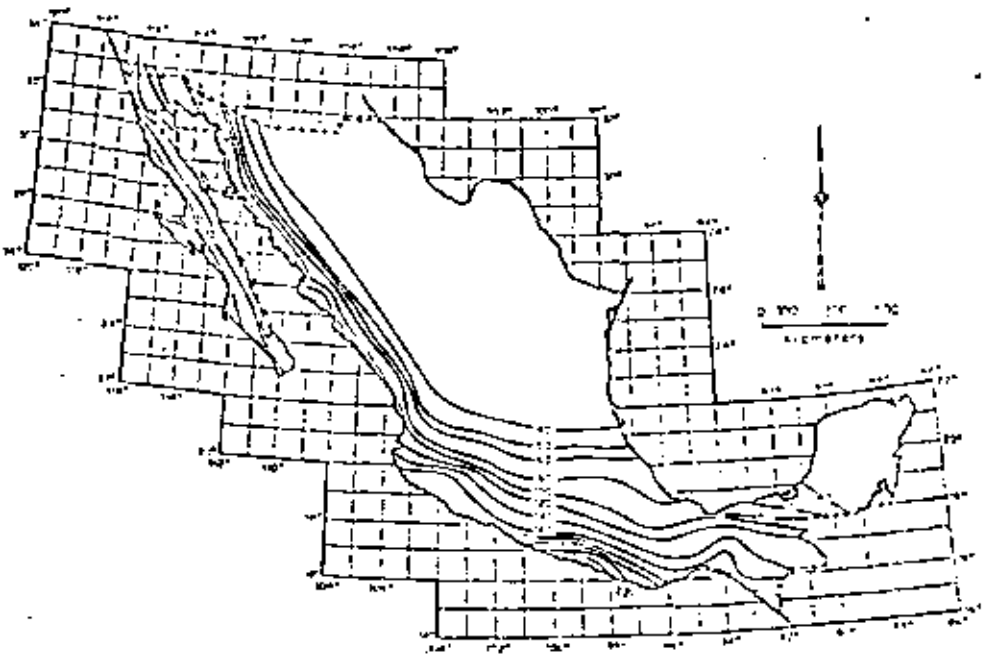

Fig. 6.20. Peak ground accelerations with return period of 100 years (cm/sec^2).

ratio of actual to predicted intensities; and geological details may significantly alter local seismicity in a small region, as well as energy radiation patterns, and hence regional seismicity in the neighbourhood. These systematic deviations are the matter of microzoning, that is, of local modification of risk maps similar to Figs. 6.19 and 6.20.

Most of the effort invested in microzoning has been devoted to study of the influence of local soil stratigraphy on the intensity and frequency content of earthquakes (see Chapter 4). Analytical models have been practically limited to response analysis of stratified formations of linear or nonlinear soils to vertically traveling shear waves. The results of comparing observed and predicted behavior have ranged from satisfactory (Herrera et al., 1965) to poor (Hudson and Udwadia, 1972). Topographic irregularities, as hills or slopes of firm ground formations underlying sediments, may introduce significant systematic perturbations in the surface motion, as a consequence of wave focusing or dynamic amplification. The latter effect was probably responsible for the exceptionally high accelerations recorded at the abutment of Pacoima dam during the 1971 San Fernando earthquake.

Present practice of microzoning determines seismic intensities or design parameters in two steps. First the values of those parameters on firm ground are estimated by means of suitable attenuation expressions and then they are amplified according to the properties of local soil; but this implies an arbitrary decision to which seismic risk is very sensitive: selecting the boundary between soil and firm ground. A specially difficult problem stems when

trying to fix that boundary for the purpose of predicting the motion at the top of a hill or the slope stability of a high cliff (Rukos, 1974).

It can be concluded that rational formulation of microzoning for seismic risk is still in its infancy and that new criteria will appear that will probably require intensity attenuation models which include the influence of local systematic perturbations. Whether these models are available or the two-step process described above is acceptable, intensity-recurrence expressions can be obtained as for the unperturbated case, after multiplying the second member of eq. 6.34 by an adequate intensity-dependent corrective factor.

REFERENCES

Aki, K., 1963. *Some Problems in Statistical Seismology*. University of Tokyo, Geophysical Institute.

Allen, C.R., 1969. Active faulting in northern Turkey. *Calif. Inst. Tech., Div. Geol. Sci., Contrib.* 1577.

Allen, C.R., St. Amand, P., Richter, C.F. and Nordquist, J.M., 1965. Relationship between seismicity and geologic structure in the southern California region. *Bull. Seismol. Soc. Am.*, 55 (4): 753—797.

Ambraseys, N.N., 1973. Dynamics and response of foundation materials in epicentral regions of strong earthquakes. *Proc. 5th World Conf. Earthquake Eng., Rome.*

Ananiin, I.V., Bune, V.I., Vvedenskaia, N.A., Kirillova, I.V., Reisner, G.I. and Sholpo, V.N., 1968. *Methods of Compiling a Map of Seismic Regionalization on the Example of the Caucasus*. C. Yu. Schmidt Institute of the Physics of the Earth, Academy of Sciences of the USSR, Moscow.

Benjamin, J.R. and Cornell, C.A., 1970. *Probability, Statistics and Decision for Civil Engineers*. McGraw-Hill, New York.

Ben-Menahem, A., 1960. Some consequences of earthquake statistics for the years 1918—1955. *Gerlands Beitr. Geophys.*, 69: 68—72

Bollinger, G.A., 1973. Seismicity of the southeastern United States. *Bull. Seismol. Soc. Am.*, 63: 1785—1808.

Bolt, B.A., 1970. Causes of earthquakes. In: R.L. Wiegel (editor), *Earthquake Engineering*. Prentice-Hall, Englewood Cliffs.

Brune, J.N., 1968. Seismic moment, seismicity and rate of slip along major fault zones. *J. Geophys. Res.*, 73: 777—784.

Burridge, R. and Knopoff, L., 1967. Model and theoretical seismicity. *Bull. Seismol. Soc. Am.*, 57: 341—371.

Cornell, C.A. and Vanmarcke, E.H., 1969. The major influences on seismic risk. *Proc. 4th World Conf. Earthquake Eng. Santiago.*

Crouse, C.B., 1973. Engineering studies of the San Fernando earthquake. *Calif. Inst. Technol., Earthquake Eng. Res. Lab.* Rep. 73-04.

Cox, D.F. and Lewis, P.A.W., 1966. *The Statistical Analysis of Series of Events*. Methuen, London.

Davenport, A.G., 1972. A statistical relationship between shock amplitude, magnitude and epicentral distance and its application to seismic zoning. *Univ. Western Ontario, Faculty Eng. Sci.*, BLWT-4-72.

Davies, G.F. and Brune, J.N., 1971. Regional and global fault slip rates from seismicity. *Nature*, 229: 101—107.

Drakopoulos, J.C., 1971. A statistical model on the occurrence of aftershocks in the area of Greece. *Bull. Int. Inst. Seismol. Earthquake Eng.*, 8: 17—39.

Esteva, L., 1968. Bases para la formulación de decisiones de diseño sísmico. *Natl. Univ. Mexico, Inst. Eng. Rep.* 182.

Esteva, L., 1969, Seismicity prediction: a bayesian approach. *Proc. 4th World Conf. Earthquake Eng. Santiago.*

Esteva, L., 1970. Consideraciones prácticas en la estimación bayesiana de riesgo sísmico. *Natl. Univ. Mexico, Inst. Eng., Rep.* 248.

Esteva, L., 1974. Geology and probability in the assessment of seismic risk. *Proc. 2nd Int. Congr. Int. Assoc. Eng. Geol., Sao Paulo.*

Esteva, L. and Villaverde, R., 1973. Seismic risk, design spectra and structural reliability. *Proc. 5th World Conf. Earthquake Eng., Rome*, pp. 2586—2597.

Figueroa, J., 1963. Isosistas de macrosismos mexicanos. *Ingeniería*, 33 (1): 45—68.

Gaisky, V.N., 1966. The time distribution of large, deep earthquakes from the Pamir—Hindu-Kush. *Dokl. Akad. Nauk Tadjik S.S.R.*, 9 (6): 18—21.

Gaisky, V.N., 1967. On similarity between collections of earthquakes, the connections between them, and their tendency to periodicity. *Fiz. Zemli*, 7: 20—28 (English transl., pp. 432—437).

Gajardo, E. and Lomnitz, C., 1960. Seismic provinces of Chile. *Proc. 2nd World Conf. Earthquake Eng., Tokyo*, pp. 1529—1540.

Gutenberg, B. and Richter, C.F., 1954. *Seismicity of the Earth*. Princeton University Press, Princeton.

Gzovsky, M.G., 1962. Tectonophysics and earthquake forecasting. *Bull. Seismol. Soc. Am.*, 52 (3): 485—505.

Herrera, I., Rosenblueth, E. and Rascón, O.A., 1965. Earthquake spectrum prediction for the Valley of Mexico. *Proc. 3rd Int. Conf. Earthquake Eng., Auckland and Wellington*, 1: 61—74.

Housner, G.W., 1969. Engineering estimates of ground shaking and maximum earthquake magnitude. *Proc. 4th World Conf. Earthquake Eng., Santiago.*

Hudson, D.E., 1971. *Strong Motion Instrumental Data on the San Fernando Earthquake of February 9, 1971*. California Institute of Technology, Earthquake Engineering Research Laboratory.

Hudson, D.E., 1972a. Local distributions of strong earthquake ground shaking. *Bull. Seismol. Soc. Am.*, 62 (6).

Hudson, D.E., 1972b. *Analysis of Strong Motion Earthquake Accelerograms. III, Response Spectra, Part A*. California Institute of Technology, Earthquake Engineering Research Laboratory.

Hudson, D.E. and Vdwadia, F.E., 1973. Local distribution of strong earthquake ground motions. *Proc. 5th World Conf. Earthquake Eng., Rome*, pp. 691—700.

Kaila, K.L. and Narain, H., 1971. A new approach for preparation of quantitative seismicity maps as applied to Alpide Belt—Sunda Arc and adjoining areas. *Bull. Seismol. Soc. Am.*, 61 (5): 1275—1291.

Kaila, K.L., Gaur, V.K. and Narain, H., 1972. Quantitative seismicity maps of India. *Bull. Seismol. Soc. Am.*, 62 (5): 1119—1132.

Kaila, K.L., Rao, N.M. and Narain, H., 1974. Seismotectonic maps of southwest Asia region comprising eastern Turkey, Caucasus, Persian Plateau, Afghanistan and Hindu-kush. *Bull. Seismol. Soc. Am.*, 64 (3): 657—669.

Kelleher, J., Sykes, L. and Oliver, J., 1973. Possible criteria for predicting earthquake locations and their application to major plate boundaries of the Pacific and the Caribbean. *J. Geophys. Res.*, 78 (14): 2547—2585.

Knopoff, L., 1964. The statistics of earthquakes in southern California. *Bull. Seismol. Soc. Am.*, 54: 1871—1873.

Lomnitz, C., 1966. Magnitude stability in earthquake sequences. *Bull Seismol. Soc. Am.*, 56: 247—249.

Lomnitz, C. and Hax, A., 1966. Clustering in aftershock sequences. In: J.S. Steinhart and T. Jefferson Smith (editors), *The Earth Beneath the Continents*. Am. Geophys. Union, pp. 502-506.

McGuire, R.K., 1974. Seismic structural response risk analysis incorporating peak response regressions on earthquake magnitude and distance. *Mass. Inst. Technol., Dep. Civ. Eng.*, R74-51.

Merz, H.A. and Cornell, C.A., 1973. Seismic risk analysis based on a quadratic magnitude–frequency law. *Bull. Seismol. Soc. Am.*, 63 (6): 1999–2006.

Milne, W.G. and Davenport, A.G., 1969. Earthquake probability. *Proc. 4th World Conf. Earthquake Eng., Santiago.*

Mogi, K., 1962. Study of elastic shocks caused by the fracture of heterogeneous materials and its relations to earthquake phenomena. *Bull. Earthquake Res. Inst. Tokyo*, 40: 125–173.

Molnar, P. and Sykes, L.R., 1969. Tectonics of the Caribbean and Middle America regions from focal mechanisms and seismicity. *Geol. Soc. Am. Bull.*, 80: 1639.

Newark, N.M. and Rosenblueth, E., 1971. *Fundamentals of Earthquake Engineering.* Prentice-Hall, Englewood Cliffs.

Omori, F., 1894. On the aftershocks of earthquakes. *J. Coll. Sci. Imp. Univ. Tokyo*, 7: 111–200.

Parzen, E., 1962. *Stochastic Processes.* Holden Day, San Francisco.

Petrushevsky, B.A., 1966. *The Geological Fundamentals of Seismic Zoning.* Scientific Translation Service, order 5032, Ann Arbor, USA.

Raiffa, H. and Schlaifer, R., 1968. *Applied Statistical Decision Theory*, MIT Press.

Rosenblueth, E., 1964. Probabilistic design to resist earthquakes. *Am. Soc. Civ. Eng., J. Eng. Mech. Div.*, 90 (EM5): 189–249.

Rosenblueth, E., 1969. Seismicity and earthquake simulation. *Rep. NSF-UCEER Conf. Earthquake Eng. Res., Pasadena*, pp. 47–64.

Rosenblueth, E., 1975. *Point Estimates for Probability Moments.* National University of Mexico, Institute of Engineering, Mexico City.

Rosenblueth, E., in preparation. Optimum design for infrequent disturbances.

Rukos, E., 1974. *Análysis dinamico de la margen izquierda de Chicoasén.* National University of Mexico, Institute of Engineering, Mexico City.

Salt, P.E., 1974. Seismic site response. *Bull. N. Z. Natl. Soc. Earthquake Eng.*, 7 (2): 63–77.

Scholz, C.H., 1968. The frequency–magnitude relation of microfracturing and its relation to earthquakes. *Bull. Seismol. Soc. Am.*, 58: 399–417.

Shlien, S. and Toksöz, M.N., 1970. A clustering model for earthquake occurrences. *Bull. Seismol. Soc. Am.*, 60 (6): 1765–1787.

Singh, S.K., 1975. *Mexican Volcanic Belt: Some Comments on a Model Proposed by F. Mooser.* National University of Mexico, Institute of Engineering, Mexico City.

Trifunac, M.D., 1973. Characterization of response spectra by parameters governing the gross nature of earthquake source mechanisms. *Proc. 5th World Conf. Earthquake Eng.*, Rome, pp. 701–704.

Tsuboi, C., 1956. Earthquake province. Domain of sympathetic seismic activities. *J. Phys. Earth.*, 6 (1): 35–49.

Utsu, T., 1961. A statistical study on the occurrence of aftershocks. *Geophys. Mag., Tokyo*, 30: 521–605.

Utsu, T., 1962. On the nature of three Alaska aftershock sequences of 1957 and 1958. *Bull. Seismol. Soc. Am.*, 52: 179–297.

Veneziano, D. and Cornell, C.A., 1973. Earthquake models with spatial and temporal memory for engineering seismic risk analysis. *Mass. Inst. Technol., Dep. Civ. Eng.*

Vere-Jones, D., 1970. Stochastic models for earthquake occurrence. *J. R. Stat. Soc.*, 32 (1): 1–45.

Wallace, R.E., 1970. Earthquake recurrence intervals on the San Andreas Fault. *Geol. Soc. Am. Bull.*, 81: 2875–2890.

Yegulalp, T.M. and Kuo, J.T., 1974. Statistical prediction of the occurrences of maximum magnitude earthquakes. *Bull. Seismol. Soc. Am.*, 64 (2): 393–414.

IX CURSO INTERNACIONAL DE INGENIERIA SISMICA

ANALISIS DE RIESGO SISMICO

NOCIONES ELEMENTALES

DR. GUSTAVO AYALA MILLAN
Julio, 1983

Nociones Elementales

Para iniciar el problema de propagación estudiemos primeramente el caso unidimensional. La ecuación que gobierna este movimiento es llamada 'ecuación de onda unidimensional' y se escribe como

$$\frac{\partial^2 \phi}{\partial x^2} = \frac{1}{c^2} \frac{\partial^2 \phi}{\partial t^2} \qquad (1)$$

donde ϕ es por ejemplo la elevación de una onda en el que y c es un coficiente conocido como celeridad o velocidad de propagación.

Pa obtener la solucion general de la ec 1 es conveniente hacer el siguiente cambio de variables,

$$u = x - ct$$
$$v = x + ct \qquad (2)$$

este método conocido como de D'Alembert conduce a las siguientes transformaciones

$$\frac{\partial \phi}{\partial x} = \frac{\partial \phi}{\partial u} + \frac{\partial \phi}{\partial v} \quad , \quad \frac{\partial^2 \phi}{\partial x^2} = \frac{\partial^2 \phi}{\partial u^2} + 2\frac{\partial^2 \phi}{\partial u \partial v} + \frac{\partial^2 \phi}{\partial v^2} \qquad (3)$$

$$\frac{\partial \phi}{\partial t} = -c\frac{\partial \phi}{\partial u} + c\frac{\partial \phi}{\partial v} \quad \text{y} \quad \frac{\partial^2 \phi}{\partial t^2} = c^2\left(\frac{\partial^2 \phi}{\partial u^2} - 2\frac{\partial^2 \phi}{\partial u \partial v} + \frac{\partial^2 \phi}{\partial v^2}\right)$$

mismas que al substituirse en la ec (1) dan la ecuación

$$\frac{\partial^2 \phi}{\partial u \, \partial v} = 0 \qquad (4)$$

cuya solución general se escribe como

$$\phi = f(u) + g(v) \qquad (5)$$

Si en las ecs. 2 se tiene

$$\phi = f(x-ct) + g(x+ct) \qquad (6).$$

donde f y g son funciones arbitrarias de sus argumentos.

De la interpretación física de la ec 6 se tiene que para un tiempo dado la función $f(x-ct)$ representa una perturbación moviendose en la dirección positiva del x con una velocidad de propagación c. Similarmente la función $g(x+ct)$ representa una perturbación que se mueve con una celeridad c en dirección negativa del eje x.

La anterior interpretación física se ilustra en la siguiente figura

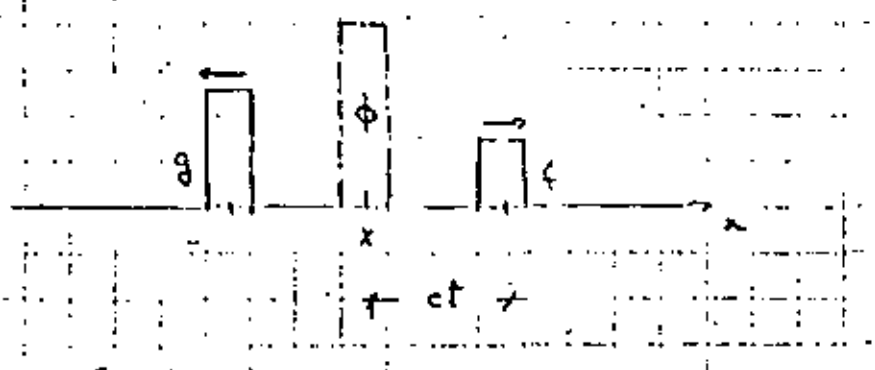

Fig 1

Para definir algunos parámetros de interés en el problema de propagación consideremos, sin pérdida de generalidad una onda armónica que se mueve con una velocidad de propagación constante y sin cambio de forma, en la dirección positiva del eje x. Así

$$\phi = a \operatorname{sen} k(x - ct) \qquad (7)$$

Definiciones:

- A el valor máximo de la perturbación, en este caso 'a', se le denomina amplitud.
- A la forma de la perturbación cuando $t = 0$ se le denomina 'perfil de onda'.
- A la distancia para la cual se repite el perfil de onda, 'λ', se le denomina longitud de onda. En este caso

$$\lambda = \frac{2\pi}{m} \qquad (8)$$

o sea la (7) se puede escribir como:

$$\phi = a \operatorname{sen} \frac{2\pi}{\lambda}(x - ct) \qquad (9)$$

- El Tiempo que toma una onda en pasar por un punto se llama periodo y se escribe como

$$T = \frac{\lambda}{c} \qquad (10)$$

- La frecuencia n, es el número de ondas que pasan

por un punto fijo en una unidad de tiempo, esto es

$$n = \frac{1}{T} \qquad (11)$$

A el número de ondas en una distancia 2π, k, se le llama número de onda y resulta ser

$$k = \frac{2\pi}{\lambda} \qquad (12)$$

Las definiciones anteriores son válidas para cualquier perturbación cuyo perfil de onda se repite regularmente.

Ondas Planas

La generalización de la solución dada por la ec 6 a un problema tridimensional permite la definición de 'ondas planas', esto es, ondas para las cuales la perturbación es constante en todos los puntos contenidos en cada plano perpendicular a la dirección de propagación. Así si la dirección de propagación se define por sus cosenos directores l, m, n, la ec 6 en un espacio tridimensional se escribe como

$$\phi = f(lx + my + nz - ct) + g(lx + my + nz + ct) \qquad (13)$$

Ondas esféricas.

Si estamos interesados en la solución de la ecuación de onda para problemas que posean simetría esférica. Se tiene que la

Ecuación que gobierna al problema:

$$\frac{\partial^2\phi}{\partial r^2} + \frac{2}{r}\frac{\partial\phi}{\partial r} = \frac{1}{c^2}\frac{\partial^2\phi}{\partial t^2} \qquad (14)$$

o bien

$$\frac{\partial^2(r\phi)}{\partial r^2} = \frac{1}{c^2}\frac{\partial^2(r\phi)}{\partial t^2} \qquad (15)$$

De los conceptos establecidos anteriormente se demuestra que la ec. (15) tiene la solución general

$$\phi = \frac{1}{r} f(r-ct) + \frac{1}{r} g(r+ct) \qquad (16)$$

donde f y g son nuevamente funciones arbitrarias de sus argumentos. Vemos que la amplitud de las ondas esféricas decrece con $\frac{1}{r}$.

Se puede demostrar que, en el caso de ondas cilíndricas con simetría axial, la atenuación de las ondas es con $\frac{1}{\sqrt{r}}$

Propagación de Ondas en un Medio Infinito

Las ecuaciones que gobiernan el movimiento de un medio plástico lineal, homogeneo e isotropo, conocidas como ecuaciones de Navier, se pueden escribir como

$$\begin{aligned}
\rho\frac{\partial^2 u}{\partial t^2} &= (\lambda+G)\frac{\partial e}{\partial x} + G\nabla^2 u + \rho X \\
\rho\frac{\partial^2 v}{\partial t^2} &= (\lambda+G)\frac{\partial e}{\partial y} + G\nabla^2 v + \rho Y \qquad (17)\\
\rho\frac{\partial^2 w}{\partial t^2} &= (\lambda+G)\frac{\partial e}{\partial z} + G\nabla^2 w + \rho Z
\end{aligned}$$

donde u, v y w son las componentes del vector desplazamiento, λ y G los coeficientes elásticos del material, ρ la densidad de masa, X Y y Z las componentes del vector de fuerzas de cuerpo por unidad de masa y e la dilatación definida como

$$e = \frac{\partial u}{\partial x} + \frac{\partial v}{\partial y} + \frac{\partial w}{\partial z} \qquad (18)$$

El sistema de ecuaciones de movimiento se puede desacoplar si el vector desplazamiento se define como

$$\underset{\sim}{u} = \text{grad}\,\phi + \text{rot}\,\underset{\sim}{\Psi} \qquad (19)$$

donde $\underset{\sim}{u}$ es el vector desplazamiento con componentes u, v y w, ϕ y $\underset{\sim}{\Psi}$ son potenciales, uno escalar y otro vectorial ambos conocidos como potenciales de Helmholtz.

De las ecs 17 y 19 se muestra que las ecs 17 se satisfacen simultáneamente si los potenciales ϕ y $\underset{\sim}{\Psi}$ son soluciones de las ecuaciones de onda

$$\nabla^2\phi = \frac{1}{C_p^2}\frac{\partial^2\phi}{\partial t^2} \qquad (20)$$

y

$$\nabla^2\underset{\sim}{\Psi} = \frac{1}{C_s^2}\frac{\partial^2\underset{\sim}{\Psi}}{\partial t^2} \qquad (21)$$

donde

$$C_p = \sqrt{\frac{\lambda + 2G}{\rho}} \quad \text{y} \quad C_s = \sqrt{\frac{G}{\rho}} \qquad (22)$$

De simples transformaciones se puede demostrar que las ecs. 20 y 21 se pueden escribir respectivamente como

$$\nabla^2 e = \frac{1}{c_p^2} \frac{\partial^2 e}{\partial t^2} \qquad (23)$$

y

$$\nabla^2 \underset{\sim}{w} = \frac{1}{c_s^2} \frac{\partial^2 \underset{\sim}{w}}{\partial t^2} \qquad (24)$$

donde $\underset{\sim}{w}$ es el vector rotación.

Usando los conceptos establecidos en el capítulo anterior se observa que las ecs 23 y 24 son ecuaciones de onda asociadas a ondas de tipo dilatacional o P y distorcionales o S, respectivamente. De aquí se concluye que en un medio elástico de extensión infinita solo pueden existir dos tipos de ondas, las ondas dilatacionales que se propagan con una velocidad c_p y las distorcionales que se propagan con una velocidad c_s.

Con el objeto de dilucidar más ampliamente el problema de propagación de ondas en un medio infinito nos interesa investigar algunas soluciones particulares.

Sea la solución asociada a una onda plana viajando

en la dirección positiva del eje x

$$u = a \operatorname{sen} \frac{2\pi}{\lambda}(x - ct)$$

$$v = 0 \qquad (26)$$

$$w = 0$$

Esta solución satisface las ecs 17 si y solo si $c = c_p$. y representa un tren de ondas planas distintacionales propagando con una velocidad c_p. Notese que para este tipo de ondas el movimiento de la particula coincide con la dirección de propagación y que además este tipo de movimiento produce cambios volumétricos.

Consideremos ahora las soluciones

$$u = w = 0$$

$$v = a \operatorname{sen} \frac{2\pi}{\lambda}(x - ct) \qquad (2c)$$

o'

$$u = v = 0$$

$$w = a \operatorname{sen} \frac{2\pi}{\lambda}(x - ct) \qquad (27)$$

De la substitución de cualquiera de las soluciones anteriores en las ecs 17 se puede concluir que estas representan una solución si y solo si $c = c_s$. Además se observa que en el caso de ondas S el movimiento de la parti-

cula es normal a la dirección de propagación

Las ondas distorcionales son generalmente polarizadas, estas, ondas SH en las que el movimiento de la partícula es horizontal y ondas SV en las que el movimiento de la partícula ocurre en el plano vertical. En los casos en que el medio tiene isotropía transversal, como es el caso de muchas formaciones geológicas, en una perturbación propagandose en dirección horizontal la onda SH se propaga mas rápido que la onda SV.

De la existencia de distintas velocidades de propagación asociadas distintos tipos de onda se puede concluir una propiedad importante de las ondas sísmicas, esto es, que una onda plana arbitraria compuesta de movimientos P y S no se puede propagar. En cada instante las distintas ondas tienen diferentes distancias y es de esta propiedad que la velocidad de propagación de las ondas P y S a cualquier profundidad es fácilmente calculable.

Propagación de Ondas en un Semiespacio Elástico

Consideremos ahora el caso de propagación de ondas en un

medio que consiste de un semiespacio elástico. Por conveniencia en la formulación escogemos el eje z dirigido verticalmente hacia abajo, así, la superficie del semiespacio está definida por el plano $z=0$. Esta superficie está libre de esfuerzos por lo que las condiciones de frontera son

$$\nabla_z = \sigma_{zx} = \sigma_{zy} = 0 \qquad (28)$$

Si consideramos una onda plana dilatacional incidendo con un ángulo i a la superficie del terreno se puede demostrar que ésta produce 2 ondas reflejadas una P y una SV

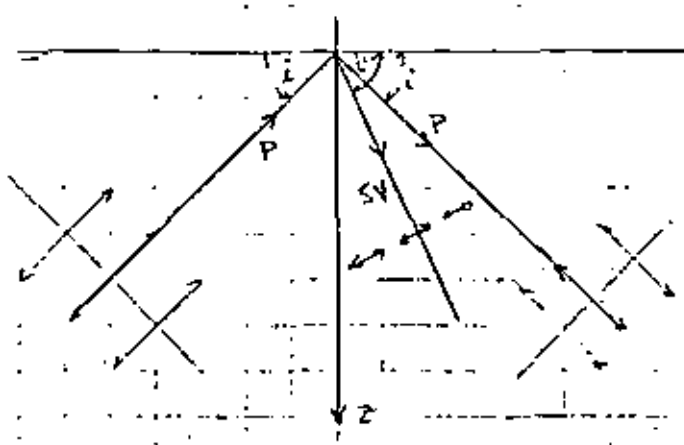

i = ángulo de incidencia
i' = ángulo de reflexión

así para las ondas dilatacionales se tiene

$$e = \underbrace{f\left(t - \frac{x\cos i - z\sin i}{c_p}\right)}_{\text{incidente}} + \underbrace{Af\left(t - \frac{x\cos i + z\sin i}{c_p}\right)}_{\text{reflejada}} \qquad (29)$$

y para las ondas distorsionales

$$w_2 = \underbrace{Bf\left(t - \frac{x\cos i' + z\sin i'}{c_s}\right)}_{\text{reflejada}} \qquad (30)$$

las condiciones de frontera dadas por las ecs 28. nos

permiten determinar los coeficientes desconocidos A y B, definidos como

$$A = \frac{4\sqrt{\xi^2-1}\sqrt{k^2\xi^2-1} - (\xi^2-2)^2}{4\sqrt{\xi^2-1}\sqrt{k^2\xi^2} + (\xi^2-2)}$$

$$B =$$

(distortional) propagates at the same velocity ($c_s = \sqrt{G/\rho}$) in both the rod and the infinite medium.

3.3 Waves in an Elastic Half-Space

In Sec. 3.2 it was found that two types of waves were possible in an infinite elastic medium—waves of dilatation and waves of distortion. In an elastic half-space, however, it is possible to find a third solution for the equations of motion which corresponds to a wave whose motion is confined to a zone near the boundary of the half-space. This wave was first studied by Lord Rayleigh (1885) and later was described in detail by Lamb (1904). The elastic wave described by these investigators is known as the *Rayleigh wave* (*R*-wave) and is confined to the neighborhood of the surface of a half-space. The influence of the Rayleigh wave decreases rapidly with depth.

Rayleigh-Wave Velocity

A wave with the characteristics noted above can be obtained by starting with the equations of motion (Eqs. 3-42, 3-43, and 3-44) and imposing the appropriate boundary conditions for a free surface. We define the surface of the half-space as the xy plane with z assumed to be positive toward the interior of the half-space, as shown in Fig. 3-12. For a *plane wave* traveling in the x-direction, particle displacements will be independent of the y-direction. Displacements in the x- and z-directions, denoted by u and w respectively, can be written in terms of two potential functions Φ and Ψ:

$$u = \frac{\partial \Phi}{\partial x} + \frac{\partial \Psi}{\partial z} \quad \text{and} \quad w = \frac{\partial \Phi}{\partial z} - \frac{\partial \Psi}{\partial x}$$

The dilatation ϵ of the wave defined by u and w is

$$\epsilon = \frac{\partial u}{\partial x} + \frac{\partial w}{\partial z} = \frac{\partial}{\partial x}\left(\frac{\partial \Phi}{\partial x} + \frac{\partial \Psi}{\partial z}\right) + \frac{\partial}{\partial z}\left(\frac{\partial \Phi}{\partial z} - \frac{\partial \Psi}{\partial x}\right) = \nabla^2 \Phi$$

and the rotation $2\bar{\omega}_y$ in the xz plane is

$$2\bar{\omega}_y = \frac{\partial u}{\partial z} - \frac{\partial w}{\partial x} = \frac{\partial}{\partial x}\left(\frac{\partial \Phi}{\partial x} + \frac{\partial \Psi}{\partial z}\right) - \frac{\partial}{\partial z}\left(\frac{\partial \Phi}{\partial z} - \frac{\partial \Psi}{\partial x}\right) = \nabla^2 \Psi$$

Now it can be seen that the potential functions Φ and Ψ have been chosen

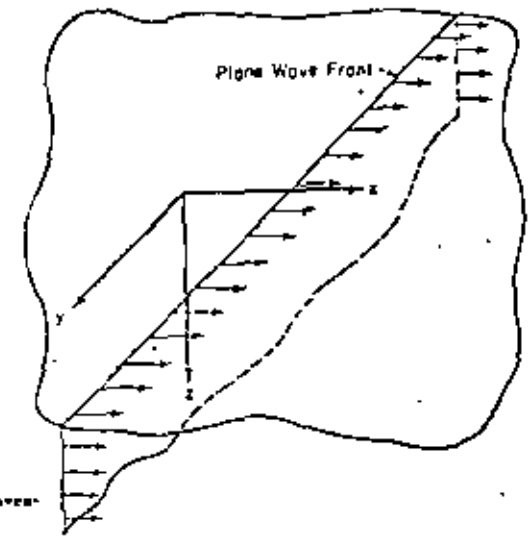

Figure 3-12 Coordinate convention for elastic half-space.

such that Φ is associated with dilatation of the medium and Ψ associated with rotation of the medium.

Substituting u and w into Eqs. (3-42) and (3-44) yields

$$\rho \frac{\partial}{\partial x}\left(\frac{\partial^2 \Phi}{\partial t^2}\right) + \rho \frac{\partial}{\partial z}\left(\frac{\partial^2 \Psi}{\partial t^2}\right) = (\lambda + 2G)\frac{\partial}{\partial x}(\nabla^2 \Phi) + G\frac{\partial}{\partial z}(\nabla^2 \Psi) \quad (3\text{-}49)$$

and

$$\rho \frac{\partial}{\partial z}\left(\frac{\partial^2 \Phi}{\partial t^2}\right) - \rho \frac{\partial}{\partial x}\left(\frac{\partial^2 \Psi}{\partial t^2}\right) = (\lambda + 2G)\frac{\partial}{\partial z}(\nabla^2 \Phi) - G\frac{\partial}{\partial x}(\nabla^2 \Psi) \quad (3\text{-}50)$$

Equations (3-49) and (3-50) are satisfied if

$$\frac{\partial^2 \Phi}{\partial t^2} = \frac{\lambda + 2G}{\rho}\nabla^2 \Phi = v_p^2 \nabla^2 \Phi \quad (3\text{-}51)$$

and

$$\frac{\partial^2 \Psi}{\partial t^2} = \left(\frac{G}{\rho}\right)\nabla^2 \Psi = v_s^2 \nabla^2 \Psi \quad (3\text{-}52)$$

Now, by assuming a solution for a sinusoidal wave traveling in the positive x-direction, expressions for Φ and Ψ can be written

$$\Phi = F(z)\exp[i(\omega t - Nx)] \quad (3\text{-}53)$$

and

$$\Psi = G(z) \exp [i(\omega t - Nx)] \tag{3-54}$$

The functions $F(z)$ and $G(z)$ describe the variation in amplitude of the wave as a function of depth, and N is the wave number defined by

$$N = \frac{2\pi}{L}$$

where L is the wave length.

Now, substituting the expressions for Φ and Ψ from Eqs. (3-53) and (3-54) into Eqs. (3-51) and (3-52) yields

$$-\frac{\omega^2}{c_p^2} F(z) = -N^2 F(z) + F''(z) \tag{3-55}$$

and

$$-\frac{\omega^2}{c_s^2} G(z) = -N^2 G(z) + G''(z) \tag{3-56}$$

By rearranging Eqs. (3-55) and (3-56), we get

$$F''(z) - \left(N^2 - \frac{\omega^2}{c_p^2}\right) F(z) = 0 \tag{3-57}$$

and

$$G''(z) - \left(N^2 - \frac{\omega^2}{c_s^2}\right) G(z) = 0 \tag{3-58}$$

where $F''(z)$ and $G''(z)$ are derivatives with respect to z. Now, letting

$$q^2 = \left(N^2 - \frac{\omega^2}{c_p^2}\right) \tag{3-59}$$

and

$$s^2 = \left(N^2 - \frac{\omega^2}{c_s^2}\right) \tag{3-60}$$

Eqs. (3-57) and (3-58) can be rewritten as

$$F''(z) - q^2 F(z) = 0 \tag{3-61}$$

and

$$G''(z) - s^2 G(z) = 0 \tag{3-62}$$

The solutions of Eqs. (3-61) and (3-62) can be expressed in the form

$$F(z) = A_1 \exp(-qz) + B_1 \exp(qz) \tag{3-63}$$

$$G(z) = A_2 \exp(-sz) + B_2 \exp(sz) \tag{3-64}$$

A solution that allows the amplitude of the wave to become infinite with depth cannot be tolerated; therefore,

$$B_1 = B_2 = 0$$

and Eqs. (3-53) and (3-54) become

$$\Phi = A_1 \exp [-qz + i(\omega t - Nx)] \tag{3-65}$$

and

$$\Psi = A_2 \exp [-sz + i(\omega t - Nx)] \tag{3-66}$$

Now, the boundary conditions specifying no stress at the surface of a half-space imply that $\sigma_z = 0$ and $\tau_{xz} = 0$ at the surface $z = 0$. Therefore, at the surface,

$$\sigma_z = \lambda\varepsilon + 2G\varepsilon_z = \lambda\varepsilon + 2G\frac{\partial w}{\partial z} = 0$$

and

$$\tau_{xz} = G\gamma_{xz} = G\left(\frac{\partial w}{\partial x} + \frac{\partial u}{\partial z}\right) = 0$$

Using the definitions of u and w and the solutions for Φ and Ψ from Eqs. (3-65) and (3-66), the above equations for boundary conditions can be written

$$\sigma_{z\,z=0} = A_1[(\lambda + 2G)q^2 - \lambda N^2] - 2iA_2GNs = 0 \tag{3-67}$$

and

$$\tau_{xz\,z=0} = 2iA_1Nq + A_2(s^2 + N^2) = 0 \tag{3-68}$$

Upon rearranging, Eqs. (3-67) and (3-68) become

$$\frac{A_1}{A_2}\frac{(\lambda + 2G)q^2 - \lambda N^2}{2iGNs} - 1 = 0 \tag{3-69}$$

and

$$\frac{A_1}{A_2}\frac{2qiN}{(s^2 + N^2)} + 1 = 0 \tag{3-70}$$

Now we add these two equations to get

$$\frac{(\lambda + 2G)q^2 - \lambda N^2}{2GNs} = -\frac{2qN}{s^2 + N^2} \tag{3-71}$$

and cross-multiply in Eq. (3-71) to obtain

$$4qGsN^2 = (s^2 + N^2)[(\lambda + 2G)q^2 - \lambda N^2] \tag{3-72}$$

Squaring both sides of Eq. (3-72) and introducing q from Eq. (3-59) and s from Eq. (3-60), we get

$$16G^2N^4\left(N^2 - \frac{\omega^2}{v_p^2}\right)\left(N^2 - \frac{\omega^2}{v_S^2}\right) = \left[(\lambda + 2G)\left(N^2 - \frac{\omega^2}{v_p^2}\right) - \lambda N^2\right]^2\left[N^2 + \left(N^2 - \frac{\omega^2}{v_S^2}\right)\right]^2 \tag{3-73}$$

Now, dividing through by G^2N^8, we obtain

$$16\left(1 - \frac{\omega^2}{v_p^2N^2}\right)\left(1 - \frac{\omega^2}{v_S^2N^2}\right) = \left[2 - \left(\frac{\lambda + 2G}{G}\right)\left(\frac{\omega^2}{v_p^2N^2}\right)\right]^2\left(2 - \frac{\omega^2}{v_S^2N^2}\right)^2 \tag{3-74}$$

Then, using the following relationships derived in the footnote* gives

$$\frac{\omega^2}{v_p^2N^2} = \frac{v_R^2}{v_p^2} = a^2K^2 \tag{3-75}$$

$$\frac{\omega^2}{v_S^2N^2} = \frac{v_R^2}{v_S^2} = K^2 \tag{3-76}$$

$$\frac{\lambda + 2G}{G} = \frac{1}{a^2} = \frac{2 - 2\nu}{1 - 2\nu} \tag{3-77}$$

* By definition,

$$N = \frac{2\pi}{L}$$

or

$$L = \frac{2\pi}{N}$$

(Let L_R and v_R be the wave length and velocity, respectively, of the surface wave.)

Eq. (3-74) can be written

$$16(1 - a^2K^2)(1 - K^2) = \left(2 - \frac{1}{a^2}a^2K^2\right)^2(2 - K^2)^2 \tag{3-78}$$

After expansion and rearrangement, Eq. (3-78) becomes

$$K^6 - 8K^4 + (24 - 16a^2)K^2 + 16(a^2 - 1) = 0 \tag{3-79}$$

Equation (3-79) can be considered a cubic equation in K^2 and real valued solutions can be found for given values of ν. The quantity K represents a ratio between the velocity of the surface wave and the velocity of the shear wave.

Also,

$$L_R = \frac{v_R}{f} = \frac{2\pi v_R}{\omega}$$

and, from above,

$$L_R = \frac{2\pi}{N} = \frac{v_R 2\pi}{\omega}$$

therefore,

$$N = \frac{\omega}{v_R}$$

and

$$N^2 = \frac{\omega^2}{v_R^2}$$

Let K and a be defined such that

$$\frac{v_R^2}{v_S^2} = K^2 \quad \text{and} \quad \frac{v_R^2}{v_p^2} = a^2K^2$$

Then

$$\frac{\omega^2}{v_p^2N^2} = \frac{v_R^2}{v_p^2} = a^2K^2$$

and

$$\frac{\omega^2}{v_S^2N^2} = \frac{v_R^2}{v_S^2} = K^2$$

Substitution of v_p and v_S from Eqs. (3-46) and (3-48) gives

$$\frac{1}{a^2} = \frac{v_S^2}{v_p^2} = \frac{\frac{\mu}{\rho}}{\frac{\lambda + 2G}{\rho}} = \frac{G}{\lambda + 2G}$$

and using

$$\nu = \frac{\lambda}{2(\lambda + G)}$$

we get

$$\frac{\lambda + 2G}{G} = \frac{2 - 2\nu}{1 - 2\nu} = \frac{1}{a^2}$$

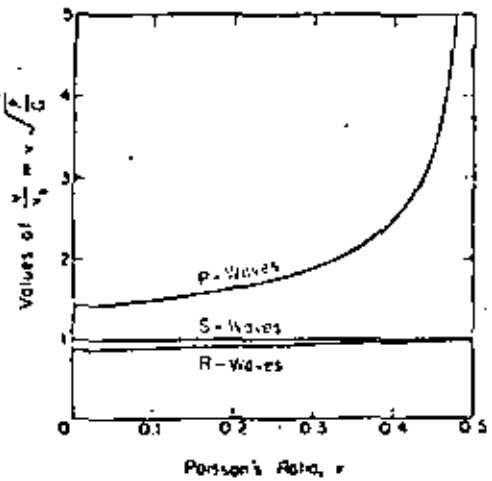

Figure 3-13. Relation between Poisson's ratio, ν, and velocities of propagation of compression (*P*), shear (*S*), and Rayleigh (*R*) waves in a semi-infinite elastic medium (*from* Sezawa, 1942).

From this solution it is clear that K^2 is independent of the frequency of the wave; consequently, the velocity of the surface wave is independent of frequency and is nondispersive.

Ratios of r_p/r_R and r_s/r_R can be obtained from Eq. (3-79) for values of Poisson's ratio ν from 0 to 0.5. Curves of these ratios as a function of ν are shown in Fig. 3-13.

Rayleigh-Wave Displacement

So far, a relationship for the ratio of the Rayleigh-wave velocity to the shear-wave velocity has been obtained, but additional information about the Rayleigh wave can be determined by obtaining the expressions for u and w in terms of known quantities. Upon substituting the expressions for Φ and Ψ from Eqs. (3-65) and (3-66) into the expressions for u and w, we get

$$u = \frac{\partial \Phi}{\partial x} + \frac{\partial \Psi}{\partial z}$$
$$= -A_1 iN \exp\left[-qz + i(\omega t - Nx)\right] - A_2 s \exp\left[-sz + i(\omega t - Nx)\right] \tag{3-80}$$

and

$$w = \frac{\partial \Phi}{\partial z} - \frac{\partial \Psi}{\partial x}$$
$$= -A_1 iN \exp\left[-qz + i(\omega t - Nx)\right] + A_2 iN \exp\left[-sz + i(\omega t - Nx)\right] \tag{3-81}$$

From Eq. (3-70) we can get

$$A_2 = -\frac{2qiNA_1}{s^2 + N^2}$$

and substitution of A_2 into Eqs. (3-80) and (3-81) gives

$$u = A_1\left[-iN \exp(-qz) + \frac{2iqsN}{s^2 + N^2} \exp(-sz)\right] \exp i(\omega t - Nx) \tag{3-82}$$

and

$$w = A_1\left[\frac{2qN^2}{s^2 + N^2} \exp(-sz) - q \exp(-qz)\right] \exp i(\omega t - Nx) \tag{3-83}$$

Equations (3-82) and (3-83) can be rewritten

$$u = A_1 N i\left\{-\exp\left[-\frac{q}{N}(zN)\right] + \frac{2\frac{q}{N}\frac{s}{N}}{\frac{s^2}{N^2} + 1} \exp\left[-\frac{s}{N}(zN)\right]\right\}$$
$$\times \exp i(\omega t - Nx) \tag{3-84}$$

and

$$w = A_1 N\left\{\frac{2\frac{q}{N}}{\frac{s^2}{N^2} + 1} \exp\left[-\frac{s}{N}(zN)\right] - \frac{q}{N} \exp\left[-\frac{q}{N}(zN)\right]\right\}$$
$$\times \exp i(\omega t - Nx) \tag{3-85}$$*

Now, from Eqs. (3-84) and (3-85), the variation of u and w with depth can be expressed as

$$U(z) = -\exp\left[-\frac{q}{N}(zN)\right] + \frac{2\frac{q}{N}\frac{s}{N}}{\frac{s^2}{N^2} + 1} \exp\left[-\frac{s}{N}(zN)\right] \tag{3-86}$$

and

$$W(z) = \frac{2\frac{q}{N}}{\frac{s^2}{N^2} + 1} \exp\left[-\frac{s}{N}(zN)\right] - \frac{q}{N} \exp\left[-\frac{q}{N}(zN)\right] \tag{3-87}$$

* The significance of the presence of i in the expression for u (Eq. 3-84) and its absence in the expression for w (Eq. 3-85) is that the u-component of displacement is 90° out of phase with the w-component of displacement.

The functions $U(z)$ and $W(z)$ represent the spatial variations of the displacements u and w. Equations (3-59) and (3-60) can be rewritten

$$\frac{q^2}{N^2} = 1 - \frac{\omega^2}{N^2 v_P^2} \tag{3-88}$$

and

$$\frac{s^2}{N^2} = 1 - \frac{\omega^2}{N^2 v_S^2} \tag{3-89}$$

and then, using Eqs. (3-75) and (3-76), Eqs. (3-88) and (3-89) can be reduced to

$$\frac{q^2}{N^2} = 1 - z^2 K^2 \tag{3-90}$$

and

$$\frac{s^2}{N^2} = 1 - K^2 \tag{3-91}$$

Now, $U(z)$ and $W(z)$ can be evaluated in terms of the wave number N for any given value of Poisson's ratio. For example, if $\nu = \frac{1}{4}$, $U(z)$ and $W(z)$ are given by

$$U(z) = -\exp[-0.8475\,(zN)] + 0.5773 \exp[-0.3933\,(zN)] \tag{3-92}$$

and

$$W(z) = 0.8475 \exp[-0.8475(zN)] - 1.4679 \exp[-0.3933(zN)] \tag{3-93}$$

Figure 3-14 shows curves for $U(z)$ and $W(z)$ vs. distance from the surface in wave lengths of the Rayleigh wave (L_R) for Poisson's ratios of 0.25, 0.33, 0.40, and 0.50.

Wave System at Surface of Half-Space

In preceding paragraphs expressions have been determined for the wave velocities of the three principal waves which occur in an elastic half-space. Knowing these velocities, we can easily predict the order in which waves will arrive at a given point due to a disturbance at another point. In addition to predicting the order of arrival of the waves along the surface, Lamb (1904) described in detail the surface motion that occurs at large distances from a point source at the surface of an ideal medium.

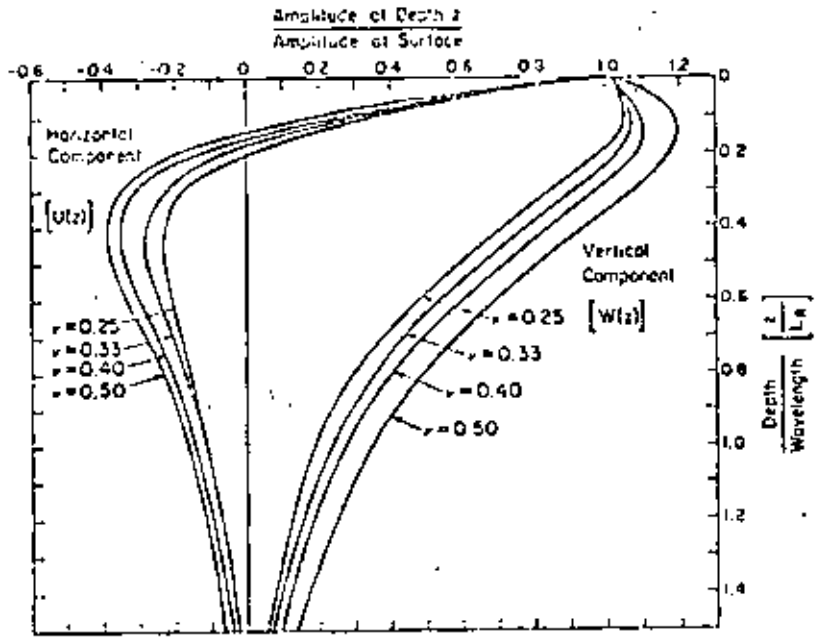

Figure 3-14. Amplitude ratio vs. dimensionless depth for Rayleigh wave.

Under the conditions considered by Lamb, a disturbance spreads out from the point source in the form of a symmetrical annular-wave system. The initial form of this wave system will depend on the input impulse; but if the input is of short duration, the characteristic wave system shown in Fig. 3-15 will develop. This wave system has three salient features corresponding to the arrivals of the *P*-wave, *S*-wave, and *R*-wave. The horizontal and vertical components of particle motion are shown separately in Fig. 3-15. A particle at the surface first experiences a displacement in the form of an oscillation at the arrival of the *P*-wave, followed by a relatively quiet period leading up to another oscillation at the arrival of the *S*-wave. These events are referred to by Lamb as the *minor tremor* and are followed by a much larger magnitude oscillation, the *major tremor*, at the time of arrival of the *R*-wave.

The time interval between wave arrivals becomes greater and the amplitude of the oscillations becomes smaller with increasing distance from the source. In addition, the minor tremor decays more rapidly than the major tremor. It is evident, therefore, that the *R*-wave is the most significant disturbance along the surface of a half-space and, at large distances from the source, may be the only clearly distinguishable wave.

7.10. LOVE WAVES

In the Rayleigh waves examined in the previous section the material particles move in the plane of propagation. Thus, in Rayleigh waves over the half-space $y > 0$ along the surface $y = 0$, propagating in the x-direction, the z-component of displacement w vanishes. It may be shown that surface waves with displacements perpendicular to the direction of propagation (the so-called *SH waves*) is impossible in a homogeneous half-space. However, *SH* surface waves are observed as prominently on the Earth's surface as other surface waves. Love showed that a theory sufficient to include *SH* surface waves can be constructed by having a homogeneous layer of a medium M_1 of uniform thickness H_1, overlying a homogeneous half-space of another medium M.

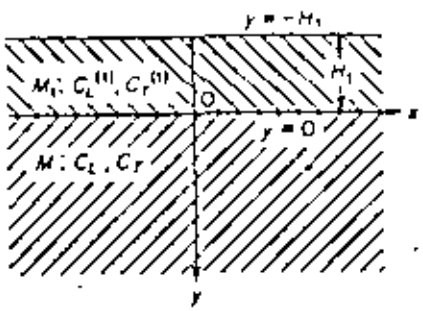

Fig. 7.10:1. A layered half-space.

Using axes as in Fig. 7.10:1, we take $u = v = 0$, and

$$(1) \qquad w = A \exp\left[-k\sqrt{1 - \frac{c^2}{c_T^2}}\, y\right] \exp\{ik(x - ct)\}$$

in M, and

$$(2) \qquad w = \left\{A_1 \exp\left[-k\sqrt{1 - \left(\frac{c}{c_T^{(1)}}\right)^2}\, y\right] + A_1' \exp\left[k\sqrt{1 - \left(\frac{c}{c_T^{(1)}}\right)^2}\, y\right]\right\} \times \exp\{ik(x - ct)\}$$

in M_1. It is easily verified that these equations satisfy the Navier's equations. If $c < c_T$, then $w \to 0$ as $y \to \infty$, as desired.

The boundary conditions are that w and σ_{zy} must be continuous across the surface $y = 0$, and σ_{zy} zero at $y = -H_1$. On applying these conditions to (1) and (2), we obtain

$$(3) \qquad A = A_1 + A_1',$$

$$(4) \qquad GA[1 - (c/c_T)^2]^{1/2} = G_1(A_1 - A_1')[1 - (c/c_T^{(1)})^2]^{1/2},$$

$$(5) \qquad A_1 \exp\{kH_1[1 - (c/c_T^{(1)})^2]^{1/2}\} = A_1' \exp\{-kH_1[1 - (c/c_T^{(1)})^2]^{1/2}\}.$$

Eliminating A from (3) and (4), and then using (5) to eliminate A_1 and A_1', we have

$$\frac{G[1 - (c/c_T)^2]^{1/2}}{G_1[1 - (c/c_T^{(1)})^2]^{1/2}} = \frac{A_1 - A_1'}{A_1 + A_1'} = i \tan\{ikH_1[1 - (c/c_T^{(1)})^2]^{1/2}\}.$$

Hence, we have

$$(6) \qquad G[1 - (c/c_T)^2]^{1/2} - G_1[(c/c_T^{(1)})^2 - 1]^{1/2} \tan\{kH_1[(c/c_T^{(1)})^2 - 1]^{1/2}\} = 0$$

as the equation to give the *SH* surface wave velocity c in the present conditions.

If $c_T^{(1)} < c_T$, Eq. (6) yields a real value of c which lies in the range $c_T^{(1)} < c < c_T$ and depends on k and H_1 (as well as on G, G_1, c_T, and $c_T^{(1)}$), because for c in this range the values of the left-hand-side terms in (6) are real and opposite in sign. Thus, *SH* surface waves can occur under the stated boundary conditions, provided the shear velocity $c_T^{(1)}$ in the upper layer is less than that in the medium M. These waves are called *Love waves*.

Love waves of general shape may be derived by superposing harmonic Love waves of the type (2) with different k. The dependence of the wave speed c on the wave number k introduces a dispersion phenomenon which will be considered later.

PROBLEMS

7.2. Derive Navier's equation in spherical polar coordinates.

7.3. From data given in various handbooks, determine the longitudinal and shear wave speeds in the following materials:

(a) Gases: air at sea level, and at 100,000 ft altitude.

(b) Metals: iron, a carbon steel, a stainless steel, copper, bronze, brass, nickle, aluminium, an aluminium alloy, titanium, titanium carbide, berylium, berylium oxide.

(c) Rocks and soils: a granite, a sandy loam.

(d) Wood: spruce, mahogany, balsa.

(e) Plastics: lucite, a foam rubber.

7.4. Sketch the instantaneous wave surface, particle velocities, and particle paths of a Love wave.

7.5. Investigate plane wave propagations in an anisotropic elastic material. Apply the results to a cubic crystal. *Note:*

$$\rho \frac{\partial^2 u_i}{\partial t^2} = C_{ijkl} \frac{\partial u_j}{\partial x_k \partial x_l}, \qquad u_i = A_i e^{i(\omega t - k_j x_j)}$$

where $k(k_1, k_2, k_3)$ is the wave vector normal to the wave front.

7.6. Determine the stress field in a rotating, gravitating sphere of uniform density.

EFFECT OF LOCAL SOIL CONDITIONS UPON EARTHQUAKE GROUND MOTIONS

by Robert V. Whitman

1. INTRODUCTION

It has long been recognized that local soil conditions can have a profound effect upon the damage caused by an earthquake. Such an effect was clearly evident in accounts of the great Lisbon earthquake of 1755, and in the accounts of almost every subsequent major earthquake that affected a large city. The effect of soil conditions upon damage during the 1906 San Francisco earthquake was well recognized in studies of that earthquake. The topic received considerable study following the Kanto (Tokyo) earthquake of 1923. The effect of local soil conditions upon earthquake damage is hardly a new problem. The seismic codes of most countries specifically require different earthquake resistance for different soil conditions. Codes now in effect in the United States contain no such requirement, but not because soil conditions are thought to be unimportant. The writers of the U.S. codes recognized the importance of soil conditions, but felt the problem was so complex and poorly understood that adequate code provisions could not be written. Without a doubt, soil conditions will be incorporated into U.S. seismic codes in the very near future.

Much of the earthquake damage to buildings built upon poor soils results from partial or complete failure of the soil. Such failures include slumping of river banks, failure of waterfront retaining structures, large landslides, foundation settlement and foundation failures. Seed (1970) has provided an excellent summary description of such failures. Many such failures are caused by total or partial liquefaction of loose saturated cohesionless soils. The possibility of such failures, especially liquefaction failures, in any given locale or site requires individual study by experts. Appendix B contains a very brief discussion of liquefaction.

This chapter considers the effect of local soil conditions upon earthquake ground motions, and hence upon the shaking of buildings.

when there is no failure of the soil. Field observations and theoretical studies of this effect have been summarized in recent papers by Ohsaki (1969) and Seed (1963). Much is now known about the problem, although by no means is there complete understanding. There are several ways in which this new knowledge can be put to practical use. One way is the development of site-conditioned earthquake motions for input to the analysis of important structures; this approach is now being used in the design of tall buildings in San Francisco and Tokyo. The second way is to guide the development of new building code provisions. This chapter deals primarily with the latter application. That is, the chapter will discuss how the base shear coefficient C should vary with soil conditions. A plot of C vs. T, the fundamental period of the building, will be called a seismic coefficient diagram.

Figure 1 illustrates several different forms of seismic coefficient diagrams incorporating soil conditions. The simplest forms are those in Figures 1a and 1b; here all ordinates are multiplied by a factor that is independent of period. That is:

$$C(T) = S\, C_0(T) \qquad (1)$$

where S is a soil factor and $C_0(T)$ is the seismic coefficient function for a reference soil condition. Ohsaki (1969) has tabulated values of S required by the codes of 13 countries. Table 1 gives examples of such factors, ranging from the very simple table used in Canada to the somewhat complex table in effect in Japan.

Figures 1c through 1f show more complicated proposals for introducing the effect of local soil conditions into seismic coefficient diagrams; now the effect of soil is varied depending upon the period T.

1. Figure 1c comes from the new Chilean code. The curve of C vs. T varies in shape depending upon a parameter T_0. The parameter T_0 is related to the characteristic frequency of the site of the building being designed.
2. Figure 1d shows a seismic coefficient diagram proposed by Muto in Japan in 1963. Both the maximum seismic coefficient and the period scale are adjusted in accordance with the type of ground.

3. According to the proposed curves shown in Figure 1e, low stiff buildings having a small period I would be designed for a larger seismic coefficient if on hard ground than if on soft ground. For tall flexible buildings, the reverse would be true.

4. Figure 1f shows the code provisions developed for Mexico City, so as to account for the effect of the unusually soft and deep clay which underlies much of that city.

Thus, a great variety of methods have been proposed for incorporating the effects of soils conditions into the seismic provisions of building codes. A building official faced with the selection of a suitable provision, or an engineer faced with implementing such provisions, must understand the basic thinking lying behind the various proposals. To develop such basic understanding, it is useful to consider four categories of soil conditions:

I. Shallow soil deposit with a distinct characteristic frequency.
II. Deep deposit of firm soil.
III. Shallow soft soil overlying deep deposit of firm soil.
IV. Deep deposit of soft soil.

While these four cases do not encompass all possible soil conditions, they serve to bring out the fundamental considerations.

2. ROLE AND STATUS OF THEORY

In order to understand adequately the effect of local soil conditions, we must combine interpretations of actual accelerograph records together with theoretical analysis. Within the recent past, it has been necessary to rely very heavily upon theory, since the field data from accelerographs has been very scanty indeed. Because of the many accelerographs which have been installed within the past few years and will be installed within the near future, there soon should be many more records involving a variety of soil conditions. However, theory will continue to be of vital importance in helping to sort out and understand the potentially staggering quantity of rather confusing data.

The theory of ground amplification* as it exists today is by no means perfect. However, in many cases predictions from the theory are in accord with observations (Seed, 1969). There now has been considerable experience in the practical use of the theory, and we understand both its limitations as well as how it can be used. Used with judgement, this theory is a very useful tool for understanding the effects of local soil conditions.

3. CASE I: SHALLOW SOIL DEPOSIT WITH DISTINCT CHARACTERISTIC FREQUENCY

For a uniform soil deposit (Fig. 2a), the fundamental period is given by:

$$T_o = \frac{4H}{C_s} \qquad (2)$$

where H = thickness of deposit
C_s = shear wave velocity

Case I is typified by $T_o < 0.5$ sec. The following tabulation indicates typical combinations of C_s and H satisfying this condition.

C_s(m/sec)		H(m)
100	(Very soft clay or silt)	< 12.5
200	(Loose sand, soft clay)	< 25
300	(Dense sand, stiff clay)	< 37.5
400	(Compact sand, hard clay)	< 50

Soil deposits with a depth greater than about 50 meters probably do not belong in Case I. The soil descriptions in the table are intended to give a very general idea of typical shear wave velocities in soils; for further discussion of the evaluation of soil properties for specific cases, see Appendix A and Whitman (1969). Since the soil is nonlinear, the shear wave velocity and hence the fundamental period depend upon the intensity of the earthquake, decreasing as the intensity increases.

* The nature of this theory is outlined in Appendix A.

Theoretical Considerations

The theory of soil amplification may conveniently be used to indicate the expected effects of a shallow soil deposit.

Amplification spectrum: An amplification spectrum is the ratio of the Fourier amplitude spectra for motions atop the soil to the Fourier amplitude spectra for motions of the underlying rock. Thus an amplification spectrum shows how the various frequency components in earthquake motion are amplified by the soil.

Figure 2b shows a typical amplification spectrum for a shallow soil deposit. It is characterized by a predominant peak, which occurs at the period given by Eq. 3. Smaller, unimportant peaks may occur at very small periods. The peak amplification ratio is a function of:

1. The ratio of the seismic impedance of the soil to the seismic impedance of the underlying rock:

$$\frac{(\gamma c_s)_{soil}}{(\gamma c_s)_{rock}} \qquad (3)$$

where γ denotes unit weight. As discussed in Appendix A, this factor accounts for the loss of energy back into the underlying rock. The smaller this ratio, the greater the amplification. Thus, for a given rock, the peak amplification ratio increases as the overlying soil becomes softer.

2. The internal damping within the soil: This damping is determined primarily by the magnitude of the dynamic strains which occur within the soil. Thus, the stronger the earthquake, the greater the damping and the smaller the amplification.

One point from the theory is worth emphasizing: the amplification from an outcropping of rock to the surface of soil is less than the amplification from the interface between soil and rock to the surface of the soil. Thus, comparison of motions measured at several depths may overestimate the amplification between the surface outcroppings of different soil or rock.

For cases of interest, the peak amplification ratio between soil and an outcropping of underlying rock is typically between 3 and 6, with the larger values applying to the softer soils during smaller earthquakes.

Peak acceleration: For Case I, T_o lies within the range of the predominant periods in earthquake ground motions. Hence the amplifying effect of a shallow soil layer causes the peak acceleration at the ground surface to exceed that at an outcrop of the underlying rock. Figure 3 compares computed ground motions for the case corresponding to Fig. 2. As the peak of the amplification spectrum increases, the ratio of peak accelerations increases; however, the increase in peak acceleration is less than the peak amplification ratio. For typical cases the computed ratio of peak accelerations is from 1.5 to 4, with the larger values during smaller earthquakes. In Figure 3, note also the obvious change in predominant frequency.

Response spectra: Figure 4 compares response spectra computed from the motions on soil and on rock. At a period corresponding to the fundamental period of the soil, the ordinates of the spectra from soil motions are considerably greater than those for the spectra from rock motions. Thus, a building whose fundamental period is approximately the same as the fundamental period of the soil will respond much more strongly if on the soil than if on the rock.

A diagram formed by taking the ratio of the response spectra at each period is very similar to the amplification spectrum, although the peak of the former is not so high as the peak of the latter.

Field Evidence

While there are many pieces of evidence which support the general conclusions of the theory (see the papers by Ohsaki and Seed), it is not possible at this time to present evidence which totally substantiates the theory. In particular, there are very few instances of records from instruments placed over very different soils in the same immediate vicinity. A sampling of the available evidence is presented in the following subsections.

Amplification spectra: Figure 5 shows a comparison of actual and predicted amplification spectra [Dobry, 1971]. The heavy line is an average of amplification spectra for six earthquakes at a given site, based on measurements made at different depths in Japan. Considering that there are uncertainties in the actual amplification data introduced by the processing of the data, the theoretical curve follows the actual behavior very well.

Peak accelerations: There are a number of examples within the Japanese literature showing that peak acceleration increases as the ground surface is approached, in accordance with the theory. As observed in rather small earthquakes, during which the internal damping is small, this increase is typically in the ratio of 3 or 4. Figure 6 shows peak accelerations observed, mostly in basements of buildings, at various depths beneath the surface of the ground in Tokyo. It should be emphasized that such an increase occurs in rock as well as in soil, because the stiffness of soil decreases near the surface, partly because of weathering and partly because of decrease in overburden stress.

Response spectra: Figure 7 compares response spectra computed from ground motions measured on soft soil and firm soil during the same earthquake. In each diagram, the spectral ordinates have been normalized to the peak acceleration, and hence the effect of soil conditions shows only in the shape and not in the ordinates of the spectra. The shift in the period at which the spectra peak is the result of amplification by the soil.

Damage to buildings: Most of the evidence concerning the effect of local soil conditions is indirect: in the form of differences in damage to buildings founded over different soils (Ohsaki, 1969; Duke and Leeds, 1959). Small buildings, whose fundamental period is in the range from 0.2 to 0.5 second, generally experience greater damage when founded over soft soil than when founded upon firm soil. These observations for the most part are consistent with the theory. However, some of the differences in damage may have resulted from partial failure of softer soils in addition to differences in ground motions.

Perspective from field evidence: Considering the available comparisons between predictions and observations, it may be concluded that the theory may be used to guide the choice of seismic coefficient diagrams for practical work. However, it also is clear that more actual experience is necessary before greater accuracy can be expected from theory.

Microtremor Studies

Kanai and Tanaka (1961) have proposed a method of microzoning based upon measurement of ambient vibrations. The measured vibrations are plotted in the form of an amplitude spectra; in Kanai's original work this spectra was constructed in an approximate way, but more recently Fourier analysis has been used for this purpose. Figure 8 shows some typical results; for identification of the soil types, see Table 1. Both the period and the magnitude of the peak of the spectra are used to determine the seismic zone; the longer the period and the higher the peak, the more severe the expected damage during an earthquake. Kanai has correlated the observed period and amplitude to the four types of ground considered in the Japanese seismic code.

This approach was specifically developed to predict the effect of shallow soil deposits upon damage to buildings having only a few stories. For these conditions, the predictions made by Kanai's approach are entirely consistent with the predictions of amplification theory. Thus, there is a sound reason why Kanai's approach has been in accord with experience during actual earthquakes.

Medvedev's Method

The Russian seismologist Medvedev (1962) has proposed a method for estimating the effect of ground conditions upon earthquake intensity, based upon two factors:

1. The ratio

$$\frac{(\gamma C_p)\ \text{soil}}{(\gamma C_p)\ \text{granite}} \qquad (4)$$

where C_D is the dilatational, or compressive, wave velocity. The wave velocity for granite serves as a reference against which a soil is rated. The smaller this ratio, the more severe the expected damage during an earthquake.

2. The depth to the water table. The shallower the water table, the greater the expected damage.

These two factors are combined in the equation

$$n = 1.67 \log_{10}\left[\frac{(\gamma C_D)\ \text{rock}}{(\gamma C_D)\ \text{soil}}\right] + e^{-0.04h^2} \qquad (5)$$

where n is the increment in intensity units on a scale equivalent to the modified Mercalli scale, and h is the depth to the water table in meters. Eq.5 typically gives an increase in 1 to 2 intensity units (equivalent to a 2 or 4 fold increase in acceleration) for soft ground as compared to firm ground. Medvedev's method was originally developed for use in connection with shallow soil deposits and buildings having only a few stories.

The relationship between Medvedev's method and amplification theory may be understood by means of the example in Figure 9. When the water table is very low, then the ratio C_D/C_S is the same for both the soil and the rock. Thus ratios 3 and 4 are equivalent, and Medvedev's method and amplification theory will predict the same trends. The soil in Figure 9b has the same C_S as in Figure 9a, and thus amplification theory would predict the same behavior for both cases. Raising the water table means that C_D increases considerably in the soil, and thus the first term in Medvedev's equation decreases. However, this decrease is compensated by an increase in the second term. Thus, Medvedev's two factors taken together give roughly the same result as amplification theory. Moreover, the increases in intensity predicted by Medvedev are consistent with increases in acceleration predicted by amplification theory.

Summary

For the common case of shallow soil deposits, the predictions of amplification theory are generally in accord with actual experience during earthquakes and moreover are in accord with the semi-empirical methods of microzoning proposed by Kanai and Medvedev.

Figure 10 summarizes the effect of local soil and rock conditions upon response spectra (say for 5% damping) at a given distance from the epicenter of an earthquake. With increasing softness of the earth material, the peak of the spectra increases and shifts to a larger period. Thus, the response of low stiff buildings is strongly affected by soil conditions. On the other hand, a shallow soil deposit has little or no effect upon the response of the fundamental period of tall buildings having long natural periods (although the shallow soil will affect the response of the higher modes of such a building).

Based upon current knowledge, a seismic coefficient diagram such as type (b) in Figure 1 should be used to account for differences in near surface earth materials within a small region. That is to say, the soil factor S should be independent of period. There are several reasons for this recommendation.

1. Because of uncertainties in both the fundamental period of the soil and the predominant periods in the input ground motion, it is difficult to predict the predominant period in motion at the top of soil. Use of constant S for $T < 0.5$ sec. covers these uncertainties.
2. Use of constant S for $T > 0.5$ sec. recognizes that the contribution of the higher modes will be affected by soil conditions, and provides extra conservatism with regard to the design of tall buildings.

With further research, it may be possible to use a reduced value of S for $T > 0.5$ sec.

Table 2 gives recommended soil factors. These factors are based upon both theory and experience, and consider possible settlement problems in addition to amplification effects. In the 2nd column of the table, hard crystalline rock found at considerable depth has been taken as the reference; the soil factor for a soft soil is 4. However, it generally is more practical to use surface exposures of rock as a reference (3rd column), and then the soil factor for soft soil is 2.2. In some localities, it may even be desirable to use firm soil as a reference (4th column), in which case the soil factor for soft soil is only 1.6.

4. CASE II DEEP DEPOSIT OF FIRM SOIL

Several areas that have experienced major earthquakes are underlain by more than 100 meters of compact alluvium. Los Angeles, Caracas, Venezuela, and Santiago, Chile are prime examples.

Theoretical Considerations

Amplification spectra: Figure 11 illustrates the general nature of the amplification spectrum for this case. Now several peaks occur within the range of building periods of practical interest.

The fundamental period is greater than in Case I, and tends to coincide with the period of taller structures. Because the shear wave velocity of compact alluvium is rather high (300 to 450 m/sec) the radiation damping also is greater than in Case I, and hence the amplification at the fundamental peak generally is less than in Case I. Nonetheless, this amplification can be quite important.

The higher order peaks typically occur at periods less than 0.5 second; that is, within the same range of periods for which amplification occurred in Case I. Radiation damping is less important for these higher modes, and hence when internal damping is small--as during small earthquakes--the peaks corresponding to these modes may be nearly as high as the fundamental peak.

Peak accelerations: Figure 12 shows computed acceleration at ground surface, for conditions corresponding to Figure 10 (the input is the same as in Fig. 3, but with a peak acceleration of 0.03g). Peak acceleration is increased: typical increases are factors of 1.5 to 3, with the larger values applying to smaller earthquakes. This increase is caused by the higher modes of the soil; these modes have amplification peaks in the range of the predominant periods of the input motion. The fundamental mode does not cause an increase in peak acceleration, but does amplify the longer period components of ground motion.

Response spectra: Figure 13 compares response spectra for motions at the surface of several different depths of compact alluvium. Changing the depth of the alluvium has relatively little effect upon the general position of the spectra for T < 0.5 second. However, increasing the depth of the alluvium has a very significant effect upon the spectra at larger periods corresponding to taller buildings.

Field Evidence

There is, to the author's knowledge, no adequate direct confirmation of these theoretical results, although Gutenberg (1957) has shown that deep deposits amplify the long period components of ground motion. Actual accelerograph records from nearby sites with very different depths of alluvium must be obtained before adequate confirmation is possible.

Observations of damage to buildings during the Caracas earthquake of July 1967 do provide strong indirect confirmation of the theory (Whitman, 1969; Seed et al, 1970). Caracas is underlain by a compact alluvium whose depth generally is less than 100 meters. However, under one portion of the city the depth is as much as 300 meters. Analysis of the patterns of damage shows:

1. For buildings having 8 stories or less, the percentage of buildings damaged is more-or-less constant for all parts of the city.

2. Buildings having more than 8 stories, and particularly those having more than 15 stories, were much more heavily damaged in the part of the city over the very deep alluvium than elsewhere in the city.

These observations show clearly that a great depth of alluvium significantly amplifies the earthquake threat to tall buildings.

Summary

The theory, together with the evidence from the Caracas earthquake shows the need to guard against the strong shaking that can occur when the fundamental period of a tall building coincides with the fundamental period of a deep soil deposit. Thus, the fundamental period of the soil must enter into the code. When differences in depth of soil, rather than differences in the nature of the soil, are of concern, it appears that a seismic coefficient diagram of type (c) in Figure 1 is suitable. An example is the following formula from the Chilean code:

$$C = \begin{cases} C_o & T \leq T_o \\ C_o \left[\dfrac{2\ T/T_o}{1+(T/T_o)^2} \right] & T \geq T_o \end{cases} \qquad (6)$$

The soil period T_o must be determined from a combination of experience, careful analysis of earthquake records and theoretical studies. Usually it is not possible to determine T_o by measurement of microtremors, since the high frequencies present in ambient vibrations mask the low frequencies associated with the fundamental period. When using Eq. 6, T_o should always be at least 0.4 even if the fundamental period is smaller than this limit.

5. CASE III SHALLOW SOFT SOIL OVERLYING DEEP DEPOSIT OF FIRM SOIL

Theoretical Considerations

As yet, this case (which is sketched in Figure 14) has not been studied completely from a theoretical standpoint. The effect of the soft shallow deposits enter through the higher modes, and the response of these higher modes is quite sensitive to the details of the analysis--especially the assumptions concerning damping. The theoretical results which have been computed are not entirely satisfactory.

However, in a general way it may be said that Case III is a combination of Case I and Case II. Thus the fundamental mode of the deep compact alluvium will amplify long period motions while the higher modes of the deep alluvium will also amplify shorter period motions. The shallow soil deposits will further amplify the short period motions. With respect to the effect upon buildings, the following can be expected:

1. Buildings with $T < 0.5$ second. Damage will be greater if these buildings are founded upon the soft soil than if they rest upon firm alluvium. The depth of the firm alluvium beneath a building has little effect upon the damage to that building. Thus conclusions applicable to Case I apply.
2. Buildings with $T > 0.5$ second. Damage will be greater if a building is founded over a great depth of firm alluvium than if it rests upon a shallow depth of this alluvium. The presence or absence of soft soil near the surface has less effect upon the damage. Thus conclusions applicable to Case II apply.

Field Evidence

Damage in Valdivia and Concepción during the 1960 earthquakes has been studied extensively (Duke and Leeds, 1963, and subsequent studies at the University of Chile). This damage was greatest where there was soft soil at the surface. The great majority of this damage was to 1 and 2 story buildings. Thus the behavior during these earthquakes is consistent with Case I. Hence it is not surprising that predictions based upon Kanai's and Medvedev's methods correlated well with the damage patterns.

At both of these cities, there exist deep deposits of firm soil. Using amplification theory, attempts have been made to correlate damage to this total depth. However, since there were very few buildings having periods greater than 0.5 second, no such correlation was possible. Moreover, since the theory for a soft shallow layer over a deep stiff layer is still not reliable, the theory often did not show correctly the effect of the shallow layer.

Thus the experience from the 1960 earthquakes showed the effect of shallow soft deposits but gave no indication as to the effect of varying depths of the compact alluvium. However, the effect of the deep alluvium must not be ignored when establishing microregionalization or building code provisions for future construction, because more and more tall buildings certainly will be constructed in these and other cities with similar soil conditions.

Summary

A seismic coefficient diagram for this case must recognize both the effect of shallow soft deposits upon buildings having $T < 0.5$ second and also the effect of deep soil upon buildings having longer periods. These requirements might be met by combining Eqs. 1 and 6:

$$C = \begin{cases} C_o S & T \leq T_o \\ C_o S \left[\dfrac{2T/T_o}{1+(T/T_o)^2} \right] & T \geq T_o \end{cases} \qquad (7)$$

The soil factor S would be chosen based upon the shear wave velocity of the near-surface soils, while T_o would bring in the effect of the deep deposit. Such a code provision might apply to many cities, such as Boston for example, where very poor soils at the surface overlie deep deposits of clay. Such a provision probably should be used only for $T < 1.5$ seconds. If the fundamental period of the soil is greater, special provisions such as that described in the next section are warranted. As before, the minimum T_o is 0.4.

6. CASE IV. DEEP DEPOSIT OF SOFT SOIL

Theoretical Considerations

Amplification spectra: Figure 15 shows an amplification spectra for a deep deposit of very soft clay. This spectrum is similar to that in Fig. 10, with one important difference: now the peak amplification at the fundamental mode is distinctly greater than that for the higher modes. This change occurs because, with a deep deposit of soft soil, radiation damping is less important and strains (and hence internal damping) are larger.

Response spectra: Figure 16 compares response spectra from motions measured on top of the soil with that from motions at an outcropping of the underlying hard soil. There is an increase in the ordinates at low periods. However, the remarkable feature is the very great increase in the range from 2 to 2.5 seconds. Now the peak of the spectra has been shifted to a much larger period.

Peak acceleration: In the case corresponding to Figure 16, peak acceleration on top of the soil was twice that on the hard outcropping. In other cases which have been investigated theoretically, peak acceleration is decreased.

Field Evidence

The classic example of this case is the soft deep deposit of clay underlying Mexico City. The examples in Figs. 15 and 16 apply for the soil conditions in Mexico City, and have been confirmed by actual accelerograph records.

It has often been suggested that a deep soft deposit can actually cause a decrease in peak acceleration. While there is little or no field evidence to prove this, such might occur during a strong earthquake when the internal damping within the soil would be increased.

Summary

For this situation, it is appropriate to use a seismic coefficient diagram of Type (f) in Fig 1. Now the seismic coefficient is less for very small periods than for intermediate periods. However, at this time use of such a diagram is justified only for sites where there is considerable actual experience which has been studied in detail.

7. PILE FOUNDATIONS

The evidence currently available suggests that piles usually do not alter the ground motions at the base of a building (Ohsaki, 1969). This is because piles generally are flexible enough to follow the horizontal motions of the soil (for example, see Yamamoto and Seki, 1970). However, piles may improve the ability of the building to resist the effects of the ground motion--by reducing both static settlements (that may use up some of the reserve strength of the building) and dynamic rocking motion. Because of the need for less conservatism, the soil factor S might be reduced somewhat for pile-supported buildings.

Large diameter caissons may be stiff enough to resist following the motions of a soft soil through which they pass (Ohsaki, 1969). Then the amplifying effect of the soil-caisson system will be more like that of a firm soil rather than a soft soil. Thus for caisson-supported buildings, T_0 used in Eq. 7 could be somewhat less than the fundamental period of the soil.

Unfortunately, at the present time there are no sound rules for deciding just how much S and T_0 might be modified in accordance with these considerations.

8. RESPONSE SPECTRA AND TIME HISTORIES

The emphasis in this chapter has been upon code provisions to

reflect soil conditions. However, there is a growing trend toward requiring dynamic analyses for tall or important buildings.

The principles discussed in connection with Cases I, II, and III can be used to suggest the possible form for a general design response spectrum incorporating soil conditions:

$$S_a = \begin{cases} S_{ao} S & T \le T_o \\ S_{ao} \dfrac{T_o}{T} \left[(S-1) \dfrac{T_o}{T} + 1 \right] & T \ge T_o \end{cases} \qquad (8)$$

where S_a is the spectral acceleration and S_{ao} is the spectral acceleration for the reference soil condition. This equation is plotted in Figure 17. The soil factor S, which brings in the effect of the near-surface soil, might be less than in Table 2, since use of dynamic analysis means less need for conservatism. For example, the following values might be used:

Ground condition	S
Exposed rock	1.0
Firm soil	1.3
Soft soil	1.8

The effect of the near-surface soil upon spectral acceleration decreases for $T > T_o$. This is in contrast to Eq. 7 where there was need to account for the contributions from higher modes; when a dynamic analysis is performed, the response of higher modes is introduced directly.

For $T > 3$ seconds and $T_o > \frac{1}{3}$ second, Eq. 8 becomes too conservative. Tezcan (1972) has recently presented a more general approach to development of response spectra including soil effects.

Time histories whose spectra lie above the spectra given by Eq. 8

would be suitable as input for dynamic analysis. Great caution should be followed in using individual time histories generated by the theoretical procedures described in Appendix A, since there are uncertainties both in the validity of the procedures and the selection of soil properties. If such procedures are used to generate site-conditioned time histories, it is very essential that a set of time histories be developed by varying the input assumptions.

9. FINAL COMMENTS

The four cases which have been discussed in this chapter certainly do not cover all possible soil conditions, and many problems remain to be solved by further theoretical research plus analysis of accelerograph records. For example, the line of demarcation between Cases II and IV is not at all clear. However, the current understanding of the effect of local soil conditions is almost equal--and perhaps even equal--to the current understanding of the nature and amplitude of earthquake ground motions for average soil conditions. That is to say, the effect of soil conditions can be evaluated with almost as much confidence as can the reference seismic coefficient C_0.

Table 1

EXAMPLES OF SOIL FACTORS

Canada

General	1.0
Soft	1.5

Argentina

Hard	0.75
Medium	1.00
Soft	1.25
Very soft	1.50

Japan

Ground/Structure		Wood	Steel	Reinf. Conc.
I	Rock	0.6	0.6	0.8
II	Diluvium	0.8	0.8	0.9
III	Alluvium	1.0	1.0	1.0
IV	Very soft	1.5	1.0	1.0

Table 2

RECOMMENDED SOIL FACTORS TO ACCOUNT FOR EFFECT OF NEAR SURFACE SOILS

Ground condition	Reference ground condition: Hard rock	Exposed rock	Firm soil
Hard crystalline rock at depth (C_s > 1200 m/sec)	1.0	0.6	0.4
Exposed rock with minimal weathering (C_s = 700 m/sec)	1.6	1.0	0.7
Firm clay, compact sand/gravel, deeply weathered rock (C_s = 350 m/sec)	2.5	1.4	1.0
Soft clay or silt (C_s = 120 m/sec)	4.0	2.2	1.6

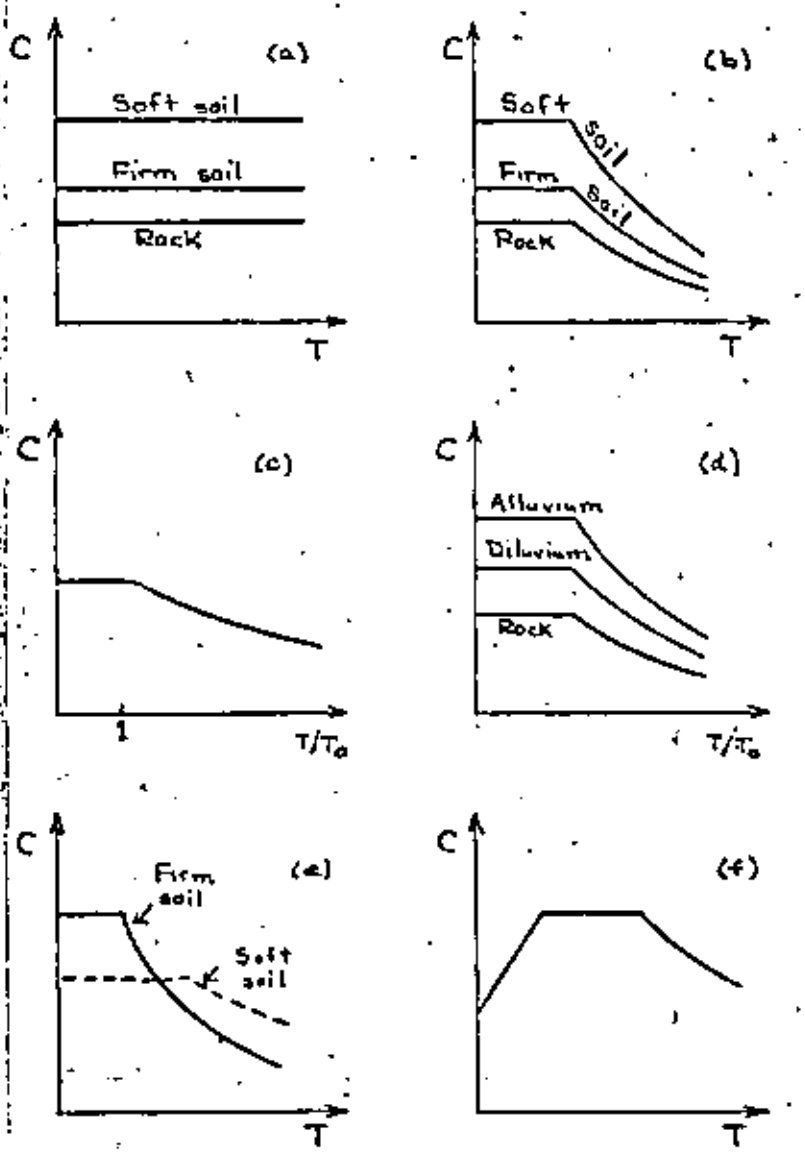

URE 1 VARIOUS TYPES OF SEISMIC COEFFICIENT DIAGRAMS

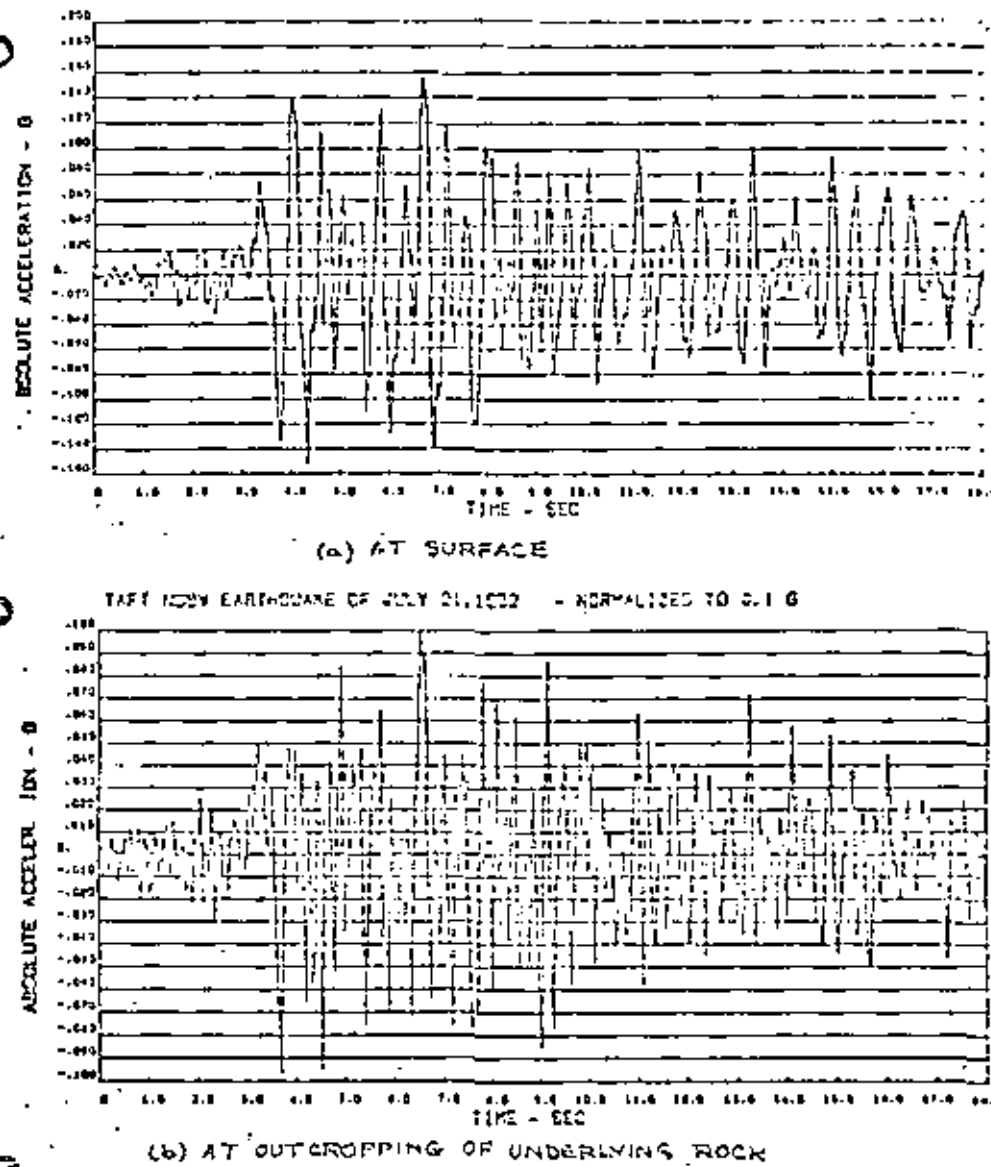

FIGURE 3 INPUT AND COMPUTED SURFACE MOTIONS FOR PROFILE IN FIGURE 2

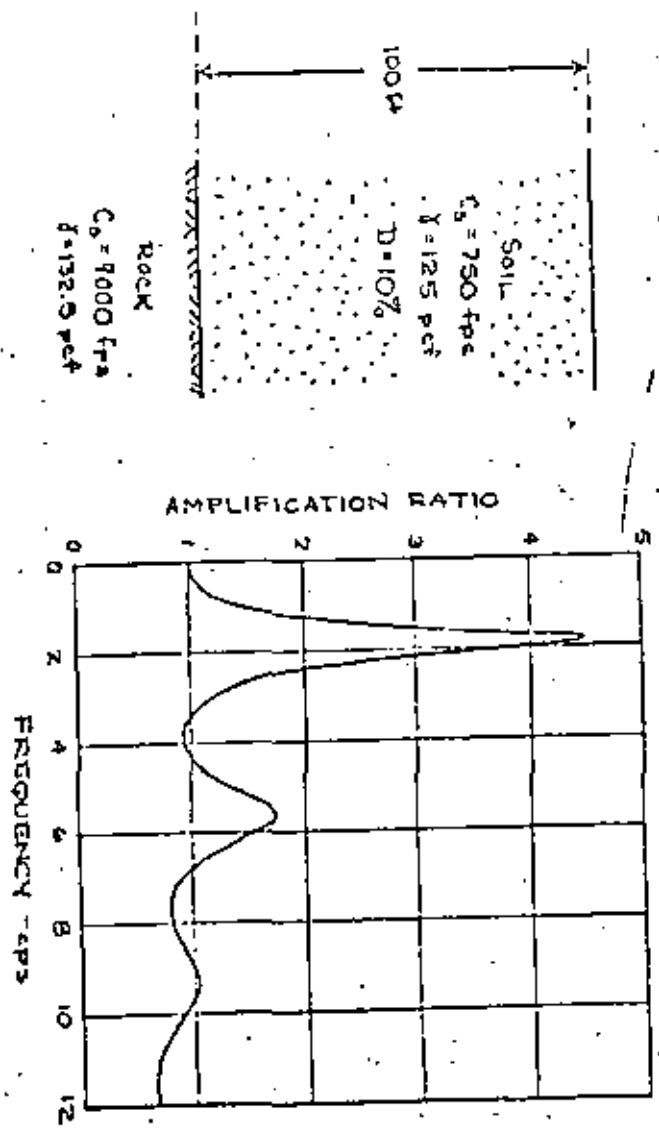

FIGURE 2 AMPLIFICATION RATIO FOR SHALLOW SOIL PROFILE

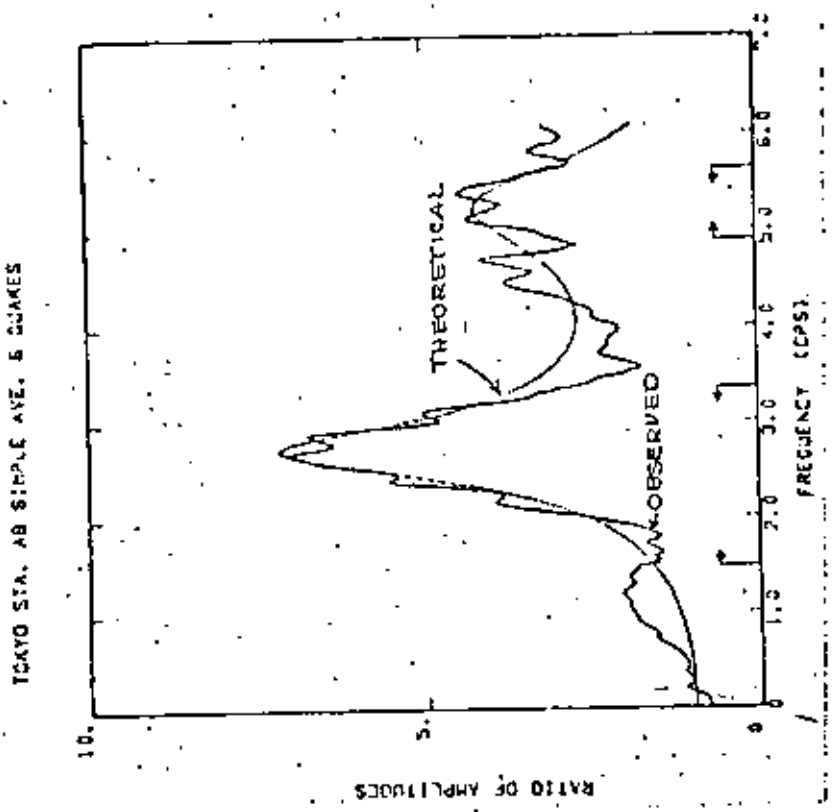

FIGURE 5 THEORETICAL AND OBSERVED AMPLIFICATION CURVES

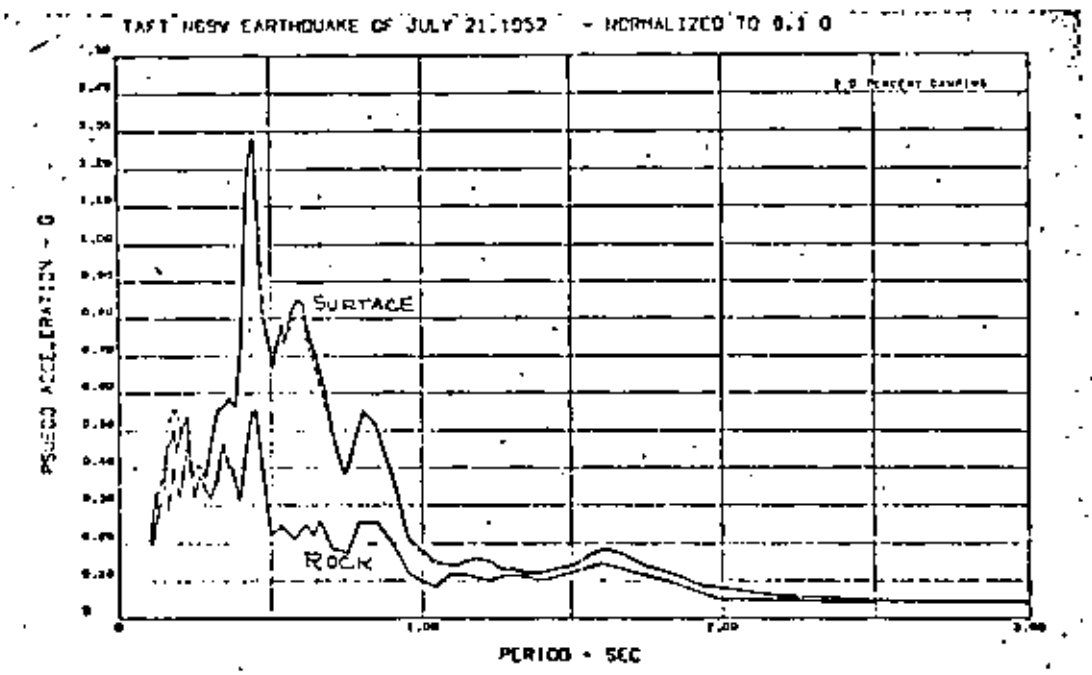

FIGURE 4 COMPARISON OF INPUT AND SURFACE RESPONSE SPECTRA FOR SHALLOW SOIL PROFILE

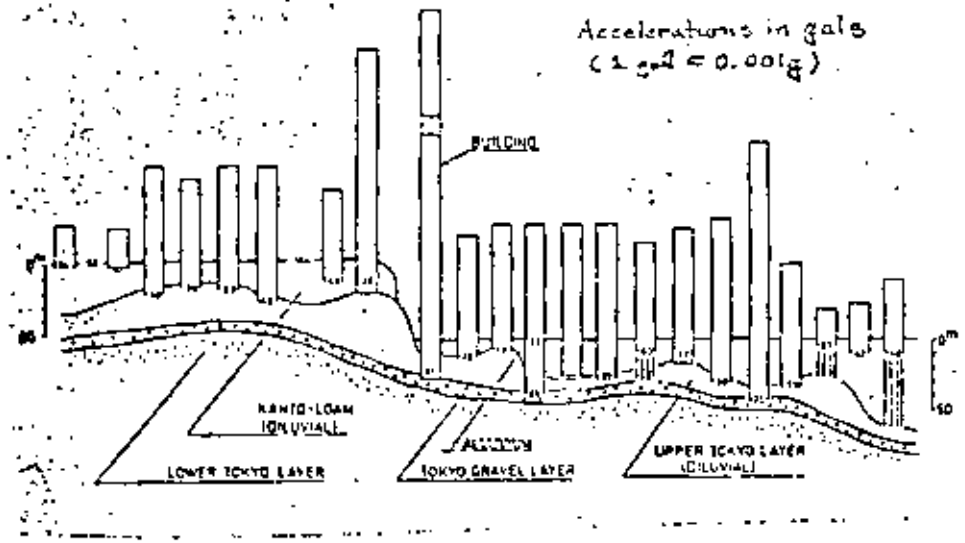

FIGURE 6 PEAK ACCELERATIONS FOR DIFFERENT SOILS AND DEPTHS IN TOKYO DURING EARTHQUAKE IN 1968 (from Ohsaki, 1969)

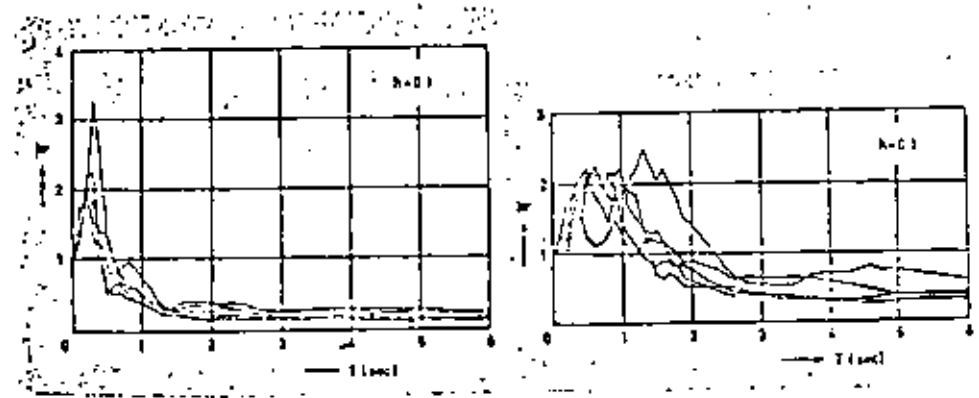

(a) Rock or hard soil (b) Soft-multi-layered soil

FIGURE 7 RESPONSE SPECTRA (normalized to peak acceleration) FOR DIFFERENT SOIL CONDITIONS IN TOKYO (from Ohsaki, 1969)

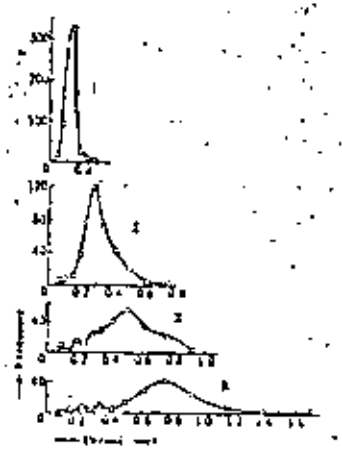

(a) Frequency of occurrence of various periods in microtremor records on different ground

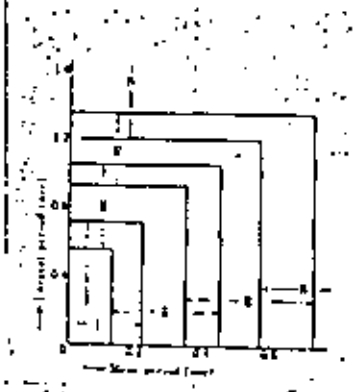

(c) Correlation of mean and largest period with ground type.

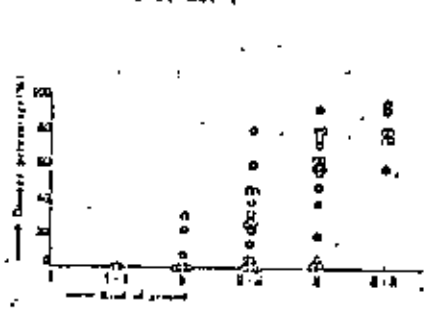

(b). Correlation between type of ground and damage to wooden buildings during 1923 earthquake.

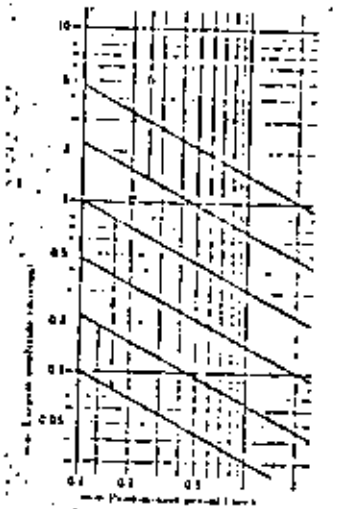

(d). Correlations of amplitude and predominant period with ground type

FIGURE 8 USE OF MICROTREMOR MEASUREMENTS TO CLASSIFY GROUND TYPE (after Kanai and Tanaka, 1961)

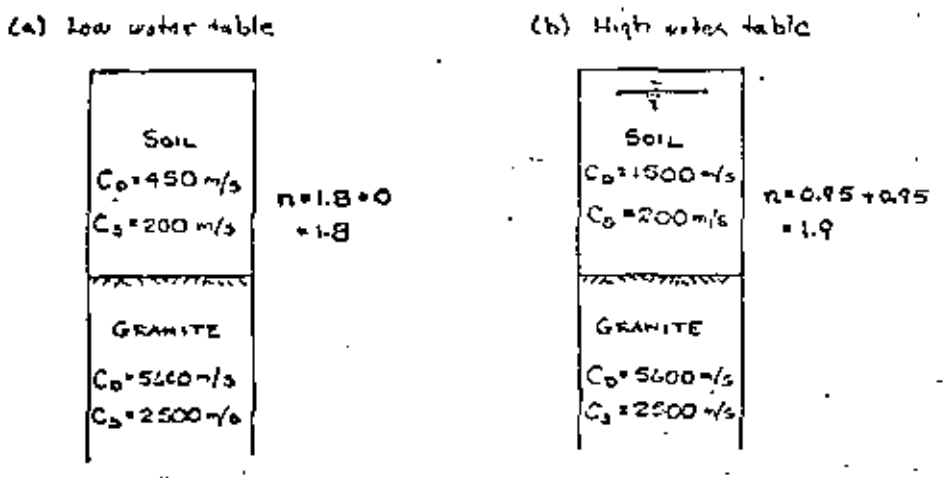

FIGURE 9 EXAMPLE OF MEDVEDEV METHOD

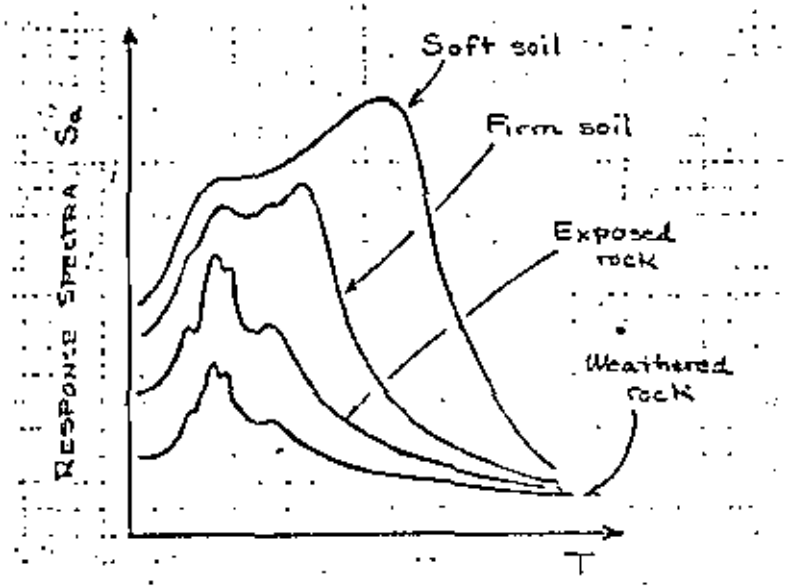

FIGURE 10 SUMMARY OF AMPLIFYING EFFECTS OF SHALLOW SOIL DEPOSIT

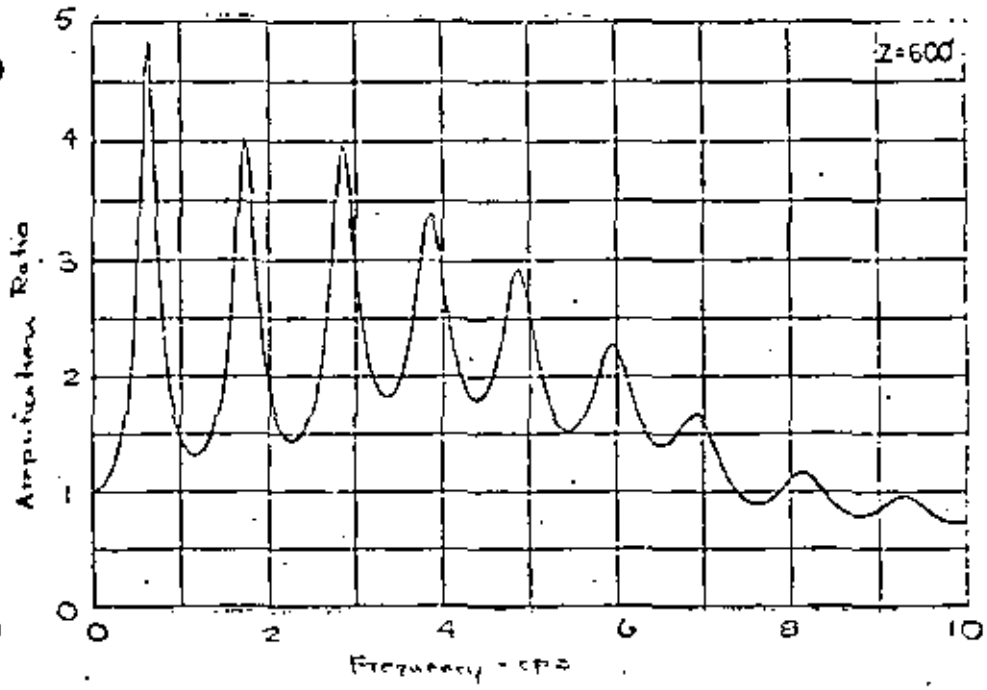

FIGURE 11 AMPLIFICATION SPECTRUM FOR 600 FOOT DEEP SOIL PROFILE

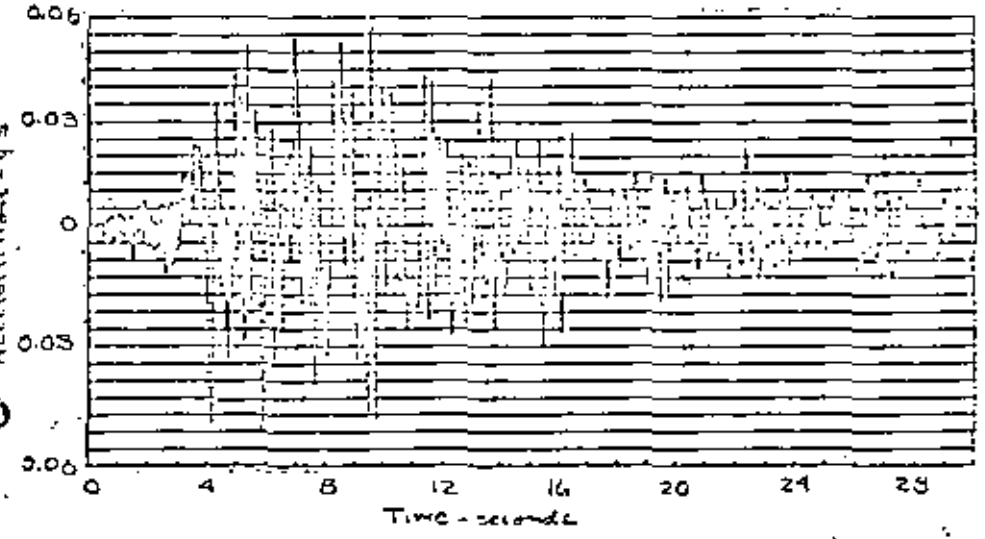

FIGURE 12 ACCELERATION COMPUTED AMP 600' OF SOIL

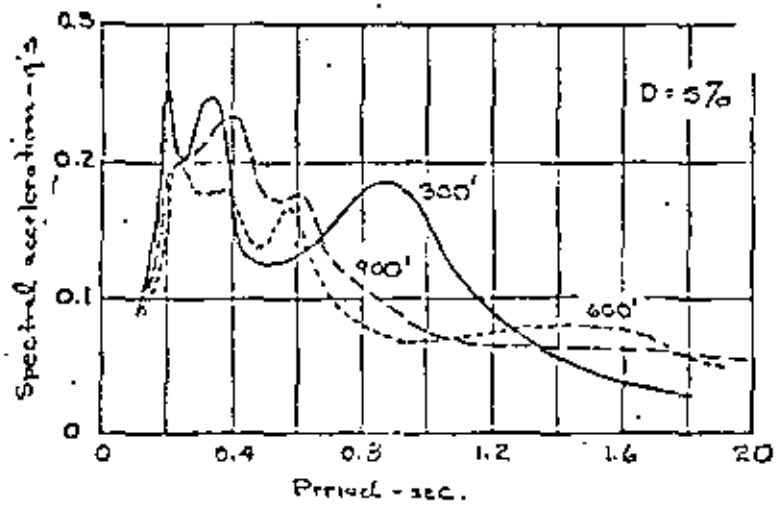

FIGURE 13 RESPONSE SPECTRA (smoothed average for several inputs) FOR DIFFERENT DEEP SOIL PROFILES

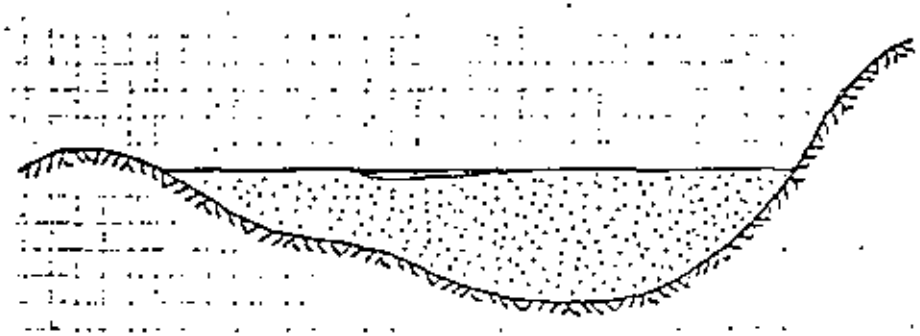

FIGURE 14 SHALLOW STRATA OF SOFT SOIL OVERLYING DEEP DEPOSIT OF FIRM SOIL

FIGURE 15 AMPLIFICATION SPECTRUM FOR DEEP PROFILE WITH VERY SOFT SOIL

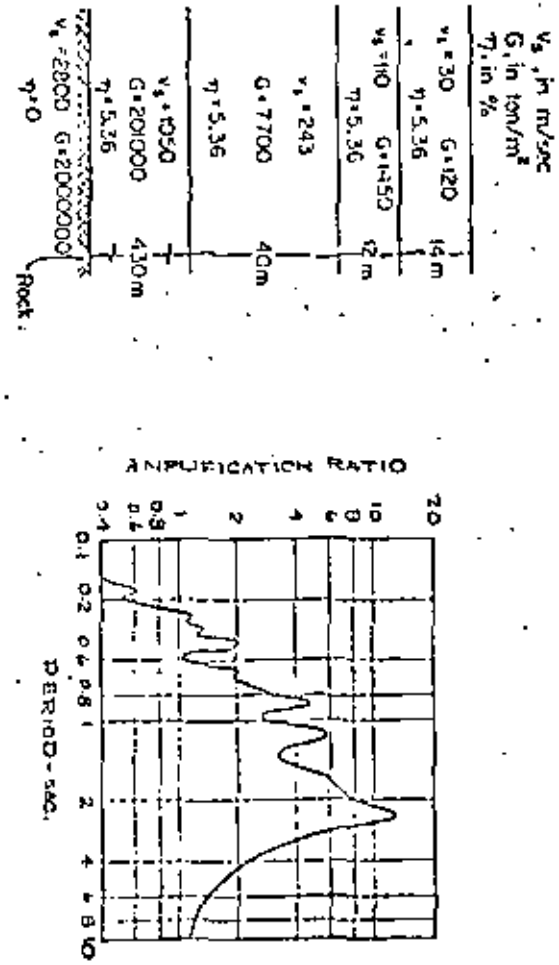

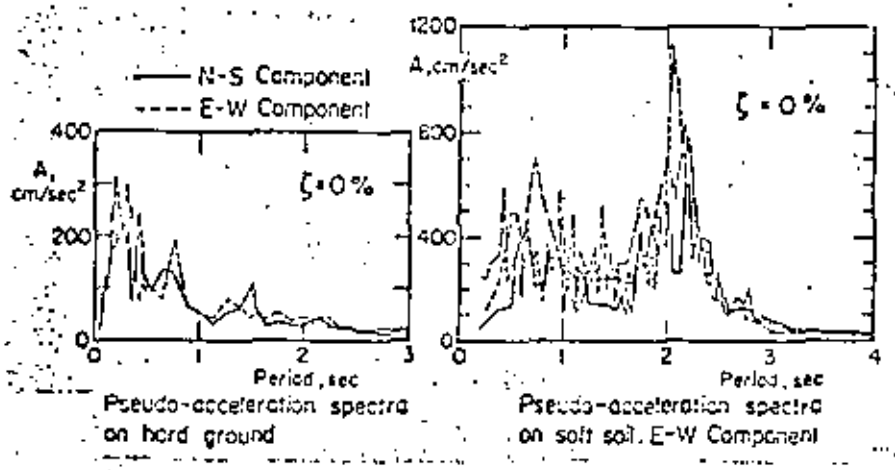

FIGURE 16 RESPONSE SPECTRA FOR HARD AND SOFT GROUND IN MEXICO CITY (from Esteva et al, 1969)

2.15

FUNDAMENTALS OF SOIL AMPLIFICATION

by

J. M. Roesset

Department of Civil Engineering

Massachusetts Institute of Technology

March 1969

Preface

The purpose of these notes is to present some of the methods now available to include the effect of local soil conditions in the derivation of design earthquakes or response spectra.

The dynamic characteristics of a soil deposit can be expressed by its transfer function representing the amplification experienced from bottom to top by a sinusoidal steady state motion. The derivation of amplification curves using both a continuous and a discrete solution is presented in II and the relative advantage of each method is discussed.

The general problem of considering an actual earthquake record and filtering it through the soil is discussed in III. Finally, approximate simplified methods are presented to obtain directly response spectra which include the effect of the soil from the knowledge of a response spectrum on firm ground or at bedrock.

Table of Contents

FUNDAMENTALS OF SOIL AMPLIFICATION*

by

J. M. Roesset

I.--INTRODUCTION

I.1 Statement of the Problem.

During the initial phases of development, Earthquake Engineering was mainly concerned with developing methods to estimate the response of a structure to given dynamic loads. While there are still many problems to be solved in the area of Structural Dynamics, particularly in the nonlinear range, it is somewhat disturbing to observe the large discrepancy between the accuracy sought by some methods of analysis and the uncertainty in the nature and magnitude of the loads to which the structure will be subjected. This inconsistency has been recognized in the last years and an increasing amount of effort is now being devoted to study the characteristics of earthquake motions as a function of magnitude, distance to the epicenter and local soil conditions. The purpose of this research is to arrive at simple, but realistic methods to represent the characteristics of the ground motion at a particular site. Among these methods one of the most powerful ones is through the use of design response spectra.

Determination of the appropriate earthquake motions at any given site involves two fundamental steps:

1. Evaluation of the seismic risk of the region. For an area with frequent strong earthquakes this step may be relatively easy and engineers may already know that a certain city is periodically subject to earthquakes of some average magnitudes with epicenters at some average distances. For regions with relatively scarce earthquake history, the determination of a design earthquake becomes much more complicated and requires in general geological and seismological studies, which attempt to identify possible sources of earthquakes or active faults.

The results of this step can take different forms, the simplest one being a series of values for probable magnitudes and associated epicentral distances. It is possible from these values, using the formulas suggested by Rosenblueth, to characterize each possible design earthquake by its maximum ground acceleration, velocity and displacement. Newmark has derived a simple approximate method by which the corresponding design spectra can be estimated, knowing these three characteristics. It is possible then to draw response spectra for each design earthquake and to find their average or envelope. Alternatively one can try to generate artificial earthquakes that would have the same average characteristics. It must be realized, however, that if this procedure is used it will not be enough to generate just one sample earthquake for a given set of values of magnitude and epicentral distance. Quite the contrary, a substantial number of samples should be generated and used for each possible earthquake, making the procedure extremely long and costly.

In any case the corresponding design earthquakes or response spectra will apply to an overall region for firm ground conditions.

2. Having obtained one or more earthquake records which could occur at the site on firm ground, or better, a set of design response spectra, the next step is to study how these motions would be modified by the local soil conditions of the particular site where the structure is going to be built. The effect of the soil is going to be one of filtering the motions, increasing their amplitude in some ranges of frequencies and decreasing it in others. This problem is normally referred to as soil amplification and will be the subject of the following discussion.

The particular problem under consideration can then be stated as: Given a soil profile and a design earthquake or response spectrum at bedrock, determine the corresponding earthquake or spectrum at the top of the soil.

It should be noticed that in order to be able to apply these results directly in the dynamic analysis of the structure, it must be

assumed that its mass is negligible in comparison to that of the underlying soil. Otherwise a third step is involved corresponding to the problem of soil-structure interaction. In other words it will not be possible to consider the structure and the soil as uncoupled systems.

1.2 General Considerations.

Earthquake motions may be decomposed into a series of waves which propagate from the focus in all directions. Given an infinite medium these waves are basically of two types: dilatational or compressional waves and shear waves. The first are normally called P waves. The second can be decomposed again by projecting the motion in two orthogonal directions. SV waves correspond to motions in a vertical plane, SH waves to horizontal motions. Of course when the direction of propagation is vertical, both SH and SV waves would correspond to horizontal motion.

When the waves propagating through a continuous medium find a free surface, a new type of wave is generated, normally referred to as surface or Rayleigh waves. If, in addition, the medium is not homogeneous, but there is a clear discontinuity at some depth from the free surface, a second type of surface wave, called Love wave, is generated. When there are several surfaces of discontinuities in the properties, other types of waves are created.

The overall problem of following an earthquake as it propagates from its focus is of course a three-dimensional wave propagation problem. By assuming for instance a line source of relatively large length or by considering only the effects at some distance from the epicenter, the problem can be reasonably reduced to a two-dimensional one for SV and P waves and a one-dimensional problem for the propagation of SH waves.

The methods described here relate all of them to the solution of the one-dimensional wave propagation equation. Their basic limitations are thus:

1. Only shear waves are considered, either SH or SV if they are propagating vertically, and only SH if they propagate at an angle. P waves propagating vertically could be considered by replacing the appropriate constants (modulus, wave propagation velocity). Surface waves are, however, neglected.

2. The different layers of soil are assumed to be parallel and extending in the horizontal direction for a distance several times larger than the total depth to bedrock.

In spite of these limitations, the solutions obtained by these methods seem to provide a useful and reasonable estimate of the filtering effect of the soil. Two-dimensional wave propagation problems can now be solved by the use of the finite element method. These techniques offer a promising future. Their application is, however, still limited and there are several questions which still have to be solved before they can be used with confidence.

The filtering effect of the soil can be measured in two different ways:

1. By considering a steady state harmonic oscillation of the soil and the underlying rock and determining the ratio of the amplitude at the free surface of the soil to the amplitude at bedrock or at the outcropping of rock (without any soil on top). This ratio will be a function of the frequency of the motion, and if there is damping, a complex function. It is normally referred to as the Transfer Function of the soil. Its modulus is the amplification function, amplification ratio or amplification spectrum.

2. By considering a given earthquake record (time history of acceleration) at bedrock or at the outcropping of rock, and determining the corresponding accelerogram at the free surface of the soil. The result in this case is not only a complete time history of acceleration at the free surface of the soil but also, if so desired, time histories of shear stresses and strains at any point within the soil. It provides therefore a much more complete solution, but it requires considerably

more computer time. Furthermore, because of the reasons previously mentioned, the complete analysis would have to be repeated for each earthquake sample, and it would make little sense to do it for just one record.

Both types of results can be obtained using two different mathematical models:

1. A continuous solution of the differential equation corresponding to the one-dimensional wave propagation problem.
2. A discrete solution replacing each layer of soil by a system of lumped masses and springs and applying standard procedures of Structural Dynamics.

The continuous model offers in general more flexibility and has an economic advantage if the results are desired only at a few points. At present the discrete model requires less computational time when complete histories of accelerations, velocities, strains and stresses are necessary at many points. Both models yield exactly the same results [except for small discrepancies due to different round-off and truncation errors] when:

a) Damping is assumed constant in all modes and viscosity for each layer directly proportional to its modulus and inversely proportional to frequency.

b) The underlying rock is assumed to be rigid or in other words the input motion is considered at bedrock with the soil on top, rather than at the outcropping of rock. For elastic rock, results can still be made to agree if an additional damping is inserted in the discrete model to simulate the loss of energy through radiation in the rock.

In the following pages the basis of both formulations will be presented, considering first the case of steady state periodic motions (determination of the amplification curve), then the case of transient motions. The application of these methods to obtain filtered earthquake records at the free surface of the soil is immediate. On the other hand, their application to design response spectra, modifying them to include the effect of the soil, is not so straightforward. This point and approximate solutions are discussed at the end.

II - STEADY STATE PERIODIC MOTIONS

The Amplification Function

II.1 Continuous Solution.

A. Uniform layer. Rigid rock.

Let us consider first a uniform layer of soil resting on rock. The equation of motion corresponding to the one-dimensional wave propagation problem is

$$\rho \frac{\partial^2 u}{\partial t^2} = G \frac{\partial^2 u}{\partial x^2} + \eta \frac{\partial^3 u}{\partial t \partial x^2}$$

where ρ = density or mass per unit volume = $\frac{\gamma}{g}$

γ = unit weight

g = acceleration of gravity

G = shear modulus

η = viscosity constant

$u(x,t)$ = displacement of a point in the soil layer

If the rock is rigid but a displacement $u_0(t)$ is imposed at the base of the soil, the boundary conditions are:

$$\frac{\partial u}{\partial x} = 0 \text{ at } x = 0$$

$$u = u_0(t) \text{ at } x = H$$

and the initial conditions:

$$u = 0 \text{ at } t = 0$$

$$\frac{\partial u}{\partial t} = 0 \text{ at } t = 0$$

By calling $y = u - u_G$ the relative displacement, the equation can be rewritten as:

$$\rho \frac{\partial^2 y}{\partial t^2} - G \frac{\partial^2 y}{\partial x^2} + \eta \frac{\partial^3 y}{\partial x^2 \partial t} = \rho \frac{\partial^2 u_G}{\partial t^2}$$

with Initial Conditions

$$y = 0, \frac{\partial y}{\partial t} = 0 \qquad \text{at } t = 0$$

and Boundary Conditions

$$y = 0 \qquad \text{at } x = H$$

$$\frac{\partial y}{\partial x} = 0 \qquad \text{at } x = 0$$

If $u_G(t) = 0$, the free vibrations can be investigated. Writing then

$$\rho \frac{\partial^2 y}{\partial t^2} = G \frac{\partial^2 y}{\partial x^2} + \eta \frac{\partial^3 y}{\partial x^2 \partial t}$$

and trying a solution of the form

$$y = U(x) \cdot V(t)$$

where U is a function only of x

V is a periodic function of t alone

$$\frac{\ddot{U}}{U} = \rho \frac{\ddot{V}}{GV + \eta \dot{V}} = -p^2$$

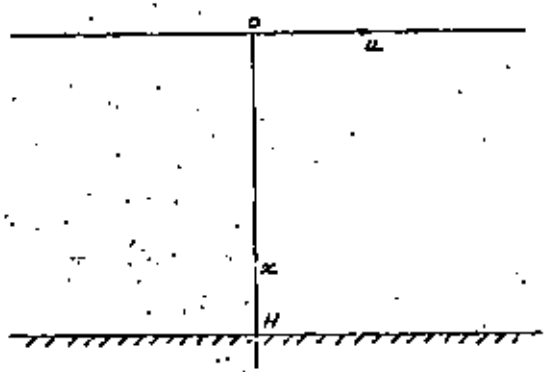

FIG. 1 - UNIFORM LAYER

The natural frequencies of the layer of soil are then given by

$$f_n = \frac{2n-1}{4H}\sqrt{\frac{G}{\rho}} = \frac{(2n-1)C_s}{4H}$$

$$\omega_n = \frac{(2n-1)\pi}{2H}\sqrt{\frac{G}{\rho}} = \frac{(2n-1)\pi C_s}{2H}$$

and the natural periods

$$T_n = \frac{4H}{2n-1}\sqrt{\frac{\rho}{G}} = \frac{4H}{(2n-1)C_s}$$

where $C_s = \sqrt{\frac{G}{\rho}}$ is the shear wave velocity of the soil.

The corresponding modal shapes are

$$U = \sin\frac{(2n-1)\pi}{2H}x$$

If the soil has viscosity $\eta \neq 0$ in order to have harmonic motion we must have

$$\eta < \frac{4H}{(2n-1)\pi}\sqrt{G\rho}$$

A critical value of viscosity can be established for each mode. In particular in order to have at least 1 mode

$$\eta < \eta_{1\,crit} = \frac{4H}{\pi}\sqrt{G\rho}$$

It is important to realize that if there is any viscosity the number of modes will be finite. (Higher modes will have damping higher than critical).

Considering now the forced vibration problem, it is convenient for a steady state periodic motion to represent the base displacement by

$$u_G(t) = C\,e^{i\omega t}$$

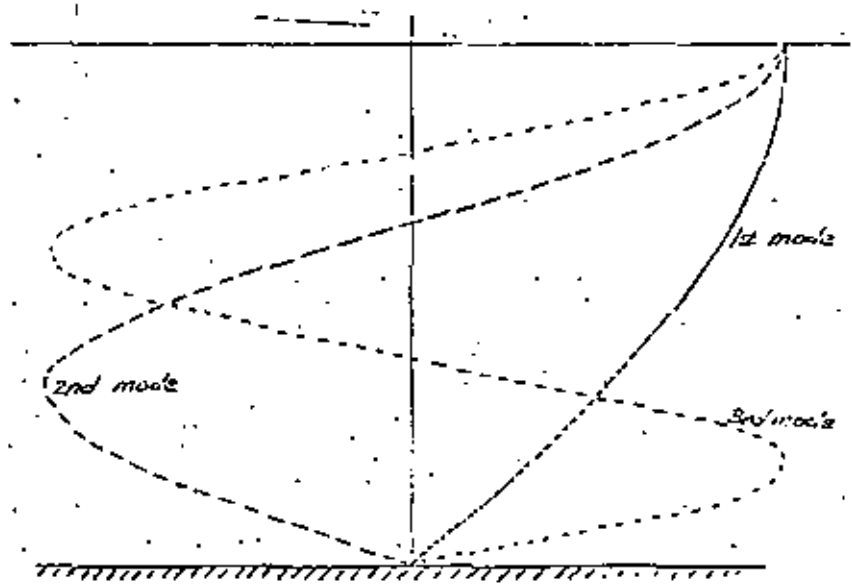

FIG-2: MODAL SHAPES FOR A UNIFORM LAYER

and the solution by

$$y(x,t) = U(x)e^{i\Omega t}$$

then

$$U = E \cos px + F \sin px - C$$

$$\text{with } p^2 = \frac{\rho \Omega^2}{G + i\eta\Omega}$$

Imposing the boundary conditions

$$F = 0$$

$$E \cos pH = C$$

$$U = C\left(\frac{\cos px}{\cos pH} - 1\right)$$

and $$\bar{y} = -\Omega^2 C \left(\frac{\cos px}{\cos pH} - 1\right)e^{i\Omega t}$$

$$\bar{u} = \bar{y} + \bar{u}_G = -\Omega^2 C \frac{\cos px}{\cos pH} e^{i\Omega t}$$

and at the free surface of the soil the absolute acceleration becomes

$$\ddot{\bar{u}} = -\Omega^2 C \frac{1}{\cos pH} e^{i\Omega t}$$

Since the base motion was $\ddot{u}_G = -\Omega^2 C e^{i\Omega t}$

$$\ddot{\bar{u}} = \frac{1}{\cos pH} \ddot{u}_G$$

The transfer function of the soil for absolute acceleration at the free surface is then defined as:

$$TF(\ddot{\bar{u}}) = \frac{1}{\cos pH}$$

It should be noticed that if there is viscosity, p is a complex variable and therefore cos pH has to be interpreted as

$$1/2\ (e^{ipH} + e^{-ipH})$$

or $$TF(\ddot{\bar{u}}) = \frac{2}{e^{ipH} + e^{-ipH}}$$

The fact that the transfer function is complex indicates that there is both a change in amplitude and in phase. If only the change in amplitude is considered the Amplification Function is defined as the modulus of the transfer function.

$$A(\Omega) = \frac{2}{\left|e^{ipH} + e^{-ipH}\right|}$$

Calling $$\alpha = \frac{1}{\sqrt{2}} H\Omega \sqrt{\frac{\rho}{G}} \sqrt{\frac{\sqrt{1 + (\eta\Omega/G)^2} - 1}{1 + (\eta\Omega/G)^2}}$$

$$\beta = \frac{1}{\sqrt{2}} H\Omega \sqrt{\frac{\rho}{G}} \sqrt{\frac{\sqrt{1 + (\eta\Omega/G)^2} + 1}{1 + (\eta\Omega/G)^2}}$$

$$A(\Omega) = \frac{1}{\sqrt{\cos h^2\alpha \cos^2\beta + \sin h^2\alpha \sin^2\beta}}$$

For small values of $\frac{\eta\Omega}{G}$

$$\alpha = \frac{1}{2} H\Omega \sqrt{\frac{\rho}{G}} \frac{\eta\Omega}{G} = \frac{1}{2} H \frac{\eta\Omega^2}{G} \sqrt{\frac{\rho}{G}}$$

$$\beta = H\Omega\sqrt{\frac{\rho}{G}}$$

and $$A(\alpha) = \frac{1}{\sqrt{\cos^2\beta + \alpha^2 \sin^2\beta}}$$

In particular if there is no viscosity $\eta = 0$

$$A(\alpha) = \frac{1}{\cos\beta}$$

and the amplification will become infinity at $\beta = \frac{(2n-1)\pi}{2}$ which corresponds to $\alpha = \frac{(2n-1)\pi}{2H}\sqrt{\frac{G}{\rho}} = \omega_n$, nth natural frequency of the layer.

On the other hand, if $\eta \neq 0$, the amplification will not become infinity. Two cases can then be considered:

1. If the value of η is constant as α increases, the first expression will have to be used since $\eta\frac{\alpha}{G}$ will not be small any longer. As α increases $A(\alpha)$ tends to zero, which means that for very large input frequencies the top of the layer remains at rest. The amplification function will have only a finite number of peaks corresponding to those natural frequencies of the layer which have damping less than critical.

For values of α such that $\eta\frac{\alpha}{G}$ is still small, the amplification at $\alpha = \omega_n$, nth natural frequency of the layer, becomes

$$A(\omega_n) = \frac{4}{(2n-1)\pi}\,\frac{1}{\eta\omega_n/G} = \frac{2}{\pi\eta}\,\frac{1}{(2n-1)^2}$$

This shows that the amplitude of the peak at the second natural frequency of the layer will be $\frac{1}{9}$ of that at the first, the amplitude of the third will be $\frac{1}{25}$ etc. ..

2. If it is assumed that the viscosity is inversely proportional to the frequency so that $\eta\frac{\alpha}{G} = \tan\delta$ is a constant, for small values of $\eta\frac{\alpha}{G}$

$$A(\omega_n) = \frac{4}{(2n-1)\pi\tan\delta} = \frac{4}{(2n-1)\pi}\cdot\frac{1}{2s}$$

with $s = \frac{1}{2}\tan\delta$ = fraction of critical damping

In this case the amplitude of the second peak will be 1/3 that of the 1st, the amplitude of the third peak 1/5 and so on.

Comparing these results with those for a lumped mass discrete system as normally encountered in Structural Dynamics, we can say that a constant value of viscosity η corresponds to an increasing percentage of damping in each mode, whereas a constant value of $\eta\frac{\alpha}{G}$ corresponds to constant damping in all modes.

Figures 3 and 4 show the amplification curve for a uniform soil layer with the following characteristics:

Depth	$h = 100'$
Shear wave velocity	$c_s = 750$ ft/sec.
Unit weight	$\gamma = 125$ lbs/cubic ft.

B. Uniform layer. Elastic rock

Taking now two sets of axes, one with origin at the free surface of the soil, the second with origin at the top of the rock, the motions in the soil and the rock can be expressed as

$$u_s = E_s e^{i(p_s x_s + \alpha t)} + F_s e^{-i(p_s x_s - \alpha t)}$$

$$u_r = E_r e^{i(p_r x_r + \alpha t)} + F_r e^{-i(p_r x_r - \alpha t)}$$

where $$p_s^2 = \frac{\rho_s \alpha^2}{G_s + i\eta_s\alpha}$$

$$p_r^2 = \frac{\rho_r \alpha^2}{G_r + i\eta_r\alpha}$$

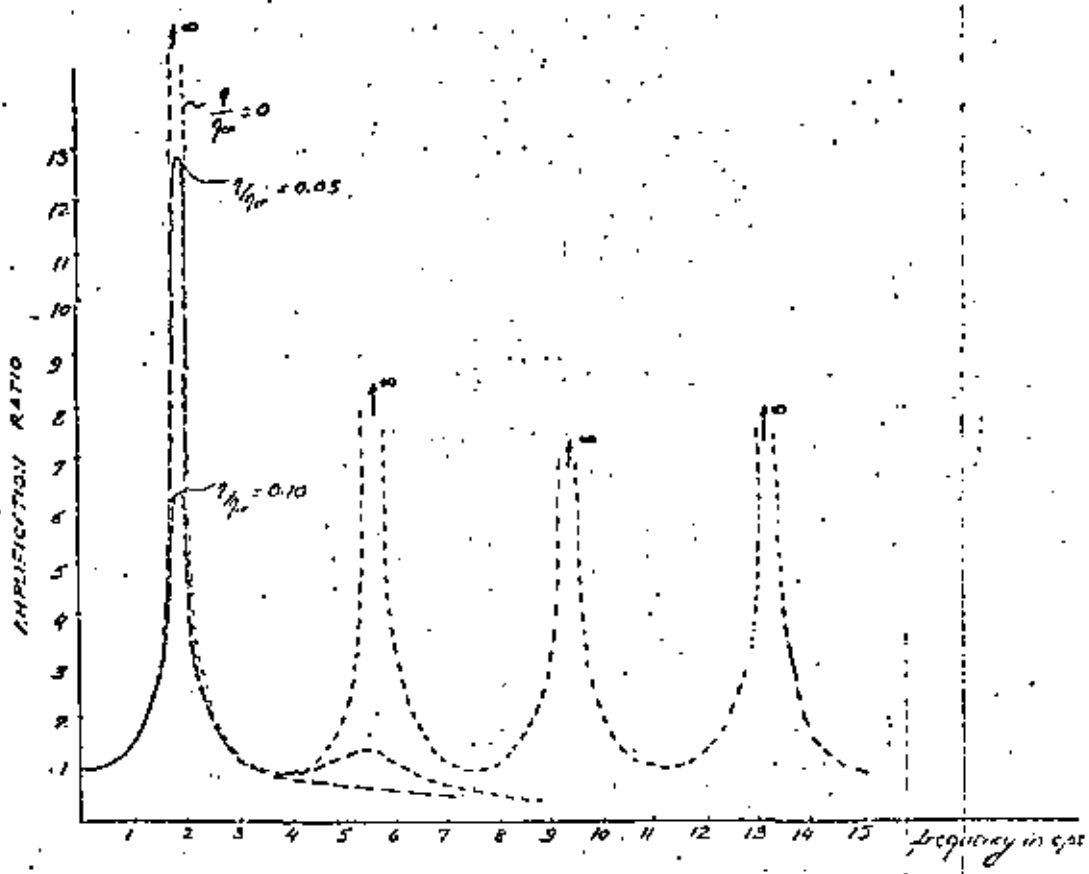

FIG. 3. AMPLIFICATION CURVE FOR UNIFORM LAYER RIGID ROCK - CONSTANT VISCOSITY

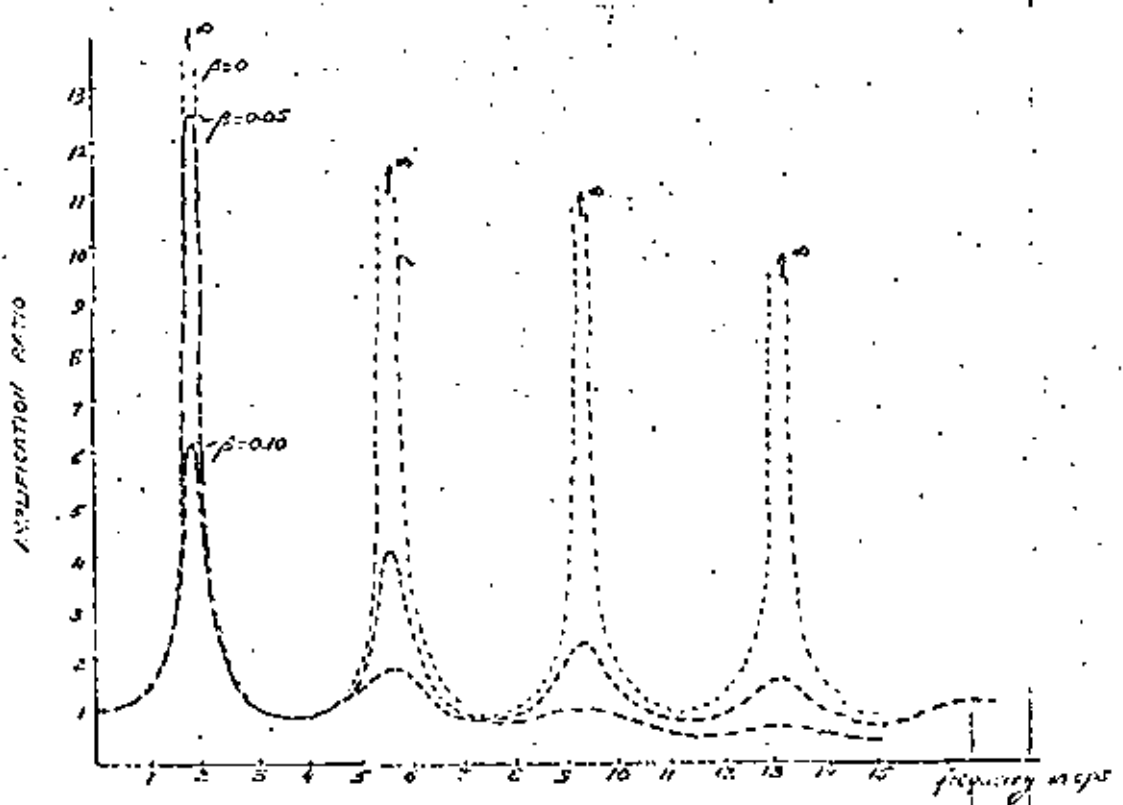

FIG. 4. AMPLIFICATION CURVE FOR UNIFORM LAYER RIGID ROCK - CONSTANT MODAL DAMPING

The boundary conditions are now

$$\frac{\partial u_s}{\partial x_s} = 0 \quad \text{at } x_s = 0$$

$$u_s(x_s = H) = u_r(x_r = 0)$$

$$(G_s + i\eta_s\omega)\frac{\partial u_s}{\partial x_s}(x_s = H) = (G_r + i\eta_r\omega)\frac{\partial u_r}{\partial x_r}(x_r = 0)$$

The result is

$$E_s = F_s$$

$$u_s = E_s e^{i\omega t}(e^{ip_s x_s} + e^{-ip_s x_s})$$

$$E_s = \frac{2E_r}{e^{ip_s H}(1+\mu) + e^{-ip_s H}(1-\mu)}$$

$$F_r = E_r \frac{e^{ip_s H}(1-\mu) + e^{-ip_s H}(1+\mu)}{e^{ip_s H}(1+\mu) + e^{-ip_s H}(1-\mu)}$$

with

$$\mu = \frac{\rho_s(G_s + i\eta_s\omega)}{\rho_r(G_r + i\eta_r\omega)}$$

$$u_s(x_s = 0) = 2E_s e^{i\omega t}$$

$$u_s(x_s = H) = u_r(x_r = 0) = (E_r + F_r)e^{i\omega t} = E_s(e^{ip_s H} + e^{-ip_s H})e^{i\omega t}$$

The ratio between the displacement (or acceleration) u at the free surface of the soil, and the displacement (or acceleration) at the interface between rock and soil can then be expressed as

$$TF = \frac{2}{e^{ip_s H} + e^{-ip_s H}}$$

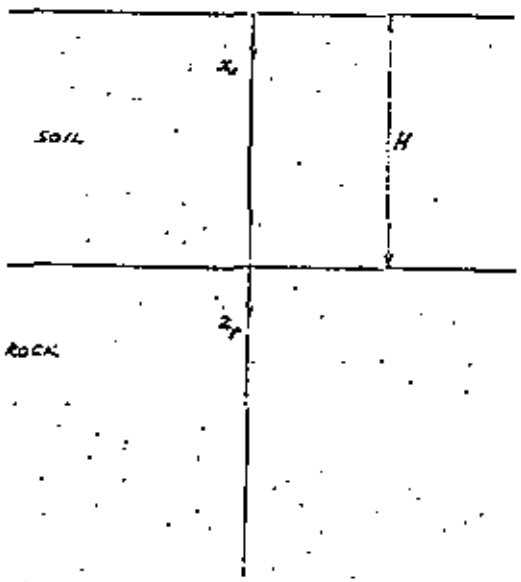

FIGURE 5. UNIFORM LAYER ON ELASTIC ROCK

which is the same expression previously obtained for rigid rock.

If on the other hand one considers the situation of the rock without soil on top, the motion at the outcropping of rock would be

$$u = 2E_r e^{i\Omega t}$$

and the ratio between the displacement (or acceleration) at the free surface of the soil, and the displacement (or acceleration) at the outcropping of rock would be

$$\frac{2}{e^{ip_s H}(1+\mu)+e^{-ip_s H}(1-\mu)}$$

A second amplification function can thus be defined by considering the elastic properties of the rock. This function gives now the ratio between amplitudes of motion on top of the soil to the amplitude of the motion that would be felt on top of the rock if the soil were not there.

$$A(\Omega) = \frac{2}{\left|e^{ip_s H}(1+\mu)+e^{-ip_s H}(1-\mu)\right|}$$

In this case if there is no viscosity $\eta_s = \eta_r = 0$

$$p_s = \frac{\Omega}{c_s} \qquad p_r = \frac{\Omega}{c_r}$$

$$\mu = \frac{\rho_s G_s}{\rho_r G_r} = \frac{G_s c_r}{G_r c_s} = \sqrt{\frac{\gamma_s \rho_s}{\gamma_r \rho_r}} = \sqrt{\frac{\gamma_s \gamma_s}{\gamma_r \gamma_r}} = \frac{\gamma_s c_s}{\gamma_r c_r}$$

and

$$A(\Omega) = \frac{1}{\left|\cos p_s H + i\mu \sin p_s H\right|}$$

At the natural frequencies of the layer $\Omega = \omega_n$ $\cos p_s H = 0$ and $\sin p_s H = (-1)^n$

$$A(\omega_n) = \frac{\gamma_r c_r}{\gamma_s c_s}$$

It can be seen that this amplification ratio does not become infinity even if the soil has no viscosity.

If the rock has no viscosity $\eta_r = 0$, and the soil has a viscosity η_s so that $\eta_s \Omega / G_s$ is small, one can again derive an approximate formula for the amplification at the natural frequencies $\Omega = \omega_n$

$$A(\omega_n) = \frac{\gamma_r c_r}{\gamma_s c_s} \cdot \frac{1}{1 + \frac{(2n-1)\pi}{4} \frac{\gamma_r c_r}{\gamma_s c_s} \cdot \frac{\eta_s \omega_n}{G_s}}$$

For the case of constant viscosity η_s

$$A(\omega_n) = \frac{\gamma_r c_r}{\gamma_s c_s} \cdot \frac{1}{1 + \frac{\gamma_r c_r}{\gamma_s c_s} \cdot \frac{\eta_s}{\eta_{s\,crit}} (2n-1)^2 \frac{\pi}{2}}$$

and for the case of constant $\frac{\eta_s \Omega}{G} = 2\delta$

$$A(\omega_n) = \frac{\gamma_r c_r}{\gamma_s c_s} \cdot \frac{1}{1 + \frac{\gamma_r c_r}{\gamma_s c_s} \cdot 2\delta \cdot \frac{(2n-1)\pi}{4}}$$

Figures 6 and 7 show amplification functions with elastic rock for the same uniform layer of soil previously considered ($\gamma_r = 140$, $C_r = 4500$).

The main difference between both cases is the fact that the rock considered as an elastic half space is dissipating energy by radiation. Both solutions are then approximately related by the

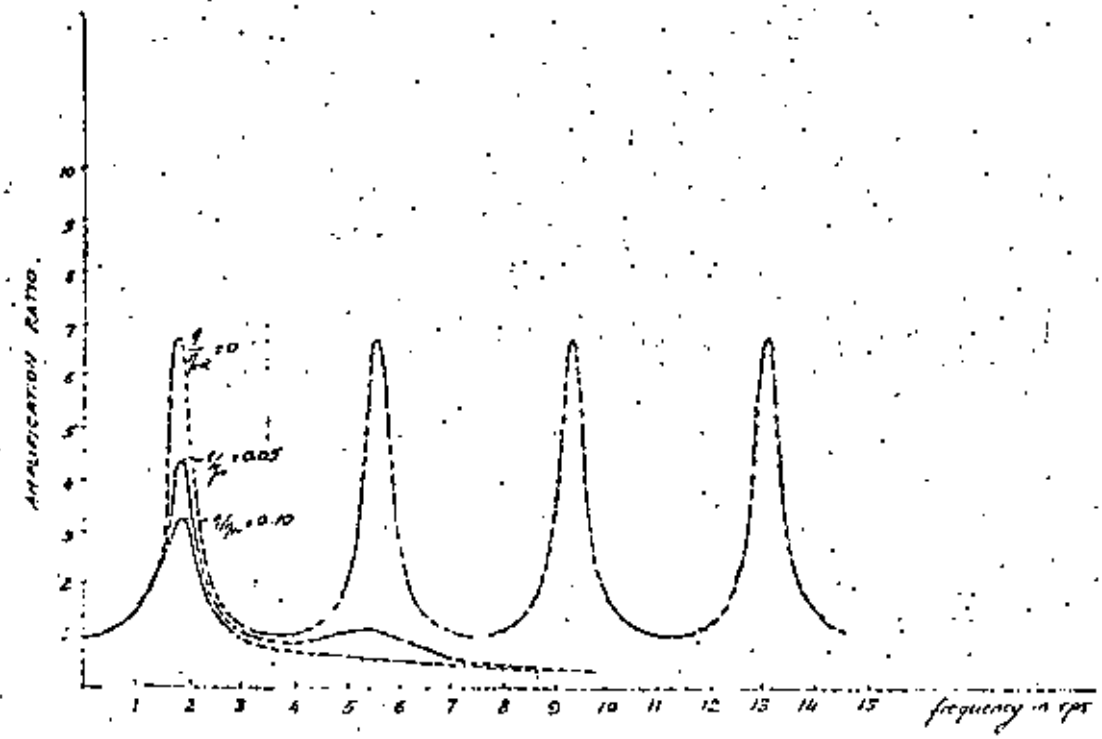

FIG 6 - AMPLIFICATION CURVE FOR UNIFORM LAYER.
ELASTIC ROCK - CONSTANT VISCOSITY

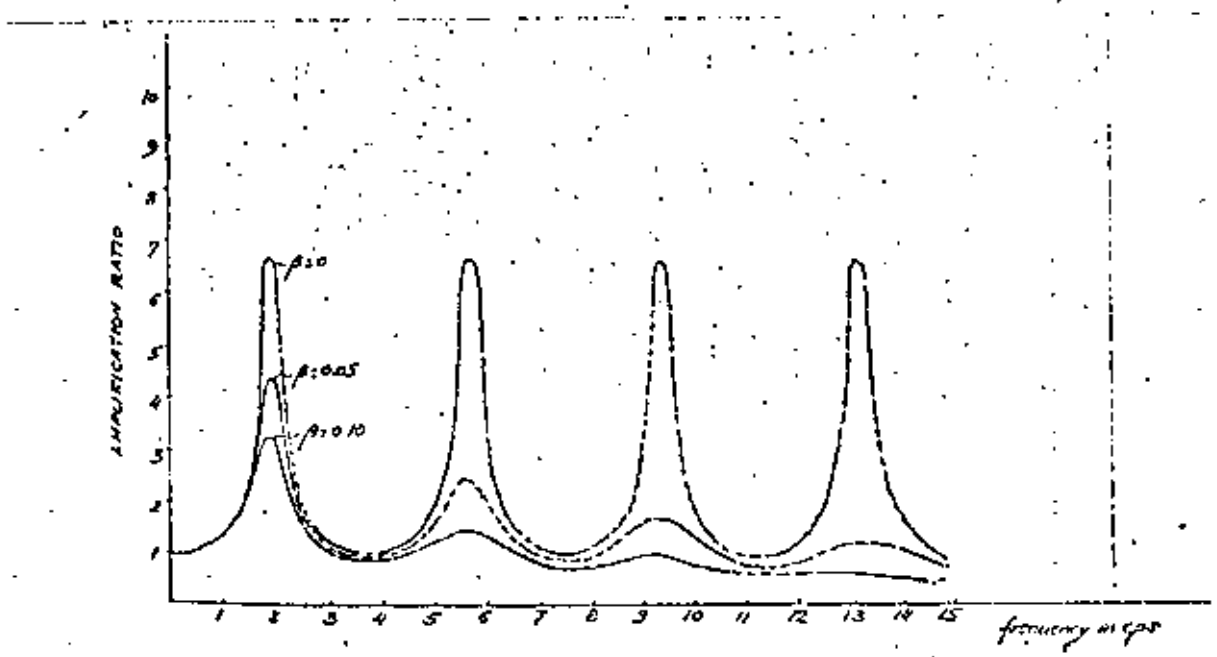

FIG 7. AMPLIFICATION CURVE FOR UNIFORM LAYER
ELASTIC ROCK - CONSTANT MODAL DAMPING

expression

$$\frac{1}{A_2(\omega)} = \frac{\gamma_s C_s}{\gamma_r C_r} + \frac{1}{A_1(\omega)}$$

where $A_1(\omega)$ is the amplification function with rigid rock

$A_2(\omega)$ is the amplification function with elastic rock.

This formula can be reproduced by adding to the first case an equivalent radiation damping, function of frequency

$$\beta_{eq} = \frac{2}{\pi} \cdot \frac{\gamma_s C_s}{\gamma_r C_r} \cdot \frac{1}{2n-1}$$

or $$\beta_{eq} = \frac{2}{\pi} \frac{\gamma_s C_s}{\gamma_r C_r} \cdot \frac{\omega_1}{\omega}$$

since $\eta \frac{\omega}{G} = 2\beta$ this represents

$$\eta_{eq} = \frac{G}{\omega} 2\beta_{eq} = \frac{4}{\pi} G_s \frac{\gamma_s C_s}{\gamma_r C_r} \cdot \frac{\omega_1}{\omega^2}$$

C. Multilayered System.

When the soil deposit is made of several layers with different properties (Fig. 8) one can define for each layer j

- h_j = thickness
- G_j = shear modulus
- γ_j = unit weight
- C_j = shear wave velocity
- η_j = viscosity coefficient

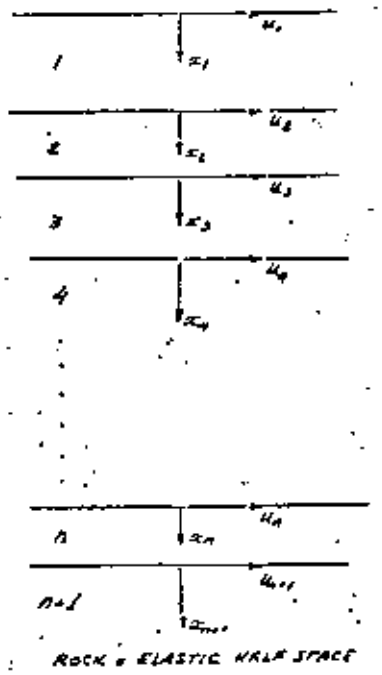

FIG 8. MULTIPLE STRATA OVER ELASTIC ROCK

$$p_j^2 = \frac{\rho_j \Omega^2}{G_j + i\eta_j \Omega}$$

and

$$\mu_j = \frac{p_j(G_j + i\eta_j \Omega)}{p_{j+1}(G_{j+1} + i\eta_{j+1}\Omega)}$$

Displacement in each layer with respect to a local set of coordinate axes with origin at the top of the layer can then be expressed as

$$u_j = E_j e^{i(p_j x_j + \Omega t)} + F_j e^{-i(p_j x_j - \Omega t)}$$

By establishing compatibility between each layer and the next, one can write

$$F_1 = E_1 \text{ (because of the free surface condition)}$$

$$2E_2 = E_1[e^{ip_1h_1}(1+\mu_1) + e^{-ip_1h_1}(1-\mu_1)]$$

$$2F_2 = E_1[e^{ip_1h_1}(1-\mu_1) + e^{-ip_1h_1}(1+\mu_1)]$$

$$2E_3 = E_2(1+\mu_2)e^{ip_2h_2} + F_2(1-\mu_2)e^{-ip_2h_2}$$

$$2F_3 = E_2(1-\mu_2)e^{ip_2h_2} + F_2(1-\mu_2)e^{-ip_2h_2}$$

and

$$2E_{n+1} = E_n(1+\mu_n)e^{ip_nh_n} + F_n(1-\mu_n)e^{-ip_nh_n}$$

$$2F_{n+1} = E_n(1-\mu_n)e^{ip_nh_n} + F_n(1+\mu_n)e^{-ip_nh_n}$$

By replacing into the expressions for E_3, F_3 the values of E_2F_2 in terms of E_1, then these ones into the expressions for E_4, F_4 and so on one can finally obtain

$$E_{n+1} = aE_1$$

The amplification function with rigid rock (ratio of displacement or acceleration at top of soil to displacement or acceleration at bedrock) is then

$$A_1(\Omega) = \left| \frac{2E_1}{E_{n+1} + F_{n+1}} \right| = \frac{2}{|a+b|}$$

The amplification function with elastic rock (ratio of displacement or acceleration at top of soil to displacement or acceleration at the outcropping of rock) is

$$A_2(\Omega) = \frac{|2E_1|}{|2E_{n+1}|} = \frac{1}{|a|}$$

The explicit expression for the amplification function in terms of the soil properties becomes too long even for two layers. However, the numerical computation proceeding from layer to layer is simple and adapts itself very well to be programmed in a digital computer.

It is possible to have any kind of viscosity (constant or an arbitrary function of frequency) in any layer. On the other hand for the purpose of comparing the results with those obtained by other methods (modal analysis of the discrete model) a case which becomes easy to interpret is that in which η/G is equal for all layers.

Then if $\frac{\eta_j}{G_j}$ is constant, independent of frequency, the resulting amplification function will have in each natural frequency a percentage of critical damping increasing linearly with the frequency ω. The magnitude of the amplification in the nth natural frequency will thus be proportional to $1/\omega_n^2$.

If $\frac{\eta_j}{G_j} \cdot \Omega = 2\beta$ is constant, the resulting amplification function will have a constant percentage of critical damping in all the modes. The magnitude of the amplification will thus be proportional to $1/\omega_n$.

While it is not possible to find an exact simple formula to reproduce the effect of the elastic rock, it has been found that good results can be obtained by taking some average properties for the soil

$$\gamma_{s\ average} = \frac{\sum \gamma_j h_j}{\sum h_j}$$

$$c_{s\ average} = \frac{\sum c_{sj} h_j}{\sum h_j}$$

and writing $$\frac{1}{A_2(\omega)} = \frac{\gamma_{save}\, c_{save}}{\gamma_r c_r} + \frac{1}{A_1(\omega)}$$

or adding an equivalent radiation damping

$$\beta_{eq} = \frac{2}{\pi} \cdot \frac{\gamma_{save}\, c_{save}}{\gamma_r c_r} \frac{\omega_1}{\omega}$$

(The correct formula would be

$$A_2(\omega) = \frac{A_1(\omega)}{1 + \frac{\tau_b}{\rho_r c_r u_b(\omega)}} = \frac{A_1(\omega)}{1 - \frac{\tau_b(\omega)}{\rho_r c_r \ddot{u}_b}}$$

where τ_b is the shear stress at the base of the soil
u_b the base displacement
$\ddot{u}_b$ the base acceleration.

Figures 9 and 10 show the amplification functions for a multilayered soil profile with the following characteristics:

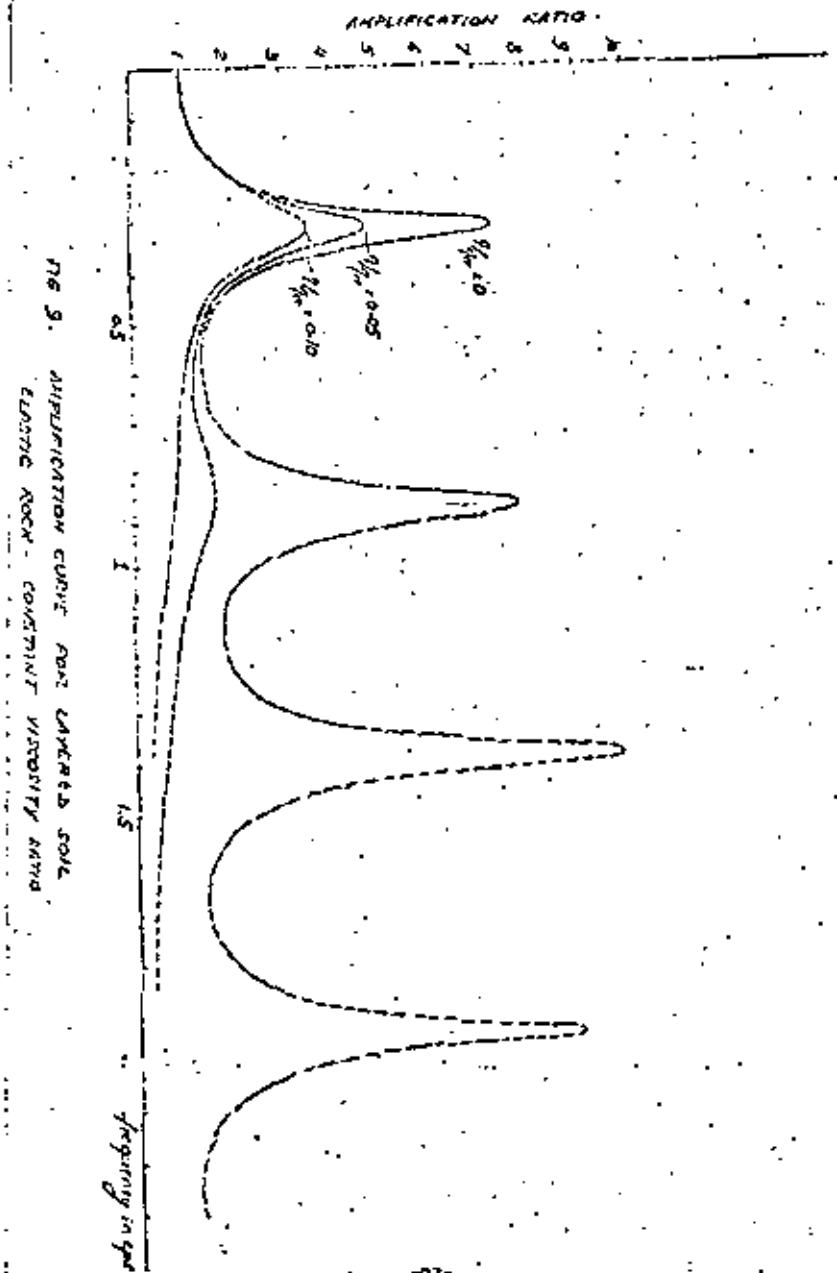

FIG 9. AMPLIFICATION CURVE FOR LAYERED SOIL ELASTIC ROCK - DAMPING RATIO

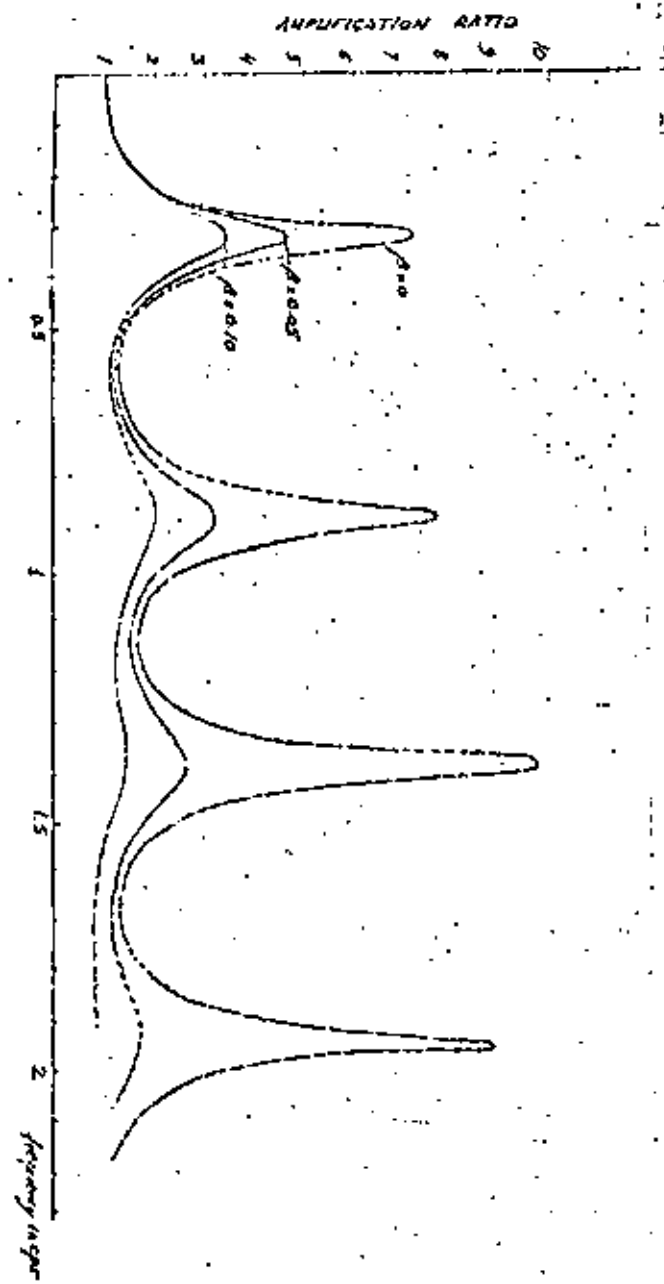

FIG 10. AMPLIFICATION CURVE FOR LAYERED SOIL RESTING ROCK. CONSTANT MODAL DAMPING

Layer No.	Thickness ft.	Shear Wave Velocity ft./sec.	Unit Weight Lb./ft.^{3}
1	10	714	100
2	150	897	120
3	70	1200	125
4	500	1300	125
5	400	1500	135
Rock		8000	150

In both cases it has been assumed that the ratio η/G is the same for all layers. It should be noticed that for η = 0 the maximum amplification does not occur at the first natural frequency but at the third one. This effect is more evident when different values of damping are considered for each layer, particularly in the case of soft layers of soil over relatively hard strata. Figure 11 shows the amplification curve for a soil profile which would correspond to the conditions at El Centro, California. It can be seen in this case that the amplification curve is basically the product of two functions: one corresponding to the relatively hard bottom of 11,000 feet with a fundamental frequency of about 0.1 cps, the other corresponding to the top 100 feet of soft soil with a fundamental frequency of about 1.5 cps. The amplification due to these top 100 feet is larger than that due to the remainder of the soil and the maximum peak in the combined amplification curve occurs in the range of 1.5 cps. It is important to notice that this simplified approach, lumping several layers of soil with similar properties into one layer with average properties and reducing the total system to just two layers which can be considered independently, can often be successfully applied for preliminary estimates. Of course to be able to treat the two resulting layers independently, multiplying the corresponding amplification functions at each point, it is necessary to be able to treat them as uncoupled, or what is the same, the mass of the top layer should be considerably smaller than that of the bottom layer.

layer	h	G_0	γ	β
1	1100	6500	125	0.11
2	1000	27700	139	0.03
3	3000	35500	139	0.005
4	3500	40000	147	0.002
5	3500	72000	147	0.
rock		160000	172	

FIG. 11. AMPLIFICATION CURVE FOR LAYERED SOIL (EL CENTRO) ELASTIC ROCK - VARIOUS DAMPING IN LAYERS.

11.2 Discrete Model.

The basis for the discrete model is to replace each layer of soil by a series of lumped masses connected by a spring and dashpot. The resulting system (Fig. 12) is of course a familiar one for engineers working in Structural Dynamics.

For any given layer of thickness h_j, shear modulus G_j, unit weight γ_j and viscosity coefficient η_j, replaced by n_j discrete masses, one would have

$$M_1 = \frac{1}{2}\frac{\gamma_1}{g}\cdot\frac{h_1}{n_j}$$

$$M_2 = M_3 = M_4 = \ldots = M_{n_j} = \frac{\gamma_j}{g}\frac{h_j}{n_j}$$

Of course at the interface between two layers the total lumped mass would be

$$\frac{1}{2g}\left(\frac{\gamma_j h_j}{n_j} + \frac{\gamma_{j+1} h_{j+1}}{n_{j+1}}\right)$$

$$k_1 = k_2 = k_3 = \ldots = k_{n_j} = \frac{G_j n_j}{h_j}$$

and

$$C_1 = C_2 = C_3 \quad \ldots = \frac{\eta_j n_j}{h_j}$$

where C_1 are the dashpot constants.

It is thus possible to write the equation of motion for each mass forming a stiffness matrix, a damping matrix and a mass matrix (diagonal). The solution of the problem falls then within the classical methods of Structural Dynamics and requires no further explanation here. It is important to notice, however, that if the dashpot constants are arbitrary (n/G variable from one layer to another) it is necessary to solve the problem by physical integration of the equations of motion.

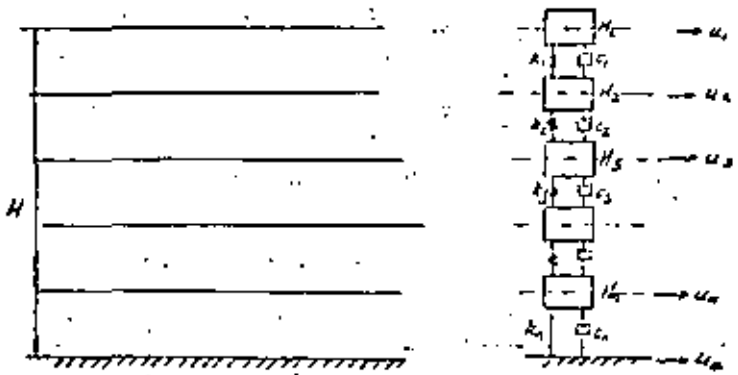

FIG 12. EQUIVALENT LUMPED MASS SYSTEM

In other words it is not possible in general to find an equivalent system with modal damping. If on the other hand the damping matrix can be expressed as a polynomial expression of $K^{-1}M$ or $M^{-1}K$ of the form

$$C = \sum_{r=m}^{r=n-1} a_r K(M^{-1}K)^r$$

or

$$C = \sum_{r=m}^{r=n-1} a_r M(K^{-1}M)^r$$

corresponding values of modal damping can be found and a normal modal analysis can be performed with damping in the ith mode.

$$2\beta_i\omega_i = \sum_{r=m}^{r=n-1} a_r \omega_i^{2r+2}$$

or

$$\beta_i = \frac{1}{2} \sum_{r=m}^{r=n-1} a_r \omega_i^{2r+1}$$

It can be shown that for the free vibration problem as the number of masses increases the natural periods and modal shapes tend to those given by the continuous solution. It has been found that a period T is reproduced with sufficient accuracy if the number of masses is

$$n \geq 5 \left(\frac{H}{TC_s} + \sqrt{\frac{H}{TC_s}}\right)$$

For a multilayered soil this condition should be verified for each layer independently and for the total deposit with an average shear wave velocity.

Knowing the natural periods or frequencies and the corresponding modal shapes, the participation factor of each mode for a base motion is

$$\Gamma_n = (-1)^{n+1} \frac{4}{(2n-1)\pi} \quad \text{for a uniform layer.}$$

In general the participation factor can be found by the normal procedures of Structural Dynamics. If M is the mass matrix and ϕ_n the nth eigenvector

$$\Gamma_n = \frac{\phi_n^T M I}{\phi_n^T M \phi_n}$$

where I is a vector with all components unity.

If ϕ_{n1} is the component of the eigenvector at the free surface of the soil calling $g_n = \Gamma_n \phi_{n1}$ the amplification function can be written as

$$A(\Omega) = \sqrt{\left[\sum_{i=1}^{n} \frac{g_i(\omega_i^2(\omega_i^2 - \Omega^2) + 4\beta_i^2\omega_i^2\Omega^2)}{(\omega_i^2-\Omega^2)^2+4\beta_i^2\omega_i^2\Omega^2}\right]^2 + \left[\sum_{i=1}^{n} \frac{g_i 2\beta_i\omega_i\Omega^3}{(\omega_i^2-\Omega^2)^2+4\beta_i^2\omega_i^2\Omega^2}\right]^2}$$

or alternatively

$$A(\Omega) = \sqrt{\left[\sum_{i=1}^{n} \frac{g_i\Omega^2(\omega_i^2 - \Omega^2)}{(\omega_i^2-\Omega^2)^2+4\beta_i^2\omega_i^2\Omega^2} + 1\right]^2 + \left[\sum_{i=1}^{n} \frac{g_i 2\beta_i\omega_i\Omega^3}{(\omega_i^2-\Omega^2)^2+4\beta_i^2\omega_i^2\Omega^2}\right]^2}$$

If all the modes are considered both formulas give the same results. If only the first few modes are included the results will differ slightly in the high frequency range.

Results obtained with these formulas (taking sufficient number of masses and modes) agree with the amplification curves obtained with the continuous model for the case of rigid rock. Adding to the values of modal damping β_i the equivalent radiation damping previously suggested results for elastic rock are again reproduced.

For all practical purposes it can be considered that the continuous and the discrete model will both be applicable to determine amplification functions and will yield the same results provided modal damping can be specified and an additional radiation damping is added to the lumped system. The continuous model is, however, more flexible since it allows for arbitrary variations of damping from one layer to another. Furthermore, it requires in general less computer time. The discrete model has the advantage that it is easier to visualize since it reduces the problem to a classical case of Structural Dynamics.

III - TRANSIENT MOTIONS

The amplification function has several important properties:

a) It gives a clear graphical picture and qualitative information on the effect of the soil. A simple look at the curve is sufficient to determine in what ranges of frequencies the soil can have a serious damaging effect, and in what ranges this effect would not be important or might even be beneficial.

b) It is independent of any given earthquake and it represents therefore a property or characteristic of the soil itself.

c) For some of the methods that will be described here, the determination of the amplification curve is a necessary first step to determine accelerograms or response spectra at the top of the soil. For other methods, however, this step may be bypassed.

In spite of these features the amplification curve is by no means the ultimate goal of this type of studies. From the point of view of the structural designer the main objective is to have a set of response spectra which apply to the surface of the soil or less frequently a set of earthquake records which could characterize the motions to be expected. From the point of view of the soils engineer it is important to be able to estimate the magnitude of shear

stresses in the soil during an earthquake to determine the factor of safety against liquefaction and to guide in the selection of suitable values for modulus and damping ratios.

In order to obtain these results several methods are still available using either the continuous or the discrete model.

III.1 - Continuous Solution

Given a certain time history of acceleration representing an earthquake record at the outcropping of rock, or at the interface between soil and rock, the corresponding accelerogram at the free surface of the soil can be obtained by:

a) Obtaining the Fourier transform of the input earthquake.
b) Multiplying it by the Transfer function of the soil.
c) Obtaining the inverse Fourier transform of the resulting function.

The Fourier transform of a function of time f(t) can be visualized as a limiting case of a Fourier series expansion. It is given by the formula

$$F(\omega) = \int_0^\infty f(t)e^{-i\omega t}dt = \int_{-\infty}^{+\infty} f(t)e^{-i\omega t}dt \quad \text{(if } f(t) = 0 \text{ for } t \leq 0\text{)}$$

f(t) is then said to be the inverse Fourier transform of F(ω)

$$f(t) = \frac{1}{2\pi}\int_{-\infty}^{+\infty} F(\omega)e^{i\omega t}\,d\omega$$

It should be noticed that F(ω) is a complex function. writing it as

$$F(\omega) = C(\omega) - iS(\omega)$$

$$C(\omega) = \int_0^\infty f(t)\cos\omega t\,dt \quad \text{(is the cosine transform)}$$

$$S(\omega) = \int_0^\infty f(t)\sin\omega t\,dt \quad \text{(is the sine transform)}$$

If on the other hand it is written as

$$F(\omega) = E(\omega)\,e^{-i\phi(\omega)t}$$

$$E(\omega) = \sqrt{C(\omega)^2 + S(\omega)^2}$$

$$\phi(\omega) = \tan^{-1}\frac{S(\omega)}{C(\omega)}$$

E(ω) represents the amplitude Fourier spectrum, and φ(ω) the phase spectrum. The amplitude spectrum has an important physical meaning. Given two values of frequency, ω_1, ω_2, the area under the curve E(ω) from ω_1 to ω_2 gives the amplitude of the motion in this range of frequencies. A simple look at the Fourier amplitude spectrum (often referred to for short as Fourier spectrum) gives immediately an idea of the range of frequencies where most of the amplitude of the motion is contained. In fact Hudson has shown that this spectrum is a lower bound to the undamped velocity response spectrum and in general a very good approximation to it (they would coincide if the maximum response occurred after the end of the excitation). Arias has also shown that if E(ω) is computed for different durations of the earthquake, the envelope of these spectra is an upper bound to the undamped velocity response spectrum.

The amplitude Fourier spectrum is of course closely related to the spectral density function S(ω)

$$S(\omega) = \frac{1}{2\pi}\,\frac{E(\omega)^2}{T}$$

and

$$S^*(\omega) = \frac{1}{\pi}\,\frac{E(\omega)^2}{T}$$

where T is the duration of the excitation f(t)

The area under the spectral density function between two frequencies ω_1 and ω_2 gives a measure of the energy of the excitation in that range.

The Fourier transform has not been used normally in Structural Dynamics. Its determination is, however, extremely fast and simple with a digital computer. Even if this method of analysis is not going to be used, the Fourier transform will provide significant information on the nature of the excitation and will help to answer such questions as how many modes should be included in a modal analysis.

The transfer function of the soil as determined in II is again a complex function. The product of these two complex functions can be accomplished by

Multiplying the Fourier amplitude spectrum of the input by the amplification function of the soil. The result is the Fourier amplitude spectrum of the earthquake at the free surface of the soil.

Adding to the Fourier phase spectrum the change in phase curve of the soil. The result is the Fourier phase spectrum of the output.

The inverse Fourier transform of this product will be again a real function representing the time history of acceleration on top of the soil. Notice that if the input represents the accelerogram at the interface between rock and soil the transfer function corresponding to rigid rock should be used. If on the other hand the input represents the accelerogram which would be recorded on the rock without any soil on top, the transfer function for elastic rock has to be used. The second approach seems more logical. However, at the present time, there is no clear way to determine what the earthquake records should be at bedrock with soil on top or at the outcropping of rock, since most accelerograms of real earthquakes have been obtained on ground (even if firm ground).

Figures 13 through 17 summarize the procedure as outlined. (The phase spectra are not plotted). Figure 13 shows a record of the Taft earthquake and Figure 14 its amplitude Fourier spectrum. Figure 15

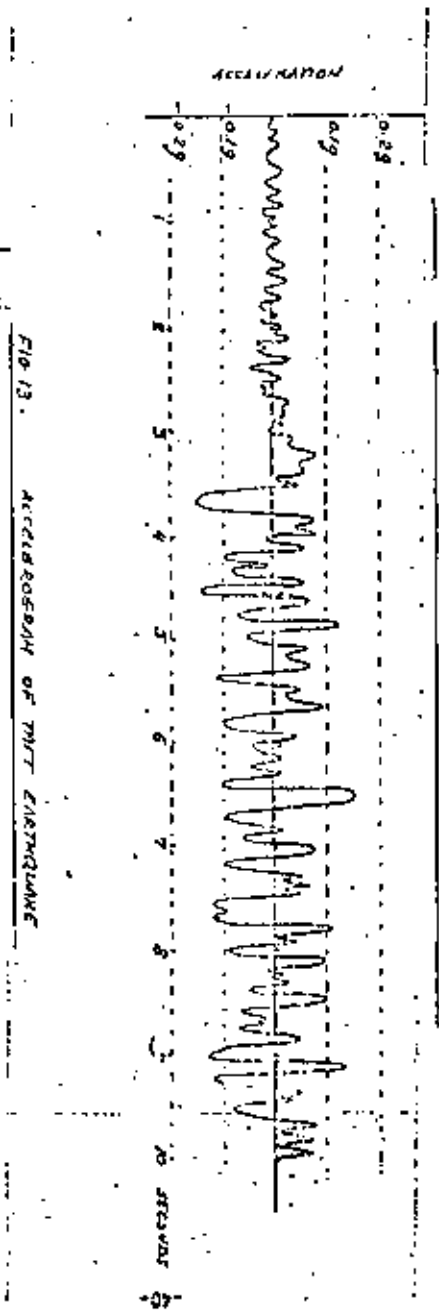

FIG 13. ACCELEROGRAM OF TAFT EARTHQUAKE

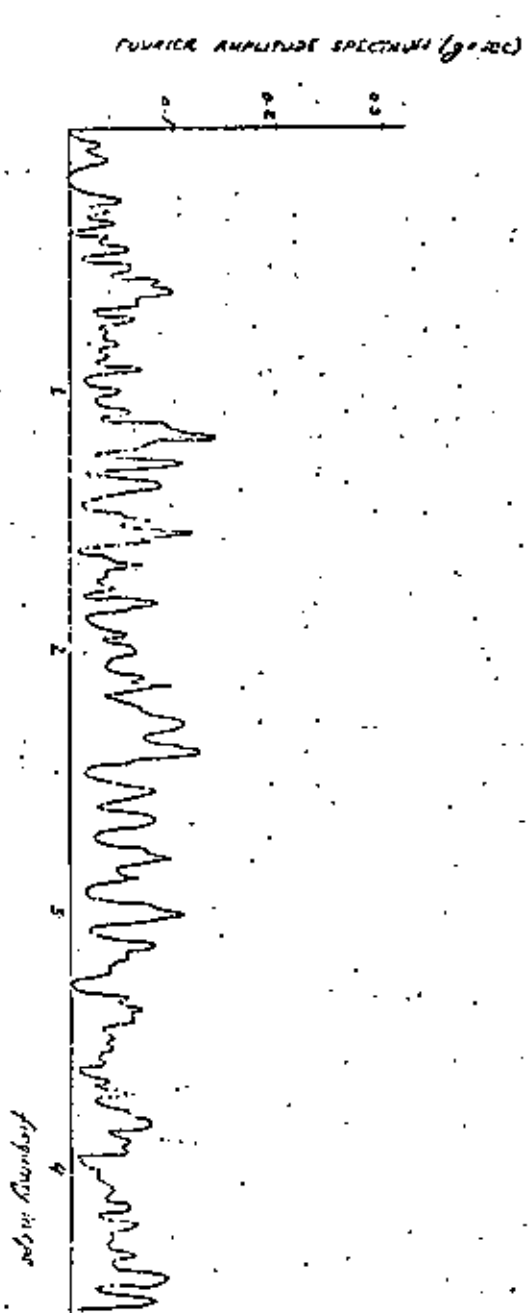

FIG 14 FOURIER AMPLITUDE SPECTRUM FOR TAFT EARTHQUAKE

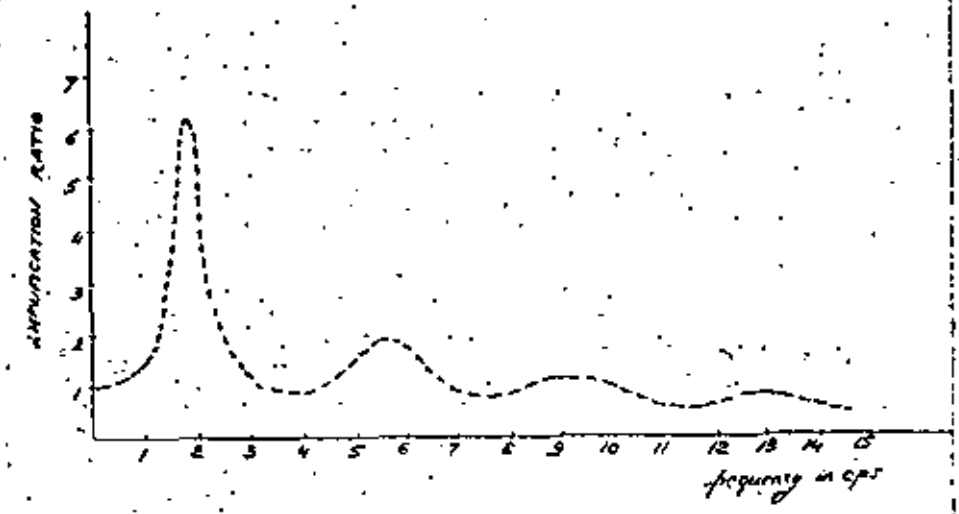

FIGURE 15. AMPLIFICATION FUNCTION OF SOIL

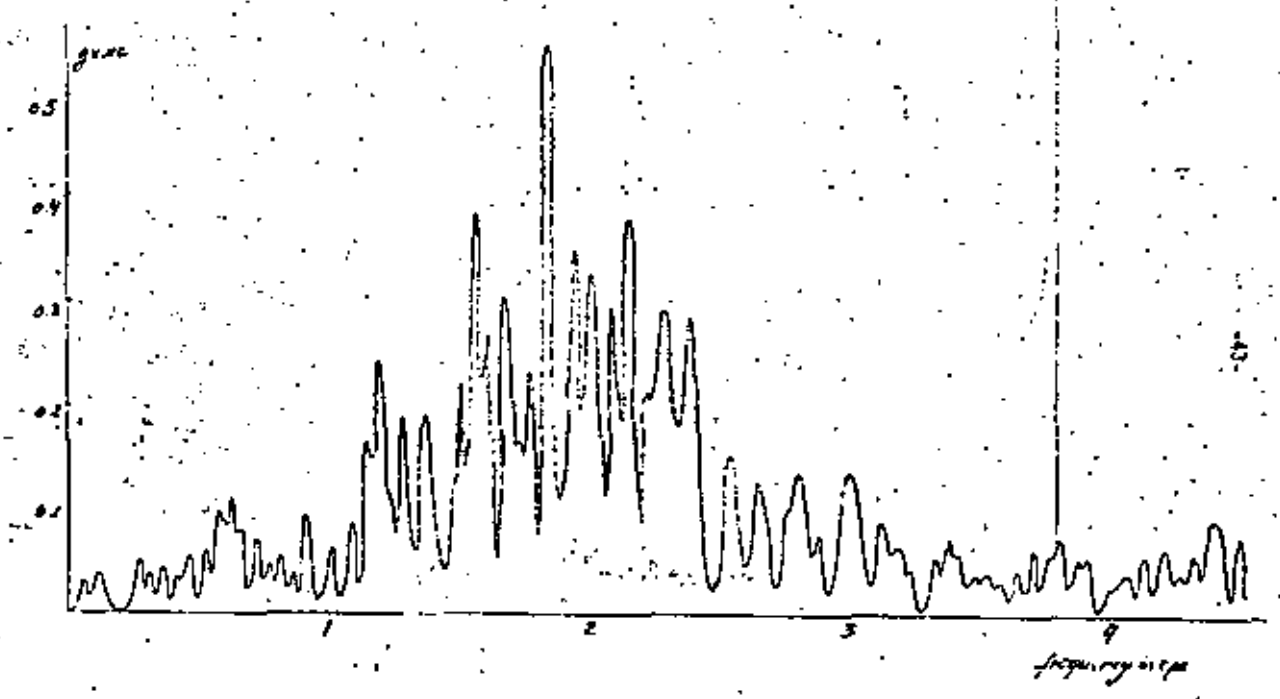

FIG 16. FOURIER AMPLITUDE SPECTRUM OF ACCELEROGRAM AT TOP OF SOIL

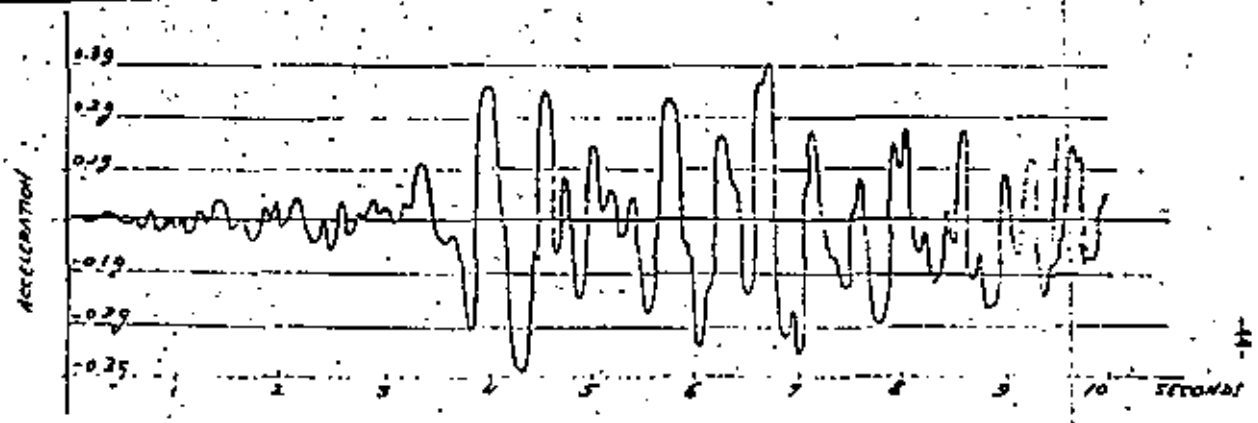

FIGURE 17. ACCELEROGRAM AT TOP OF SOIL

shows the amplification curve for a given soil profile (the uniform layer previously considered with rigid rock). The product of the Fourier spectrum of the input by the amplification function is shown in Figure 17.

Once the earthquake record at the surface of the soil has been obtained, design response spectra can be obtained in two different ways:

a) From the Fourier transform of the output (before inverting it), by multiplying it by the Transfer function of a one-degree-of-freedom linear oscillator, then inverting the result and finding the maximum. The Transfer function of the one-degree-of-freedom system with frequency ω_n and damping β_n is

$$H(\omega) = \frac{\omega_n^2 + 2i\beta_n\omega_n\omega}{\omega_n^2 - \omega^2 + 2i\beta_n\omega_n\omega}$$

b) By integrating through a step-by-step procedure, the equation of motion of a one-degree-of-freedom system

$$y + 2\beta_n\omega_n\dot{y} + \omega_n^2 y = -u_s$$

where u_s is the acceleration time history on top of soil.

The first procedure is normally referred to as integration in the frequency domain whereas in the second case the solution is said to be carried out in the time domain" While the first method would represent a consistent continuation of the procedure followed up to that moment at the present time the second seems more economical as far as computer time is concerned.

Figure 18 shows the pseudo-acceleration response spectrum for the Taft earthquake filtered through the uniform soil deposit. The response spectrum of the input is also shown in the same figure. Figure 19 shows the ratio of both response spectra for 2 and 5%

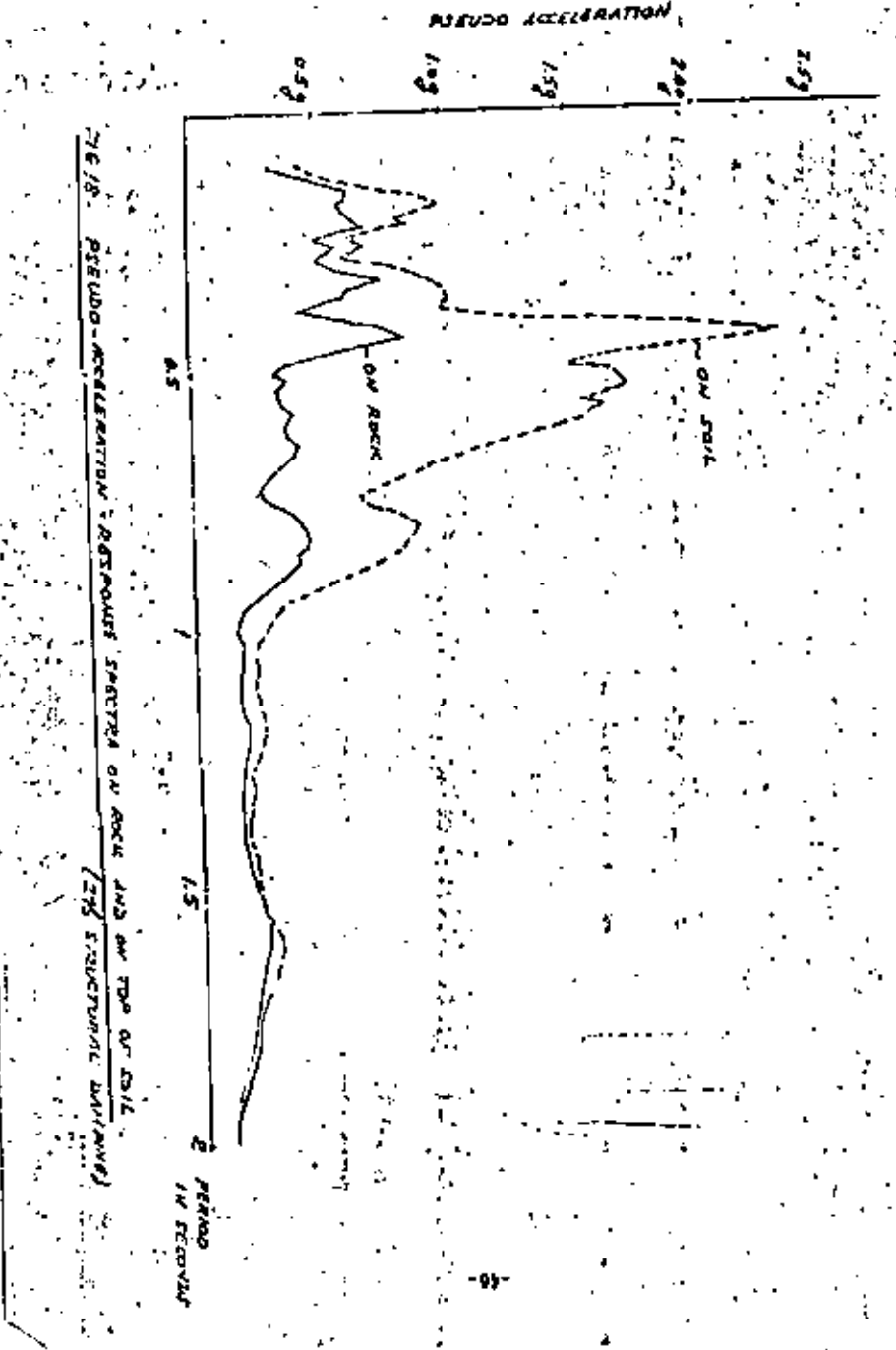

FIG 18. PSEUDO-ACCELERATION RESPONSE SPECTRA ON ROCK AND ON TOP OF SOIL (2% STRUCTURAL DAMPING)

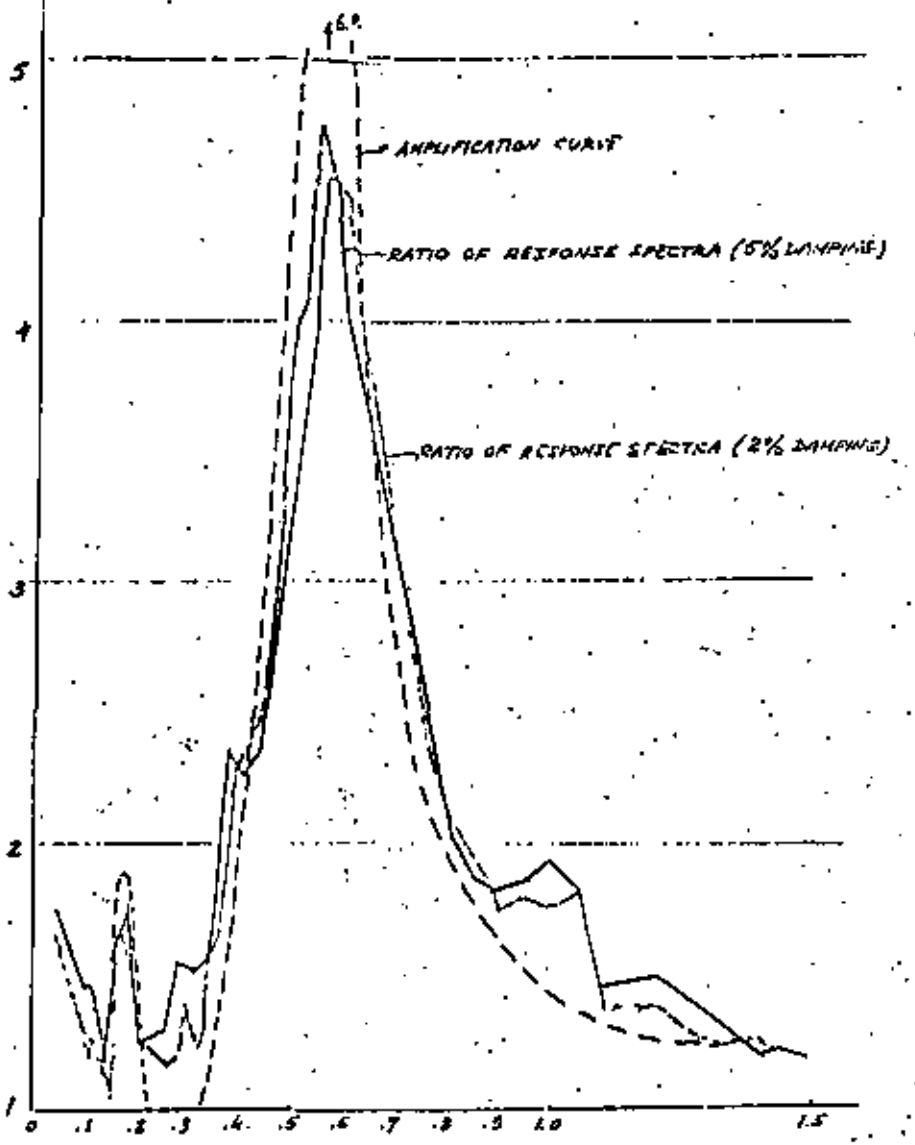

FIGURE 19

damping together with the amplification curve. The similarity between these curves is of course striking, and their relationship will be further discussed later.

III.2 - Discrete Model

In the discrete model the soil is represented by a close-coupled set of masses, springs and dashpots. The equations of motion can be written in terms of relative displacements

$$M_1\ddot{y}_1 + C_1(\dot{y}_1 - \dot{y}_2) + k_1(y_1 - y_2) = -M_1\ddot{U}_G$$

$$M_2\ddot{y}_2 + C_1(\dot{y}_2 - \dot{y}_1) + C_2(\dot{y}_2 - \dot{y}_3) + k_1(y_2 - y_1) + k_2(y_3 - y_3) = -M_2\ddot{U}_G$$

$$\vdots$$

$$M_n\ddot{y}_n + C_{n-1}(\dot{y}_n - \dot{y}_{n-1}) + C_n\dot{y}_n + k_{n-1}(y_n - y_{n-1}) + k_n y_n = -M_n\ddot{U}_G$$

or in matrix form

$$M\ddot{Y} + C\dot{Y} + KY = -MI\,\ddot{U}_G$$

where

$$M = \begin{vmatrix} M_1 & & & & \\ & M_2 & & & \\ & & M_3 & & \\ & & & \ddots & \\ & & & & M_n \end{vmatrix} \qquad C = \begin{vmatrix} C_1 & -C_1 & & & \\ -C_1 & C_1+C_2 & -C_2 & & \\ & -C_2 & C_2+C_3 & -C_3 & \\ & & & -C_{n-1} & C_{n-1}+C_n \end{vmatrix}$$

$$K = \begin{vmatrix} k_1 & -k_1 & & & \\ -k_1 & k_1+k_2 & -k_2 & & \\ & -k_2 & k_2+k_3 & -k3 & \\ & & & -k_n & k_{n-1}+k_n \end{vmatrix} \qquad \text{and} \quad I = \begin{vmatrix} 1 \\ 1 \\ 1 \\ \vdots \\ 1 \end{vmatrix}$$

Replacing $\ddot{u}_G$ by the accelerogram of the earthquake at bedrock and integrating numerically this set of differential equations, one can obtain the time history of displacements, velocity or acceleration at any of the masses, or what is equivalent at any point in the soil. Once $\ddot{u}$, absolute acceleration = $\ddot{y} + \ddot{U}_G$ is obtained at the surface of the soil as a function of time, the procedure to determine response spectra is the same as that described for the continuous modal, second approach.

The integration of the set of differential equations as outlined above is normally referred to as physical integration of the equations of motion. This procedure is the only one which can be used if the properties of the soil are considered non-linear. On the other hand, for linear systems if modal damping can be specified it is normally preferred to carry out the solution by modal superposition.

If ω_i are the natural circular frequencies of the soil deposit, ϕ_i, its modal shapes (eigenvectors), normalized so that $\phi_i^T M \phi_i = 1$ and Γ_i the participation factor of the ith mode

$$\Gamma_i = \phi_i^T M \bar{1} = (M_1\phi_{i1} + M_2\phi_{i2} + \cdots + M_n\phi_{in})$$

the solution can be expressed as

$$Y = \sum_i \Gamma_i \phi_i a_i(t)$$

where $a_i(t)$ is the solution of the one-degree-of-freedom equation

$$\ddot{a}_i + 2\beta_i\omega_i\dot{a}_i + \omega_i^2 a_i = -\ddot{u}_G(t)$$

In particular at the surface of the soil

$$\ddot{u}_s = \sum_i \Gamma_i \phi_{i1} \ddot{a}_i + \ddot{u}_G = \sum_i g_i \ddot{a}_i + \ddot{U}_G$$

The advantage of this type of solution is that it requires only the solution of a one-degree-of-freedom equation for each mode, once the modal shapes, participation factors and natural frequencies are known. Moreover in general only the first few modes contribute significantly to the solution. For the case of the uniform layer, previously considered with the continuous solution the coefficients g_i are

first mode $g_1 = 1.27$
second mode $g_2 = -0.416$
third mode $g_3 = 0.24$

Only three modes are enough in this case to obtain a good solution. The maximum acceleration in the first mode is of the order of 0.27g, in the second of 0.15g, and in the third of 0.05g.

Response spectra obtained by this method show good agreement with those obtained by the continuous solution, although not as perfect as in the case of the amplification function. The discrepancies are, however, very small and are easy to understand if the large number of computations involved is considered. Each method has its own round-off and truncation errors and they will affect each procedure differently. For all practical purposes the results can, however, be considered equivalent.

Again if the effect of the elastic rock has to be included, it can be done by adding the equivalent radiation damping in each mode.

If the only result desired is the time history of acceleration at the free surface of the soil (or at a small number of points) the continuous solution has an advantage both from the point of view of flexibility (being able to consider different values of damping in each layer) and from the point of view of time of computation. On the other hand, if the time history of acceleration and stresses is desired at many points the modal solution becomes more economical. Damping in the soil does not really come from viscosity but from non-linear

hysteretic dissipation of energy. Correspondingly both shear modulus and damping are functions of strain. If a non-linear analysis is to be performed only the discrete model with physical integration of the equations of motion would be applicable. Often, however, the system is considered linear, assuming values of shear modulus and damping, determining histories of strains, computing new values of modulus and damping and cycling until convergence of the process is obtained. For these preliminary runs the discrete model with modal analysis is convenient and it provides a faster, more economical solution. Once appropriate values of modulus and damping have been obtained, the continuous model can be used for a final series of analyses with different values of damping in each layer. (In the modal solutions the values of damping are averaged and expressed as modal damping, constant in all modes).

IV. DERIVATION OF RESPONSE SPECTRA

The methods previously outlined are mainly intended to consider an earthquake at the base of the soil, filter it and obtain the resulting time history of acceleration at the free surface. While it is possible to obtain then design response spectra on top of the soil, the procedure has for this purpose several difficulties:

a) It requires as an input an actual accelerogram, be it that of a real earthquake, scaled or not, or an artificial earthquake obtained by a simulation process. While the area of Earthquake Simulation has seen a considerable progress in the last years, it is still harder to derive the time history of an earthquake corresponding to a certain magnitude and epicentral distance than it is to derive a response spectrum.

b) In order to obtain reliable results the analysis cannot be done for just one input earthquake, but should be repeated for several inputs representing samples of earthquakes with the same average characteristics. The resulting response spectra should finally be smoothed by drawing an average or envelope. The process becomes then too long and expensive.

It would be therefore desirable to have simple and approximate ways by which smooth response spectra on top of the soil would be derived from response spectra at bedrock or on firm ground. Figure 19 showed the amplification curve for a given soil profile and the ratio of response spectra for 2 and 5% of structural damping. The similarity of these curves is apparent. In fact, if the Fourier spectrum were exactly the undamped velocity response spectrum, the amplification curve should coincide with the ratio of response spectra for no damping.

There are, however, several important differences between these two curves:

1. The amplification curve tends to zero as the frequency increases or as the period becomes very small. The ratio of response spectra on the other hand tends to a finite value which is the ratio of the maximum acceleration on top of the soil to the maximum acceleration of the input. (This ratio can be estimated from the design response spectra at bedrock if the modes of the soil are known). The ratio of response spectra is therefore highly dependent on the input earthquake in the high frequency range (or for very short periods, say T smaller than 0.1 seconds).

2. The amplification curve is a function of the soil properties only. The ratio of response spectra on the other hand will depend on the soil properties (periods and damping), the amount of structural damping and the selected earthquake input.

3. The ratio of response spectra is in general smoother than the amplification curve with lower peaks and higher valleys and it becomes smoother as the structural damping increases. For damping values of 20 or 25% the ratio of response spectra is practically constant over a long range of periods. On the other hand for very small values of structural damping or for undamped spectra, the ratio of the response spectra should be close to the amplification curve except in the range of very small periods.

4. It should also be expected that the agreement between the amplification curve and the ratio of response spectra would be better for

high values of damping in the soil since this would tend to eliminate the transients and furnish a motion closer to a periodic one.

In order to determine the applicability of the amplification curve to reproduce the ratio of response spectra, the ratio between both curves b has been obtained at several points for uniform soils with varying fundamental periods and damping, subject to different earthquake inputs. The earthquake records considered are El Centro, Taft and five artificial earthquakes with a Tajimi type spectral density function.

Figure 20 shows for one of the cases studied the amplification curve and the ratio of response spectra for El Centro and Taft earthquakes. Figure 21 shows the average ratio of response spectra for the five artificial earthquakes, together with the 95% confidence levels (mean + 2σ). Most of the points of the curves for El Centro and Taft fall within this band. It must be therefore realized that even within samples of earthquakes with the same properties (magnitude and epicentral distance) a substantial variation is to be expected in the ratio of response spectra.

Figure 22 shows the effect of the natural period of the soil and the amount of damping in the soil in the value of b at different points. For $T = 2T_1$ (1st natural period) the ratio is practically constant, independent of T_1. For $T = T_1$ it has again little variation for periods larger than 0.3 seconds. For $T = 0.5\ T_1$ the variation is large for periods smaller than 0.5 seconds and for $T = \frac{1}{3} T_1$ for periods smaller than 0.8 or 0.9 seconds. It should be noticed that in all cases the variation is small for values of T larger than 0.2 or 0.3 seconds. If it is accepted that in this range (say 0 to 0.2 or 0.3 seconds) the maximum acceleration at top of the soil controls the response spectrum, the values of b can be considered only slightly depending on the natural period of the soil over the range of application.

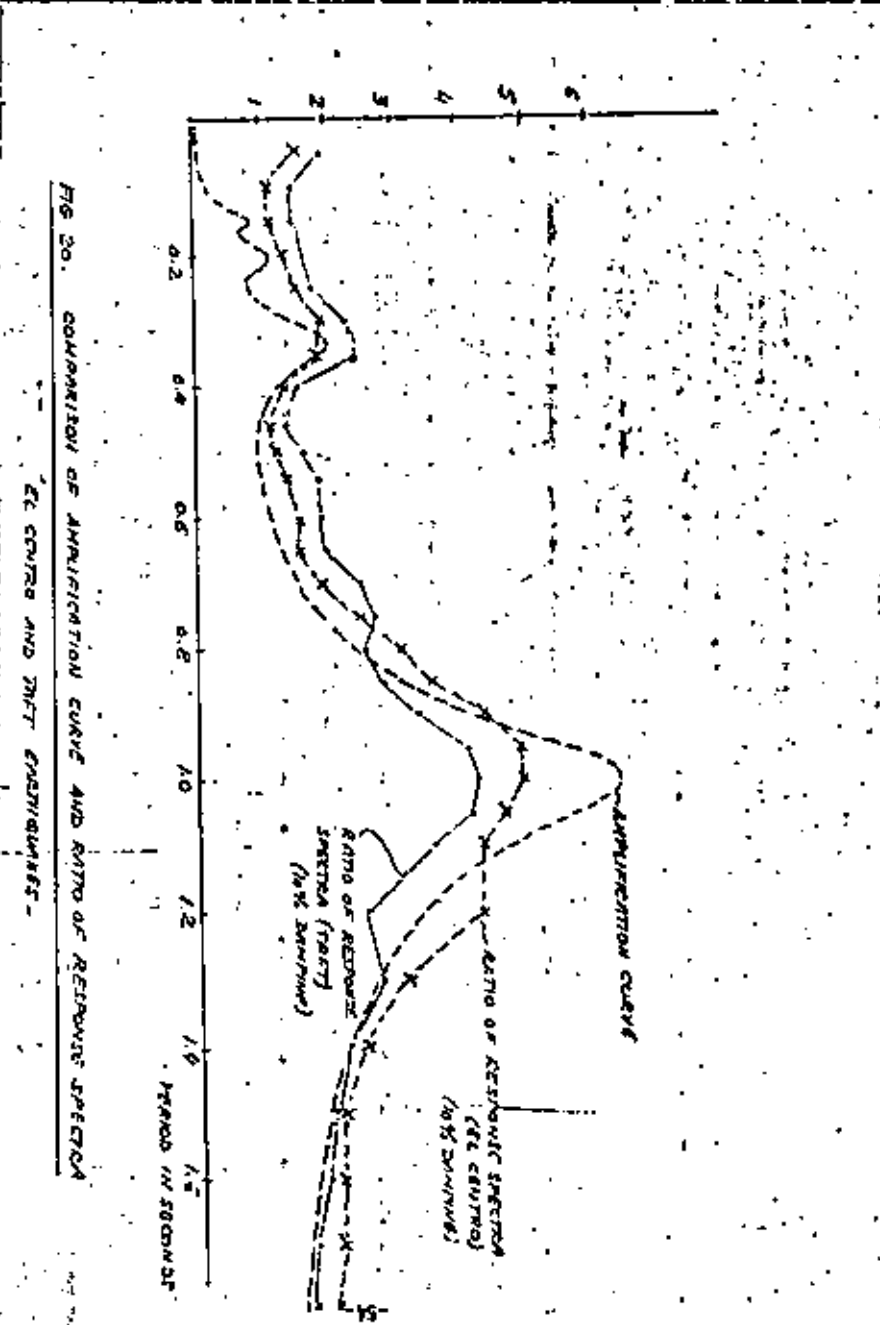

FIG 20. COMPARISON OF AMPLIFICATION CURVE AND RATIO OF RESPONSE SPECTRA - EL CENTRO AND TAFT EARTHQUAKES -

FIG. 21. COMPARISON OF AMPLIFICATION CURVE AND RATIO OF RESPONSE SPECTRA

S. PETROVSKI EARTHQUAKE.

FIG. 22. RATIO BETWEEN RATIO OF RESPONSE SPECTRA AND AMPLIFICATION CURVE AT DIFFERENT POINTS

EFFECT OF NATURAL PERIOD OF SOIL

Figure 23 shows the effect of structural damping in the values of a. It can be noticed that as it should be expected the value of b is closer to unity as the damping in the soil increases and the structural damping decreases. While the effect of the structural damping is large in the range 0 to 20% in the normal range of structures (say 0 to 5%) this effect may be considered slight, particularly compared to the variation from one input record to another within a family of earthquakes.

Curves like those shown in Figures 22 and 23 have been obtained for different values of T/T_1. Using these curves the following procedure is suggested to derive the ratio of response spectra from the amplification curve.

1. At each one of the peaks ($T = T_1$, $T = \frac{1}{3} T_1$, $T = \frac{1}{5} T_1$ etc.) find the value of b from the curves and obtain the corresponding point (multiplying the amplification by the factor b). A horizontal segment is then drawn passing by each one of these points and cutting the peak of the amplification curve if b is smalle. than 1.

2. At each one of the valleys ($T = \frac{1}{2} T_1$, $T = \frac{1}{4} T_1$ etc.) the ratio b is obtained from the curves and a point is drawn. These points are then joinsd by smooth curves to those resulting from step 1.

3. At $T = 2T_1$, the value of b is again found or can be taken approximately equal to 1. For $T > 2 T_1$ the amplification curve can be used. This point is then joined to the point immediately next to T_1 by a smooth curve if the curve is plotted versus period or a straight line if plotted versus frequency.

4. In the range of small periods or large frequencies the response spectrum has to be controlled by the acceleration at top of the soil. The ratio of this acceleration to the maximum input acceleration can be obtained. At a period of 0.1 seconds (or a frequency of 10 cycles per second) this value may be taken as the ratio of response spectra. Between the value at a period of 0.2 seconds and this value a straight line may be drawn if the curve is plotted versus period or a smooth transition curve if plotted versus frequency.

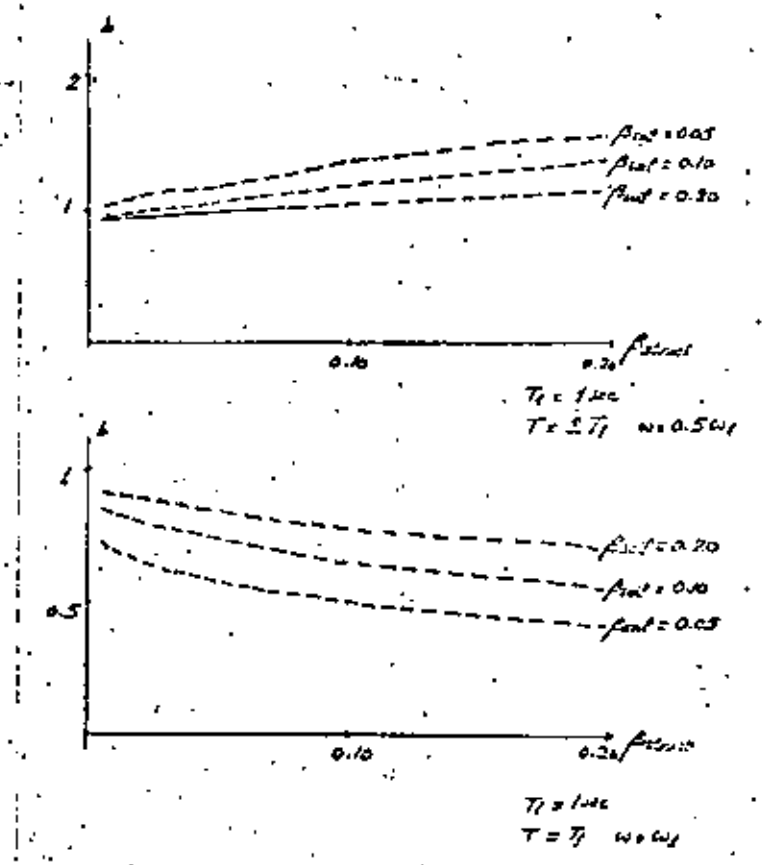

FIG 23. RATIO BETWEEN RATIO OF RESPONSE SPECTRA AND AMPLIFICATION CURVE AT DIFFERENT POINTS

EFFECT OF STRUCTURAL DAMPING

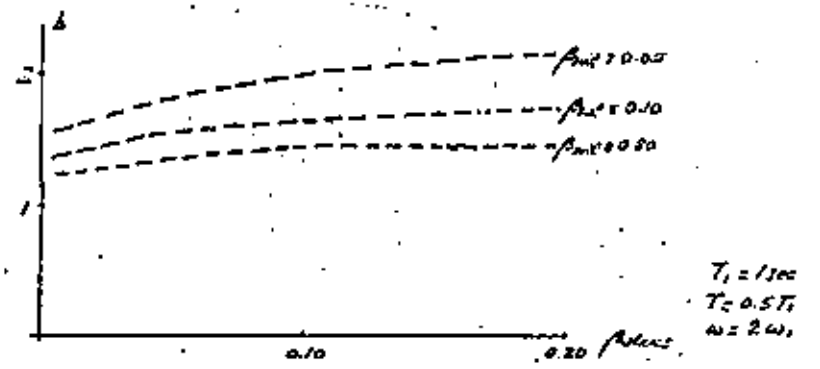

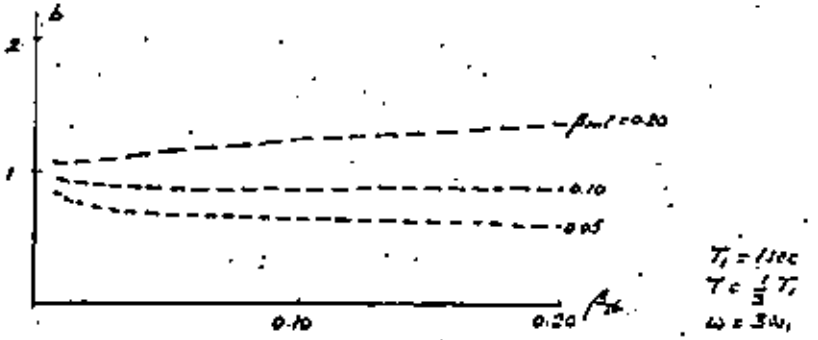

FIG 23 (CONTINUED)

While all the cases considered to derive the curves for the values b have corresponded to a uniform soil profile and further testing is necessary for multilayer systems, it is believed that such a procedure could also be applied for the latter taking the T_1 as the period at which the maximum amplification occurs rather than the first fundamental period.

Figure 24 shows an example of application of the method. Curves of the standard deviation σ have also been obtained. From these curves it is then possible to draw not only the average ratio of response spectra but also confidence levels.

FIGURE 14. SUGGESTED RATIO OF RESPONSE SPECTRA (SOIL BEDROCK)

REFERENCES

1. Seed and Idriss, "Influence of Soil Conditions on Ground Motions during Earthquakes. State of the Art Symposium, Earthquake Engineering of Buildings, San Francisco, California - Feb. 1968 and Journal of Soil Mechanics and Foundations Division ASCE, Jan. 1969.

2. Donovan and Matthiesen, "Effects of Site Conditions on Ground Motions During Earthquakes." Same Symposium.

3. Herrera, Rosenblueth and Rascon, "Earthquake Spectrum Prediction for the Valley of Mexico. 3rd World Conference on Earthquake Engineering, 1965.

4. Idriss and Seed, "Seismic Response of Horizontal Soil Layers," Journal of the Soil Mechanics and Foundations Division, ASCE, July 1968.

5. Roesset and Whitman, "Effect of Local Soil Conditions upon Earthquake Damage - Theoretical Background." M.I.T. Dept. of Civil Engineering Report, 1969.

6. "The Use of Amplification Functions to Derive Response Spectra, Including the Effect of Local Soil Conditions," M.I.T. Civil Engineering Dept. Report, 1969.

IX CURSO INTERNACIONAL DE INGENIERIA SISMICA
ANALISIS DE RIESGO SISMICO

SISMOLOGIA Y TECTONICA DE PLACAS
ONDAS SISMICAS
SISMOMETROS Y SISMOGRAMAS
DETERMINACION DEL EPICENTRO
ESCALAS DE MAGNITUD E INTENSIDAD
CONSTITUCION DE LA TIERRA
SISMICIDAD
SISMICIDAD EN MEXICO
PREMONITORES Y REPLICAS
PREDICCION
QUE HACER EN CASO DE UN SISMO

DR. JUAN M. ESPINDOLA C.

JULIO , 1983

INDICE

APENDICES

1. Sismología y Tectónica de Placas
(Teoría del rebote elástico)

SISMOLOGIA Y TECTONICA DE PLACAS

La ciencia que estudia los aspectos relacionados con la ocurrencia de temblores de tierra o sismos es llamada Sismología. Esta es una ciencia joven ya que gran parte de sus métodos e instrumental fueron desarrollados durante este siglo.

A pesar de ésto, la Sismología ha logrado avances notables. Quizá una de sus más valiosas contribuciones al entendimiento de nuestro planeta lo constituya su aportación a la llamada TECTONICA DE PLACAS.

Para esbozar esta teoría consideremos en primer lugar la estructura interna de la tierra. En la figura 1 podemos ver esquemáticamente su constitución. El núcleo terrestre está probablemente compuesto de fierro y niquel. El manto terrestre tiene una composición a base de silicatos ferromagnesianos mientras que la corteza está compuesta por silicatos abundantes en potasio, sodio y calcio. El cascarón más externo de la tierra, el cual comprende la corteza y parte del manto, con un espesor de aproximadamente 100 km parece comportarse como un cuerpo rígido "flotando" en el resto del manto en con-

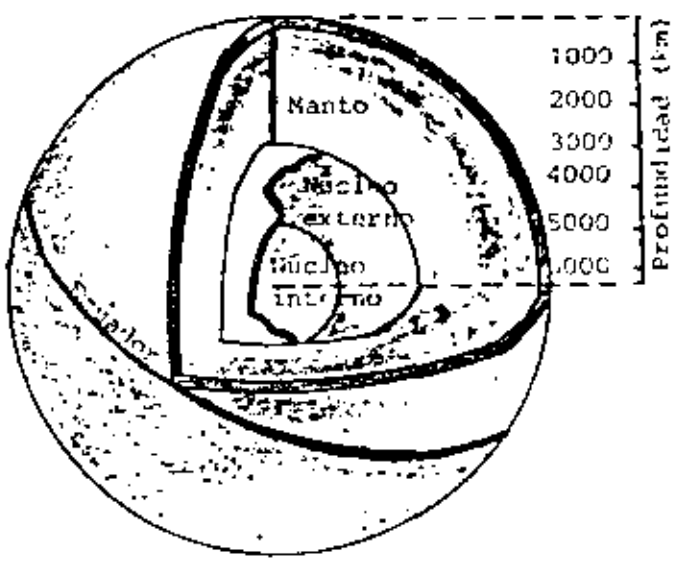

Fig. 1

de pueden presentarse movimientos como si se tratara de un fluido. Esta conducta semejante a la de un fluido tiene sentido solamente en tiempos geológicos, es decir en tiempos del orden de millones de años.

El cascarón exterior llamado litósfera no es continuo sobre la superficie de la tierra sino que está formado por diferentes "placas" en contacto una con otra.

las placas sufren movimientos relativos debidos a fuerzas de origen aún no completamente conocidos, aplicadas a lo largo de las mismas. Estos mismos esfuerzos producen en algunos de sus márgenes la subducción de una placa bajo la otra y en otras la creación de nueva litósfera (Figura 2). Debido a estos movimientos los continentes han variado su posición relativa a través del tiempo geológico y se cree que en un tiempo estuvieron todos reunidos en un gran continente llamado Pangea. Esto nos explica el ajuste que existe entre, por ejemplo, las costas de Sudamérica y África. ¿Cuál es la distribución geográfica de estas placas? La Figura 3 nos la muestra. Las zonas de creación de nueva litósfera se presentan como cordilleras submarinas y las zonas de subducción forman a menudo trincheras submarinas de

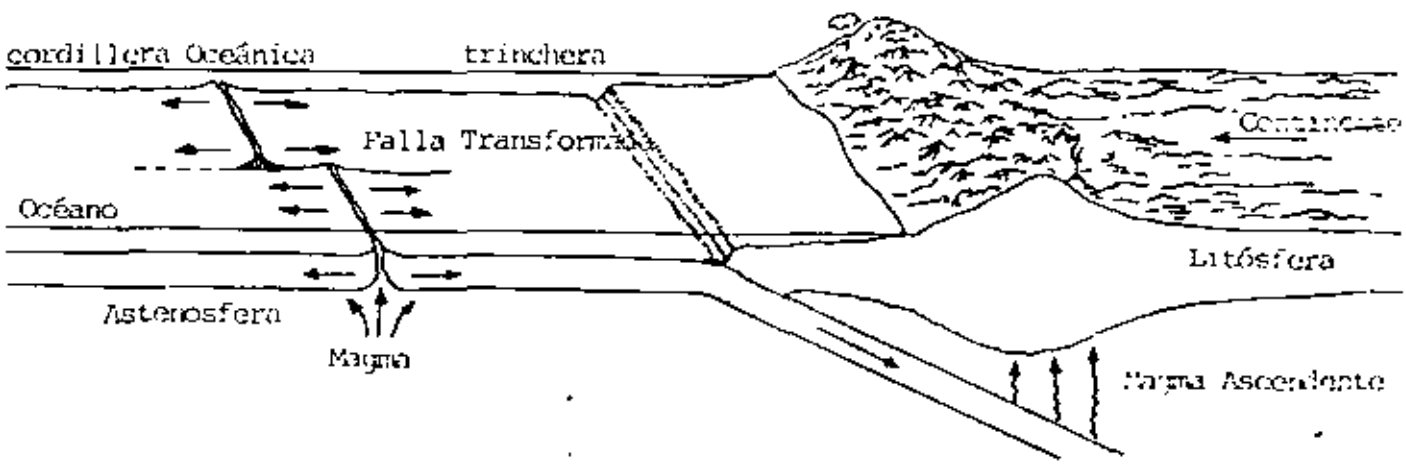

Fig. 2

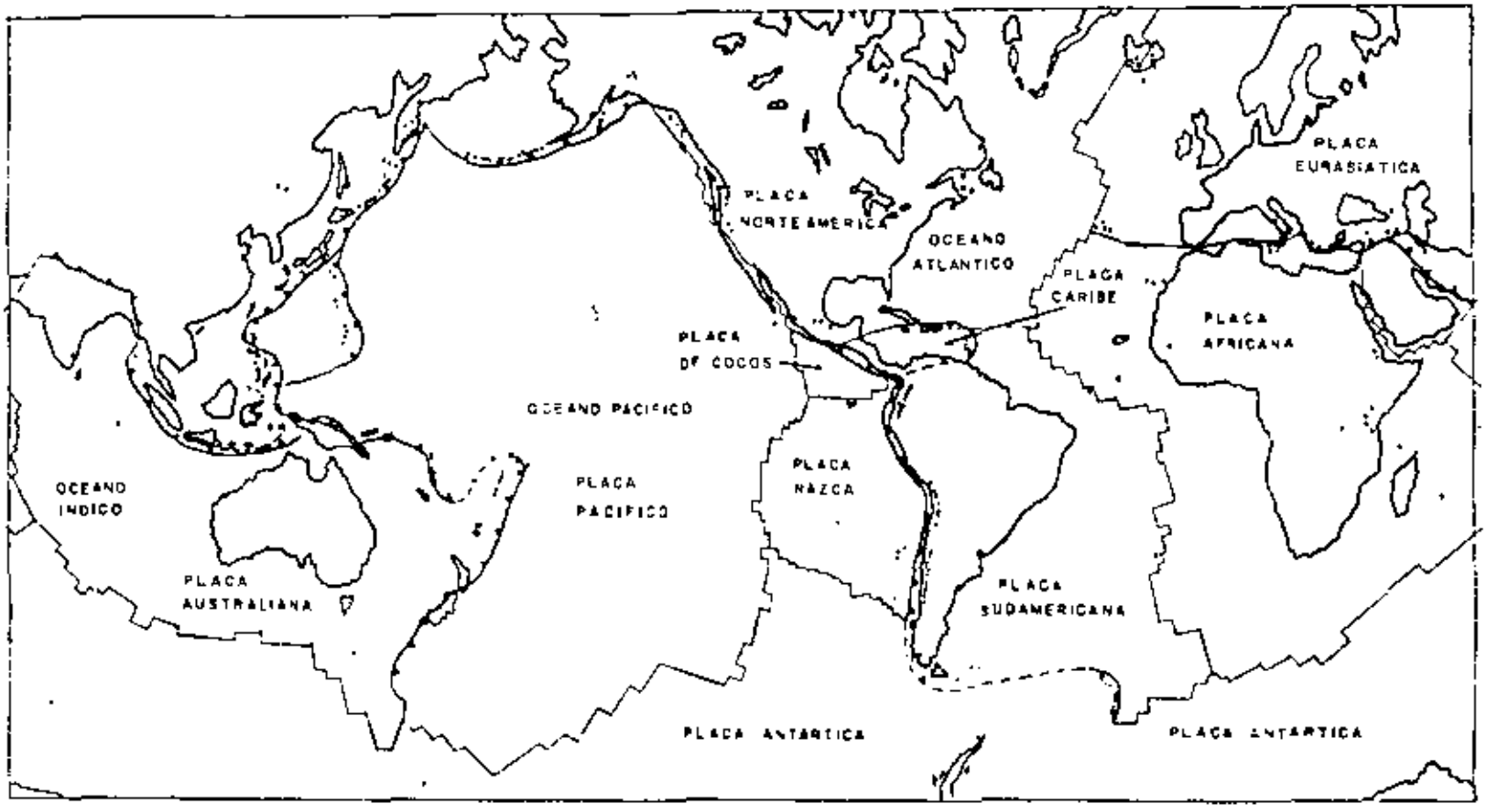
PLACA EURASIATICA
PLACA NORTEAMERICA
OCEANO ATLANTICO
PLACA CARIBE
PLACA AFRICANA
PLACA DE COCOS
OCEANO PACIFICO
PLACA NAZCA
OCEANO INDICO
PLACA PACIFICO
PLACA AUSTRALIANA
PLACA SUDAMERICANA
PLACA ANTARTICA
PLACA ANTARTICA
ZONA DE SUBDUCCION
EJE DE CORDILLERA
TRANSFORMACION
VOLCAN

Fig. 3

gran profundidad. Podemos también notar que las diferentes placas no coinciden con los continentes y los océanos, sino que pueden tener corteza continental y oceánica.

No se sabe con certeza que causa los esfuerzos que producen los movimientos de las placas pero se cree que éstos son producidos por transferencia convectiva de calor, de la misma manera como ocurre cuando se hierve agua o cualquier otro líquido. El fluido más cercano a la fuente de calor se expande, se vuelve de esta manera menos denso y tiende por lo tanto a subir a la superficie donde es enfriado y desplazado hacia el fondo por nuevas parcelas ascendentes (Figura 4).

Este tipo de corrientes de convección pueden existir en el manto terrestre aunque no debe por ésto suponerse que el mismo se encuentra en estado de fusión como las lavas. Ya se ha mencionado que ésto sólo tiene sentido en tiempos muy largos. Una manera de visualizar ésto es considerar un cierto

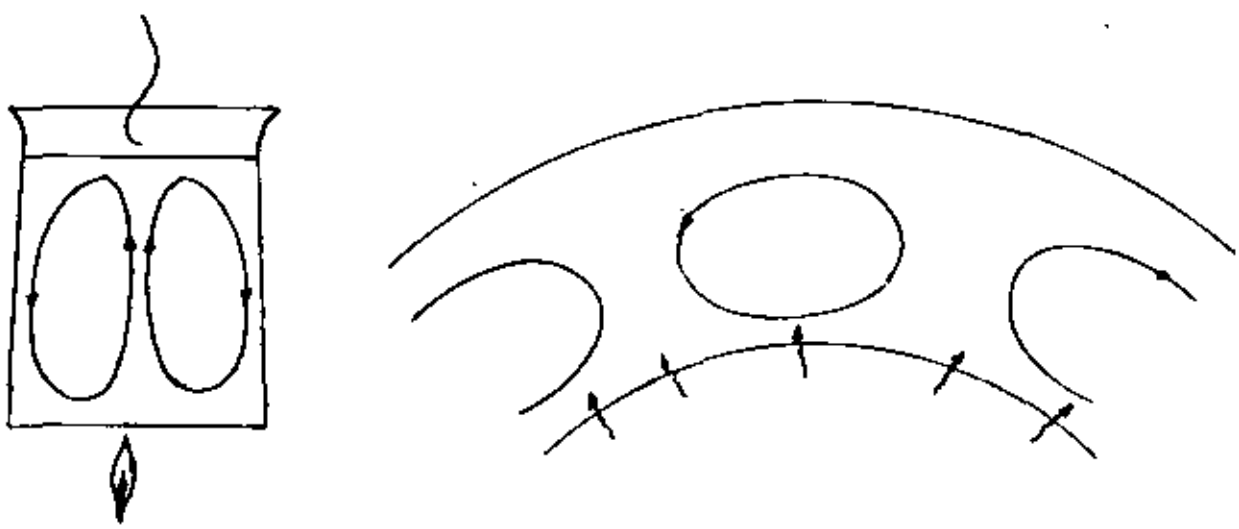

Fig. 4

volumen de roca. Si aplicamos a ésta un esfuerzo tensional por un tiempo corto la roca vuelve a su posición inicial. Si por el contrario aplicamos el esfuerzo por un período prolongado de tiempo la roca quedará deformada permanentemente (Fig. 5). En este último caso la roca "fluye" y se parece, en este sentido, a un fluido, ya que en éstos las deformaciones son permanentes. Esto nos explica también los plegamientos que observamos muchas veces en las cortaduras hechas en las carreteras.

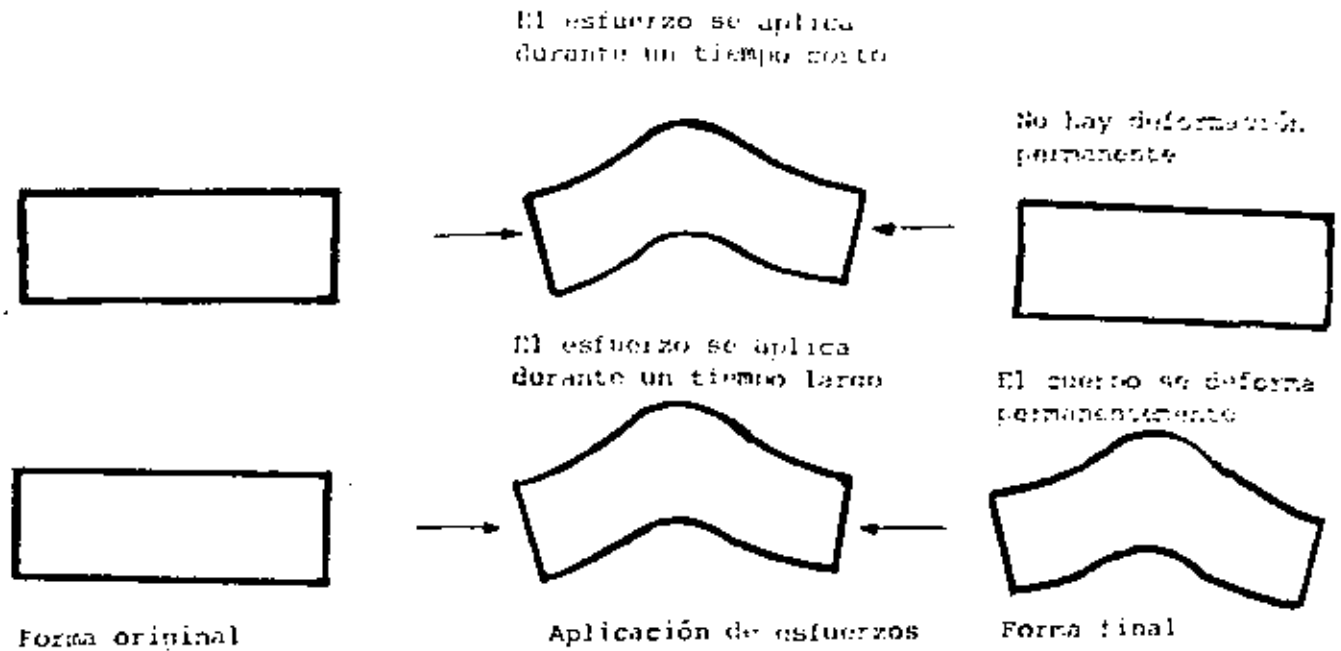

Figura 5

¿Cuál es la relación de ésto con los temblores? En primer lugar notaremos que en una zona de subducción el movimiento de una placa bajo la otra se realiza venciendo las fuerzas de fricción generadas en el contacto entre ambas. A lo largo de este contacto, llamado zona de Wadati-Benioff (WB), el movimiento de una placa contra la otra tiene lugar dicontinuamente, por "brincos". Es ésto precisamente lo que genera los temblores en esas regio

nes. Para visualizar estos procesos pensemos en un bloque de cemento sobre una mesa como se muestra en la Figura 6.

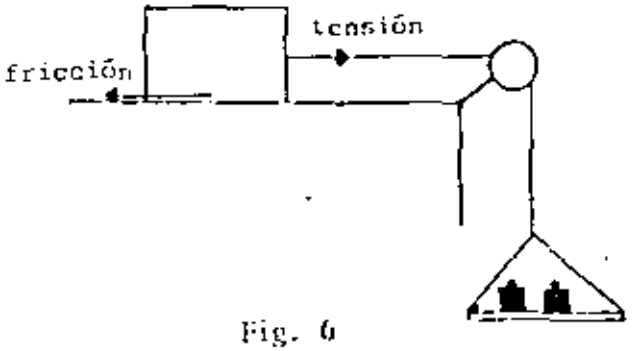

Fig. 6

Si colocamos un peso pequeño en la canastilla el bloque no se moverá debido a la fuerza de fricción entre el bloque y la mesa. Conforme aumentamos el peso la tensión en el cable continúa acumulándose hasta que iguala a la fuerza de fricción, a partir de ese momento el bloque empezará a moverse.

Análogamente en la zona W-B se acumula gradualmente hasta que rebasa un límite, en ese momento comienza a presentarse un fallamiento en algún punto llamado foco desde donde se propaga a toda una superficie (Fig. 7).

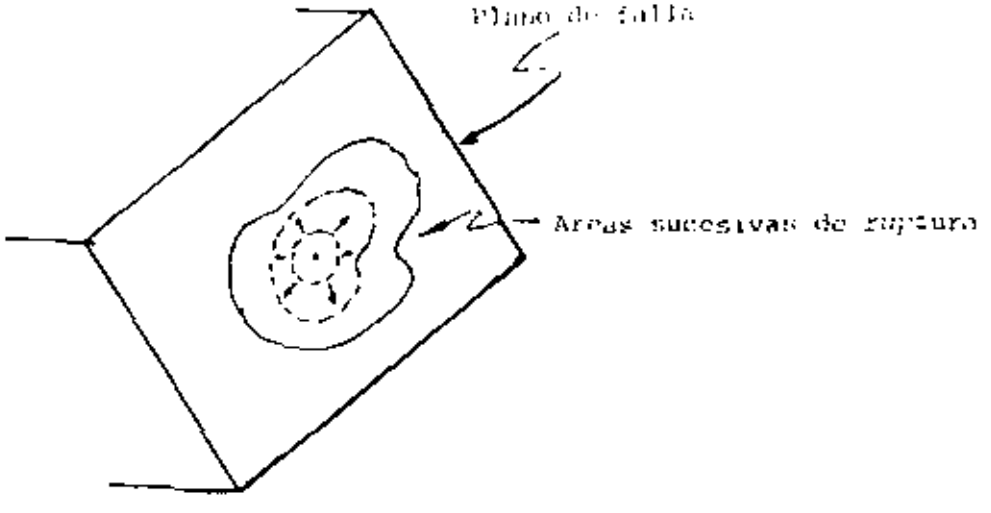

Fig. 7

Este comportamiento puede ser observado cuando el contacto entre placas aflora en la superficie de la tierra como en la famosa Falla de San Andrés en California. De hecho, fue en observaciones hechas en esta falla que pudo deducirse este mecanismo que es conocido como la TEORIA DEL REBOTE ELASTICO. Esto ocurrió durante el sismo de San Francisco en 1906. La Figura 8a muestra las dos placas durante el movimiento lateral que produce la acumulación de esfuerzos. En la Figura 8b los esfuerzos rebasan cierto límite y el fallamiento se produce en un punto y se propaga en ambas direcciones. La Figura 8c muestra la situación después del temblor; existe ahora

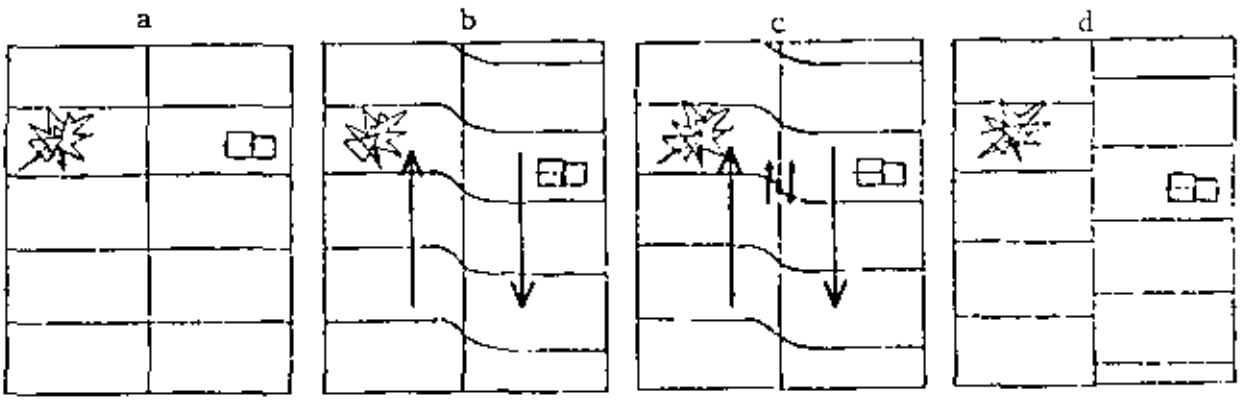

Fig. 8

un desplazamiento permanece entre ambas caras de la falla.

Aunque este proceso puede parecer intuitivamente obvio, en realidad no lo es. Durante mucho tiempo se pensó que el fallamiento de la corteza era un efecto de los temblores y no su origen. Como fuentes de éstos se pensaba en intrusiones de magma o colapso de volúmenes por cambios de densidad de las rocas que componen la corteza. Aunque estos mecanismos pueden ocurrir, se piensa en la actualidad que la mayoría de los temblores en las regiones de subducción se originan por el mecanismo expuesto y son llamados "tectó-

nicos". Otros tipos de sismos están asociados a fenómenos locales como son los volcánicos o algunos otros debido p. ej. al colapso del subsuelo por pérdida de agua, etcétera.

ONDAS SISMICAS

Si desplazamos un diapazón de su posición de equilibrio y lo soltamos repentinamente percibimos su sonido característico (Fig. 9). Lo mismo sucede

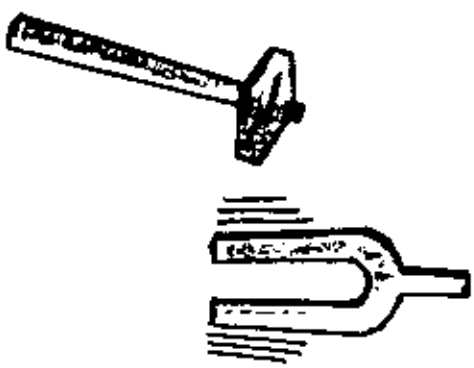

Fig. 9

en la tierra, hemos visto que el fallamiento de la roca consiste precisamente en la liberación repentina de los esfuerzos impuestos al terreno. De esta manera, la tierra es puesta en vibración. Esta vibración es debida a la propagación de ondas como en el caso del diapasón.

Ahora bien, en un sólido pueden transmitirse dos tipos de ondas. El primer tipo de ondas es conocido como compresional porque consiste en la transmisión de compresiones y rarefacciones como en el caso de la transmisión del sonido, en este caso las partículas del medio se mueven en el mismo sentido en que se propaga la onda. El segundo tipo es conocido como ondas transversales o de cizallamiento; las partículas se mueven ahora en dirección perpendicular a la dirección de propagación de la onda.

La figura 10 muestra esquemáticamente la propagación de estas ondas en un bloque sólido.

Las ondas compresionales y transversales han sido llamadas P y S respectivamente por razones que se verán más adelante. Son también conocidas como ondas internas porque pueden viajar en el interior de un sólido elástico.

Además de estas dos clases de ondas pueden existir otros dos tipos más llamadas superficiales. Estas ondas viajan en la superficie de la tierra y su

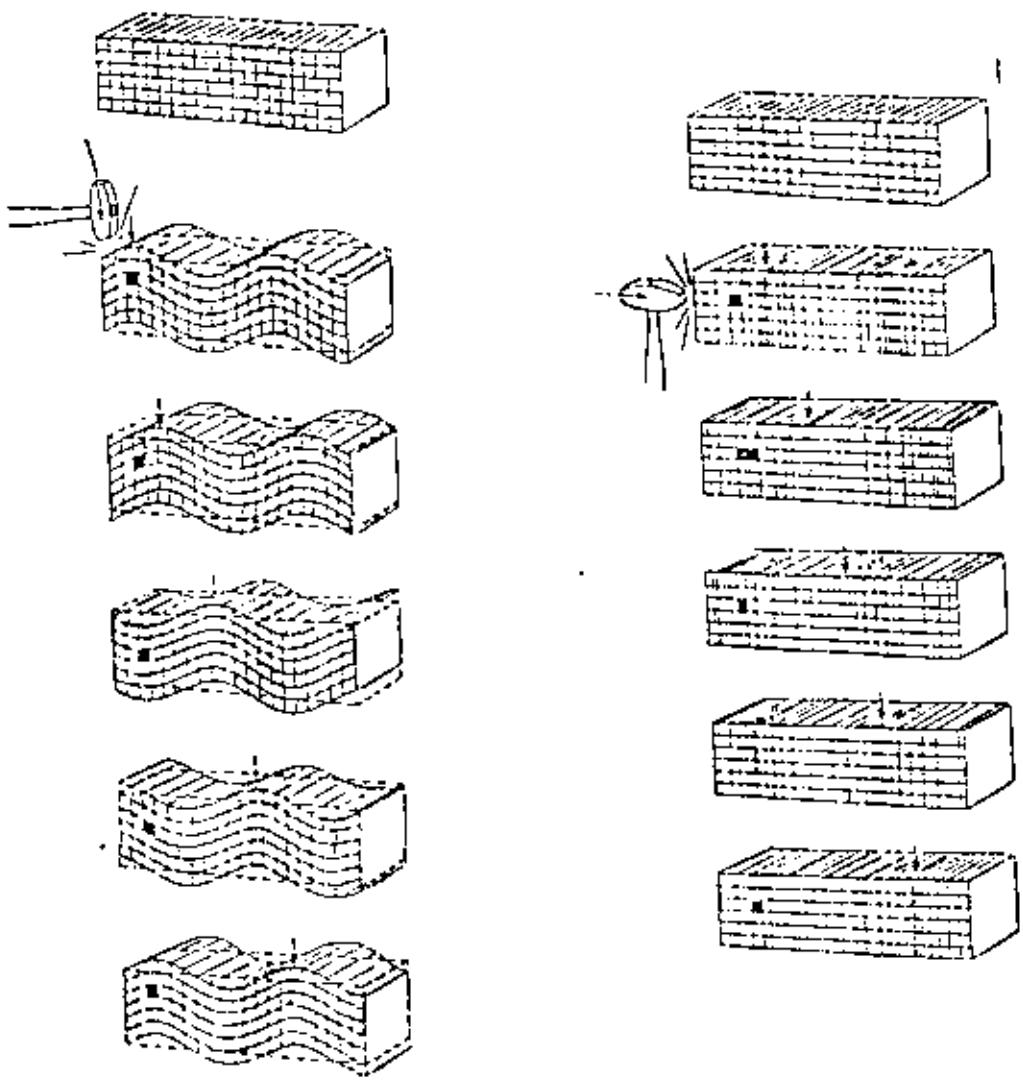

Fig. 10

amplitud decrece con la profundidad. Se les ha denominado con el nombre de los científicos que demostraron teóricamente su existencia: Rayleigh y Love.

Las ondas de Rayleigh se originan en la superficie de un sólido elástico, es decir, estas ondas no podrían generarse en un medio infinito y se caracterizan por la trayectoria elíptica retrógrada que describen las partículas al propagarse la onda. Esta trayectoria ocurre en el plano de propagación de la onda (Fig. 11).

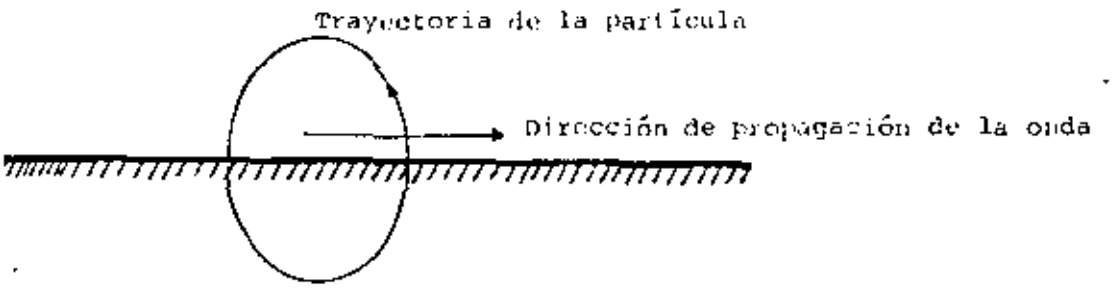

Fig. 11

Por otro lado, las ondas de Love ocurren cuando existe una interfase entre dos medios elásticos de distintas propiedades. Como las ondas S, las ondas de Love ocurren con un movimiento de las partículas perpendicular a la dirección de propagación, sólo que, polarizado en el plano de la superficie terrestre (Fig. 12).

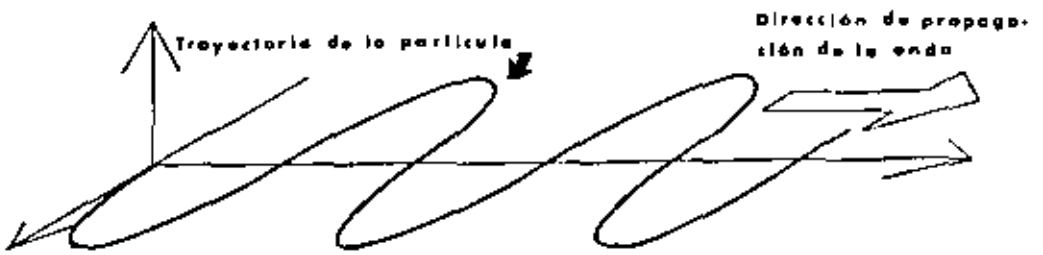

Fig. 12

¿Cuál es la velocidad de estas ondas? Se puede demostrar teóricamente y se observa experimentalmente que la velocidad de las ondas es tal que:

$$V_L < V_S < V_P$$

donde V_P, V_S y V_L son las velocidades de la onda P, S y superficiales respectivamente.

Las velocidades de las diferentes ondas dependen de las características del medio; por ejemplo, en rocas ígneas la velocidad de las ondas P es del orden de 6 km/seg mientras que en rocas poco consolidadas es de aproximadamente 2 km/seg o menor. Así, las ondas P de un terremoto originado en la Costa de Acapulco serían sentidas en la ciudad de México en menos de 2 minutos.

SISMOGRAFOS Y SISMOGRAMAS.

Los mecanismos para detectar los temblores fueron ideados a fines del siglo pasado y perfeccionados a principios de éste. Actualmente estos instrumentos han alcanzado un alto grado de sofisticación, pero el principio básico empleado no ha cambiado. Si tomamos en cuenta que al ocurrir un temblor el suelo se mueve, entonces para poder observar este movimiento tendríamos que estar en un punto fijo fuera de la tierra para no sufrir nosotros mismos ese movimiento y poder detectarlo; ésto obviamente es imposible. Sin embargo, es posible construir un mecanismo que pueda medir este movimiento relativo.

El mecanismo consiste de una masa suspendida de un resorte atado a un soporte acoplado al suelo (Fig. 13), cuando el soporte se sacude al paso de las

ondas sísmicas, la inercia de la masa hace que ésta permanezca un instante

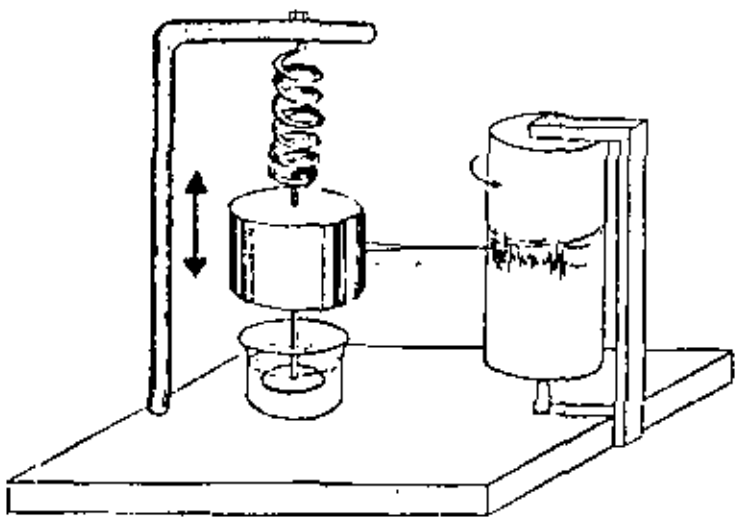

Fig. 13

en el mismo sitio de reposo. Posteriormente cuando la masa sale del reposo, oscila. El movimiento posterior del péndulo no refleja el movimiento del suelo, por lo cual se ha ideado un método para volver a la masa a su sitio original, ésto es lo que se conoce como amortiguamiento del aparato. En la Figura 13 se representa el amortiguamiento como una lámina sumergida en un líquido (comúnmente aceite).

Si se sujeta un lápiz de la masa suspendida para que pueda inscribir sobre un papel pegado sobre un cilindro que gira a velocidad constante, se podrá registrar sucesivamente el movimiento del suelo. El instrumento, hasta aquí descrito, para detectar la componente vertical del movimiento del suelo, se conoce como sismógrafo vertical y el papel donde se inscribe se llama registro o SISMOGRAMA. Sismogramas típicos se muestran en la Figura 14.

Los movimientos del suelo también tienen componente horizontal y para re-

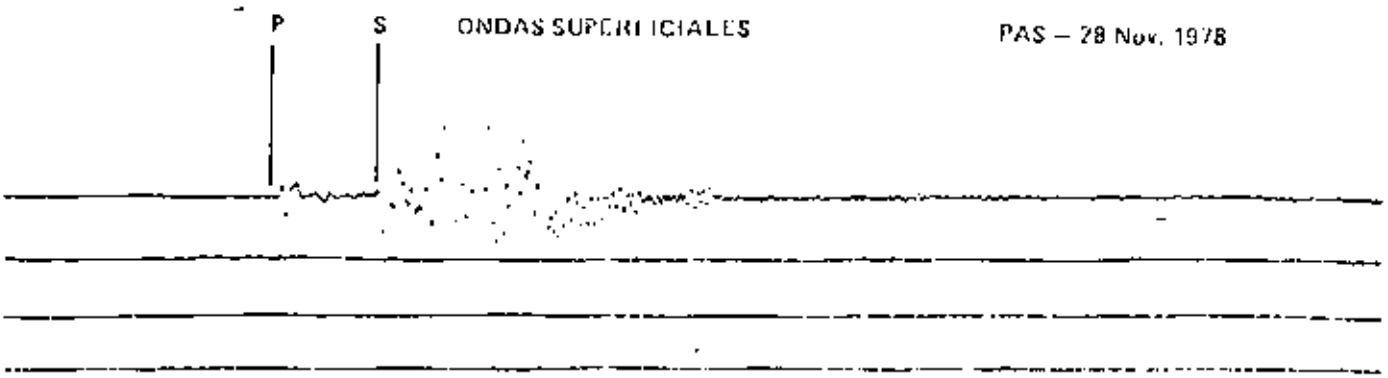

Sismograma de la estación sismológica de Pasadena (E.E.U.U.) correspondiente al temblor de Oaxaca del 28 de noviembre de 1978 $\Delta \simeq 3\,060$ km.

Sismograma de la estación sismológica de Tacubaya correspondiente al temblor del día 22 de febrero de 1979, registrado a las 03h 36'55" y localizado en el "Eje Volcánico Central". Distancia (Δ) de la estación de Tacubaya 120 km

Fig. 14

dir este movimiento se requiere de péndulos horizontales que oscilan como una puerta que tiene su eje inclinado (Fig. 15a). El sismógrafo horizontal se representa en la (Fig. 15b).

Los sismógrafos que se emplean actualmente, en general tienen masas que pueden ser de unos gramos hasta 100 kg, mientras que los sismógrafos antiguos de amplificación mecánica solían tener grandes masas con el fin de vencer las fuerzas de rozamiento, tal es el caso del sismógrafo horizontal Wiechert de 17000 kg de la estación sismológica de Tacubaya (apéndice A); el amortiguamiento se hace por corrientes parásitas o imánes, etcétera, la amplificación por medio de palancas y galvanómetros y la inscripción en papel ahumado, papel fotográfico o cinta magnética.

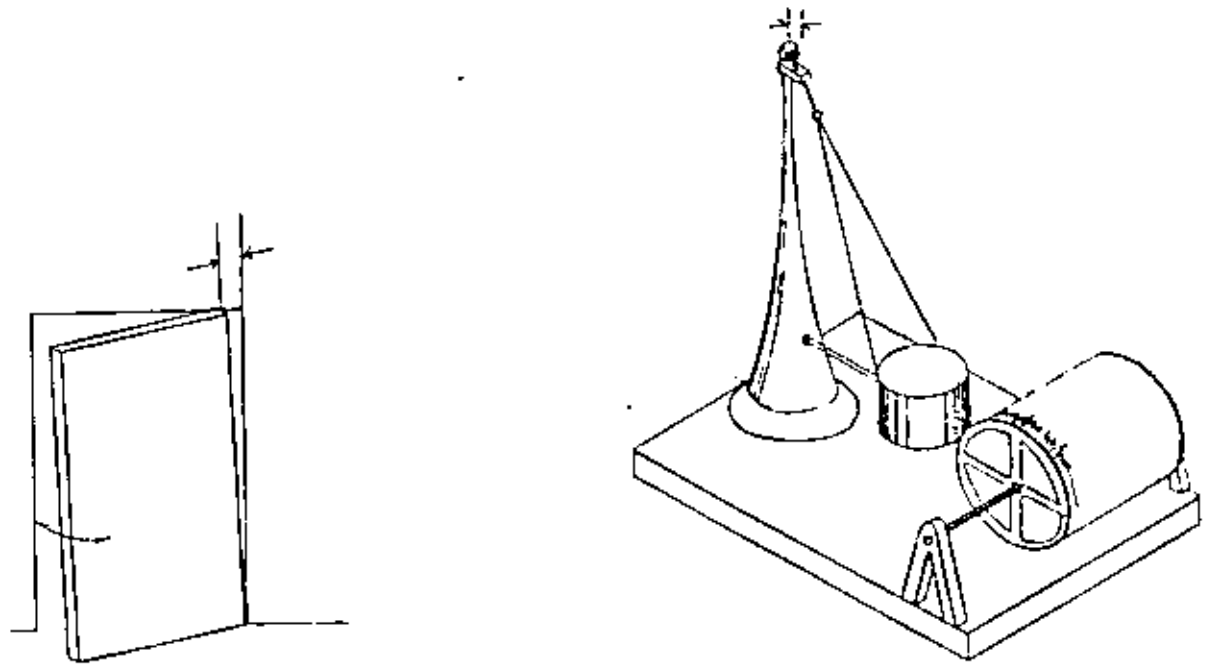

Fig. 15

Los Sismómetros son los sismógrafos cuyas constantes físicas son conocidas de tal manera que se puede conocer el movimiento real del suelo calculado directamente de los sismogramas.

Para determinar con precisión el epicentro de un temblor se requiere del auxilio de varias estaciones sismológicas, por lo cual los observatorios sismológicos requieren por lo menos de tres estaciones sismológicas o formando redes de éstas. Tal como la Red Sismológica Mexicana (ver apéndice B) que controla el Servicio Sismológico Nacional, organismo encargado de la generación de datos e información sismológica. En México existen otras redes de proyectos específicos como RESMAC*, RESNOR**, y SISMEX***. A ni-

---

* "RED SISMICA MEXICANA DE APERTURA CONTINENTAL" operada por el Instituto de Matemáticas Aplicadas y Sistemas de la UNAM.

** "RED SISMOLOGICA DEL NOROESTE" operada por el Centro de Investigación y Enseñanza Superior de Ensenada, B.C.

*** "SISTEMA DE INFORMACION SISMOTECTONICA DE MEXICO" operada por el Instituto de Ingeniería de la UNAM.

vel mundial existen convenios para el intercambio de datos entre los diferentes observatorios, formando así todas las estaciones la red mundial.

DETERMINACION DEL EPICENTRO

Hemos mencionado que el lugar en que comienza el fallamiento que produce los temblores es llamado foco. A grandes distancias el plano completo de ruptura aparece como un punto y lo llamamos foco; la proyección de éste sobre la superficie terrestre recibre el nombre de epicentro (Figura 16).

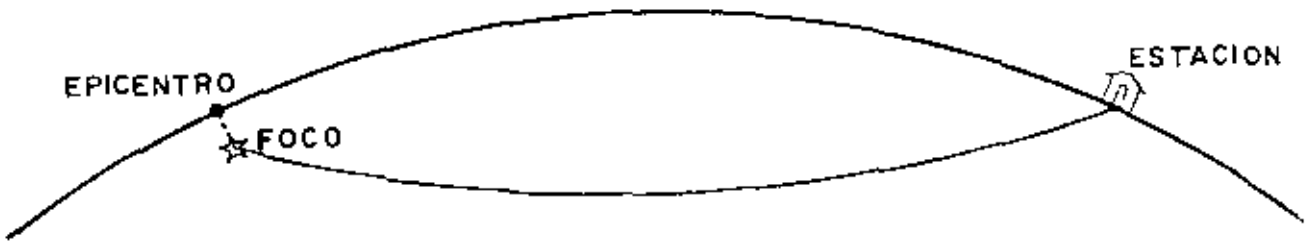

Fig. 16

¿Cómo determinan los sismólogos la ubicación del epicentro?. Ya se dijo que los sismógrafos amplifican e inscriben el movimiento del suelo en una tira de papel (o cualquier otro tipo de material similar) que se llama registro o sismograma. En el sismograma se registran en orden sucesivo de tiempo los diferentes tipos de ondas generadas por un temblor y que arriban a la estación sismológica, como se puede apreciar en la Figura 14. La ubicación del epicentro de un temblor se hace analizando sus registros e identificando los diferentes tipos de ondas como se muestra en la Figura

20. Se ha mencionado ya que la velocidad de las ondas P es mayor que la de las ondas S. Este hecho es utilizado en una de las técnicas más comunes de la Sismología para determinar el epicentro. En efecto, supongamos que la persona A es más veloz que la persona B (Fig. 17). Si ambas empiezan a correr desde el punto 0 en el momento que están juntas a medida que se alejan de 0 la distancia entre ellas será mayor. Puede utilizarse la separación entre ellas en un punto dado para calcular la posición del origen a partir de ese punto.

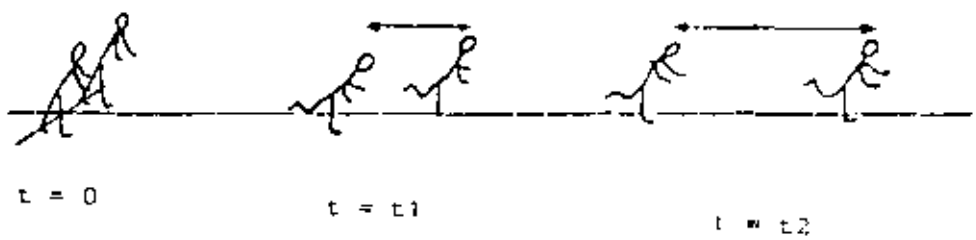

Fig. 17

Sobre la superficie de la tierra, una estación puede proporcionar la distancia al epicentro pero no su dirección de manera que son necesarias al menos tres estaciones para determinarlo sin ambiguedad (Fig. 18).

En la práctica, la intersección de los círculos correspondientes a las tres estaciones no coincide en un solo punto sino comprende una región más o menos grande dependiendo de la calidad de los datos utilizados. La información obtenida de estaciones adicionales es tratada estadísticamente en otras técnicas sismológicas para refinar la posición.

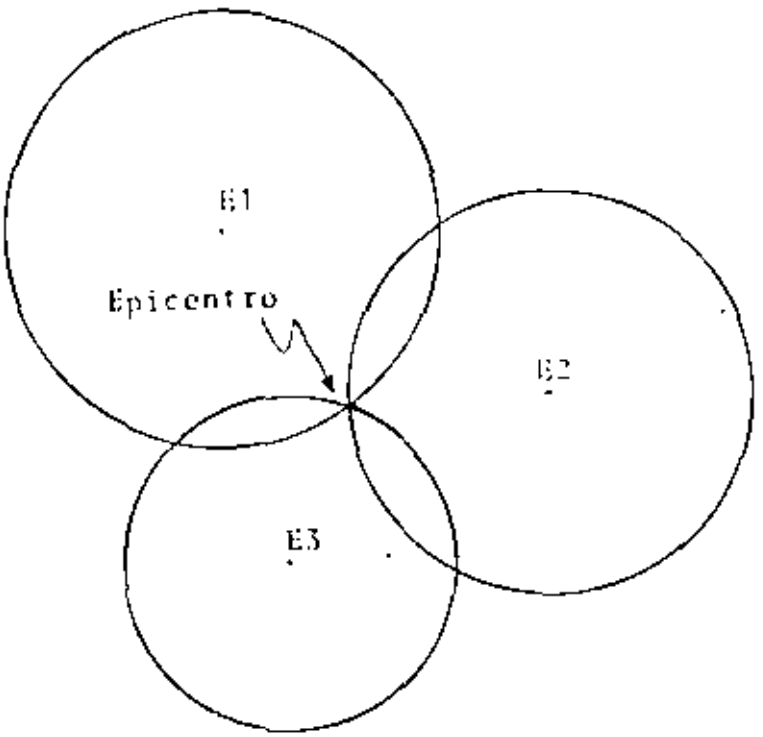

Fig. 18

ESCALA DE MAGNITUD E INTENSIDAD.

Las escalas de magnitud e intensidad son utilizadas para cuantizar o medir los temblores. La escala de magnitud está relacionada con la energía liberada como ondas sísmicas; la de intensidad con los daños producidos por el sismo. Ambas escalas son necesarias puesto que miden aspectos diferentes de la ocurrencia de un temblor. Así la escala de magnitud está relacionada con el proceso físico mismo mientras que la de intensidad lo está con el impacto del evento en la población, las construcciones y la naturaleza.

Como es natural, una clasificación de los temblores por medio de sus efectos, que son observables, fue el primer intento de catalogarlos. Escalas

de intensidad fueron propuestas desde los últimos años del siglo pasado. En 1902 Mercalli propuso una tabla, que fue posteriormente modificada en 1931 y desde entonces se le ha llamado escala Modificada de Mercalli (MM). Esta no es la única;pero si la más frecuentemente usada en nuestro continente. Consta de 12 grados como puede apreciarse en la Tabla I donde se muestran también las características de cada grado.

Podemos ver que la escala de intensidad es en gran medida subjetiva. No nos da información sobre la energía liberada en el temblor puesto que por ejemplo un sismo pequeño puede causar más daños a una población, si ésta está cercana al epicentro, que uno grande pero a mayor distancia.

Así pues es necesario catalogar temblores de acuerdo con los procesos físicos de la fuente; pero también de manera tal que puedan ser medidos. Desde el punto de vista físico sería conveniente clasificar los temblores de acuerdo con la energía que disipan y aunque podríamos hacerlo, no tenemos instrumentos que puedan medirla directamente.

Resulta entonces necesario encontrar una metodología para poder precisar no sólo el epicentro del sismo sino la magnitud y fecha del mismo.

Poseemos sin embargo sismogramas y éstos pueden ser utilizados para catalogar temblores de una manera racional como se verá a continuación.

De dos temblores ocurridos en el mismo epicentro y registrados en el mismo lugar, el más débil producirá un trazo pequeño en el papel y el más fuerte un trazo grande. Para un mismo sismo y estaciones que se alejan gradualmente del epicentro la traza se hace igualmente menor (Fig. 19).

TABLA I

ESCALA MODIFICADA DE MERCALLI

I. Microsismo.
Detectado por instrumentos.

II. Sentido por algunas personas
(generalmente en reposo).

III. Sentido por algunas personas dentro de edificios.

IV. Sentido por algunas personas fuera de edificios.

V. Sentido casi por todos.

VI. Sentido por todos.

VII. Las construcciones sufren daño moderado.

VIII. Daños considerables en estructuras.

IX. Daños graves y pánico general.

X. Destrucción en edificios bien construidos.

XI. Casi nada queda en pie

XII. Destrucción total.

* Una escala más detallada aparece en el Apéndice D.

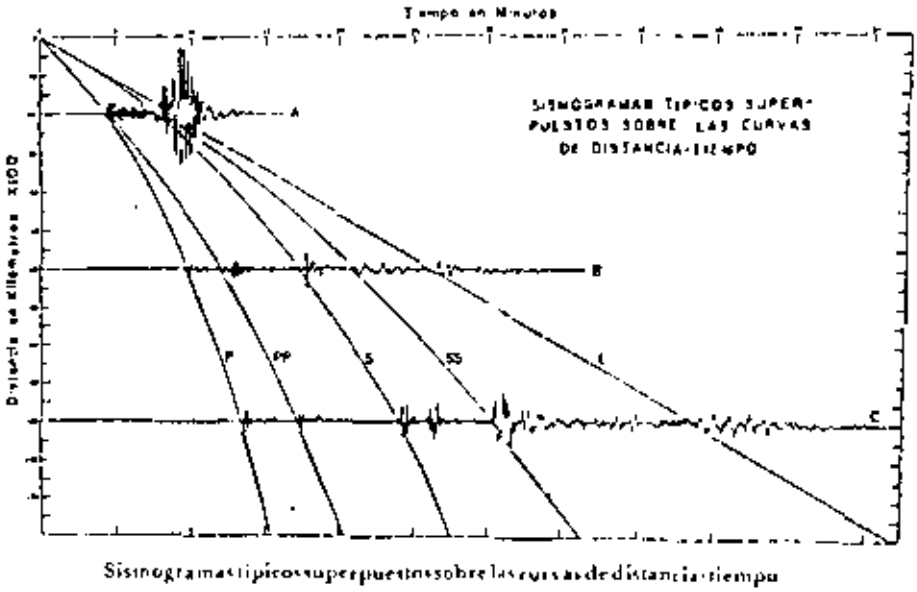

Sismogramas típicos superpuestos sobre las curvas de distancia-tiempo

Fig. 19

Si se grafican los valores del logaritmo de la amplitud de la traza contra la distancia, se obtienen gráficas como las mostradas en la Fig. 20. En esa misma figura, la curva más baja representa un temblor más pequeño. Resulta entonces lógico tomar cualquiera de estos sismos como el sismo patrón

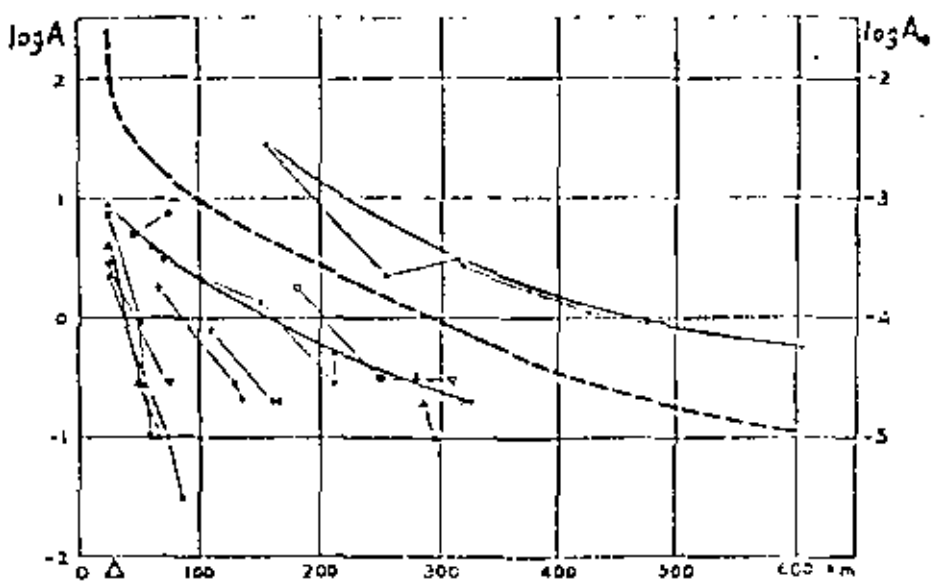

Fig. 20

y asignarle la magnitud cero, los demás pueden ser medidos a partir de éste midiendo la separación entre ellos para cualquier distancia del epicentro. Se tiene entonces que:

$$M = \log a - \log A_o$$

El temblor patrón, de magnitud cero se define como aquel que teniendo su epicentro a 100 km de distancia deja una traza de una micra en un sismógrafo Wood-Anderson elegido también como sismógrafo patrón.

Se tiene ahora una fórmula que nos proporciona un valor relacionado con el "tamaño" del sismo e independiente de los daños que pueda ocasionar. Este mismo valor ha sido relacionado por los sismólogos con la energía liberada por el sismo. Existen diferentes fórmulas que relacionan la energía con la magnitud de un sismo, éstas varían porque la amplitud medida en el sismograma puede ser la de cualquiera de las distancias fases (P, S, superficiales) que son registradas.

Un temblor de magnitud 5.5 libera una energía del orden de magnitud de la de una explosión atómica*, es decir unos 10^{20} ergs. Sin embargo, la energía de un sismo de magnitud 8.5 no es tres veces esa energía sino la equivalente a la de unas 27,000 de estas bombas atómicas, ésto es, la energía aumenta aproximadamente 30 veces por cada grado. Esto puede verse más claramente en las fórmulas que relacionan magnitud y energía; éstas son de la forma:

$$\log E = a + bM$$

donde a y b dependen de la forma en que es calculada M.
Notemos que la escala de magnitud no tiene límites; sin embargo, no se han

* como la de Hiroshima (20 Ktn de TNT).

encontrado temblores mayores de 8.6. Esto está relacionado con el hecho de que la corteza tiene un límite de ruptura más allá del cual ya no pueden acumularse más esfuerzos. Un ejemplo de un temblor de esta magnitud es el de Alaska del 28 de marzo de 1964.

Notemos también que pueden existir temblores de magnitud negativa, puesto que el sismo patrón (de magnitud cero), es elegido, hasta cierto punto arbitrariamente.

La determinación de magnitudes ha sido mejorada en las últimas décadas utilizando la disponibilidad de más información y modelos teóricos. Sin embargo el principio básico es el mismo.

En el Apéndice C se detallan algunos de los sismos mexicanos más destructivos.

LA CONSTITUCION DE LA TIERRA.

En el primer apartado de este artículo se consideró la estructura de la tierra. ¿Cómo fue posible conocerla si las perforaciones más profundas no alcanzan sino unos pocos kilómetros?. La respuesta está nuevamente en la Sismología.

De igual manera que un médico puede saber si existe fractura en los huesos de un accidentado por medio de rayos X, el sismólogo ha deducido la estructura de la tierra por medio de las ondas sísmicas que viajan a través de ella como los rayos X a través del cuerpo humano.

Supongamos que ocurre un sismo en un punto dado si la tierra fuera completamente homogénea los rayos viajarían en líneas rectas del foco al observador

(Fig. 21a).

Los sismogramas observados serían relativamente simples. los científicos han hallado que los rayos no viajan en línea recta sino que van curvándose hacia la superficie debido a que la velocidad de las ondas aumenta con la profundidad. (Ver Fig. 21b). Además de ésto se encuentra que éstas sufren refracciones y reflecciones que sólo pueden explicarse si la tierra está compuesta por las diferentes regiones de que se habló en el primer apartado. Los temblores resultan entonces, tener un aspecto positivo y es éste el de darnos a conocer el interior de nuestro planeta.

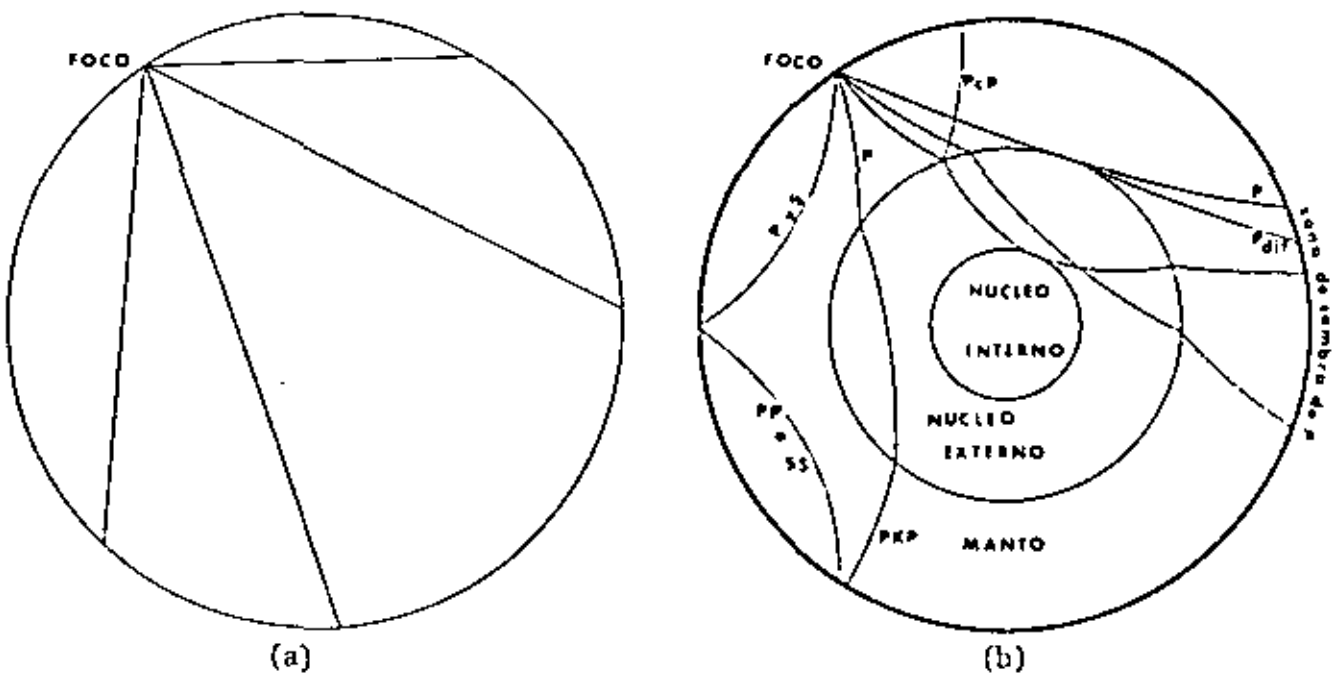

Fig. 21

SISMICIDAD

En los últimos 80 años se han podido registrar todos los temblores más importantes (en cuanto a energía) de manera que se han podido hacer estudios cualitativos de la sismicidad de la tierra, así se ha obtenido un esquema

global de la sismicidad mundial. El mapa de la Figura 22 muestra la distribución geográfica de sismos. Se puede observar que la mayor parte de energía sísmica se libera en las costas del Océano Pacífico región que se conoce como cinturón de fuego debido a que en esta zona ocurre también gran actividad volcánica. Hay otras regiones, como el Atlántico medio y el cintu-

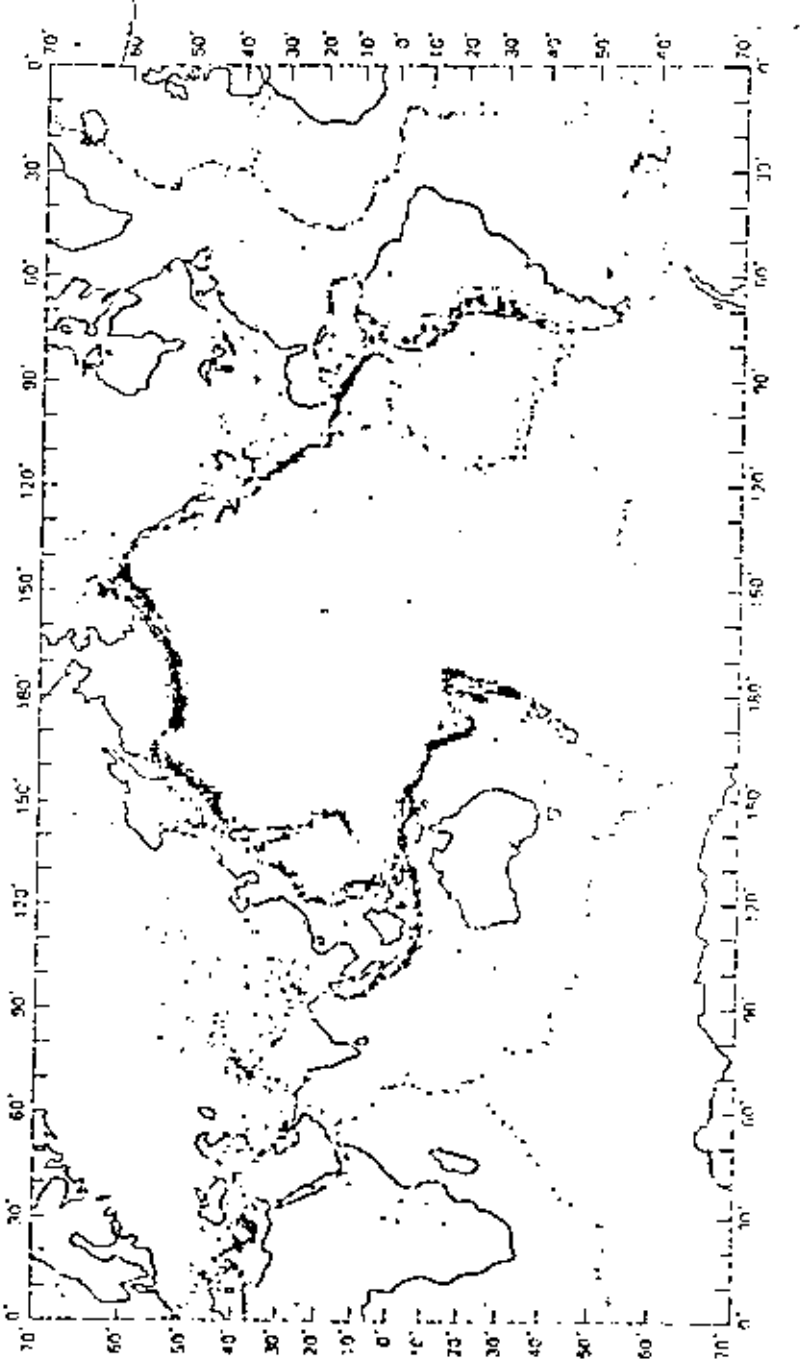

Fig. 22

rón Eurásico pero con una actividad sísmica menor. Nótese que estas franjas coinciden con los límites de placas de la Figura 3. Existen también regiones donde la actividad sísmica es casi nula o desconocida. A estas regiones se les suele llamar escudos. Desde luego que los países que se sitúan en zonas sísmicas serán más afectados por los sismos.

SISMICIDAD GLOBAL.

Observando la actividad sísmica mundial se puede estimar el número de temblores de cierta magnitud que ocurren en un año. Se ha visto que por lo menos ocurren dos grandes terremotos actualmente (ver Tabla II). Por otra parte están ocurriendo varios cientos de miles de temblores de magnitud inferior a 3 que pasan desapercibidos.

TABLA II
PROMEDIO ANUAL DE TEMBLORES

MAGNITUD	NUMERO PROMEDIO
8	2
7	20
6	100
5	3000
4	15000
3	150000

SISMICIDAD DE MEXICO

A fines del siglo pasado se conocía la historia acerca de la actividad sísmica de México desde 1400. Posteriormente con el desarrollo técnico sismológico hacia 1910 se inauguró la red sismológica mexicana (ver apéndice A). De esa fecha a la actualidad se han generado sismogramas que se conservan

en el Servicio Sismológico, en la estación Sismológica de Tacubaya.

Durante los últimos 70 años se han registrado y localizado, utilizando los datos de la red sismológica mexicana, sismos ocurridos en la República Mexicana hecho por el cual actualmente se conoce bastante bien la sismicidad de México (Fig. 23).

PREMONITORES Y REPLICAS

Los sismólogos han observado que inmediatamente después de que ocurre un gran temblor, éste es seguido por temblores de menor magnitud llamados réplicas y que ocurren en las vecindades del foco del temblor principal. Se piensa que la ocurrencia de éstos se debe probablemente al reajuste mecánico de la región afectada. Inicialmente la frecuencia de ocurrencia es grande pero decae gradualmente con el tiempo dependiendo de la magnitud del Temblor principal. Por ejemplo para el temblor de Oaxaca del 29 de noviembre de 1978 de magnitud 6.8 inicialmente se observaron hasta 200 réplicas de magnitud mayor que 2.0 diariamente y fue decayendo esta actividad durante 5 meses aproximadamente. El estudio de las réplicas de un gran temblor se ha aprovechado para estimar las dimensiones de la región focal.

Frecuentemente algunos temblores grandes son precedidos por temblores de menor magnitud llamados temblores premonitores que comienzan a fracturar la región focal del gran temblor. No es fácil determinar cuando un temblor queño es un premonitor de un gran temblor ya que se suele confundir con cualquier otro no relacionado. En la generalidad de los casos se sabe que un temblor es premonitor sólo en el contexto de la actividad posterior.

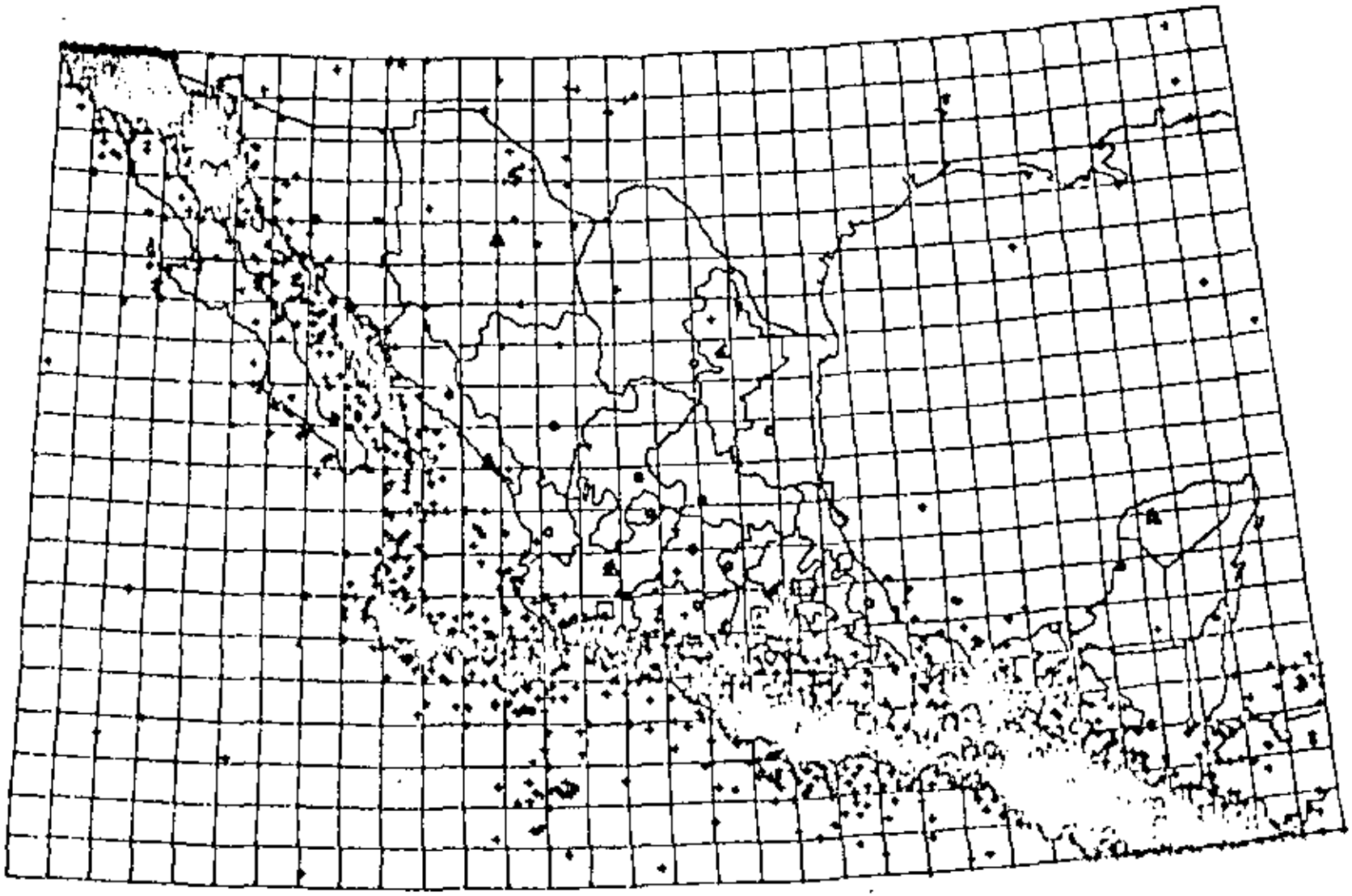

Fig. 23 Sismicidad de México, de 1900 a 1974.

PREDICCION

¿Se pueden predecir los temblores? La respuesta a esta pregunta depende de lo que se entienda por predicción. Año tras año podemos leer en los periódicos las declaraciones hechas por adivinadores, mediums y otras gentes por el estilo, sobre la futura ocurrencia de temblores en algún lugar del planeta. Estas declaraciones distan mucho de ser predicciones. Se ha visto (Tabla II)que en promedio ocurren cerca de 120 temblores de magnitud mayor a 6 anualmente. Se conocen también las zonas sísmicas del planeta, de manera que por ejemplo el afirmar que durante el año de 1981 ocurrirá un temblor en la costa occidental de México no contiene información novedosa ni útil.

En la última década el desarrollo de la sismología ha llevado a los sismólogos a la convicción de que éstos pueden ser predichos. La investigación en este aspecto es relativamente nueva a pesar de la cual se han logrado resultados prometedores.

Existen esencialmente dos maneras de atacar el problema. En una de ellas se estudia la variación de ciertos parámetros físicos debido a la acumulación de los esfuerzos cuya relajación ocasiona el temblor. Así por ejemplo, se ha observado que la región focal sufre una dilatación que altera la velocidad de las ondas que se propagan en ella. Otros de los parámetros que se alteran son por ejemplo resistencia del terreno al paso de corriente eléctrica y el nivel freático. Todos estos factores pueden ser medidos y correlacionados con la ocurrencia final del temblor.

En otra de las formas de enfrentar el problema se ha estudiado la sistematicidad en la ocurrencia de los temblores. Se ha observado que los epicentros a lo largo de una zona de subducción no se distribuyen al azar sino siguiendo un patrón geográfico y temporal. Puede entonces estudiarse la his-

toria sísmica de una región, estimar los períodos de recurrencia de temblores de cierta magnitud y evaluar de esta manera la posibilidad de ocurrencia de un temblor.

Este breve bosquejo trata solamente de poner de manifiesto que los sismólogos actuales se encuentran trabajando sobre bases científicas para la futura predicción de temblores. Cuanto tiempo tomará el desarrollar un sistema eficiente para predecir temblores es difícil de precisar pero seguramente será de algunas décadas. Indudablemente ésto requerirá del desarrollo de nuevas metodologías tanto teóricas como instrumentales.

¿QUE HACER CUANDO OCURRE UN TEMBLOR?

Existen varias medidas que deben tomarse en caso de ocurrir un temblor, pero ante la eminencia de un suceso de esta naturaleza, en regiones sísmicamente activas es mejor prepararse mentalmente para una eventualidad. Por otra parte conviene buscar las condiciones adecuadas de seguridad de los sitios donde se permanece más tiempo como son: la casa, el trabajo, la escuela, etcétera.

La seguridad de las casas en caso de temblores se garantiza construyendo a éstas según los códigos de construcción antisísmica de la región, si en los centros de trabajo se observa poca seguridad en las instalaciones pedir que sean reforzadas. En México las escuelas, y en general, obras civiles son construidas tomando en cuenta el código de construcción pero si se observa alguna anomalía conviene reportarlo a las autoridades competentes. Debe evitarse el colocar objetos pesados o peligrosos como lámparas, etcétera en repisas y lugares elevados a no ser que estén bien sujetos.

APENDICES

BIBLIOGRAFIA

Z. Jiménez (1979). Algunos aspectos relevantes de la interpretación de sismogramas. Ciencia y Desarrollo, No. 26.

I.P.G.H. (1979). Temblores de Tierra. Cartilla Popular publicación No. 363.

B. Bolt (19). Earthquakes. A primer. Freeman Publishing Co. San Fco. Calif.

M. Muñoz L. (1918). La Sismología en México hasta 1917. Instituto Geológico de México, Boletín No. 36.

J. Yamamoto (1980). Cronología de Terremotos: Historia del miedo. Comunidad CONACYT, No. 111, 1980.

APENDICE A.

HISTORIA DE LA SISMOLOGIA EN MEXICO.

La República Mexicana está situada en una de las regiones sísmicamente más activas del mundo como se puede apreciar en la Figura 24. El estudio de la actividad sísmica en México es relativamente reciente, sin embargo su observación tiene antecedentes remotos. Sabemos que los primeros pobladores de México se percataron de la actividad sísmica y volcánica en estas regiones y posiblemente hasta existieron personas dedicadas a estudiar estos fenómenos.

En la época de la colonia la descripción de los temblores la hicieron principalmente los monjes en algunos conventos y se encuentran anotadas en algunas obras de Clavijero y Sahagún. Con el uso generalizado de la imprenta se reportaban datos sismológicos en los periódicos de la época con descripciones a veces pintorescas y exageradas. Posteriormente los temblores eran observados por naturalistas, publicistas y por el público en general, pues en todos los folletos antiguos se encuentran notas sobre temblores, cuyas áreas se empezaban a delimitar a medida que las communicaciones se establecían entre pueblos.

Cuando se instaló la red telegráfica en la República Mexicana los telegrafistas suministraban datos referentes a temblores y se publicaban mensualmente en boletines.

La medición de los temblores por medio de instrumentos se inició a fines del siglo pasado, en la época de Mariano Bárcena, se instaló en el Observatorio Meteorológico Central un sismógrafo del Padre Sechi. Por ese tiempo Juan Orozco y Berra se dedicó a observar estos fenómenos y formar estadísti

cas, reuniendo importantes datos de temblores desde tiempos precolombianos, coleccionados con cuidado y publicados en la sociedad científica Antonio Alzate. Sin embargo es hasta el 5 de septiembre de 1910 que por Decreto Presidencial se crea e inaugura el Servicio Sismológico Nacional. Este evento se enmarcó dentro de los festejos conmemorativos del primer centenario de la iniciación de la Independencia Nacional. Dicho servicio dependía del Instituto Geológico Nacional.

La red inicial consistió del Observatorio Central de Tacubaya y estaciones ubicadas en Oaxaca, Mérida, Zacatecas, Mazatlán, Guadalajara y Monterrey. Se eligieron como sensores los sismógrafos Wiechert de período corto. Básicamente, estos sismógrafos con algunas modificaciones y mejoras continúan operando.

Hacia 1929, el Instituto Geológico Nacional pasó a ser el Instituto de Geología de la UNAM y el Servicio Sismológico formó parte de este nuevo Instituto. En 1949 con la creación del Instituto de Geofísica, el Servicio Sismológico pasó a formar parte de este Instituto.

El Servicio Sismológico vuelve a cobrar vida hacia 1965-1967 cuando se instalaron estaciones de mayor sensibilidad en Tehuantepec PRJ), Vista Hermosa (VHO), Comitán (CCM), Toluca (OXM), León (LCG), Presa Infiernillo (PIM), Presa Mal Paso (PMM), Ciudad Universitaria (UNM), Tepostlán (TPM) y Popocatépetl (PPM). También se instaló por 1970 una red de estaciones en el Noroeste, con el fin de observar la actividad sísmica del Golfo de California. Este conjunto de estaciones ahora es controlado por el Centro de Investigaciones y de Educación Superior de Ensenada, Baja California (CICESE).

Actualmente el Servicio Sismológico cuenta con una red de 14 estaciones

TABLA II

Fecha	Magnitud Richter Mb	Ms	Región	No. de Muertos	Datos generales
1, junio 7	7		Jalisco-Colima	45	Destructor en Cd. Guzmán Jal., ha sido uno de los temblores más fuertes que han ocurrido los últimos 100 años. Se reportaron 45 muertos en el D.F.
1[illegible]7, julio 16	?		Oaxaca-Puebla	?	Grandes daños en Esperanza, Puebla
1[illegible]3, julio 29	7.8		Guerrero: San Marcos	55	Miles de heridos y daños materiales en varios estados. La población más dañada fue San Marcos, Gro.
1[illegible]8, agosto 2	6.3	7.1	Oaxaca: Pinotepa	?	Se estima que hubo varios muertos y miles de heridos. Grandes daños materiales en Pinotepa.
1[illegible], enero 30	6.2	7.5	Colima	50	300 heridos y 30 poblaciones afectadas severamente.
1[illegible]1, agosto 28	6.8		Oaxaca-Puebla	600	Miles de heridos y damnificados. Cd. Serdán destruída: daños considerables en las ciudades de Puebla, Orizaba, Oaxaca y México. 77 pueblos dañados seriamente.
1[illegible], noviembre 28	6.8		Oaxaca	?	Daños en Jamiche, Oaxaca. Es aquí el temblor que más se ha estudiado en México.
1[illegible], octubre 24	6.5		Oaxaca: Huajuapan	50	Fuertes daños en la región fronteriza de los estados de Puebla, Oaxaca y Guerrero. Principalmente en Huajuapan de León, Oax.

LOS SIGUIENTES ANEXOS DAN INFORMACION ADICIONAL

SOBRE LOS TEMAS TRATADOS

Deriva Continental. Esparcimiento del Fondo Marino. Tectónica de Placas

A principios de siglo el geofísico alemán Alfredo Wegener propuso la teoría conocida como Deriva Continental, en la que se supone que las masas continentales han sufrido largos desplazamientos horizontales que determinaron la posición y distribución actual de tierras y mares.

Wegener se basó fundamentalmente en la concordancia de algunas líneas de costa, como las de América del Sur y Africa (figura 1); en datos paleoclimáticos y paleontológicos y en la distribución de las cadenas montañosas. Propuso la existencia de un gran continente primario al cual llamó Pangea que en el transcurso de las edades geológicas se fracturó y sus partes navegaron sobre la capa basáltica del piso marino, hasta ocupar diferentes posiciones.

Otros investigadores anteriores ya habían avanzado en la idea de movimientos continentales; sin embargo Wegener en 1912 presentó una considerable cantidad de evidencias y una descripción de las posiciones de los continentes en las diferentes épocas.

La teoría pronto encontró un gran número de objeciones, principalmente por el mecanismo propuesto para explicar el desplazamiento de los continentes así como por la similitud de edades de los océanos, y la existencia de los cratones continentales y de regiones de lentos levantamientos y sub-

sidencias entre otras. Pronto la teoría cayó en desuso.

Con el advenimiento de la Segunda Guerra Mundial las técnicas e instrumentos para la exploración marina experimentaron un fuerte avance, principalmente en los sistemas de navegación así como de registro del fondo, lo que fomentó la investigación de los océanos.

En la década de los cincuenta, las investigaciones oceanográficas se incrementaron enormemente. Se hicieron mediciones de gravimetría, de magnetometría, de flujo de calor de sismología de refracción y reflexión y se tomaron muestras de sedimentos del fondo oceánico. Todos estos estudios aportaron información novedosa cuya interpretación hizo necesaria la revisión cuidadosa de la hipótesis de Wegener.

Dietz en 1961 y Hess en 1962 propusieron la teoría llamada de Esparcimiento del Fondo Oceánico, para explicar sus observaciones sobre el lecho marino. En esta teoría se considera a las dorsales oceánicas como centros generadores de material nuevo proveniente del manto y trasladado a la superficie por corrientes de convección.

La idea general asume que el valle medio de una dorsal oceánica representa una fisura, la cual se rellena por material del manto, probablemente peridotita, que al enfriarse bajo los 500 °C sufre un proceso de serpentinización. Esto hace que disminuya la densidad de 3.3 a 2.6 gr/cm^3 y aumente su volumen, lo que provoca la elevación de las montañas que rodean al valle. Este proceso también justifica el espesor

casi uniforme de la corteza oceánica reportado por los estudios sísmicos (Figura 2).

La teoría explica además, la falta de sedimentos antiguos anteriores al Cretácico, los espesores inferiores a 1.3 Km, la distribución de edades (mayores al aproximarse a los continentes) la forma y localización de los guyots (mesetas submarinas, algunas de ellas situadas a gran profundidad), la ausencia de la discontinuidad de Mohorovicic bajo las dorsales y el elevado flujo térmico sobre ellas, y explica la presencia de las fosas profundas en algunas márgenes continentales como zonas en donde el piso oceánico retorna al manto.

La interpretación de las anomalías magnéticas de Campo Total tomadas sobre las cordilleras submarinas empleando las inversiones de polaridad del Campo Geomagnético hecha por Vine y Mattews en 1963, proporcionó un fuerte apoyo a la teoría.

Los años siguientes fueron de intensa actividad y descubrimientos. En 1968 Isacks Oliver y Sykes publicaron un artículo ahora clásico, "Seismology and the New Global Tectonics", en el que se sintetizan la mayoría de las ideas que integran lo que es conocido como Tectónica de Placas o Nueva Tectónica Global.

Brevemente, la teoría considera que la tierra posee un casquete externo rígido de unos 100 Km de espesor. Este casquete no es continuo sino que está dividido en varios segmentos (Figura 3) con movimientos relativos entre sí.

Los movimientos a que están somedidas las placas producen en algunos de sus márgenes la subducción de una de ellas bajo la otra, mientras que en otros márgenes se produce la creación de nueva corteza. (Figura 2).

Aunque el origen de los esfuerzos que producen estos movimientos no es bien comprendido es muy posible que sean debido a la transferencia convectiva de calor hacia la superficie. Cualquiera que sea el mecanismo que produce el desplazamiento, el contacto entre las placas es zona de acumulación de esfuerzos y el lugar donde se libera la mayoría de la energía de la superficie terrestre. En la figura 4 puede verse que las zonas sísmica y volcánicamente activas definen los márgenes de las placas. Nótese también que los límites de las placas no necesariamente coinciden con las fronteras océano-continente.

La distribución de hipocentros en un corte transversal a través de una zona de subducción puede verse en la figura 5. La región definida por los focos es llamada zona de Wadati Bennioff en honor a los investigadores que describieron esta relación geométrica en los años 40.

Figura 1.

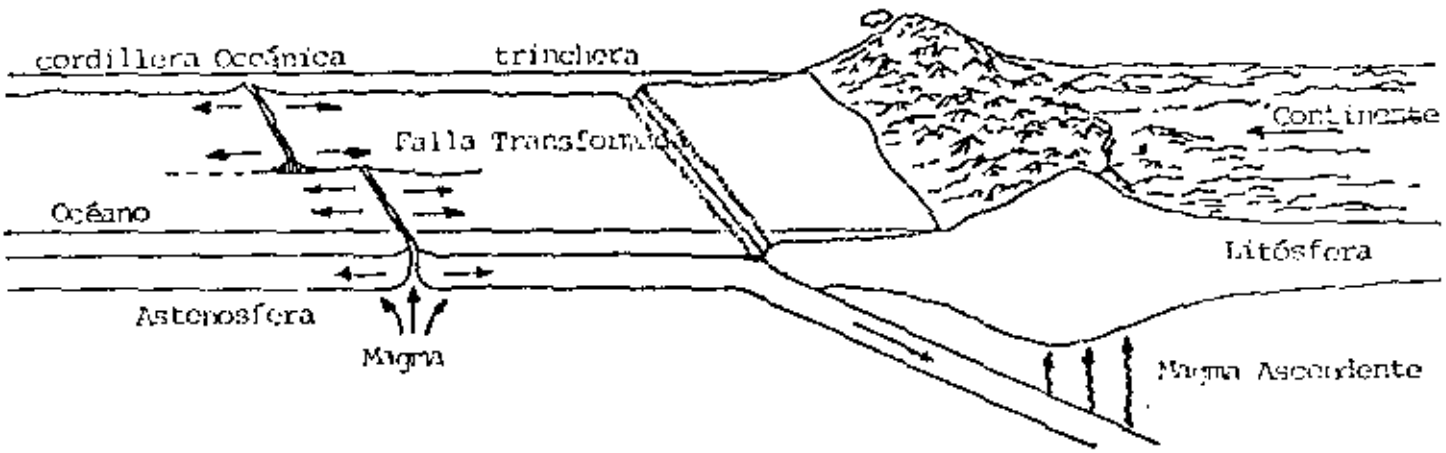
cordillera Oceánica
trinchera
Falla Transformada
Continente
Océano
Litósfera
Astenosfera
Magma
Magma Ascendente

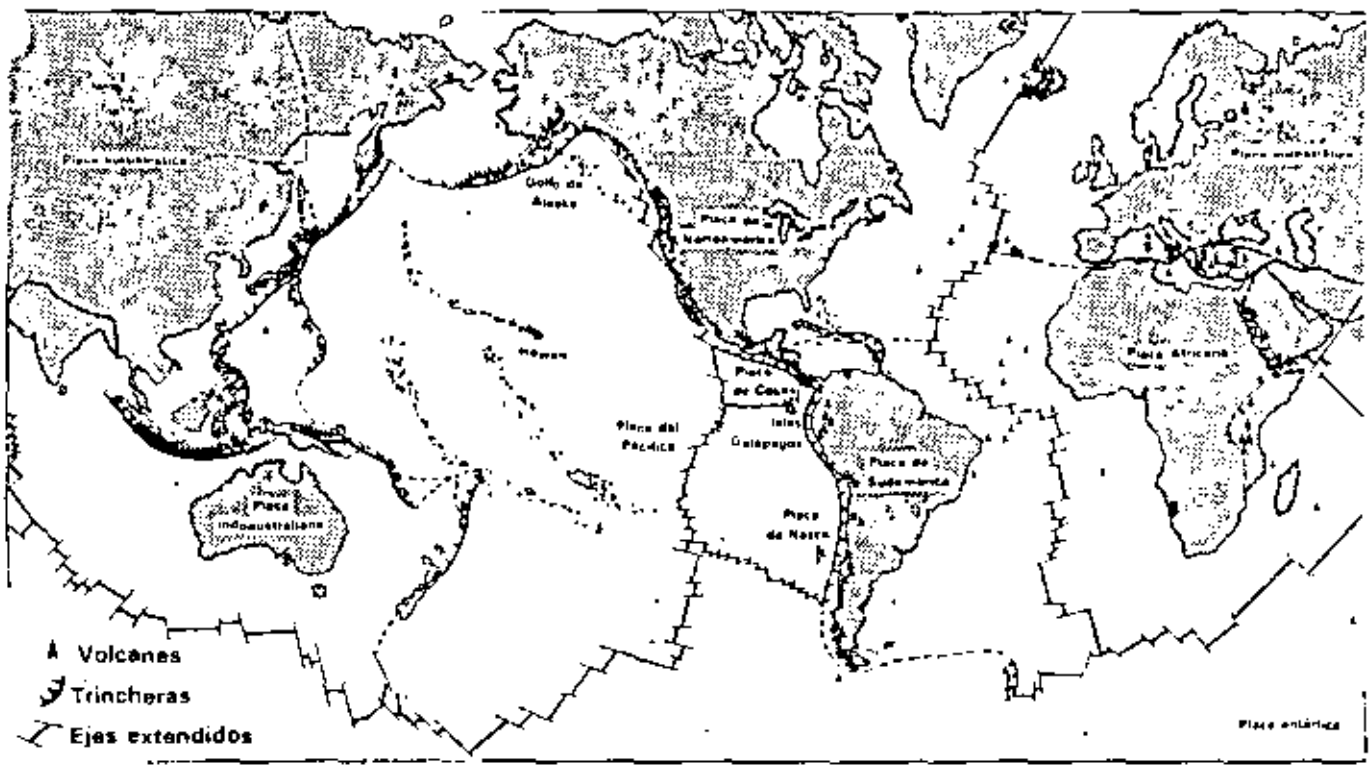

Figura 3.

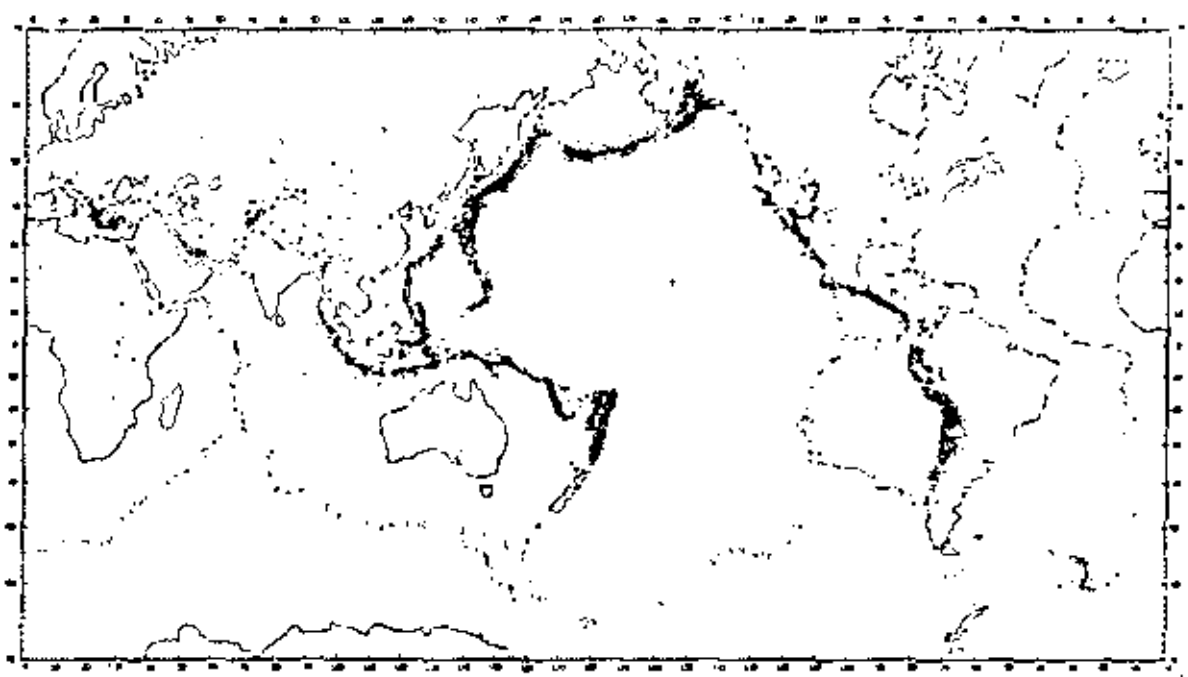

Algunos de los acontecimientos más importantes en el desarrollo de la Tectónica de Placas.

1620	Se notó la concordancia entre las líneas de costa de Africa y América del Sur. (Bacon)
1839	Ideas de convección térmica en el manto (Hopkins).
1855	Teoría isostática (Airy).
1858	Mapa mostrando el movimiento de los continentes - (Snider).
1859	Teoría isostática (Pratt).
1889	Concepto de la astenósfera (Fisher).
1906	Primeras evidencias de inversiones del Campo Magnético terrestre (Brunhes).
1910	Teoría de movimientos continentales (Taylor).
1912	Teoría de Deriva Continental (Wegener).
1914	Concepto de la astenósfera (Barrel).
1923 Zo- 28	Nuevo método de análisis de temblores, llamado de mecanismos focales o plano de falla (Nakano y - Byerly).
1926	Concepto de la astenósfera (Gutenberg).
1929	Establecimiento de una época de polaridad inversa magnética en el Pleistoceno (Matuyama).
1939	Celdas de Convección en el manto (Griggs).
1940	Determinaciones de edades radiométricas K-Ar (Evans).
1944	Mecanismos de deriva continental (Holmes).
1946	Descubrimiento de los guyots en el Océano Pacífico. (Hess).
1949	Descubrimiento de las zonas de Benioff (Benioff).
1950	Estudios de las cordilleras submarinas (Instituto Scripps).
	Comienzo de las mediciones de flujo térmico en el mar (Bullard).
	Empleo de los magnetómetros de Campo total en estudios marinos (Instituto Scripps).
1952	Descubrimiento de las zonas de fractura en el - Océano Pacífico (Menard y Dietz).
1955	Investigaciones teóricas del origen del Campo Magnético (Bullard y Elsasser).
	Ideas de fuentes térmicas "Hot spots" (Wilson).
1956	Descubrimiento del valle medio de las dorsales y reconocimiento de los temblores que en ellos ocurren (Ewing y Haten).
	Demostración de la Deriva Continental con datos Paleomagnéticos (Irving y Runcorn).
1957	Levantamiento marino con gravímetro de superficie.
1957	Año Geofísico Internacional
1958	Reconocimiento de lineamientos magnéticos sobre las dorsales (Mason). Confirmado por Vacquir, 1961 y Mason y Raff 1961.

1960 Primeras perforaciones del proyecto Mohole.

1961-1962 Hipótesis de esparcimiento de los fondos marinos (Hess).

1963 Interpretación de los lineamientos magnéticos empleando las ideas de inversiones del Campo Geomagnético y de esparcimiento de los fondos marinos (Vine y Matthews; Morley).

Primera escala de tiempo cuantitativa de inversiones del Campo Geomagnético usando edades de K.Ar (Cox).

1960-70 Proyecto Internacional del Manto Superior bajo la dirección del profesor V.V. Beloussov.

1965 Concepto de fallas transformadas (Wilson).

1967-69 Modelo de una litósfera capaz de soportar tensiones como mecanismo de hundimiento en las trincheras (Elsasser).

1967 Conceptos e implicaciones geométricas de las placas (Mc Kenzie y Parker).

1968 Estudios sobre las placas y sus límites (Morgan).

Nueva Tectónica global (Isacks).

1969 Concepto de juntas triples (Mc Kenzie y Morgan).

Relaciones entre la edad, la elevación topográfica y el flujo térmico en los fondos oceánicos -- (Selater y Franchetau).

1964 Programas del JOIDES (Muestreo de la tierra profunda)

Información del proyecto de perforación en mar profundo (Deep sea drilling Project) dentro de los programas del JOIDES (From Oceanographic Institutions Deep Earth Sampling).

1970 Proyecto Internacional Geodinámica. Con la participación del Grupo de Trabajo No. 2, Grupo de Estudio No. 2, Placa de Cocos, Comité Mexicano de Geodinámica.

1970 Proyecto CICAR (Cooperative Investigations of the Caribbean and Adjacent Regions). Participación de México.

1971 Proyecto IDOE (International Decade Oceanographic Exploration). Participación de México.

Predicción de Temblores

Como hemos visto, la mayoría de los temblores ocurren en los márgenes de las placas como respuesta a la acumulación de esfuerzos en esas áreas. Los esfuerzos son debidos al movimiento relativo entre placas. Este movimiento, que es del orden de algunos centímetros por año no cambia en plazos cortos de tiempo (geológicamente hablando) por consiguiente es posible estudiar los márgenes sísmicamente activos en términos estadísticos.

Los períodos de recurrencia de los temblores grandes ($M \geq 7.0$) son altamente variables (30 - 100 años) por lo tanto es necesario contar con un record histórico tan completo como sea posible.

Si el período de recurrencia es conocido, la probabilidad de ocurrencia de un temblor es proporcional al tiempo transcurrido desde el último. Este último aspecto nos lleva a lo que se ha definido como tramo de quietud sísmica a falta de una mejor traducción del inglés "seismic gap".

El concepto anterior fue originalmente desarrollado por Fedotov y Mogi y posteriormente por Sykes y Kelleher y colaboradores*. Estos últimos autores* publicaron un mapa de "gaps sísmicos" para el cinturón del Pacífico.

* Kelleher et al. (1973). Journal of Geophysical research.

El mapa ha sido revisado recientemente por Mc Cann y colaboradores*. Las siguientes figuras son mapas de "gaps sísmicos" para Mesoamérica, Sudamérica y el Caribe.

Este tipo de mapas es muy útil no sólo para evaluar el riesgo sísmico sino también como parte de un programa de predicción a largo plazo. Una vez que una región es reconocida como "gap", pueden utilizarse técnicas para determinar cambios físicos asociados con la acumulación de esfuerzos.

Los cambios físicos observados se relacionan al aumento de volumen, previo al temblor, llamado dilatancia. Asociado a la dilatancia se encuentran el cambio en la velocidad de las ondas P y S, el aumento de la resistividad eléctrica, el cambio en el campo magnético y el aumento de gas radón en pozos cercanos así como cambios en temperatura y nivel de los fluidos en los mismos.

Para explicar la dilatancia se desarrollaron dos modelos que han sido llamados el modelo americano y el modelo ruso. Ambos coinciden en las fases iniciales pero divergen en la descripción del episodio final. Quizá la situación real sea una combinación de ambos.

* Mc Cann et al. (1979). JGR

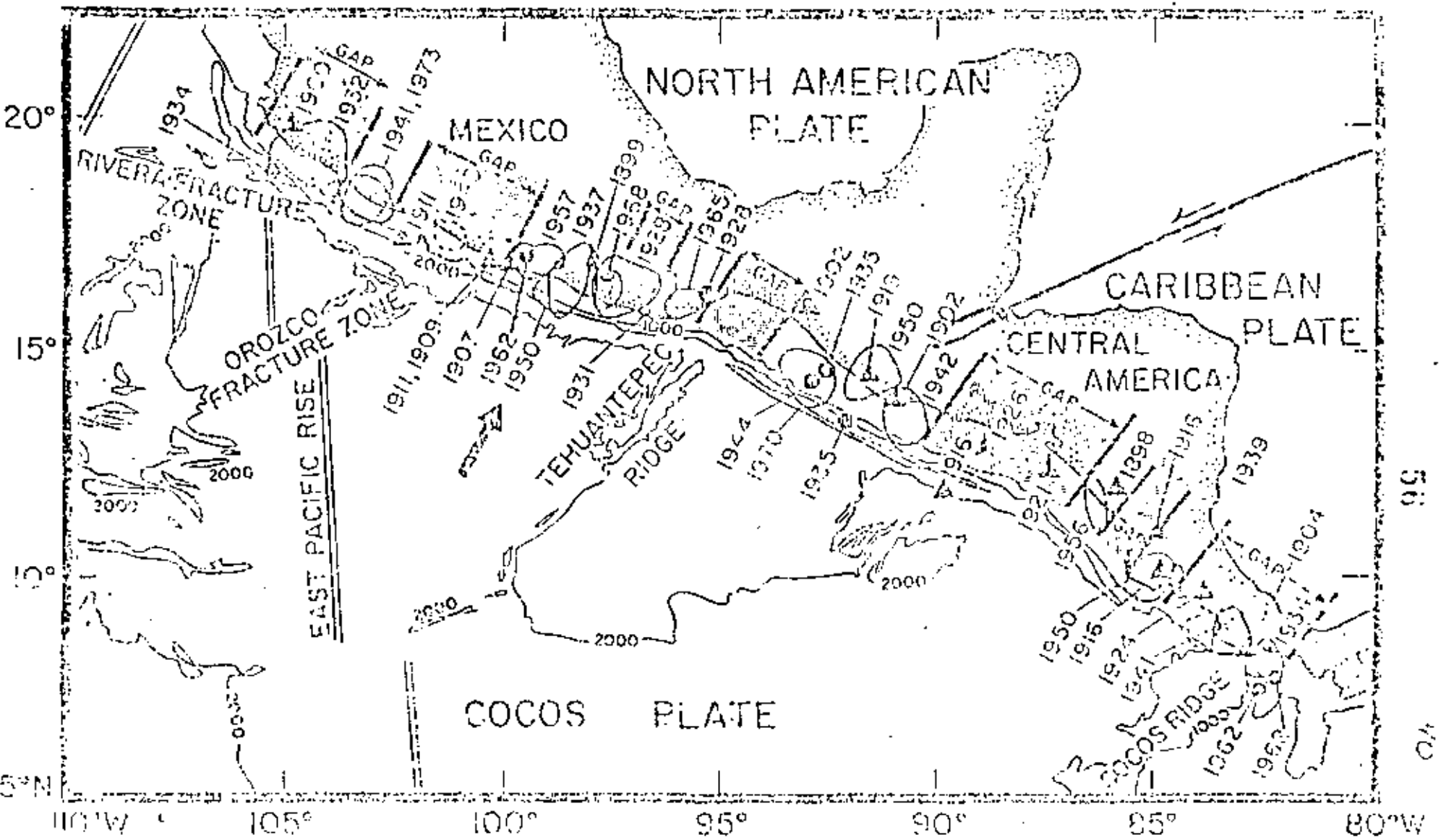
NORTH AMERICAN PLATE
MEXICO
CARIBBEAN PLATE
CENTRAL AMERICA
COCOS PLATE
COCOS RIDGE
RIVERA FRACTURE ZONE
OROZCO FRACTURE ZONE
EAST PACIFIC RISE
TEHUANTEPEC RIDGE
GAP
2000
3000
20°
15°
10°
5°N
110°W
105°
100°
95°
90°
85°
80°W

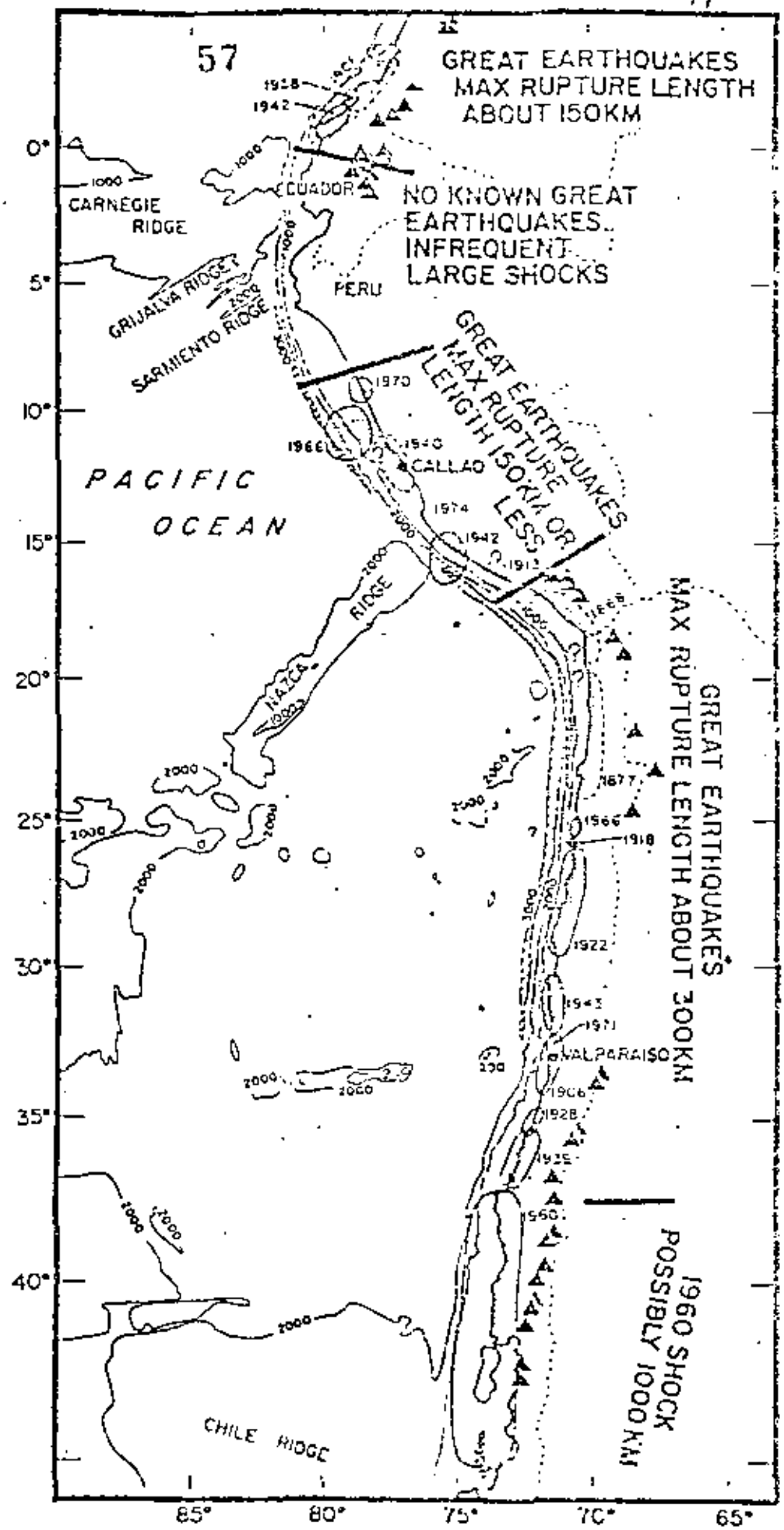
57
GREAT EARTHQUAKES
MAX RUPTURE LENGTH
ABOUT 150KM
NO KNOWN GREAT
EARTHQUAKES..
INFREQUENT
LARGE SHOCKS
GREAT EARTHQUAKES
MAX RUPTURE
LENGTH 150KM OR
LESS
GREAT EARTHQUAKES
MAX RUPTURE LENGTH ABOUT 300KM
1960 SHOCK
POSSIBLY 1000 KM
PACIFIC
OCEAN
ECUADOR
PERU
CARNEGIE
RIDGE
GRIJALVA RIDGE
SARMIENTO RIDGE
NAZCA
RIDGE
CHILE RIDGE
CALLAO
VALPARAISO
1958
1942
1970
1966
1940
1974
1942
1913
1877
1966
1918
1922
1943
1971
1906
1928
1939
1960
0°
5°
10°
15°
20°
25°
30°
35°
40°
85°
80°
75°
70°
65°

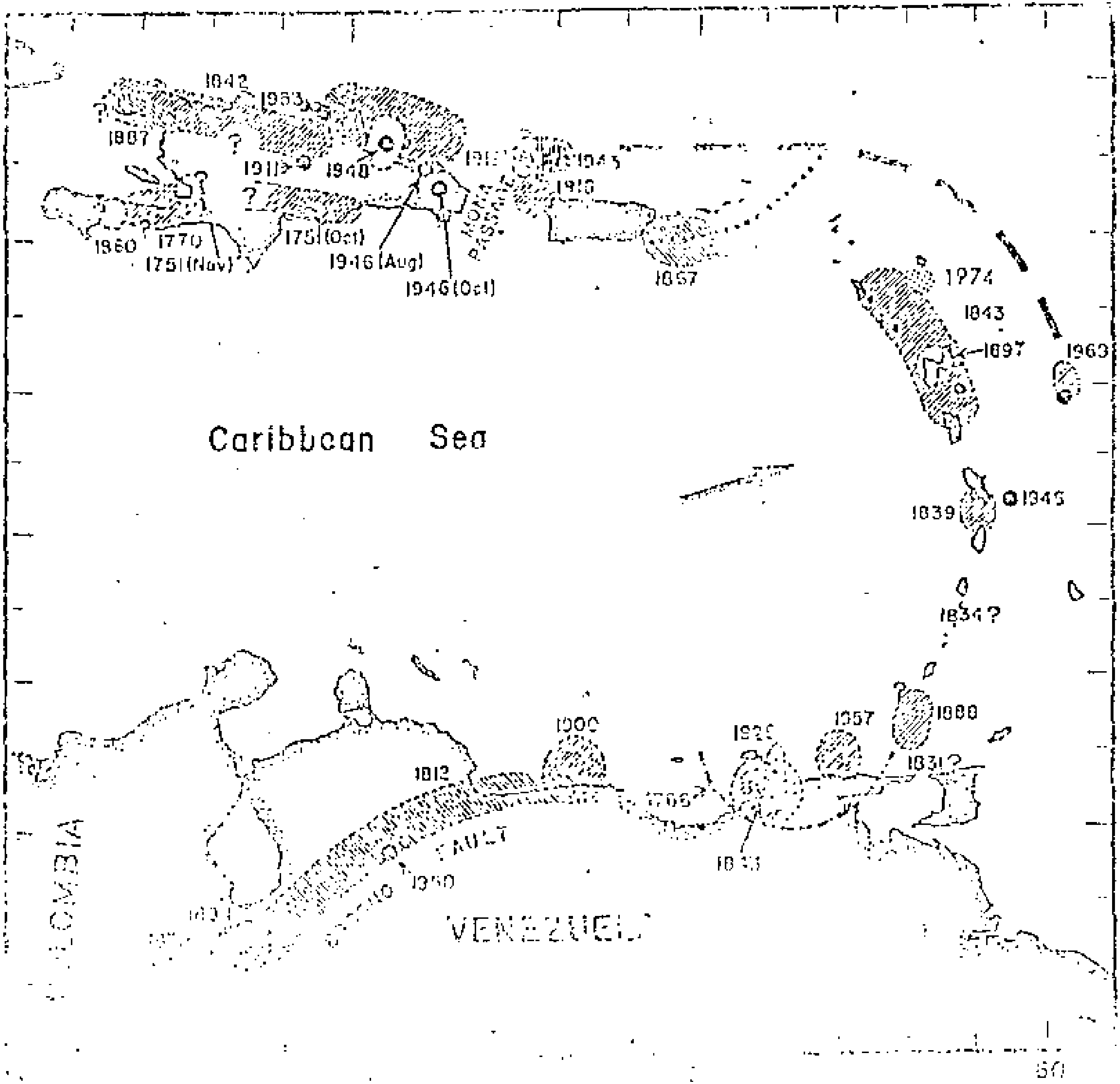

20
18
16
14
12
10
60
Caribbean Sea
1842
1953
1887
1911
1948
1946 (Aug)
1946 (Oct)
1860
1770
1751 (Nov)
1751 (Oct)
1943
1918
1867
1974
1843
1897
1963
1839
1845
1834?
1888
1957
1831?
1900
1812
1766
1950
FAULT

Ondas Sísmicas

Dentro de un cuerpo con constantes elásticas λ y μ y densidad ρ pueden viajar dos tipos de ondas llamadas "de cuerpo" o internas:

Longitudinales $Vp = \sqrt{\frac{\lambda + 2\mu}{\rho}}$ onda (de primus)

Transversales $Vs = \sqrt{\mu/\rho}$ onda s (de secundus pues arriba después de p)

En muchos casos $\lambda = \mu$ y $Vp = \sqrt{3}\ Vs$ (Sólido de Poisson)

En un sólido elástico estratificado con una superficie libre se generan además dos tipos de ondas superficiales:

Ondas de Rayleigh con velocidad C_R y ondas de Love con velocidad C_L; puede demostrarse que

$$C_R < 0.92\ Vs$$

$$V_{S_1} < C_L < V_{S_2}$$

donde V_{S_1} y V_{S_2} son las velocidades transversales de los dos estratos.

La velocidad de las ondas superficiales depende de la frecuencia y sufren por lo tanto dispersión. La dispersión i.e. la velocidad de grupo depende de la estructura interna del medio y por lo tanto su estudio puede utilizarse para inferir esta estructura.

Las fases arriba descritas quedan registradas en los sismogramas (dependiendo de la posición del instrumento con respecto a la fuente) sin embargo su estructura se complica pues también aparecen fases de ondas reflejadas y refractadas:

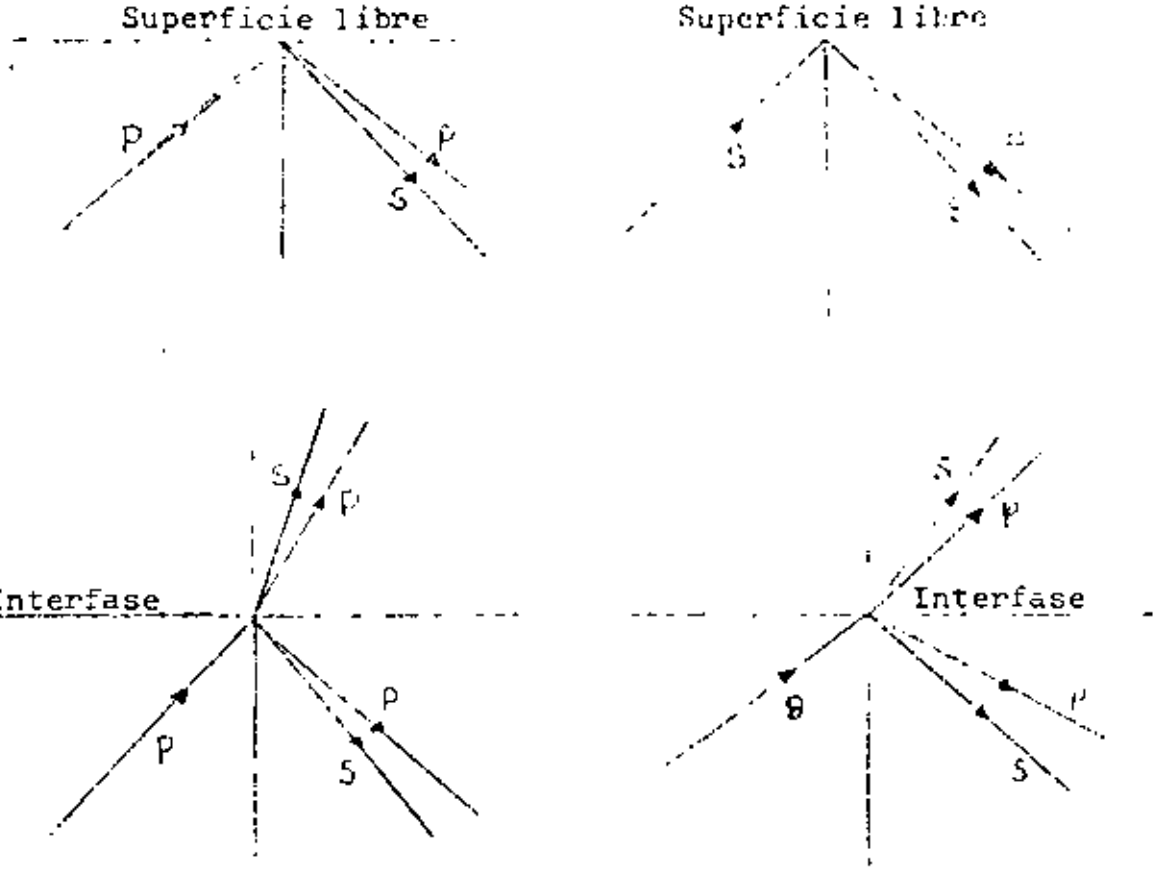

A escala global muchas de estas fases correspondientes a reflexiones y refracciones en el interior del planeta pueden ser identificadas; a continuación pueden verse las trayectorias de algunas de estas ondas y su nomenclatura, así como su distribución de velocidades con la profundidad.

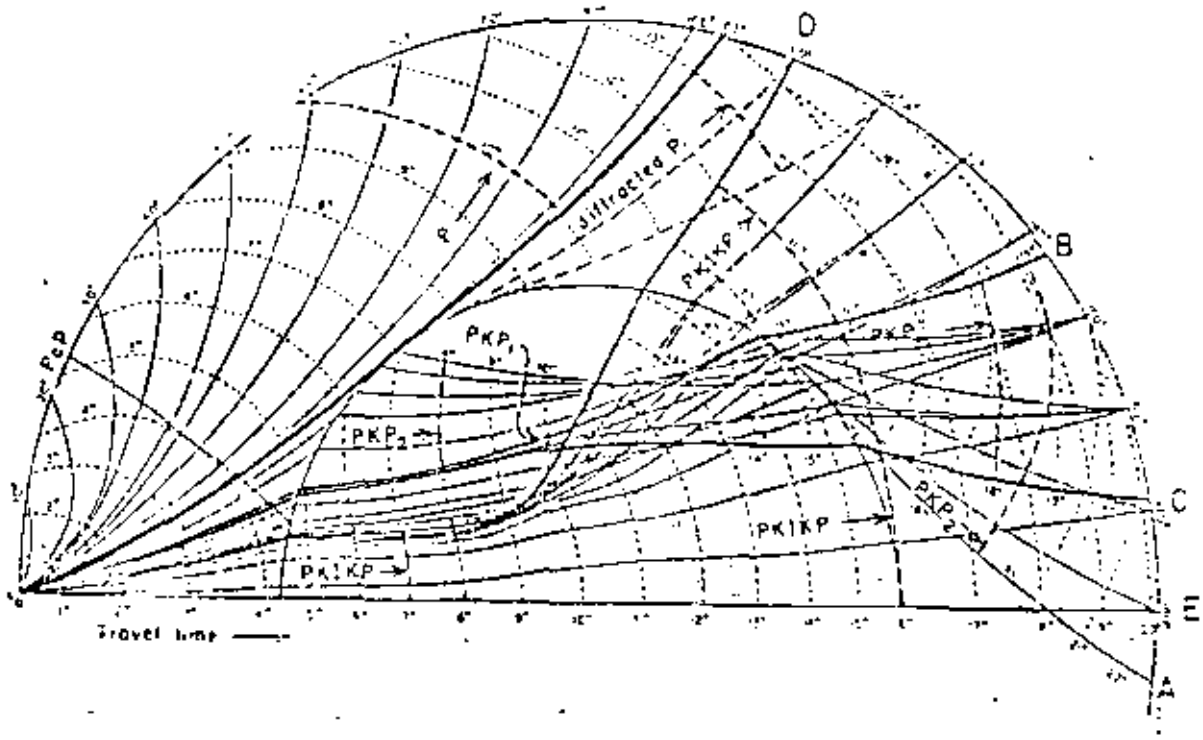

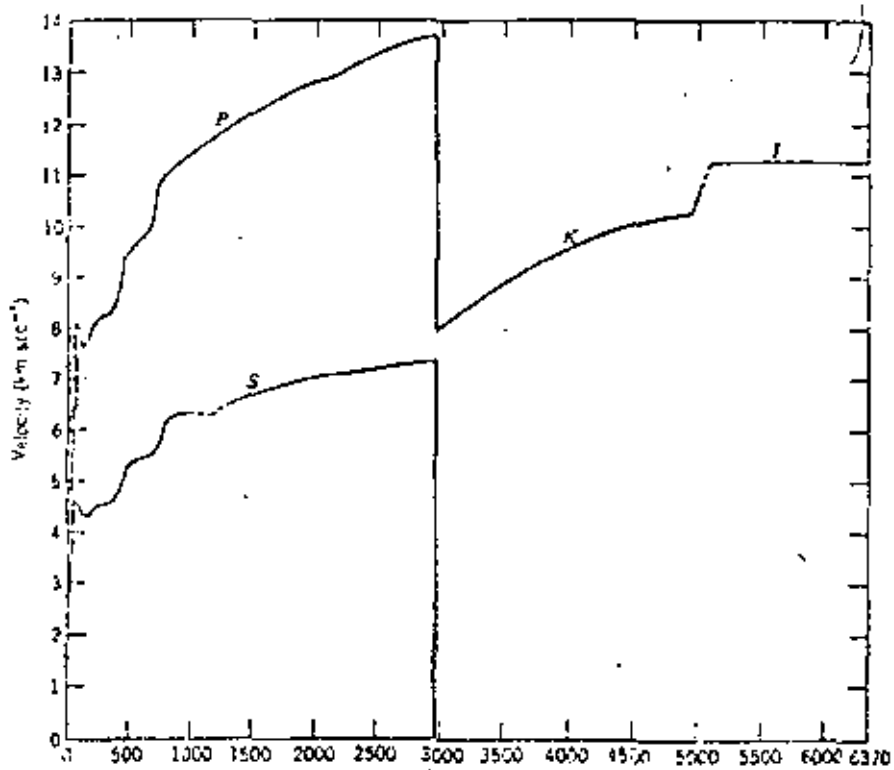

Las diferentes fases pueden identificarse en el registro con ayuda de las curvas de viaje de Jeffreys y Bullen que nos dan el tiempo de arribo en términos de la distancia al foco. Estas curvas fueron dadas por Jeffreys y Bullen en los años 40 y a pesar de la introducción de los computadores modernos han adquirido poca modificación.

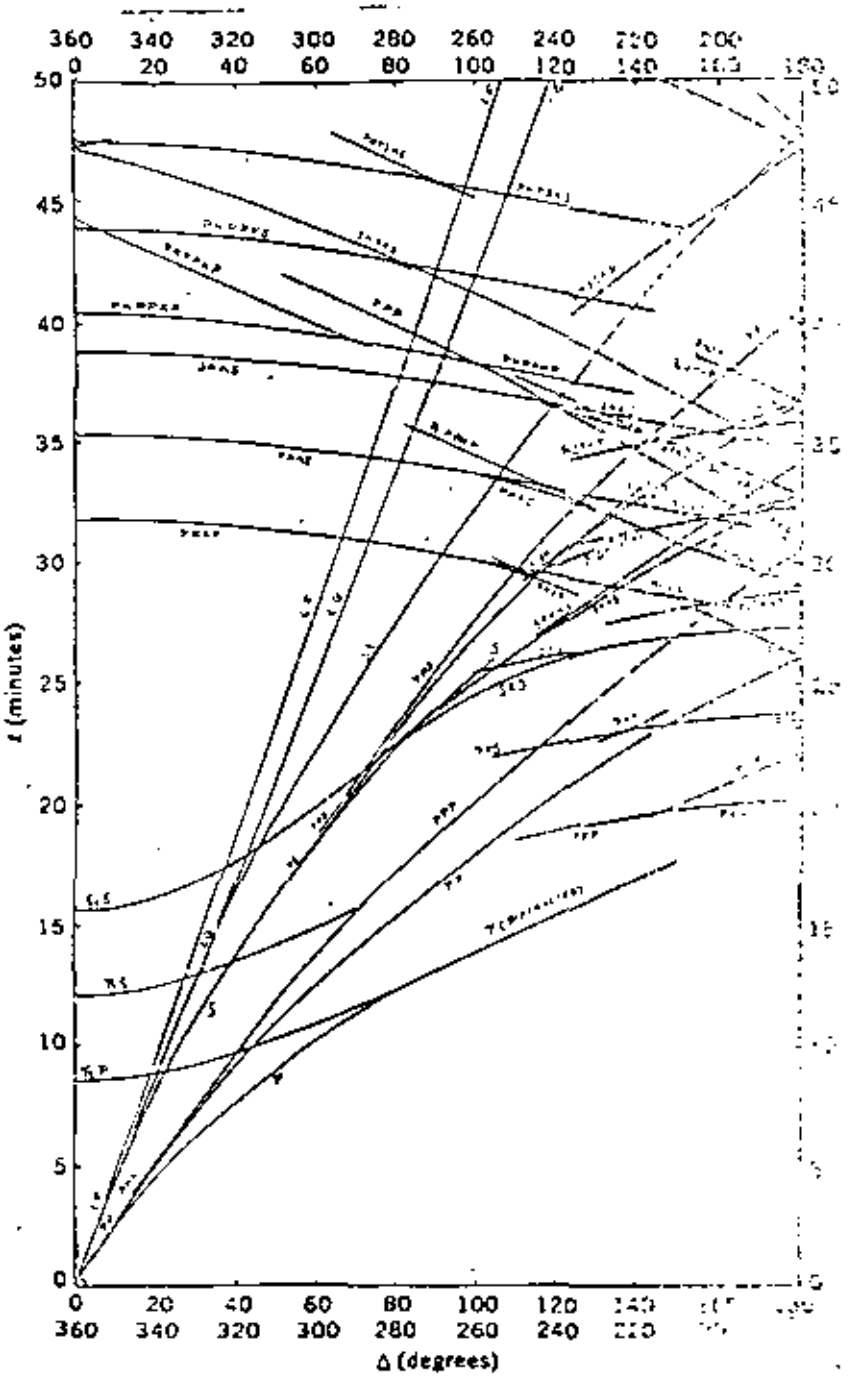

El tipo de onda para determinar M_L no está especificado es simplemente la máxima amplitud y puede ser de onda P, S o de superficie.

Otras magnitudes en uso comun además de las M_L (magnitud local) son la mb y la magnitud de ondas superficiales M_S.

La M_S fue definida por Gutenberg en 1945 para temblores superficiales como

$$M_S = \log A_H + 1.656 \log\Delta + 1.818 + C \quad (15° < \Delta < 13°)$$

donde

A_H - componente horizontal del máximo movimiento del suelo (de 0 a pico en micrones) para onda superficial de período 20 seg.

$A_H - (A_N^2 + A_E^2)^{1/2}$

A_N - Max. amplitud N-S

A_E - Max. amplitud E-W

Una fórmula adoptada por la Asociación Internacional de Sismología y Física del Interior de la Tierra (IASPEI) es

$$M_S = \log (A/T)_{max} + 1.66 \log\Delta + 3.3$$

para $T = 20$ seg la fórmula se reduce a

$$M_S = \log A_{20} + 1.66 \log\Delta + 2.0$$

y $$mb = \log (A/T) + Q$$

donde Q es un término que depende de Δ y la profundidad. A es la máxima amplitud de la onda P. En la práctica T es en general 1 segundo. También pueden usarse PP y SH.

En general M_L, mb y M_s son diferentes pues se derivan de diferentes fases. M_s y mb están relacionadas aproximadamente por

$$mb = 2.5 + 0.63\ M_s$$

La energía sísmica se relaciona empíricamente a M_s por

$$\log E_s = 1.5\ M_s + 11.8$$

Se ha demostrado, por otra parte, que para temblores grandes (dimensiones de ruptura de aprox 100 km) la escala M_s comienza a saturarse es decir que aunque aumenta la energía no aumenta la magnitud (M_s). Para evitar este problema se ha introducido la magnitud Mw.

Esta magnitud, llamada magnitud de mínima energía de deformación (Mw), fue introducida por Kanamori*. La energía total liberado en un temblor puede ser escrita como:

$$E_t = \bar{\sigma}\,\bar{u}\,A$$

con $\bar{\sigma} = (\sigma_1 + \sigma_2)/2$ valor promedio de esfuerzo

σ_1 = esfuerzo inicial

σ_2 = " final

$\bar{u}$ = dislocación promedio

A = área de ruptura

* Journal of Geophysical Research, 82, 1977, 1981-1987

Le energía total Et es la suma de la energía perdida en fricción, Ef, y la liberada como ondas sísmicas. Entonces,

$$E_t = E_f + E_s$$

$$E_s = -E_f + E_t$$

$$= -\bar{\sigma}_f \bar{u} A + \bar{\sigma} \bar{u} A$$

$$= \bar{u} A \left(\frac{\sigma_1 + \sigma_2}{2} - \sigma_f \right)$$

Si $\sigma_f = \sigma_2$ (Modelo de Orowan). Entonces,

$$E_s = \bar{u} A \left(\frac{\sigma_1 - \sigma_2}{2} \right)$$

$$= \frac{\bar{u} A \Delta\sigma}{2}$$

$$= \frac{\bar{u} A \Delta\sigma}{2} = \frac{\Delta\sigma M_o}{2\mu}$$

La experiencia demuestra que el modelo es razonable.

Ya que $\frac{\Delta\sigma}{\mu} = 1 \times 10^{-4}$ para temblores de intraplaca entonces

$$\log E_s = \log M_o - 4.3$$

Así, si podemos estimar M_o (lo cual es posible si se conoce el área de ruptura etc) entonces podemos estimar Es ya que la relación magnitud-energía de Gutenberg-Richter, válida para longitudes de ruptura máxima de 100 km es

$$\log E_s = 1.5 M_s + 11.8$$

$$\log E_s = \log M_o - 4.3$$

para todos los temblores puede definirse una magnitud Mw tal que

$$1.5 M_w + 11.8 = \log M_o - 4.3$$

o $$M_w = \frac{2}{3} \log M_o - 10.73$$

Mw es aproximadamente igual a Ms para longitudes máximas de 100 km pero para temblores mayores no sufrirá saturación.

Ejemplo: Tamblor de Chile del 22 de mayo de 1960. M_s = 8.3 pero Mw = 9.5. En la escala Mw éste es el temblor más grande del siglo.

Sample Calculation of Magnitudes and Energy of an Earthquake

The following calculations are for an Alaskan earthquake recorded at Oroville, California. The energy factor (equation 4) allows us to get an idea of the scale of energy release that is possible for earthquakes of different magnitude. For instance, we would need 30 earthquakes of magnitude 6 to release the equivalent amount of energy in the Earth's crust as released by just one magnitude 7 earthquake, and we would need 900 magnitude 5 earthquakes to produce the same energy. It follows, therefore, that even if small earthquakes occur in swarms in a particular area, they do very little to reduce the reservoir of strain energy needed for a major earthquake. But tectonic energy is drained away into heat and seismic waves in a truly gigantic way by a major earthquake like that of 1906 along the San Andreas fault with a magnitude M_s of 8¼. That earthquake released about 10^{25} ergs of strain energy within 60 seconds! (Only a fraction went into ground shaking.)

It is well known that, as the threshold of earthquake size being considered in a seismic region is lowered, the number of earthquakes above that magnitude rapidly increases. The rate of occurrence of shocks n above a given magnitude is again logarithmic and is measured by a parameter b (see equation 5). The smaller b is the more numerous are the earthquakes in a given time span. When b is determined for a seismically active region, the total seismic energy released over a period can be calculated by using the energy factor.

Magnitude is also sometimes roughly estimated from the length of surface fault rupture L (in kilometers—see equation 6).

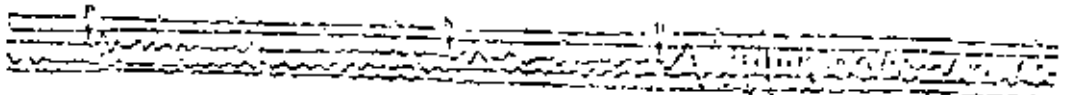

Let A be the amplitude, and T the period of a wave measured at a distance Δ from the source. One minute between gaps.

Measured values (reduced to ground motion)

P wave, A = 1.4 microns, T = 12 sec

Rayleigh wave, A = 4.3 microns, T = 20 sec

Δ = 28°

Body wave magnitude m_b ($25° < \Delta < 90°$)

$$m_b = \log A - \log T + 0.01\,\Delta + 5.9 \qquad (1)$$

$$= 0.15 - 1.08 + 0.28 + 5.9$$

$$= 5.3$$

Surface wave magnitude M_s ($25° < \Delta < 90°$)

$$M_s = \log A + 1.66 \log \Delta + 2.0 \quad (2)$$
$$= 0.63 + 2.40 + 2.0$$
$$= 5.0$$

Relation between m_b and M_s (approximate)

$$m_b = 2.5 + 0.63 M_s \quad (3)$$
$$= 2.5 + 3.2 \text{ (above earthquake)}$$
$$= 5.7 \text{ (compared with 5.3 calculated directly)}$$

Seismic energy E

$$\log E = 11.8 + 1.5 M_s \quad (4)$$
$$= 19.3$$
$$E = 2.0 \times 10^{19} \text{ ergs}$$

Relation between n and M_L

$$\log n = a - b M_L \quad (5)$$

Relation between M_s and L (worldwide data)

$$M_s = 6.03 + 0.76 \log L \quad (6)$$

Relation between M_s and S: the area of rupture (Worldwide data)

$$M_s = 3.21 + 1.92 \log S - 0.18 (\log S)^2 \quad (7).$$

For a theoretical basis for empirical relations in seismology see Kanamori and Anderson (Bull. Seism. Soc. Am., vol. 65, 1975) and Geller (Bull. Seism. Soc. Am., vol. 66, 1976).

Description of the Earthquake Source

Apart from the hypocentral location and magnitude of an earthquake there are several other source parameters (which require special study) which shed light on the details of the earthquake process, give important data on the current behavior of the area, and may help in future earthquake predictions.

Earthquake: When two sides of an earthquake suddenly move with respect to one another, seismic waves are generated and earthquake is said to have occurred. Reid in 1906 San Francisco earthquake proposed the "Elastic Rebound Theory"

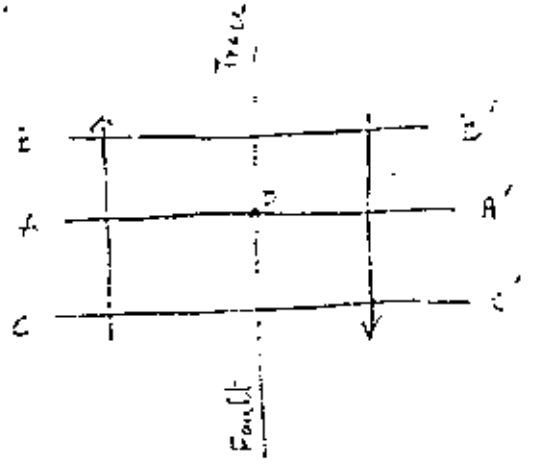

Initially

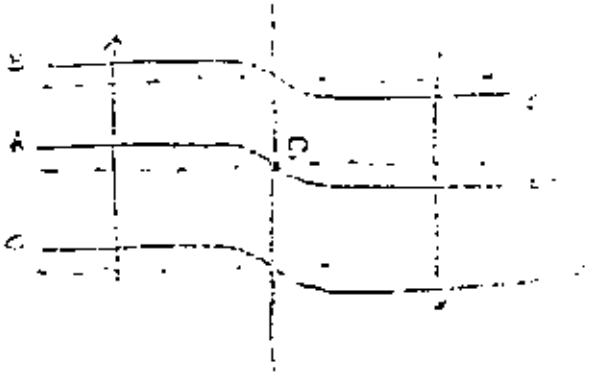

Strained state

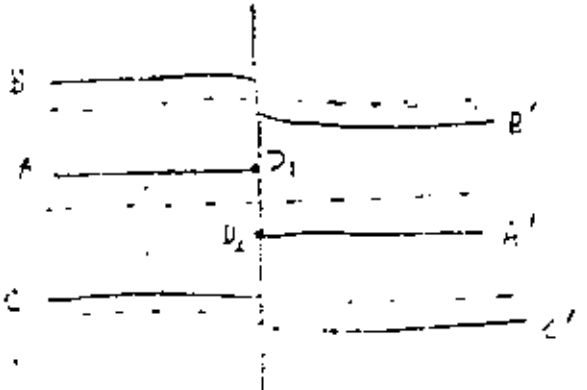

Imagine 2 parallel lines AA', BB', CC'. Due to tectonic forces these lines are deformed (strained state) till the rock breaks at a point D. This breakage at D along the fault trace is an earthquake (The breakage is not limited to point D only but to points adjacent to it as well). Since the tectonic forces causing the strain change very slowly the cycle is repeated. Reid's theory works well for atleast shallow earthquakes. Summarizing then an earthquake is a sudden dislocation in an earth mass. The following Fig. gives a schematic drawing of how a rupture may nucleates at focus & the dislocation propagates on the fault plane. Dislocation, in general, does not reach the surface although there are exceptions such as 1906 San Francisco earthquake and the recent Motagua, Guatemala earthquake. The rupture velocity in large earthquakes

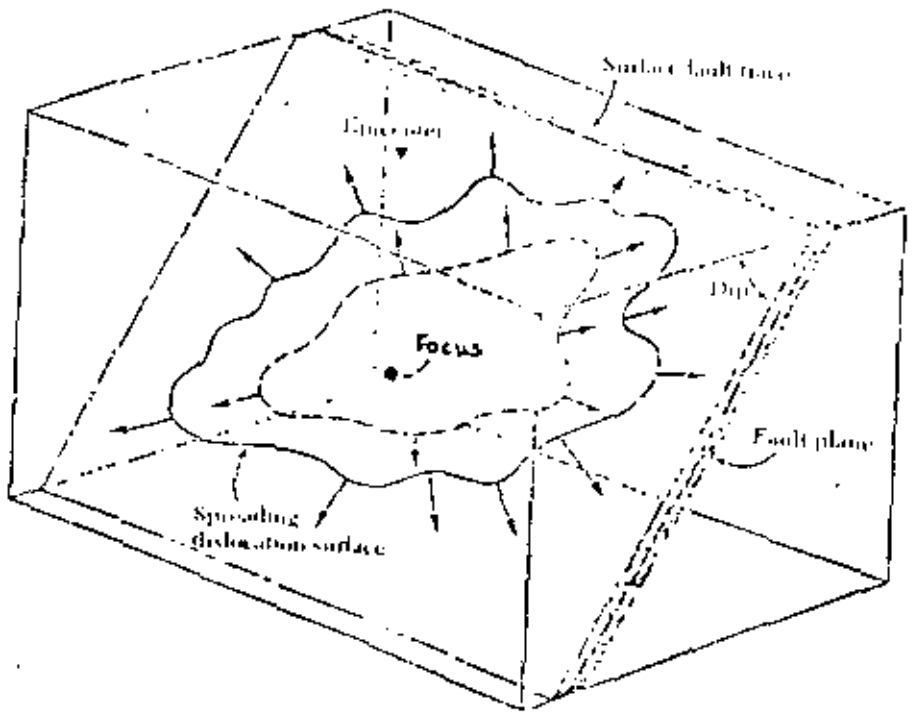

may vary. The rupture may be rather complex. The details of rupture are reflected in recorded seismic waves.

Fault Mechanism: P-wave arrives first at a seismic station. For shallow earthquake at some stations the polarity of P wave is found to be up (compressional), at others down (dilatational). Moreover distribution of compressions and dilatations forms a systematic pattern.

Remembering that an earthquake is a dislocation and that it can be shown that a dislocation can be represented by a double couple system of forces (without moment), it

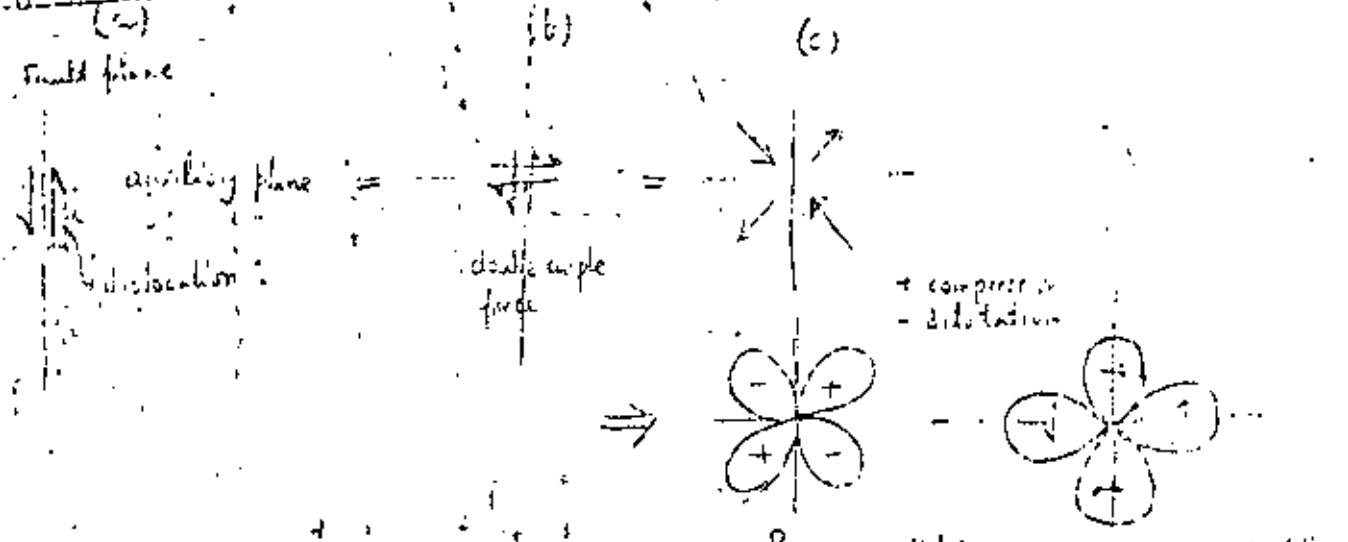

(a), (b) and (c) are equivalent

follows from the above Fig. that from the polarity of P wave first motion the polarization of S waves) 2 planes can be determined one of which is the fault plane. It is not possible to know, however, which of these 2 planes is the fault plane, except from geological information. However geological constraints, in most cases, are sufficient to identify the fault plane. This information is of great importance in tectonic studies. Also this fault plane orientation is needed for recovering other source parameters from the seismograms. From other local networks to study the local

Since $M_o = \mu A \bar{u}$, it follows that

$$\Delta\sigma = \frac{7}{16} \frac{M_o}{a^3} = \frac{7\pi^{3/2}}{16} \frac{M_o}{A^{3/2}}$$

Thus if we know M_o and the radius of the fault a, we can compute $\Delta\sigma$. Similar relations for other type of fault geometries can be deribed.

Area of Rupture:

Area of rupture associated with an earthquake can be determined from after shock locations, from synthetic modelling, or from surface rupture observed in the field (only a few earthquakes). After shock area, generally, grows with time and it seems that 1 to 2 day after-shock locations define the rupture are well.

From above,

$$M_o = \frac{16\,\Delta\sigma}{7\pi^{3/2}} A^{3/2}$$

$$\log M_o = \frac{3}{2} \log A + \log\left(\frac{16\Delta\sigma}{7\pi^{3/2}}\right)$$

Good quality data on well studied earthquakes are shown in the following Fig.

figure

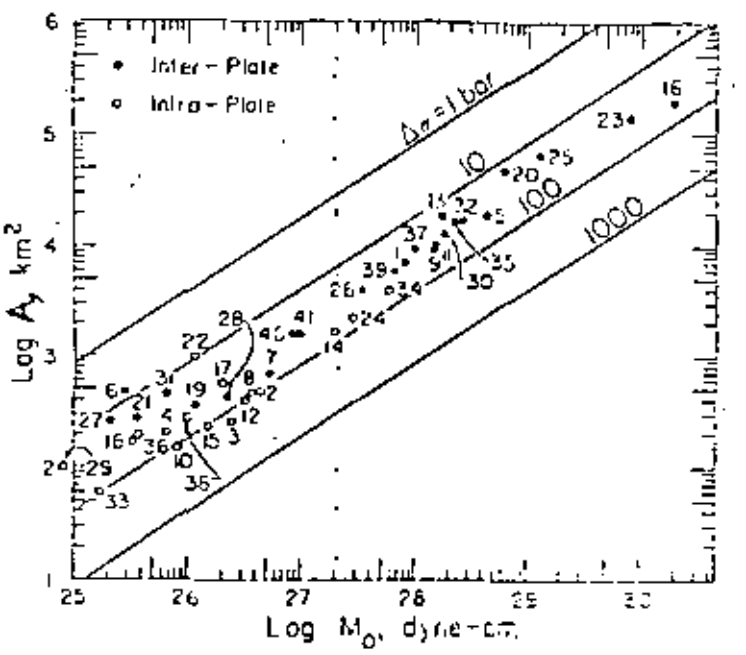

Data show that remarkable linearity with a slope of 2/3 between log A and log M_o. The linearity is explained in terms of constant stress drop. The stress $\Delta\sigma$ for interplate (boundary of plates) earthquakes is about 30 bars and for intraplate earthquakes $\Delta\sigma$ = 75 bars. The stress drop is nearly independent of the size of the earthquake. That $\Delta\sigma$ lies between 10 to 100 bars is surprising since the estimated stresses in the plates are of the order of a kilobar.

(1 bar = 10^6 dyne/cm^2 = 1 atmosphere)

if $\Delta\sigma$= 30 bars then

$$M_o = 1.23 \times 10^{22} \; A^{3/2} \text{ dyne cm} \quad (A \text{ in km}^2).$$

Thus, an estimate of Mo can be made for an earthquake from the above relation if we know A. Example: Chile earthquake of May 22, 1960; A=200,000 km ^{2} rom the above Mo=1.1x10^{30} dyne-cm, about a factor of 2 or more.

As mentioned in the section of magnitudes, knowing Mo we can compute the minimum strain energy magnitude Mw.

Equivalent radius of the fault.

The spectra of teleseismic P and S waves is schematically shown below:

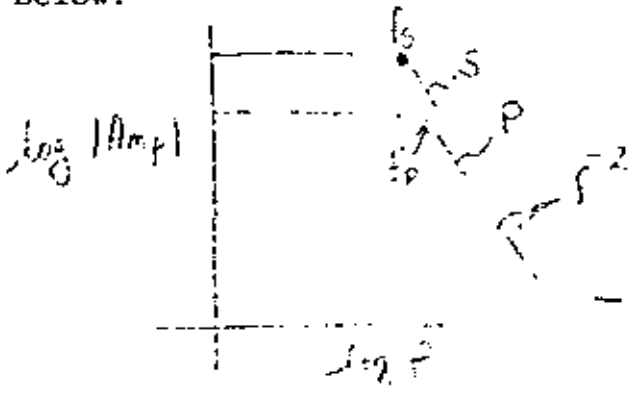

The spectra are flat at low frequencies and then decays proportional to f^{-2}. The corner frecuency fs or fp is defined by the intersection of the two slopes. Teoretically it has been shown that:

fs=0.37Vs/a , fp=0.37 Vp/a: where a is the radius of the fault.

From observed spectra fs and fp, and thus a, can be estimated

Near-Field Ground Motion: Just what ground motion can be expected near the source of an earthquake is important question in seismic engineering and is difficult question to answer. Regressions on M (magnitude), distance and recorded strong motion (say acceleration) has been carried out by several authors but since the data near the surface are very few, extrapolation of the regression curves at short distances is of dubious value. Recourse to more deterministic models is preferable.

Given a dislocation on a fault surface it is not difficult to compute the near-field ground motion but since we don't know the likely dislocation, the exercise is somewhat futile. Also the stresses associated with the dislocation may not be realistic. A simple physical argument of Brune (J. Geophys. Res., vol 75, 1970, pp. 4997-5009) leads to some interesting results.

Assume that stress drop occurs instantaneously over the fault surface. For points near the fault and for short time after the stress drop the fault can be thought as infinite.

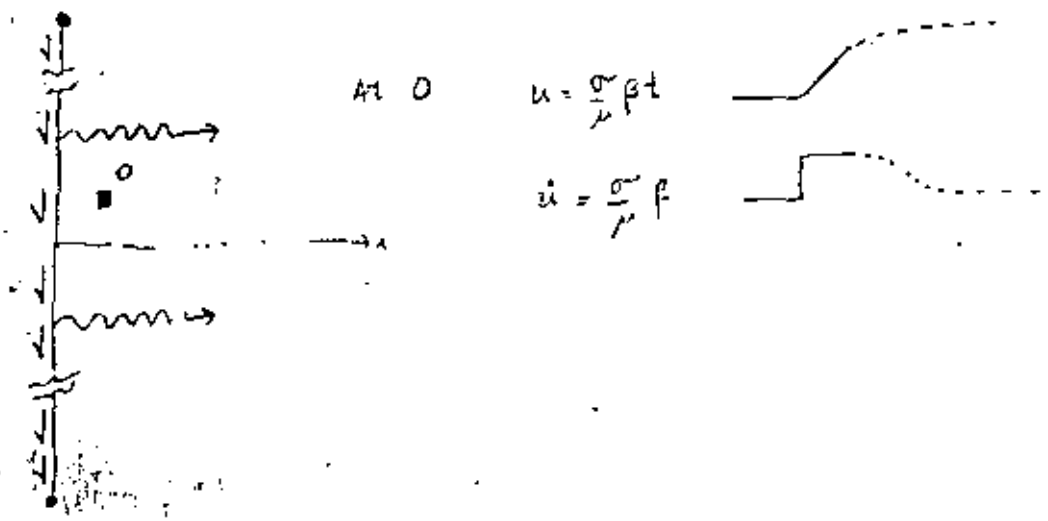

... $\sigma(x,t) = \sigma H(t - x/\beta)$ where $H(t)$ is unit step function

$$\sigma = \mu \frac{\partial u}{\partial x}$$

... At $x = 0$ $\quad u = 0 \quad , t < 0$

$u = \left(\frac{\sigma}{\mu}\right)\beta t \quad , 0 < t < T$, where T is the time required for elastic waves to propagate from the end of the ruptured surface.

$$\dot{u} = \frac{\sigma\beta}{\mu}$$

$= 100$ cm/sec if $\sigma = 100$ bars (10^8 dyn/cm^2), $\mu = 3 \times 10^{11}$ dyn/cm^2, $\beta = 3$ km/sec

Thus the initial velocity is directly proportional to the stress drop. A max^m of 150 cm/sec appears reasonable. Although acceleration is infinite as the wave arrives, it can be calculated for any finite band of frequency.

$$\ddot{u}(t) = \frac{\sigma\beta}{\mu} \delta(t) = \frac{\sigma\beta}{\mu} \frac{1}{2\pi} \int_{-\infty}^{\infty} e^{i\omega t} \, d\omega$$

If we consider a finite frequency band from 0 to ω_s then

$$\ddot{u}(t) = \frac{\sigma\beta}{\mu} \frac{1}{2\pi} \int_{-\omega_s}^{\omega_s} e^{i\omega t} \, d\omega$$

$$= \frac{1}{\pi} \frac{\sigma}{\mu} \beta \, \omega_s \left(\frac{\sin \omega_s t}{\omega_s t}\right)$$

If the cut off frequency is 10 Hz and $\sigma = 100$ bars,

$$\ddot{u}(t) \simeq 2g$$

The largest observed acceleration observed to date is about 1.25 g, for the San Fernando earthquake of 1971.

Attenuation :

A plane wave propagating in earth decreases in amplitude due to attenuation by internal friction. The decrease in amplitude can be roughly approximated by

$$A(f,t) = A_0 e^{-\pi f t/Q} = A_0 e^{-\pi f R/Q v}$$

where A_0 = initial amplitude, f = frequency, t = travel time, Q = attenuation coefficient, R = distance and v = wave velocity (α or β). Larger the Q less is the attenuation. Even if Q were constant (independent of frequency), at high frequencies the wave would be attenuated rapidly. There are many definitions of Q. An excellent review paper on Q is by Knopoff (Rev. Geophys., vol. 2, 1964, pp 625-660).

Generally it has been assumed that Q is constant over a broad frequency range. However recent work based on coda analysis of local earthquakes suggest that for a range of 1 to 25 Hz, $Q \propto f^n$ where $0.5 \leq n \leq 0.8$. Thus Q increases with frequency. The following fig. shows results on Q_β (for shear waves), from Aki (1979, preprint). The result is important since the frequency range of 1 to 10 Hz is of interest in seismic engineering. $Q_\beta \simeq 500$ at $f \leq 0.06$ ($T \geq 20$ sec). It appears to reach at minimum at $f \simeq 0.5$ ($T \simeq 2$ sec) afterwhich it increases.

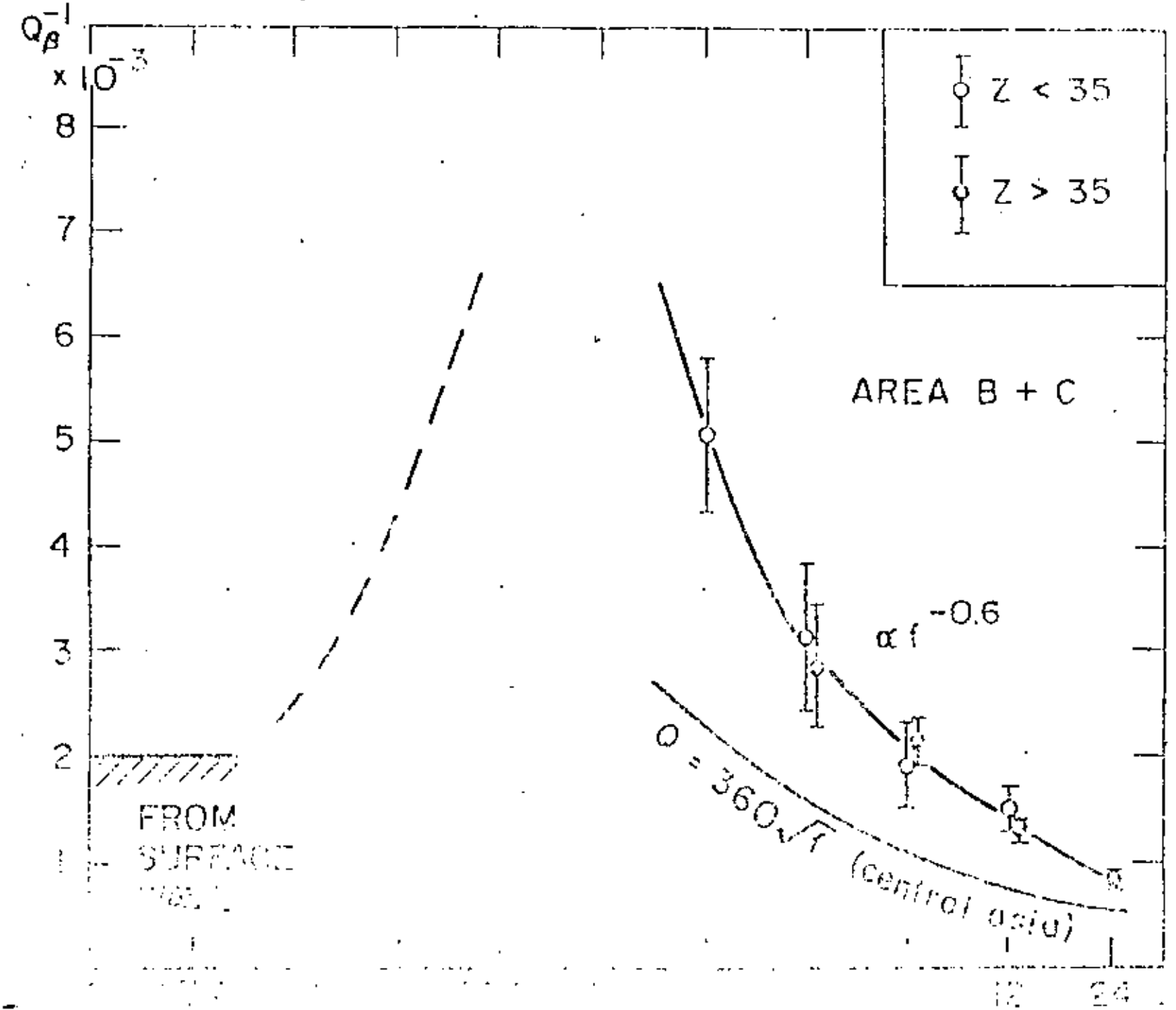
Q_β^{-1}
x 10^{-3}
8
7
6
5
4
3
2
1
Z < 35
Z > 35
AREA B + C
$\alpha f^{-0.6}$
$Q = 360\sqrt{f}$ (central axial)
FROM
SURFACE
12
24

Coming back to near-field ground motion, since the peak accelerations are associated with high frequency seismic waves (3–10 Hz), Q, along with scattering, plays an important role in determining the pattern of strong motion. High frequencies would be attenuated at short distances, independent of fault size. Geometrical spreading in the near-field is of course governed by the fault size. The effect of Q is accentuated by the fact that large amplitude waves (near the source) may act nonlinearly and drastically lower the effective Q near the source may be as low as 50. For Q = 50 at 5 Hz, e^{-1} distance is 10 km. Uncertainty in Q is the greatest source of error in estimating upper limits for particle velocity and acceleration.

An excellent reference on near-field ground motion is:

Brune, J. N. (1976) "The Physics of Earthquake Ground Motion" in C. Lomnitz and E. Rosenblueth (Editors) "Seismic Risk and Engineering Decisions", Elsevier Press.

Seismicity:

As mentioned earlier seismicity, mostly, is confined to the plate boundaries. In fact some of the boundaries of the plates (and thus their number) is defined by the seismicity. At the accretion boundary, where hot material ascends, only small earthquakes occur. It is at transform faults and subduction zones where large and great earthquakes occur. Subduction zones are, by far, the largest contributors to the energy release.

The earthquakes which occur on the plate boundaries are called interplate earthquakes and those which occur in the plates are called intraplate earthquakes. Note that in plate tectonics (the plates are assumed rigid) no intraplate earthquakes are assumed to occur.

About 75% of the shallow focus seismic energy is released along the circum Pacific belt. About 15% is released around the trans-Asiatic or Alpide belt, which extends from Indonesia through Himalayas to the Mediterranean. The intermediate (70-300 km) and deep-focus (>300 km) earthquake energy release is even more pronounced for the Pacific belt.

Table (Data from Båth and Duda, 1979)

Average annual frequency and energy for given magnitudes for the interval 1905 - 1977.

Magnitude M	Annual frequency ΣN/yr	Annual energy ΣEN/year, 10^{25} ergs
≥ 6.0	209	0.63
≥ 6.5	63	0.61
≥ 7.0	19	0.57
≥ 7.5	6	0.52
≥ 8.0	2	0.42
≥ 8.5	0.4	0.26

Recall the energy - magnitude relation

$$\log E = 1.5\,M + 11.8$$

Thus a magnitude 7 earthquake releases about 30 times as much energy as a magnitude 7 earthquake. It is the large earthquakes that contribute heavily to the energy. It also follows that small earthquakes can not act as 'valves' in releasing accumulated strain energy.

Frequency-magnitude relations for the aftershocks (M ≥ 7.0) are shown in the following figure. Dots: Single frequency N (M intervals of 0.1 unit) and stars refer to cumulative frequency ΣN.

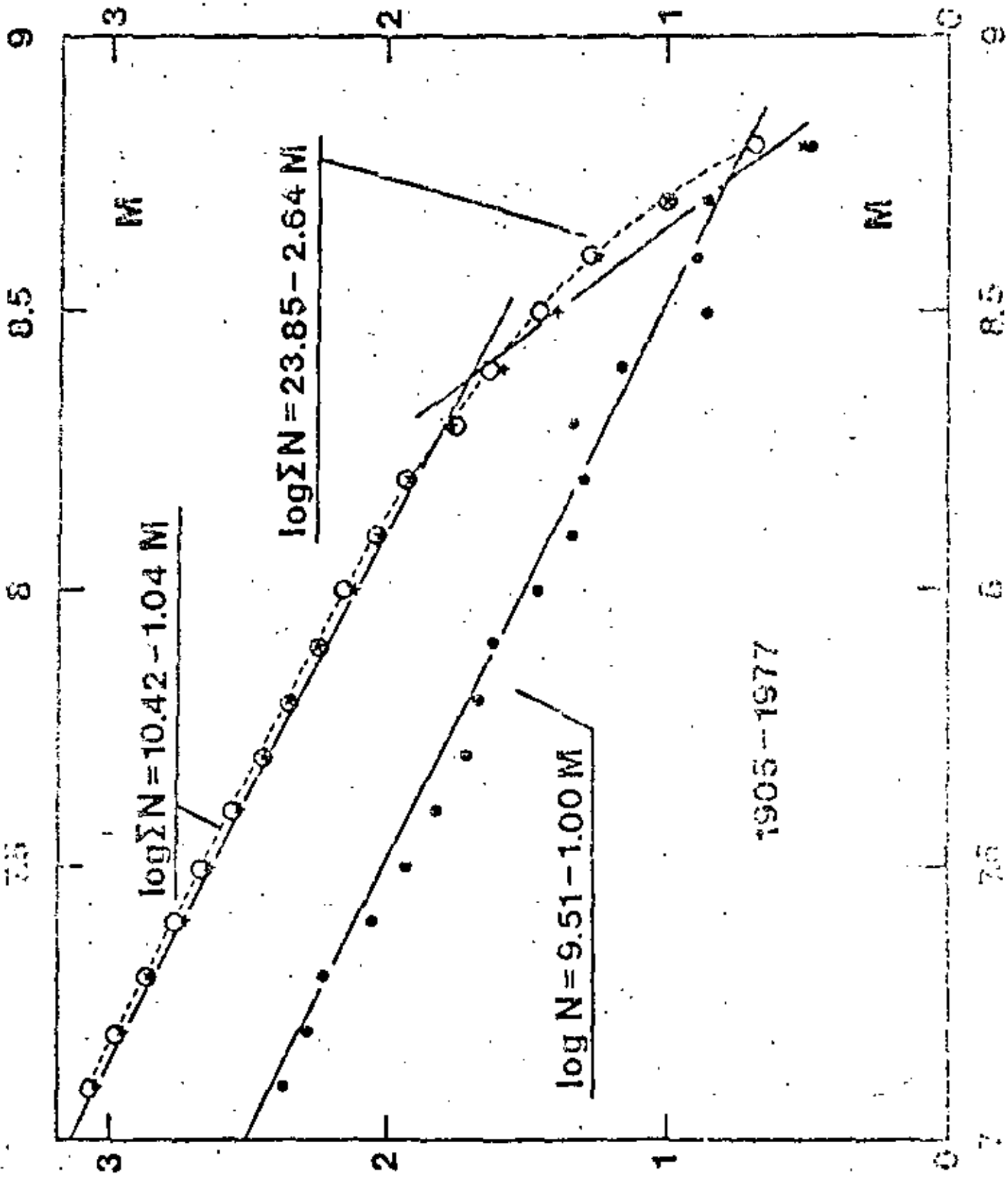

Cumulative Energy Release and number of Earthquakes (M≥7.0) since 1897

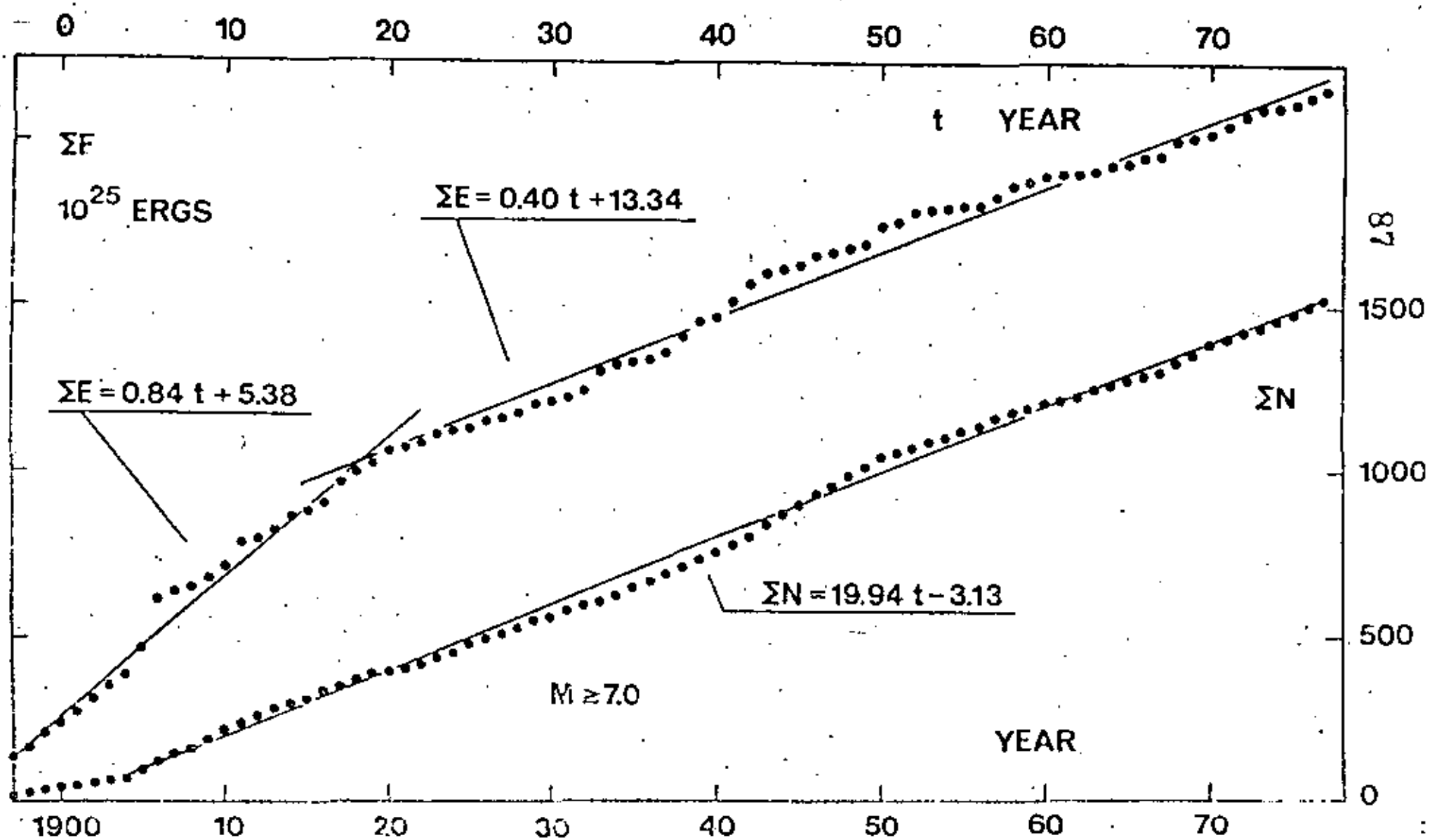

For seismic risk calculation of an area, statistics on local seismicity to smaller values of M might be needed. Data of $M \geq 5.5$ before 1965 or so are not uniform. Data of $M \geq 7.0$ since 1918 is reliable. A regional analysis of seismicity from 1897 to 1964 (inclusive) is given by S. Duda (1965, Tectonophysics, vol. 2, pp. 409–452) who also gives a catalog of earthquakes ($M \geq 7.0$).

A list of destructive earthquakes is given as the following. These are not necessarily great earthquakes.

Notable World Earthquakes and Seismicity.

YEAR	DATE (GMT)	REGION	DEATHS	MAGNITUDE	COMMENTS
526	December	Greece, Corinth	15,000		
1038	January 9	China, Shensi	23,000		
1057		China, Chihli	25,000		
1268		Asia Minor, Silicia	60,000		
1290	September 27	China, Chihli	100,000		
1293	May 20	Japan, Kamakura	30,000		
1531	January 26	Portugal, Lisbon	30,000		
1556	January 23	China, Shensi	830,000		
1663	February 5	Canada, St. Lawrence River			Max. Intensity X. Chimney's Broken in Massachusetts.
1667	November	Caucasia, Shemaka	80,000		
1693	January 11	Italy, Catania	60,000		
1737	October 11	India, Calcutta	300,000		
1755	June 7	Northern Persia	40,000		
1755	November 1	Portugal, Lisbon	70,000		Great tsunami.
[illegible]3	February 4	Italy, Calabria	50,000		
[illegible]7	February 4	Ecuador, Quito	40,000		
[illegible]11	December 16	Missouri, New Madrid	Several		Intensity XI. Also Jan. 23, Feb. 7, 1812.
1812	December 21	California, offshore Santa Barbara	Several injuries		Max. intensity X. Reported tsunami unverified.
1819	June 16	India, Cutch	1,543		
1822	September 5	Asia Minor, Aleppo	22,000		

Year	Date (GMT)	Region	Deaths	Magnitude	Comments
1828	December 18	Japan, Echigo	30,000		
1857	January 9	California, Fort Tejon			San Andreas fault rupture. Intensity X-XI
1868	August 13	Peru and Bolivia	25,000		
1868	August 16	Ecuador and Colombia	Ecuador 40,000 Colombia 30,000		
1872	March 26	California, Owens Valley,	About 50		Large-scale faulting.
1886	August 31	South Carolina, Charleston-Summerville	About 60		
1891	October 28	Japan, Mino-Owari	7,000		
1896	June 15	Japan, Riku-Ugo	22,000		Tsunami.
1897	June 12	India, Assam	1,500	8.7	
1899	September 3 & 10	Alaska, Yakutat Bay		7.8 & 8.6	
1906	April 18	California, San Francisco	700	8.25	
1908	December 28	Italy, Messina	120,000	7.5	
1915	January 13	Italy, Avezzano	30,000	7	
1920	December 16	China, Kansu	180,000	8.5	
1923	September 1	Japan, Kwanto	143,000	8.2	Great Tokyo fire.
1932	December 26	China, Kansu	70,000	7.6	
1935	May 31	India, Quetta	60,000	7.5	
1939	January 24	Chile, Chillan	30,000	7.75	
1939	December 27	Turkey, Erzincan	23,000	8.0	
1948	June 28	Japan, Fukui	5,131		
1949	August 5	Ecuador, Pelileo	6,000		
1960	February 29	Morocco, Agadir	14,000	5.9	
1960	May 21–30	Southern Chile	5,700	8.5	
1962	September 1	Northwest Iran	14,000	7.3	
1963	July 26	Yugoslavia, Skopje	1,200	6.0	
1964	March 28	Alaska	131	8.6	Prince William Sound, Tsunami.
1968	August 31	Iran	11,600	7.4	Surface faulting.
1970	May 31	Peru	66,000	7.8	$530,000,000 damage. Great rock slide.
1971	February 9	California, San Fernando	65	6.5	$550,000,000 damage.
1972	December 23	Nicaragua, Managua	5,000	6.2	
1975	February 4	China, Liaoning Province	few	7.4	Predicted.
1976	February 4	Guatemala	22,000	7.9	200-kilometer rupture Motagua fault.
1976	May 6	Italy, Friuli (Gemona)	965	6.5	Extensive damage. No surface faulting.
1976	July 27	China, Tangshan	About 650,000	7.6	Great economic damage, also perhaps 780,000 injured. Not predicted.
1977	March 4	Romania, Vrancea	2,000	7.2	Damage in Bucharest.

Source: U.S. National Oceanic and Atmospheric Administration.

Instruments :

The theory of damped seismographs is very simple and is given, for example, in Richter (pp 28 – 230). Principle

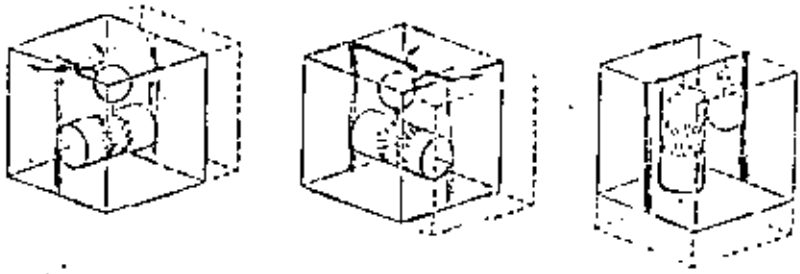

Simple models of pendulum seismographs recording vertical and two horizontal directions of ground motion. The pendulum must be damped in order to separate seismic pulses. [From Bruce A. Bolt, *Nuclear Explosions and Earthquakes*, W. H. Freeman and Company. Copyright © 1976.]

of pendulum seismographs is schematically shown above. The ground motion moves the frame but the pendulum mass tends to remain at the same point due to the inertia of its mass. The relative motion is magnified (mechanically or electronically) 100 to 100,000 times or more. The oscillation of the frame when the wave has passed needs to be avoided; this is accomplished by damping (mechanical or electronic). It is of great importance to know the response of the seismograph so that from the records, the precise ground motion can be determined.

A seismic record which includes precise time marks is not very useful. Modern seismographs have internal crystal clocks which put a time sign on the record. An ideal situation is when the seismic data from many stations are telemetered to a central station where all the data is recorded on paper (and/or magnetic tape) and a single clock puts the time marks. Italian observatories keep time to

better than 1/1000 sec accuracy.

A-36

A strong motion seismograph is designed such that even near the epicenter it does not go off the scale. Typically the magnification of such instruments is between 1 to 20. often a continuous record is not desired. The system triggers when a 'strong motion' occurs and is recorded on a photographic paper. Such records are very important from 'engineering point' since they provide ground motion near the source of an earthquake. Ordinary seismographs (with their high magnification) go off the scale if a large earthquake occurs nearby.

In the following the seismic instrumentation of important larger structures (strong motion seismograph and microseismic networks) is given.

Seismic Instrumentation of Important Large Structures

Strong Motion Instrumentation

Instrument Characteristics. The first requirement for strong-motion instrumentation is insensitivity—the strongest possible earthquake ground motions should stay on scale. In addition, a wide dynamic range is advantageous, since valuable information can be obtained from small nondamaging earthquakes. To study the dynamic response of the engineering structure, a wide frequency response range is also needed. Such a range requires high recording speeds that make continuous recording impracticable. An inertia trigger operated by the initial portion of the earthquake ground motion has been found to be a satisfactory solution to this problem.

Abstracted from Bruce A. Bolt and Donald E. Hudson, *Journal of the Geotechnical Engineering Division, Proceedings of the American Society of Civil Engineers*, Vol. 100, No. GT11, November 1974.

Accelerograph Location. Completely adequate definition of ground motions and structural response would require a large number of accelerographs at carefully selected points. For major projects in highly seismic regions, detailed studies of the optimum number and location of accelerographs would be expected by the special conditions of the particular site. For minimum recommendations, however, questions of location are secondary to the prime object of ensuring that at least some information of engineering value will be obtained for all strong shaking.

For this purpose, it is recommended that not fewer than four strong motion accelerographs be installed. Two of these should be located to record earthquake motions in the foundation, and two to measure structural response. For dams, the foundation instruments can often be mounted on abutments, or at an appropriate site in the immediate vicinity of the dam that is not obviously influenced in a major way by local geologic structural features. The instruments to measure dam response can usually be mounted at two different locations on the crest, or in upper galleries should they exist; they should not be mounted on special superstructures that may introduce localized dynamic behavior.

The purpose of requiring two instruments for each function is to give some indication of the uniformity of conditions, and to ensure some useful information in the event of instrument malfunction.

Accelerograph Installation and Maintenance. It is essential that the instruments be well protected from such environmental conditions as flooding or excessive summer temperatures, and from tampering or vandalism. The accelerograph, which is about 20 centimeters by 20 centimeters by 40 centimeters in size, can often be conveniently installed in the corner of a basement office, storage room, or gallery of a dam. If no space of this type is available near a suitable site, an insulated metal enclosure sealed against weather and interference can usually be provided by the instrument manufacturer at a reasonable cost. The accelerograph should be firmly bolted down to a concrete foundation, as specified by the instructions of the instrument manufacturer.

Checking, maintenance, and servicing of the accelerographs should be carried out on a regular schedule according to the instructions of the instrument manufacturer. Routine maintenance can usually be carried out by a regular member of the technical staff, if he is given a small degree of specialized training; instructions in the proper [illegible] of records and the initial [illegible] data processing [illegible] that they [illegible] after an earthquake [illegible]

Accelerograph Recommendations. Accelerographs meeting the performance requirements [illegible] are commercially available at 1978 prices in the $2,000 to $2,500 range. A suitable protective housing can usually be provided, if necessary, for $500 to $1,000. The only additional cost of installation will be the provision of standard electric lines to solar panels for battery trickle charging. The total 1978 cost of a typical recommended system will thus be about $12,000.

Local Seismograph Networks

Network Requirements. Sensitive seismographs to measure local earthquakes are sometimes advisable in the vicinity of projects such as large dams and nuclear reactors before major construction begins. The purposes of such instrumentation are to (1) determine the frequency of local earthquakes (if any); (2) determine the location of seismic activity and its depth; (3) determine the magnitude and some indication of focal mechanisms of the earthquakes; 4) allow prediction of the course of earthquake occurrence.

Reasonably precise location of an earthquake focus requires that the onset of P waves (and also S waves where feasible) be recorded to an accuracy of ±0.1 second or better, at a minimum of four nearby seismographs. There must be a common time base for all seismographs, and they should ideally surround the region of earthquake activity. For dams, the overall aims can be accomplished in two stages. In the preclosure stage, where the main purpose is to establish if any local earthquakes at all occur normally, a minimum network of three short-period vertical-component seismometers may be sufficient. With such a network a rough but adequate assessment of background earthquake frequency, location (using P and S waves), and magnitude can be made. If local earthquakes are prevalent the network should be expanded to at least four seismographs with the additional seismometer as near as possible to the active area.

After dam closure, it is advisable, at the least, to operate a four-station network for a period extending some years beyond the time when maximum impounding is reached. If sequences of earthquakes do occur, then the network should be densified. Such studies of reservoir-induced [illegible] usually will be of special interest. The requirements [illegible]

Network Location. The selection of sites for the sensitive seismographs often depends on practical considerations such as accessibility and avoidance of construction work. However, several general considerations should govern the configuration to the greatest extent practically possible. First, the sites should be uniformly spread in azimuth around the project.

The interstation distance should not be more than about 30 kilometers or less than 5 kilometers. Individual site selection should depend upon the local tectonic structures. It is best to locate the instruments on outcrops of basement rock, and they should be as remote as possible from construction activities, streams, quarrying, spillways, and so on. Normally, sites should be chosen so that they do not have to be shifted throughout the life of the project. It is also helpful to make field surveys of the relative background microseismic noise at prospective sites, with the use of a portable seismographic recorder before locations are finalized.

It has been found adequate to place the seismometers in shallow pits (about 1 meter deep) in the surficial rock. A generally adequate housing is a steel drum, with a watertight cover, that is set on concrete poured at the bottom of the pit.

Seismographic Characteristics. A variety of suitable components for a reliable high-gain seismographic system is now commercially available. Thus numerous systems can be designed to meet the aims previously established. The following two alternative systems—A and B—meet the minimum requirement and have been field tested. In both, the response of the overall seismographic system should be between 5 hertz and 50 hertz.

Seismographic System A. The system makes use of available portable seismometers and visual recording units. The network stations are not connected, and depend on separate crystal clocks at each recorder. Recording is normally on smoked paper and the paper records must be changed every day. This can be done by a member of the maintenance staff without special training.

The portable system for each site is in four parts: (1) seismometer; (2) waterproof single-packaged recording unit with batteries (size approximately 50 centimeters by 30 centimeters by 25 centimeters); (3) radio receiver; (4) power source and, as solar battery charger.

Seismographic System B. This system telemeters the signals from individual seismometers of the network to a central recording room by hard-wire connections. Power is needed at the individual seismometers for the amplifiers and voltage-controlled oscillators. At the recording station, additional power is needed for the signal discriminators, amplifiers, and drum and tape recorders. The system is costlier than System A because of the cost of land lines. Its great advantage is the centralization of recording at one convenient accessible location. Maintenance personnel would rarely need to visit the seismometers in the field. Components of the telemetered system are now all commercially available.

Network Operation and Analysis. Operation of either network A or B should not require instrumentation specialists or a staff seismologist. The critical requirements in all such studies of seismicity are continuity of operation and minimum system adjustments.

For either system, an operator would need to change the paper records each day of the week at about the same hour. He would need to mark the date and location on each seismogram. Any absolutely essential changes in system characteristics would need to be logged. It may be necessary, from time to time, to readjust and calibrate the seismometers in accord with the procedures specified by the equipment manufacturers.

For the telemetry system B, the discriminators, radio, clock, and recording drums can usually be located in a small room in the engineering quarters. The ac power is usually available. Seismograms can often be examined and stored in the same facility. All seismographic instrumentation should be bolted to the building structure to prevent movement and damage in the case of an earthquake.

The analysis side of the high-gain system often requires some seismological expertise. Special arrangements are not needed, of course, if no or very few local earthquakes are recorded. However, if the region is seismic or, at a dam, if the local seismicity increases on closure, or both, it is recommended that some special advice be obtained on analysis from a consultant seismologist.

Cost Estimates. The components in systems A and B are now commonly available and widely used by seismologists. At 1978 prices, the seismometers in System A cost about $1,000. A complete portable recording system can be obtained for $1,000. A suitable solar cell unit [illegible] $500 to $1,000. The cost of a four-station network of System [illegible] about $20,000. No cost is included for preparation of [illegible]

[illegible] of the preferred System B is somewhat [illegible] amplifier-oscillator package at each site is

102

listed at about $1,800 in 1978. At the central recording facility, each discriminator-amplifier-recorder package costs about $2,500. A suitable crystal clock is about $1,500 and a WWV radio receiver $500. The estimated total cost of the instrumentation at current prices is thus again about $20,000. In addition, however, there is the cost of the overland telemetry lines. In some areas commercial telephone lines may be available for rental. (In certain locations, HF radio telemetry links may be suitable.)

IX CURSO INTERNACIONAL DE INGENIERIA SISMICA

ANALISIS DE RIESGO SISMICO

MICROZONING: MODELS AND REALITY

DR. LUIS ESTEVA MARABOTO

JULIO, 1983

1

MICROZONING: MODELS AND REALITY

Contribution to a panel session on Ground Motion Characteristics

6WCEE, Delhi, 1977

by

Luis Esteva[1]

INTRODUCTION

ody doubts that local conditions usually have a significant influence on the acteristics of earthquake ground motion. What is not agreed upon, however, is the ner in which that influence must be evaluated. When one talks about microzoning, ion is usually focused on shear-beam models of stratified soil formations and in nsional, vertically traveling shear waves. But strong-motion and seismological have shown that those models can only be applied to a much narrower range of s than is usually believed, and that many other geologic or topographic features a more pronounced influence on ground motion than the presence of sediments. eneral analytical models have been developed in order to account for nsional and three-dimensional response and various types of arriving waves, but ity and range of applicability have not been determined yet. Because of this, and f the greater complexity of these models as compared with shear-beam ion models, they have not gained wide acceptance in the solution of actual g problems.

is the shear-beam amplification model the object of strong controversy with · the types of waves that significantly contribute to the earthquake motion at a also with respect to the lack of consistent criteria intended to define base rock the level at which usual intensity-attenuation laws are supposed to be valid, and ich local soil contributes to modify intensity and frequency content of seismic In other words, it cannot be uniquely defined what constitutes local conditions . is a portion of the path. Those criteria can be objected also on the grounds that ence of local soil conditions is often accounted for twice when making estimates of risk: as a random factor associated with the path when establishing empirical ation laws and as a systematic correction associated with local conditions when ying amplification.

a microzoning is not only a matter of ground-motion amplification; it also implies rmulation of consistent criteria to define design spectra at different sites, and evaluation t liquefaction potential. The former point requires consideration of the different laws that overn amplification of different types of waves and different directions of arrival, as well as eir corresponding probabilities; the latter is not covered by this discussion, as it will be ncluded in another panel session. Thus, the paper deals with the problems of ground motion haracteristics, under the framework of conceptual models, analytic results and observed facts. The paper is not intended to be a state-of-the-art report although it is based on one

[1] Institute of Engineering, National University of Mexico

(Ruiz, 1976). The intention of the author is mainly to point out some basic questions pertinent to the topic, aiming at the generation of vivid and fruitful discussion.

SEISMIC WAVES

The results of some analytical studies show that the influence of local soil on the ground motion is strongly dependent on the nature of the incoming seismic waves. Hence, analytical prediction of the amplitudes of ground motion at a site characterized by given local conditions as compared with those that would occur under standard conditions requires both the decomposition of the motion into various types of incoming waves, and the formulation of models adequate for the study of amplification and transformation of those types of waves. Despite the very significant effort devoted by seismologists to the formulation of analytical models for the study of wave amplification and transformation, very little of their contributions is either available or of use to engineers, as those models deal in general with the types of waves that are recorded at large epicentral distances (far field), or consider highly idealized topographical features. These results should not be overlooked, however, as they can provide a qualitative insight to many engineering problems.

If a reasonable degree of success is to be attained in the prediction of the influence of local conditions for a sufficiently wide range of cases, a lot of understanding has to be previously achieved about the decomposition of ground motion into different types of seismic waves in the near and intermediate fields. Obviously, the detailed source mechanism and the propagation path can be decisive in the directions and relative amplitudes of the most significant incoming waves, and hence on the laws governing ground motion amplification.

MECHANISM, PATH AND LOCAL CONDITIONS

The profusion of heterogeneities, irregularities and discontinuites in the earth's crust (Fig. 1) is responsible for the complex patterns of reflection, refraction, and scattering that seismic waves suffer in their path from source to site. Hence, it is not surprising that the influence of mechanism and path on ground motion characteristics is in some instances more pronounced than that of local conditions. This influence stems both from the modification of the surface ground motion itself, independent of local conditions, and from the fact that the different types of seismic waves resulting from mechanism and path effects are modified by local soil in different manners.

Fig 2 shows the two main paths followed by seismic energy form the source to a site of interest: through the interior of the crust, in the form of body waves, and along the surface, in the form of surface waves. But this picture still displays an oversimplified conception of the process: the source is not a point, but a large volume, and the influence of path is much more pronounced and complex than is implied by Fig 2.

The general type of source mechanism, and not only the detailed history of relative displacement along a fault, has a strong influence on the types of seismic waves generated, and hence on the motion characteristics for standard ground conditions, and in the manner in which local conditions modify them. Thus, strike-slip motion tends to produce a relative higher proportion of SH and Love waves, while subduction faults tend to produce higher proportions of P, SV and Rayleigh waves. The fact that seismic waves are generated from a large volume that may extend as far as the ground surface or its close proximity means that a significant portion of the motion at the near field should be made up of the contribution

of body waves that travel at very low angles with respect to the horizontal (Fig 3). These waves are probably guided along stratified formations and then modified by local conditions according to patterns similar to those affecting surface waves. Besides, it is likely that they give place to conventional surface waves that significantly contribute to ground motion at short epicentral distances and in the range of small and moderate frequencies. This pattern of energy travel seems plausible, and provides an explanation to the failure of conventional amplification theory to adequately predict the influence of local conditions.

The complexity of the path followed by waves is another reason for stating that surface ground motion at the near field is not the result of the superposition of a short number of wave trains: every wave impinging on a crust heterogeneity, subsurface discontinuity or topographic feature, gives place to a number of secondary trains of all types of waves (Fig 4).

Whatever the mechanism and the path of the waves for a given shock, it is of interest to assess the influence of local conditions; but, as Fig 5 shows, that influence cannot in general be made to depend only on the stratified soil formations underlying the site of interest: as an important portion of the energy may be traveling in the horizontal direction, the meaning of the term *local conditions* should be extended to include geologic and topographic features in the immediate vicinity of the site. Local amplification would hence be sensitive to the direction of wave arrival.

Even in the case that adequate tools were available for estimating the influence of local conditions on the amplification functions for the various significant types of seismic waves, the problem would remain of determining the trains of waves of different types that would arrive from a given direction. This is probably not feasible when dealing with near-field problems, first because of the possible occurrence of a large number of significant wave trains of different types incoming from different directions, and second because it is not always clear whether a given geologic or topographic accident should be taken as portion of the path –the influence of which would be included as a random factor in the experimental error of an *intensity attenuation expression* (expression relating intensity with magnitude and distance)– or of the local conditions –the influence of which should be included as a systematic correction– when trying to predict ground motion produced by seismic waves arriving from a given direction. For instance, coming back to Fig 5, a promontory such as *B* could be taken as a part of the path or of the local conditions for the purpose of assessing the contribution of surface waves coming from the left to ground motion at *A*, depending on whether the local zone is assumed to be bounded by line 1 or 2, respectively. Because the absence or presence of features such as these has not been explicitly included in empirical attenuation expressions, a unique criterion cannot be easily established. For the purpose of microzoning, however, a great deal of information is provided by ratios of surface wave amplitudes at *A* and *B* –and not necessarily their absolute values– for earthquakes originated at the left of the figure.

OBSERVED FACTS

Before the San Fernando earthquake of 1971, conceptual models of soil-related intensity amplification had gained their main support from nearly qualitative comparisons of observed differences between intensities on firm ground and on sedimentary deposits at a number of sites, notably Tokyo, San Francisco, Mexico City and Caracas. A more quantitative support to models based on the concept of vertically traveling SV waves had been provided by the comparison of predicted and observed response of the soft clay

deposits underlying Mexico City (Herrera I. *et al*, 1965); but conclusions valid for very peculiar conditions –existence of a very pronounced contrast between shear wave velocities of soil and underlying material– were being indiscriminately extrapolated, in spite of the fact that, in order to apply the same criterion, arbitrary decisions had often to be made concerning the portion of the ground profile that should be considered as a filter that would amplify standard-conditions-ground-motion. But records obtained during San Fernando earthquake disclosed the limitations of the mentioned criterion. Although a large portion of the area affected by that earthquake is known to be underlain by deep sedimentary formations (Fig 6), no pronounced contrast between shear wave velocities is apparent. Fig 7 (from Hudson, 1972) shows a sampling of peak accelerations measured at different sites. Included are all sites for which a clear distinction could be made between rock and alluvium as the basic site condition. It is evident that many factors other than distance and local site characteristics must be important.

Influence on ground motion of fault mechanism and propagation path has been disclosed by recordings obtained at a number of sites during several events. Thus, Udwadia and Trifunac (1973) analyzed a group of 15 events recorded at El Centro, California, characterized by short epicentral distances and magnitudes ranging from 3 to 6.8; the same authors (Trifunac and Udwadia, 1974) studied the records obtained at 6 stations located in the metropolitan area of Los Angeles during three different earthquakes, and Hudson (1972) analyzed the records of a number of seismoscopes and accelerographs obtained within an area of 40 square miles during San Fernando earthquake.

The 15 events recorded at El Centro were classified into four sub-groups, according to source azimuth with respect to the station, and Fourier spectra of records within each sub-group were compared. Group I included four events, three of them having the same epicenter, but different magnitudes. Spectral shapes of the components corresponding to the various events differ considerably among themselves. As propagation path and local conditions are the same, differences can only be ascribed to differences in fault mechanism and perhaps to nonlinear effects. Group II includes four events with different magnitudes and origins and, again, no similarity attributable to path or local conditions can be detected in the records. For one event in particular, predominant frequencies are very low, which can be explained in terms of predominance of surface waves. Group III includes the Imperial Valley earthquake of 1940, the record of which has been analyzed (Trifunac, 1971a) leading to the conclusion that it actually consisted of the superposition of several events, each starting a few seconds after the previous one. Horizontal components are similar, but the vertical component of the Imperial Valley earthquake shows significantly higher ordinates for high frequencies. This is probably a consequence of the short epicentral distance, that implies low attenuation of body waves, and of the peculiar source mechanism. Finally, the last group included events with large epicentral distances –about 150 km– and records were characterized by the low frequencies typical of surface waves. Despite very clear similarities between magnitude and origin of events in this group, their spectral shapes are significantly different, thus suggesting predominance of source effects over path and local conditions.

Similar conclusions are obtained from Trifunac and Udwadia's study concerning the records obtained at six stations during Borrego Mountain (1968), Lytle Creek (1970) and San Fernando (1971) earthquakes: source mechanism and epicentral distance significantly affected the records, while local conditions played only a secondary role. Of the six stations, four lie within Los Angeles Metropolitan area, two of them less than 1 km apart; two are located on base-rock and the other four –those within Los Angeles– on deep sediments of intermediate stiffness. In no case are dominant ground periods evident. An analysis of

5

records obtained at the four sites on sediments makes apparent the influence of source mechanism. For the Borrego Mountain shock, for instance, transverse displacements are systematically larger than radial ones, thus suggesting significant contribution of Love waves; the shapes of the displacement and velocity records are the same at all four sites, but their amplitudes differ, probably as a consequence of variations in the depth of alluvium from station to station, within a distance of 12 km. Records and spectra corresponding to the San Fernando earthquake are also very similar among themselves, but they differ in shape and in relative frequency content from those obtained during the other shocks. Large amplitudes of radial and transverse displacements have been ascribed (Hanks, 1975) to Rayleigh and Love waves, respectively. Fourier spectra of Borrego Mountain records at the four Los Angeles stations shown are very similar in the range of frequencies smaller than 1 hz; the similarity should not be ascribed to dominant group periods, but to the predominance of surface waves, given the long epicentral distance –about 200 km. For San Fernando earthquake, instead, the contribution of high frequencies is rather important, as could be expected, given the proximity of the source—40 km.

Hudson's observations during San Fernando earthquake covered a wide range of ground conditions, from crystalline rock to alluvial deposits 300 m deep. Notorious discrepancies were observed in seismoscope traces even for sites with very similar ground conditions, stressing the importance of other factors, such as topography or subsurface irregularities, pointed out, for instance, by Jackson (1971) and Boore (1972). A comparison of response spectra corresponding to rock and alluvium sites fails to show any systematic influence of local soil. The author concludes that the properties of response spectra at the same sites during another earthquake would probably show quite different relative variations. This implies that formulation of microzoning maps must be based on the analysis of records obtained during a sufficiently large number of intense earthquakes.

Some interesting cases have been presented in the literature, describing the overall response of some soil formations during strong earthquakes. Although the influence of local conditions was shown to be clear in those cases, it was also clear that it may not suffice to study the influence of the soil directly underneath the structure of interest, but that an analysis of the response of a wider area can explain observed facts. Two instances will be described in this respect: one corresponds to the Skopje earthquake of 1963, and the other to two records obtained at Hutt Valley, New Zealand.

Poceski (1969) describes the geological setting of Skopje: the city is located in a long valley along which flows the Vardar river. A cross section of the valley shows a large discontinuity of the sediment thickness along a line that follows the river course (Fig 8). The greatest intensity of damage on constructions was observed directly above the discontinuity, and was ascribed to the hypothetical occurrence of large rotational components of the ground motion with respect to a vertical axis, motivated by the also hypothetical difference in the horizontal response of the alluvial deposits at each side of the discontinuity.

The rotational response of a large volume of alluvium was actually detected by Stephenson (1974), when he analyzed the records obtained at two sites near Hutt Valley. The sites are 900 m apart, and are underlain by saturated recent alluvial deposits with shear wave velocities of about 100 m/sec. Spectral densities of acceleration at both sites show each a predominant direction of response, with a high statistical correlation between the corresponding predominant components, thus suggesting the torsional oscillation of a large mass of alluvium.

How should microzoning be influenced by effects such as those described in this section?

6

EFFECTS OF TOPOGRAPHY

The largest acceleration ever recorded occurred at one of the abutments of Pacoima dam during the San Fernando earthquake and implied, according to Reimer *et al* (1973) a three-fold amplification of its peak value. Ratios of up to 30 between the peak ordinates of the Fourier spectrum of the velocity record obtained at the top and at the base of Kagel mountain were computed for several aftershocks of the mentioned event, while the corresponding ratios of peak ground velocities "only" reached 3.95. This implies a resonant effect of the mountain, which was explained by Davis and West (1973) in terms of the ratio of its average width and the length of shear waves. The values indicated are not necessarily amplifications with respect to standard conditions (whatever they are), as analytical studies show (see Fig. 9) that at some frequencies wave amplitudes tend to be amplified at the top of promontories and reduced at their base (Bouchon, 1973; Aki & Larner, 1970; Boore, 1972), but the fact remains that the effects of surface topography cannot be overlooked. Similar considerations can be made regarding the significance of subsurface topography: the distribution of structural damage in Skopje in 1963 was ascribed to excessive torsional oscillations in the region directly above a sharp discontinuity of soft layer thickness (Fig. 8) for incident waves that possessed significant horizontal components parallel to the discontinuity; and analytical studies predict focusing of waves in the vicinity of subsurface irregularities (Jackson, 1971). The interaction of subsurface topography and direction of wave arrival is illustrated in Fig 10 (Trifunac, 1971b), which shows relative amplitudes of the motion produced at the surface by SH waves arriving at a semicylindrical valley. Amplitudes vary with site location and with incidence angle at a fast rate, thus suggesting that detailed knowledge of subsurface topography and of directions and types of incoming waves would be required for the deterministic prediction of the influence of topographic features. As this knowledge is not easy to achieve at present, careful judgement must be exercised when trying to employ analytical results as those shown here in the predictions of seismic risk.

A further question stemming from the significance of surface and subsurface irregularities is that related to the homogeneity of the data set that has been used by different investigators in the derivations of empirical attenuation expressions: unless those sites for which the topographic conditions are suspected to have a significant systematic influence on ground motion are eliminated from the data set used to derive those attenuation expressions, we face the danger of accounting for the mentioned conditions twice: as random effects in one step and as systematic effects in another.

MODELS AND REALITY

Theoretical considerations and observed facts concerning mechanism, path and local conditions, point at the complexities involved in the formulation of mathematical models intended to predict the influence of local conditions on ground motion.

Hence, the question arises of whether the role of those models is too limited to be of practical significance. This is probably too pessimistic an outlook although detailed simulations of near-field motions based on physical models that account for source, path and local conditions are probably beyond reach of present engineering practice, the writer believes that a fair degree of understanding of the parameters and mechanisms that affect ground motion amplification and attenuation can be gained by means of simplified analytical models that consider alternate patterns of energy liberation and propagation.

7

The significance of models as related to reality and to decision making in engineering is dramatically illustrated by the applicability of the vertically-traveling-shear wave model to the study of ground motion amplification in the valley of Mexico: this is the site on earth where that model has been most beautifully supported by instrumental evidence, and however, the shallow depths and large epicentral distances of earthquakes usually observed there imply that practically all energy must arrive in the form of surface waves. It is easy to understand that the apparent confirmation of the unidimensional-shear-wave model in this case stems from the fact that the large lengths of the incoming surface waves lead to the response of the soft soil formation far away from the borders of the valley according to a pattern very similar to that of the shear beam model. The agreement is accentuated because very little energy is radiated back to the base, and because a significant portion of it is radiated in accordance with the shear beam model. This form of soil response and the small ratio of energy radiation are responsible for the occurrence of dominant ground periods. For the same reasons, dominant ground periods determined by means of excitation applied at the surface coincide with those resulting from earthquake excitation. But the conditions that favor the practical applicability of the mentioned model in the case where a pronounced contrast exists between the soft formations and the base do not appear in the absence of that contrast, and conditions other than sediment properties may dominate the local pattern of intensity variations.

In an attempt at developing a unified approach to the combined intensity-attenuation and local-amplification effects for site underlain by stratified soil formations, Sanchez and Esteva (1977) made use of available data for the derivation of attenuation expressions that directly account for the systematic influence of local soil, while random deviations were dealt with as equation errors. Data of earthquakes recently recorded at sites where detailed information was available about local soil conditions (this means 50 horizontal components at 10 different sites) provided the basis for semiempirical attenuation expressions for Fourier spectra at the ground surface. These expressions are of the form $F(\omega) = G(\omega; R, M)\, g(\omega; s)$, where $F(\omega)$ is the ordinate of Fourier spectrum for frequency ω, G accounts for source (M) and path (R) effects, and g is a function that accounts for amplification effects in terms of local soil properties (s). G was assumed of the form $b_1(R + c)^{-b_3} \exp(b_2 M)$, and g was taken as the amplification function of an equivalent single-degree-of-freedom model of a linear shear beam assumed to represent the soil layers above firm ground. A number of expressions were derived for seven values of ω, in accordance with three alternate definitions of firm ground: the surface material itself, or those with shear wave velocities of 400 and 800 m/sec, respectively. The results were disappointing: the ratio of observed to predicted ordinates of Fourier spectra was systematically greater than unity for the components recorded at the particular site where the computed values of g were highest (i.e., where a thick layer of very soft materials existed), and the standard deviation of that ratio for the whole ensemble of sites and records was very high and independent of the definition of firm ground. But Mohraz (1976) obtained significantly different intensity attenuation expressions for different alluvium thickness. A similar study was carried out by Faccioli (1976), who classified ground properties into four categories: crystalline rock, sedimentary rock (including stiff conglomerates and very compact sands), typical alluvial deposits with intermediate stiffness and soft deposits (loose sands and soft clays). He succeeded in obtaining empirical attenuation expressions for each of these categories, for which the standard deviation of error is lower than that associated with previous expressions that neglected the influence of local conditions (Esteva and Villaverde, 1973; Mc Guire, 1974). The systematic influence of such conditions is thus confirmed, as well as the inadequacy of the shear beam model to predict them.

Two-dimensional models as shown in Fig 11 can perhaps suffice for the qualitative study of

8

the overall patterns of wave generation and transformation. They should also prove useful for the understanding of the possible influence of irregularities and discontinuites found by different types of waves along their path, and for the assessment of local variability of intensities in the neighborhood of some geological or topographical accidents. Probably, they can even help at gaining some insight into the general patterns of waves arriving at a site, thus permitting the formulation of adequate amplification models. There are instances, however, where three-dimensional models may be required. One such case is the study of the amplified motion recorded at one of the abutments of Pacoima Dam during San Fernando earthquake; another would be the study of the response of an alluvial formation where torsional oscillations might be of importance.

Given a train of incoming waves, predictions of the resulting motion at a site with heterogeneous properties or irregular topography can be dealt with as a diffraction problem. However, standard analytical formulation (Morse & Feshbach, 1953) can only be applied in practice to simplified idealizations of actual conditions (see, for instance, Aki and Larner, 1970; Bouchon, 1973; Trifunac, 1971b). For more general applications, finite difference solutions of the wave equation (Boore, 1972), finite element wave-propagation investigations (Smith, 1974) and dynamic response studies of finite-element models of small local regions (Lysmer & Drake, 1971; Ayala & Aranda, 1977) have been undertaken. The latter formulation is very attractive to engineers, because it permits direct application of standard programs of frequency-domain or time-response dynamic analysis. But adequate boundary conditions have to be defined at the edges of the region under study in order to allow transmittal of incoming and outgoing waves without excessive energy losses or reflections. When incoming and outgoing waves are of the same type and have the same direction, theoretically exact boundary conditions can be established, expressed in terms of equivalent damping units (Lysmer & Drake, 1971; Tsai, 1969). Aproximate solutions have also been formulated for the case of outgoing body waves of known type and unknown direction (Lysmer & Kuhlemeyer, 1969) and these solutions have been extended to the combination of incoming and outgoing waves (Ayala & Aranda, 1977), but the general case of known incoming waves and unknown outgoing wave types and directions has not been sufficiently studied.

Despite these problems, criteria based on the time-history analysis of finite element models will probably gain wide acceptance in view of their ability to account for nonlinear soil behavior. But despite the importance usually ascribed to nonlinearities when trying to explain discrepancies between observed and predicted local amplification effects, it must be recognized that their influence is often overshadowed by the overall patterns of shock generation and propagation. It is this consideration that supports the usefulness of frequency-domain studies as advocated above.

CONCLUDING REMARKS

Microzonation implies much more than influence of stratified soil formations. It implies a better knowledge of the fault mechanisms of earthquakes that significantly contribute to seismic risk at a site, study of the possible influence of path characteristics on the types of arriving seismic waves and hence on the manner in which local conditions will affect them. More general analytical models for the study of all factors affecting seismic waves from their source will have to be developed, adapted and implemented by engineers. But, as a consequence of the complexities inherent in the phenomena under study, those models should only play a role complementary to instrumental observations. Because path and

mechanism effects have been shown to affect local variations of ground motion, a large number of events will have to be recorded at every site of interest and its neighborhood before reliable conclusions can be drawn concerning those variations. Hence, small magnitude shocks should be given increased attention, as they will probably constitute the main source of information at some sites, in spite of their inability to provide information about the influence of nonlinear soil behavior associated with severe shocks. Deployment, operation and interpretation of the records of local instrumental networks should aim at the description of earthquake motion variability throughout small regions, and at the understanding of the patterns of seismic waves giving place to that variability.

ACKNOWLEDGEMENTS

The author wishes to express his gratitude to S. E. Ruiz for her assistance in the revision and interpretation of the literature, through the preparation of a state-of-the-art report. Critical reading of the manuscript by G. Ayala and J. Bielak is also gratefully acknowledged.

REFERENCES

Aki, K. & Larner K., 1970, "Surface motion of a layered medium having an irregular interface due to incident plane SH waves", J. Geophys Res., 75, pp. 933-954

Ayala, G. & Aranda R., 1977 "Boundary conditions in soil amplification studies", 6WCEE, Delhi

Boore D. M., 1972, "A note on the effect of simple topography on seismic SH waves", Bull. Seism. Soc. Am., Vol 62, No. 1, pp. 275-284

Bouchon, M., 1973, "Effect of topography on surface motion", Bull. Seism. Soc. Am., Vol 63, No. 3, pp.615-632

Davis, L. L. & West, L. R., 1973, "Observed effects of topography on ground motion", Bull. Seism. Soc. Am., Vol 63, No. 1, pp. 283-298

Esteva, L. & Villaverde, L., 1973, "Seismic risk, design spectra and structural reliability", Proc. 5WCEE, Rome

Faccioli, 1976, personal communication

Hanks, T. C., 1975, "Strong ground motion following the San Fernando, California, earthquake. 1. Ground displacements", mentioned by Trifunac and Udwadia, 1974

Herrera, I., Rosenblueth, E. & Rascón, O. A., 1965, "Earthquake spectrum prediction for the valley of Mexico", Proc. 3WCEE, Vol 1, pp 161-174

Hudson, D. E., 1972, "Local distribution of strong earthquake ground motions", Bull of the Seismological Soc. of America, Vol 62, No. 6, pp. 1765-1786

Jackson, P. S., 1971, "The focusing of earthquakes", Bull. Seism. Soc. Am., Vol 61, No. 3, pp. 685-695

Lysmer, J. & Drake, L. A., 1971, "A finite element method for seismology", Methods in Computational Physics, Cap. VI, University of California, Berkeley

Lysmer, J. & Kuhlemeyer, R. L., 1969, "Finite dynamic model for infinite media", Journ. Eng. Mech. Div. ASCE, Vol 95, No. EM4, pp. 859-877

Mohraz, B., "A study of earthquake response spectra for different geologic conditions", Bull. Seism. Soc. Am., Vol 66, No. 3, pp. 915-936

Morse, & Feshbach, 1953, "Methods of Theoretical Physics", McGraw-Hill, Kogakusha, Tokyo

Poceski, A., 1969, "The ground effects of the Skopje July 26, 1963 earthquake", Bull. Seism. Soc. Am., Vol 59, No. 1, pp. 1-29

Reimer, R. B., Clough, R. W. and Raphael, J. M., 1974, "Evaluation of the Pacoima Dam accelerogram", SWCEE, Vol 2, pp. 2328-2337

Ruiz, S. E., 1976, "Influencia de las condiciones locales en las características de los sismos", M S Thesis, Faculty of Engineering, National University of Mexico

Sánchez-Sesma, F. J. & Esteva, L., 1977, "Intensity attenuation and local amplification: a unified approach", Institute of Engineering, National University of Mexico

Smith, W. D., 1974, "A non reflecting plane boundary for wave propagation problems", Journal of Computational Physics, Vol 15, No. 4, pp. 492-503

Stephenson, W. R., 1974, "Earthquake induced resonant motion of alluvium", Bull. New Zealand Nat. Soc. for Earthquake Engng, Vol 7, No. 3

Trifunac, M. D., 1971a, "Response envelope spectrum and interpretation of strong earthquake ground motion", Bull. Seism. Soc. Am., Vol 61, No. 2, pp. 343-356

Trifunac, M. D., 1971b, "Surface motion of a semi-cylindrical alluvial valley for incident plane SH waves", Bull. Seism. Soc. Am., Vol 61, pp. 1755-1770

Trifunac, M. D. & Udwadia, F. E., 1974, "Variations of strong earthquake ground shaking in the Los Angeles area", Bull. Seism. Soc. Am., Vol. 64, No. 5, pp. 1429-1454

Tsai, N., 1969, "Influence of local geology on earthquake motion", Ph. D. Thesis, California Institute of Technology, Pasadena, Calif

Udwadia, F. E. & Trifunac, M. D., 1973, "Comparison of earthquake and microtremor ground motions in El Centro California", Bull. of the Seismological Soc. of America, Vol 63, No. 4, pp. 1227-1253

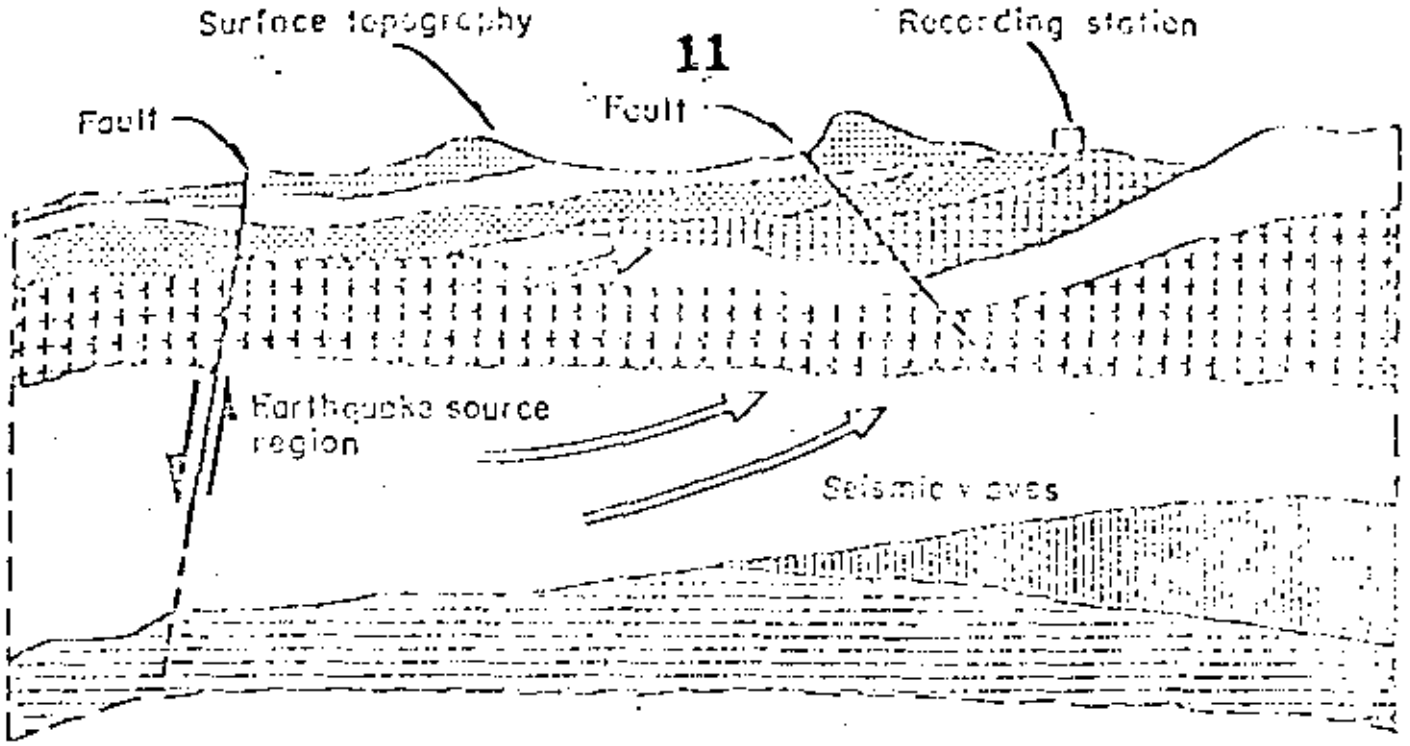

Fig. 1 Source, path and local conditions (Hudson, 1972)

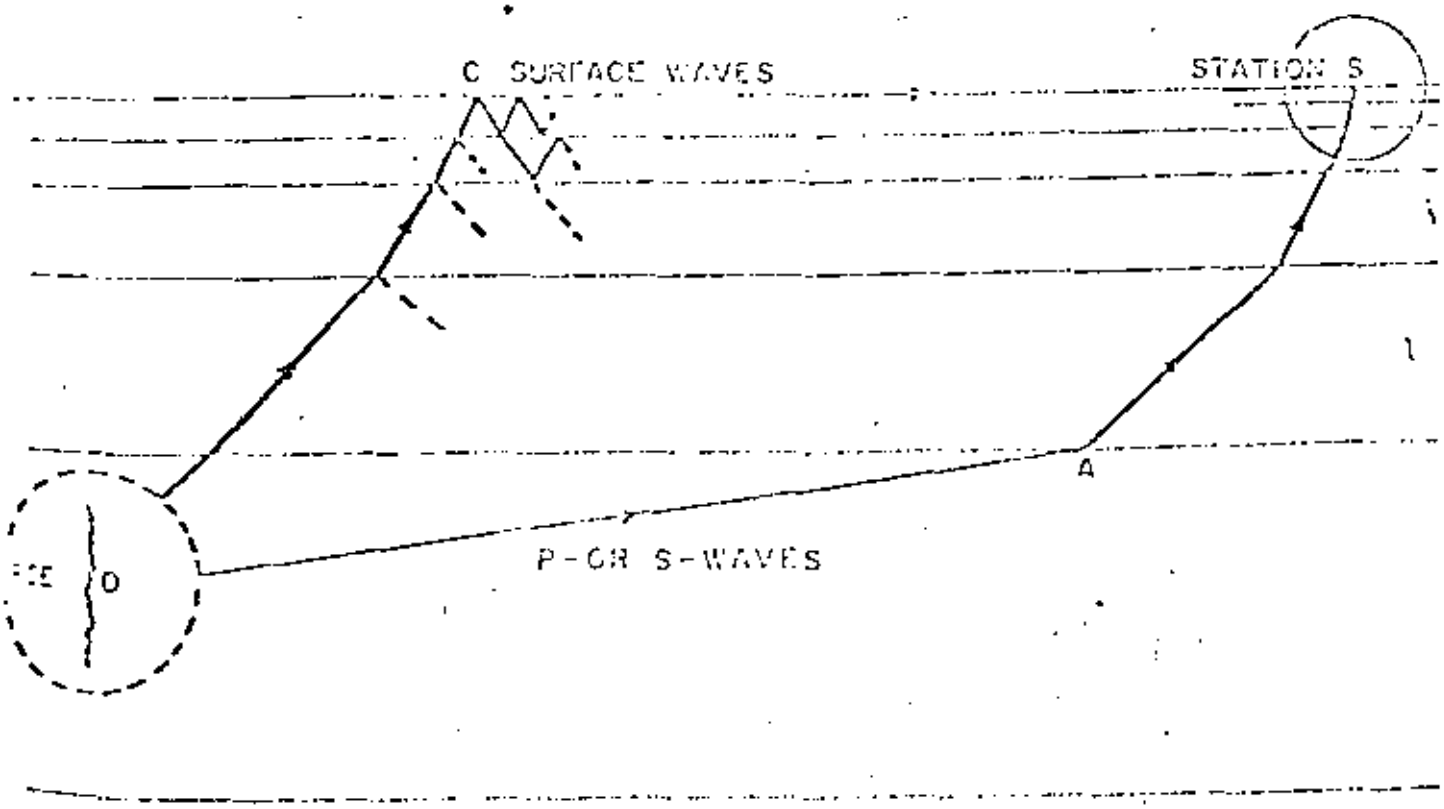

Fig. 2 Seismic waves (Duda, 1965)

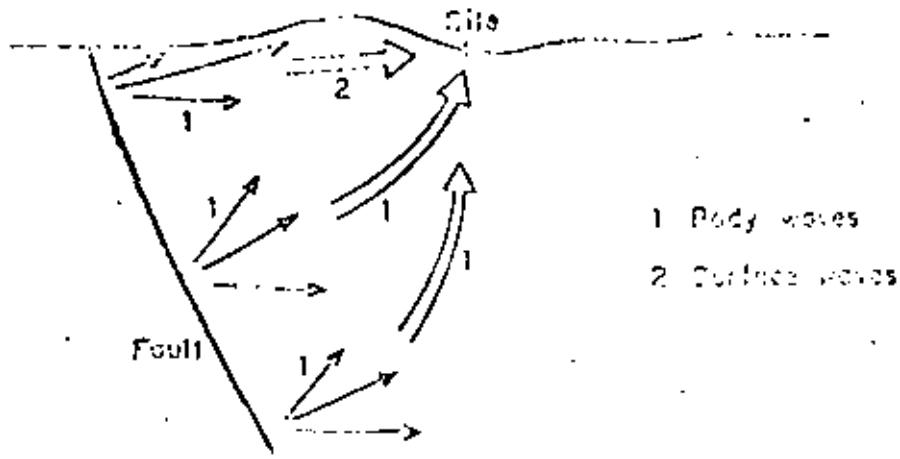

Fig. 3 Seismic waves in the near field

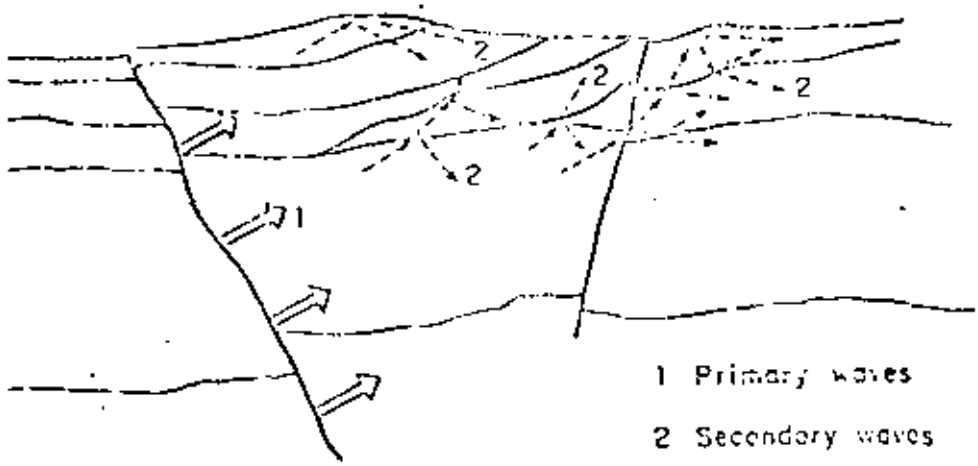

Fig. 4 Secondary wave trains

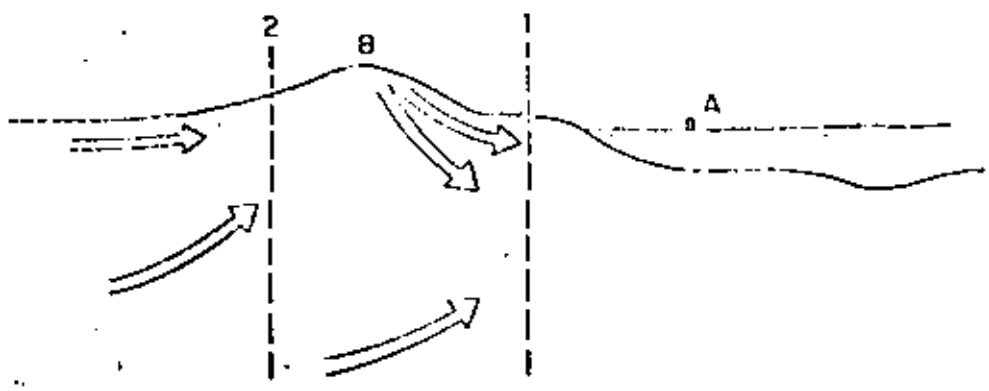

Fig. 5 Path and local conditions

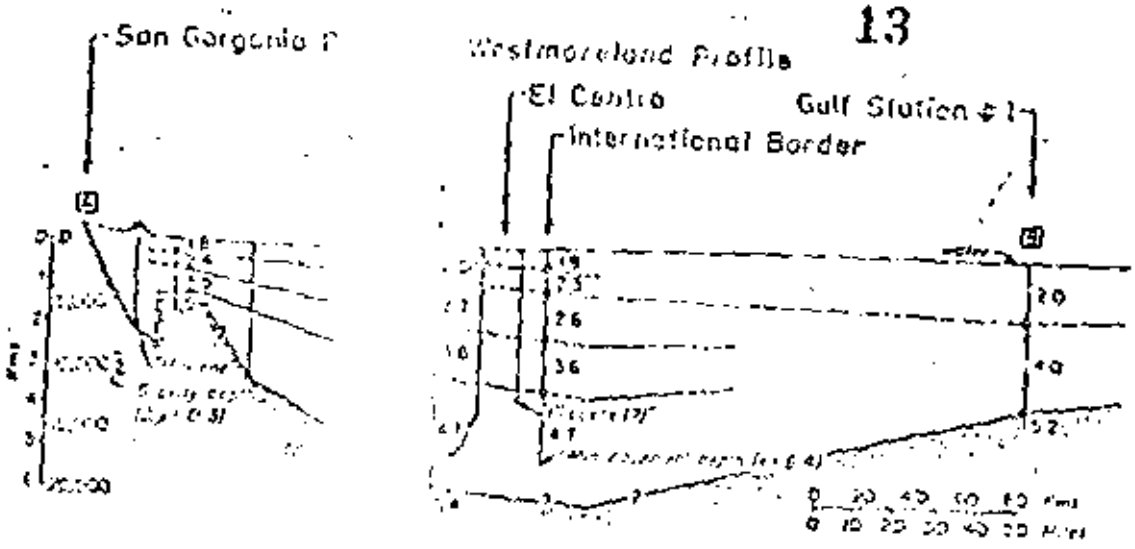

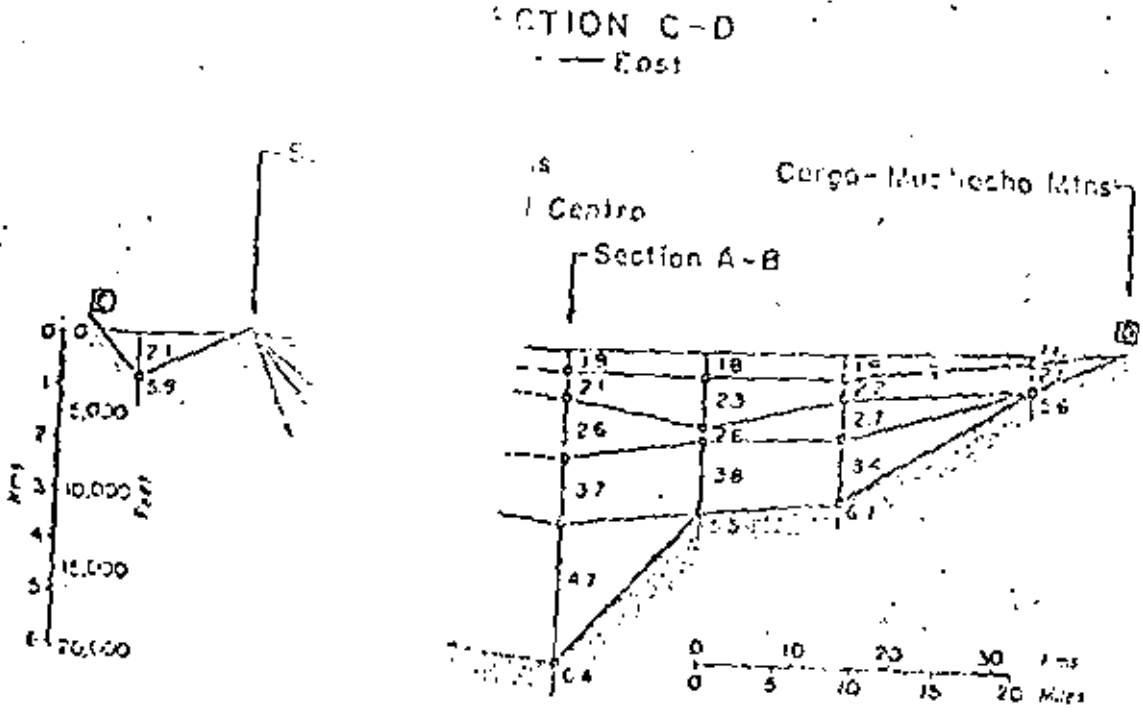

Figure ... ological cross section, Los Angeles area (Scalia and Trifunac, 1973)

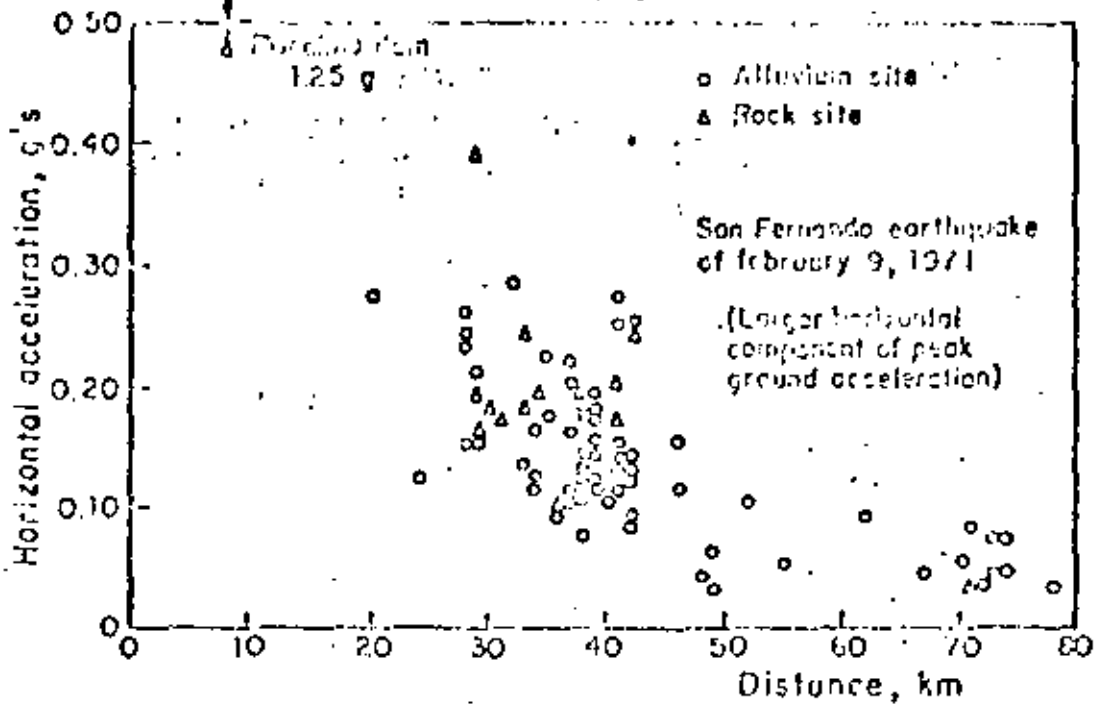

Peak ground acceleration versus distance

Fig. 7 Peak accelerations and ground conditions (Hudson, 1972)

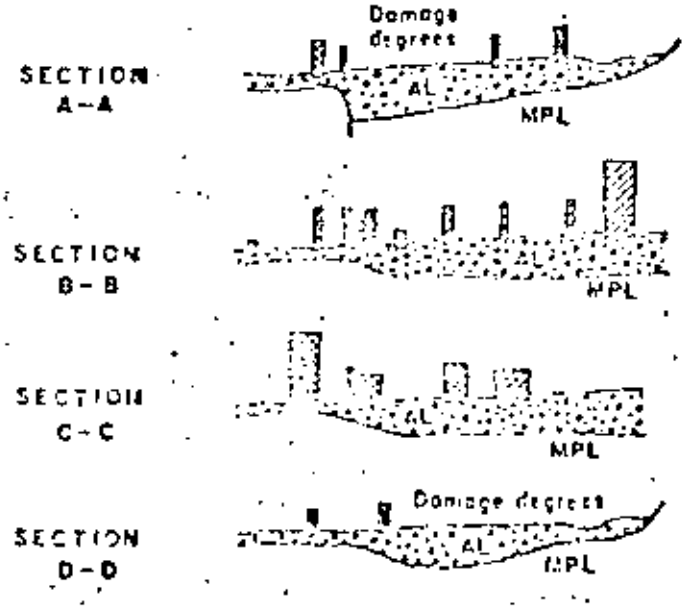

Fig. 8 Geologic cross section at Skopje (Ercelik, 1969)

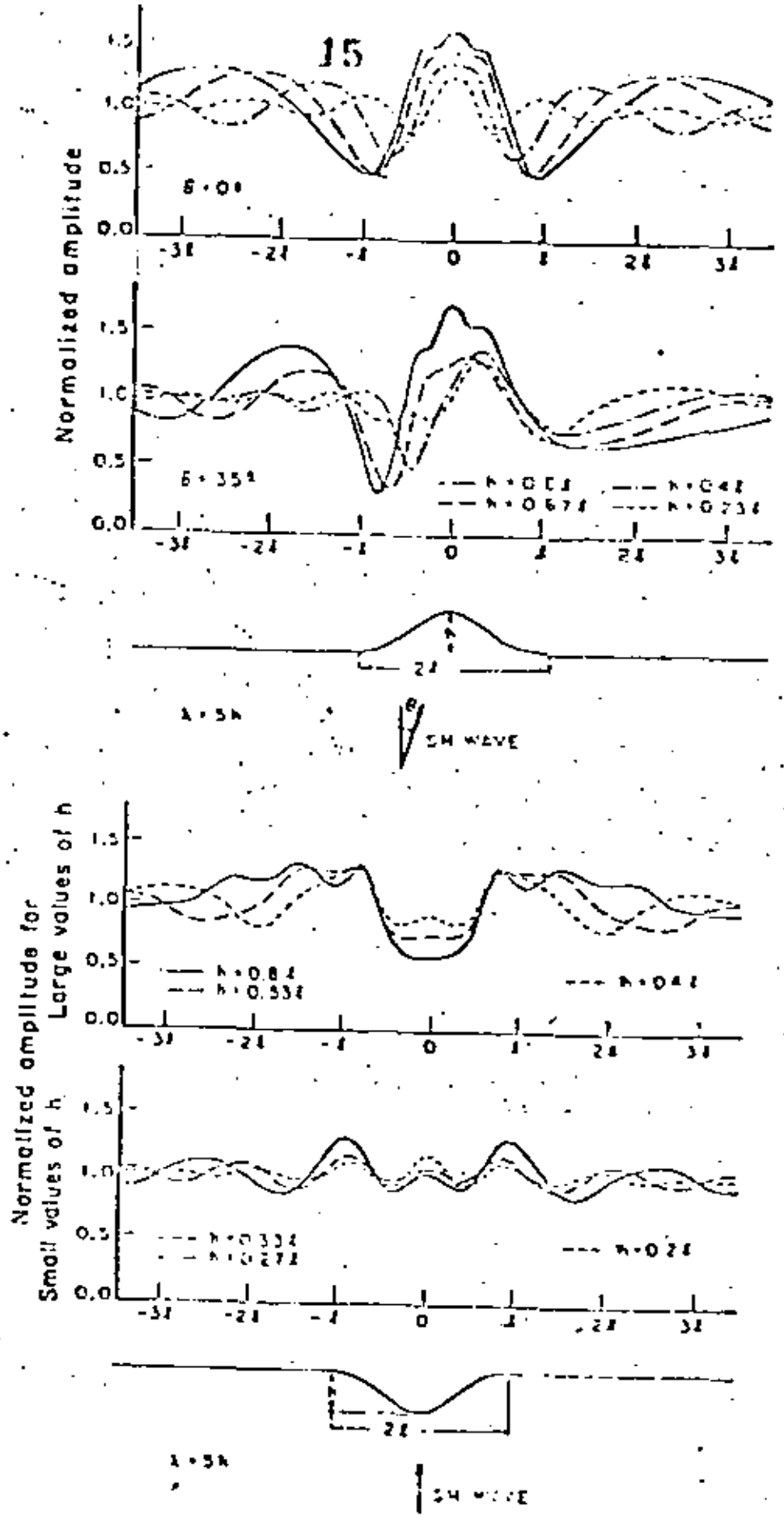

Fig. 9 Normalized amplitudes of motion produced by SH waves (Davies, 1973)

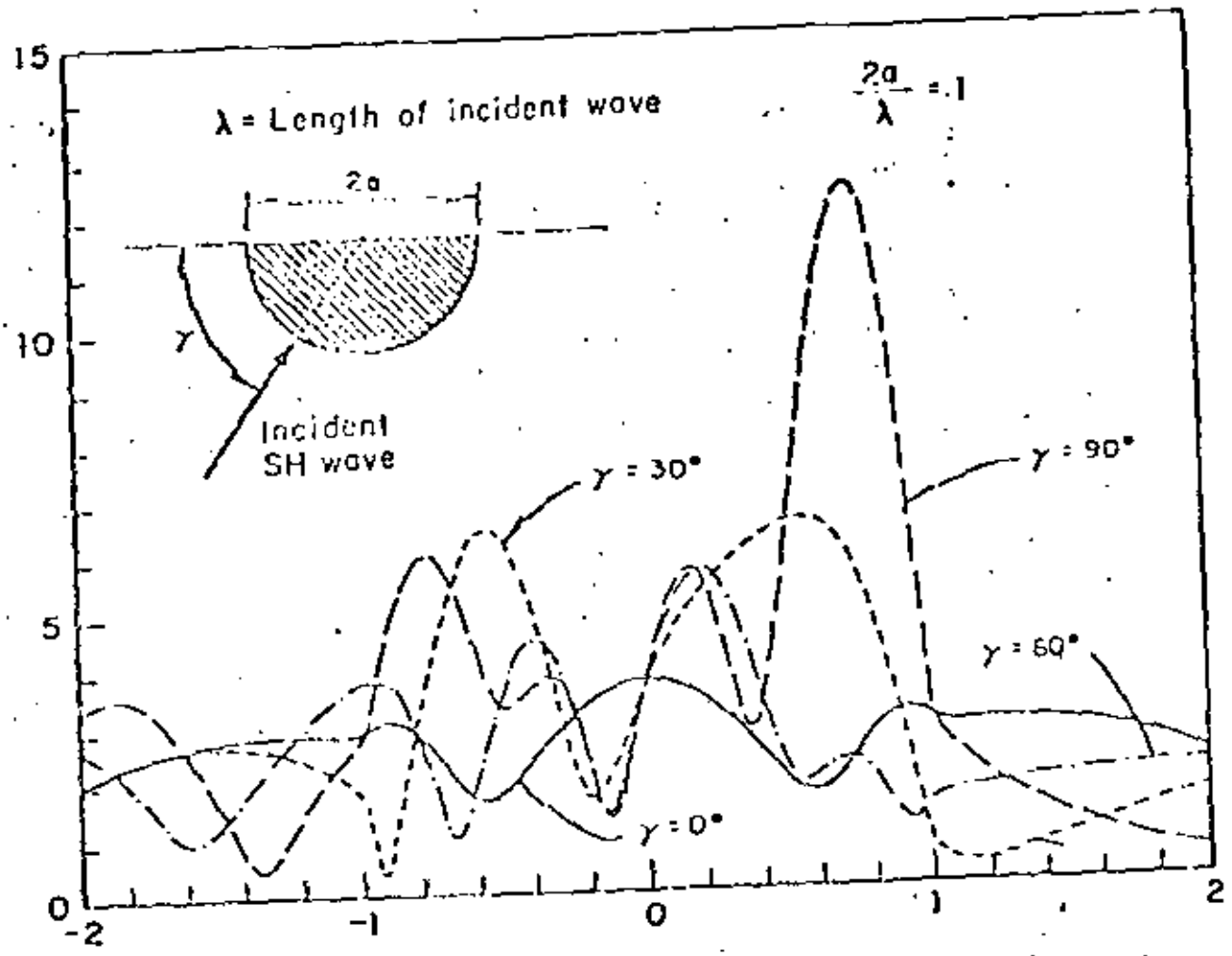

Fig. 10 Displacement amplitudes at the surface of a semicylindrical valley (Trifunac, 1971b)

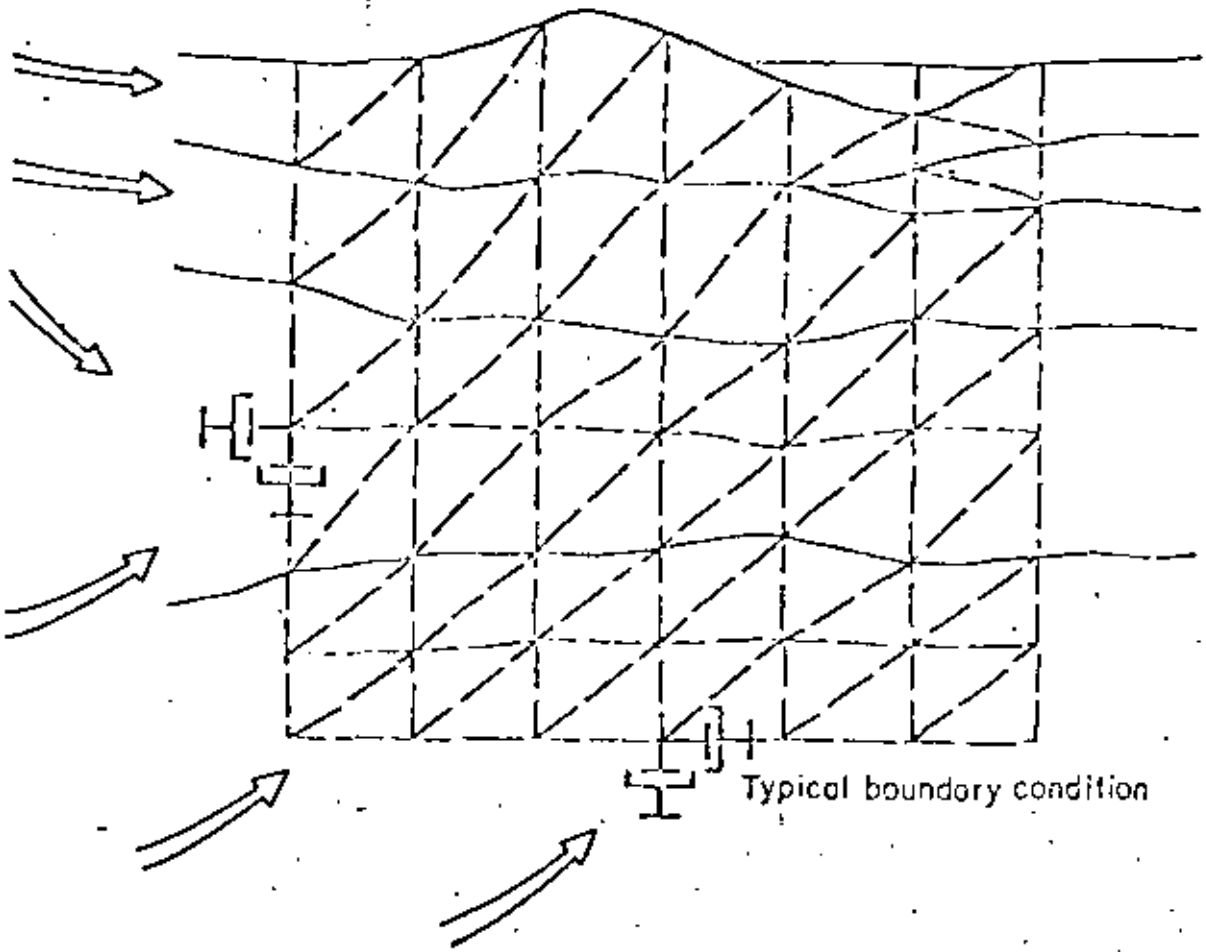

Fig. 11 Two-dimensional finite element models

SISTEMAS DE VARIOS GRADOS DE LIBERTAD CON COMPORTAMIENTO INELASTICO

Método β de Newmark. Ejemplo:

Calcular mediante el método β de Newmark los desplazamientos máximos absolutos del 1o. y 2o. niveles de la estructura mostrada abajo, cuando es excitada por un desplazamiento súbito de 2 cm en su base.

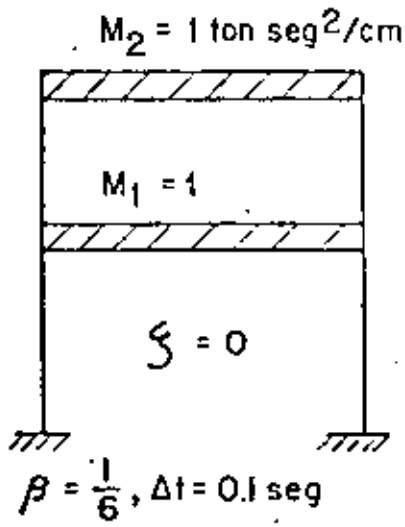

$\beta = \frac{1}{6}$, Δt = 0.1 seg

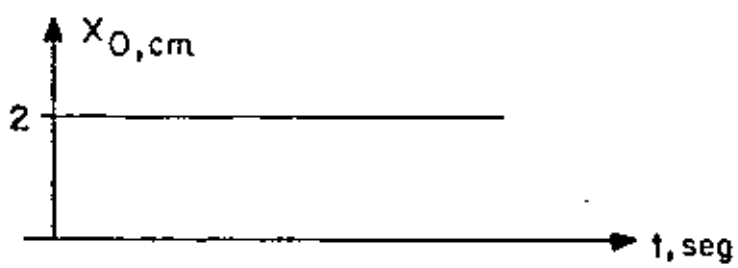

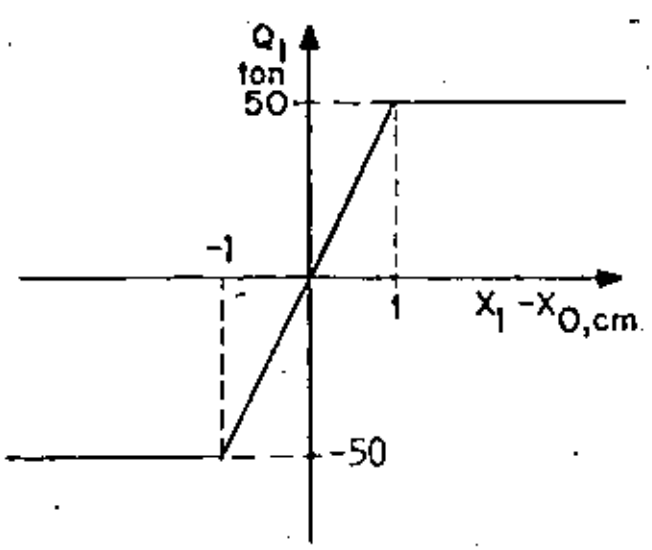

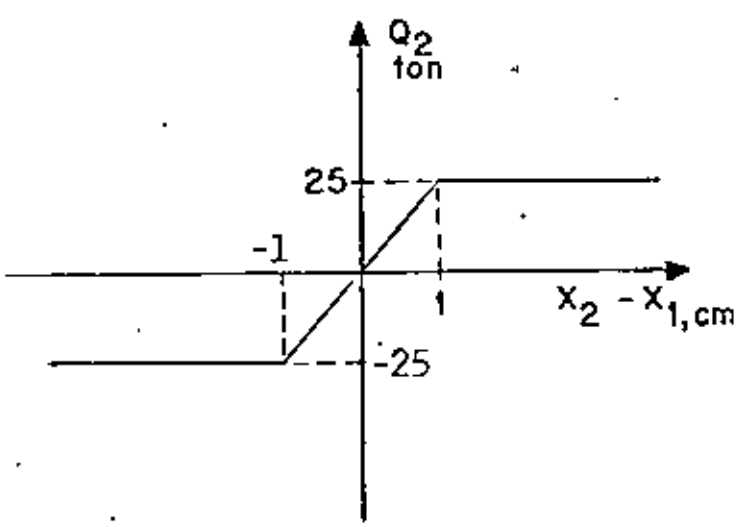

$M_2 \leftarrow F_I = m_2 \ddot{X}_2$

$\leftarrow Q_2$

$\rightarrow Q_2$

$M_1 \leftarrow F_I = m_1 \ddot{X}_1$

$\leftarrow Q_1$

$\underline{M}\ddot{\underline{X}} + \underline{Q} = 0$

$$M_1 \ddot{X}_1 + Q_1 - Q_2 = 0$$

$$M_2 \ddot{X}_2 + Q_2 = 0$$

$$\left.\begin{aligned} \ddot{X}_1 &= \frac{Q_2 - Q_1}{M_1} \\ \ddot{X}_2 &= \frac{-Q_2}{M_2} \end{aligned}\right\} \quad (1)$$

En vez de suponer $\ddot{X}_1$ y $\ddot{X}_2$ al inicio de cada ciclo, supondremos Q_1 y Q_2 y calcularemos ambas aceleraciones con base en ellas mediante la ec (1). Las ecuaciones para la velocidad y desplazamiento son:

$$\left.\begin{aligned} \dot{X}_{i+1} &= \dot{X}_i + 0.05\,(\ddot{X}_i + \ddot{X}_{i+1}) \\ X_{i+1} &= X_i + 0.1\dot{X}_1 + \frac{1}{600}(2\ddot{X}_i + \ddot{X}_{i+1}) \end{aligned}\right\} \quad (2)$$

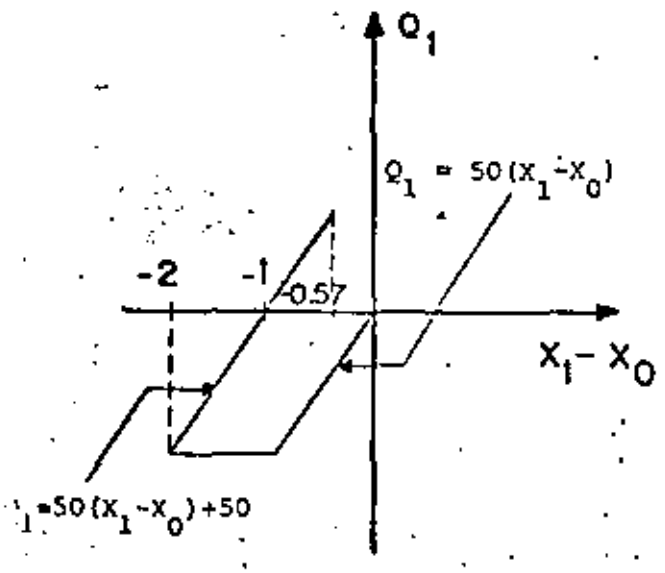

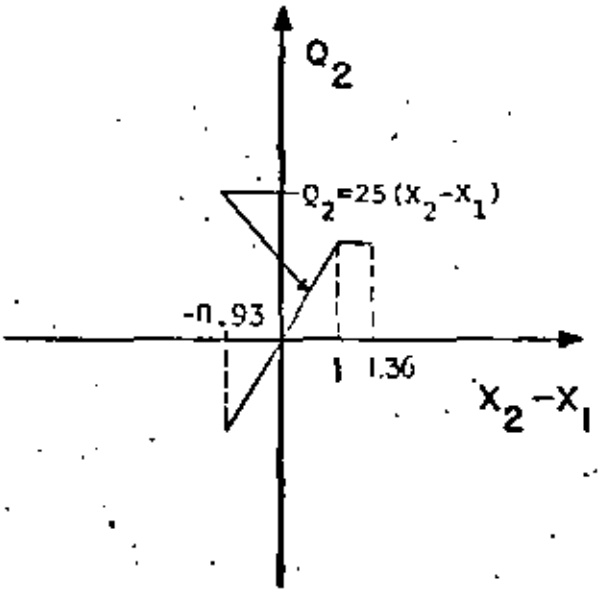

Para t=0.1 seg

1^{er} CICLO

Supongamos Q_1=-43.75 y Q_2=-6.25, entonces de la ec 1: $\ddot{x}_1$= 37.50 y $\ddot{x}_2$= 6.25 .

En tal caso:

$$\dot{x}_1 = 0+0.05(50+37.50) = 4.38$$
$$\dot{x}_1-\dot{x}_0 = 4.38-0.0 = 4.38$$
$$\dot{x}_2 = 0+0.05(0+6.25) = 0.31$$
$$\dot{x}_2-\dot{x}_1 = 0.31-4.38 = -4.07$$
$$x_1 = 0+0.1x0 + \frac{1}{600}(2x50 + 37.50) = 0.23$$
$$x_1-x_0 = 0.23 - 2.0 = -1.77$$
$$x_2 = 0 + 0.1x0 + \frac{1}{600} (2x0 + 6.25) = 0.01$$
$$x_2-x_1 = 0.01 - 0.23 = -0.22$$
$$Q_1 = 50 (x_1-x_0) + 50 = 50(-1.77) + 50 = -38.50$$
$$Q_2 = 25(x_2-x_1) = 25(-0.22) = -5.50$$

de la ec. 1 :

$$\ddot{x}_1 = \frac{-5.50 - (-38.50)}{1} = 33.00 \neq 37.50$$

$$\ddot{x}_2 = \frac{-(-5.50)}{1} = 5.50 \neq 6.25$$

2^{o} CICLO

Tomando los valores de $\ddot{x}_1$ y $\ddot{x}_2$ obtenidos en el calculo anterior:

$$\dot{x}_1 = 0.05(50 + 33.00) = 4.15$$
$$\dot{x}_2 = 0.05 (5.50) = 0.28$$
$$x_1 = \frac{1}{600} (2x50 + 33.00) = 0.22$$
$$x_2 = \frac{1}{600} (5.50) = 0.01$$
$$\dot{x}_1-\dot{x}_0 = 4.15$$
$$\dot{x}_2-\dot{x}_1 = 0.28-4.15 = -3.87$$
$$x_1-x_0 = 0.22-2.00 = -1.78$$
$$x_2-x_1 = 0.01-0.22 = -0.21$$
$$Q_1 = 50 (-1.78) + 50 = -39.00$$
$$Q_2 = 25 (-0.21) = -5.25$$

de la ec. 1:

$$\ddot{x}_1 = \frac{-5.25 -(-39.00)}{1} = 33.75 \neq 33.00$$

$$\ddot{x}_2 = \frac{-(-5.25)}{1} = 5.25 \neq 5.50$$

y así sucesivamente.

Para t=0.2 seg

1^{er} CICLO

Supongamos $Q_1 = -20.00$ y $Q_2 = -10.00$, entonces de la ec. 1 tenemos $\ddot{x}_1 = 10.00$ y $\ddot{x}_2 = 10.00$.

En tal caso:

$$\dot{x}_1 = 4.19 + 0.05(33.75 + 10.00) = 6.38$$

$$\dot{x}_1 - \dot{x}_0 = 6.38 - 0.0 = 6.38$$

$$\dot{x}_2 = 0.26 + 0.05(5.25 + 10.00) = 1.02$$

$$\dot{x}_2 - \dot{x}_1 = 1.02 - 6.38 = -5.36$$

$$x_1 = 0.22 + 0.1(4.19) + \frac{1}{600}(2(33.75) + 10.00)$$

$$= 0.77$$

$$x_1 - x_0 = 0.77 - 2.0 = -1.23$$

$$x_2 = 0.01 + 0.1(0.26) + \frac{1}{600}(2(5.25) + 10.00)$$

$$= 0.07$$

$$x_2 - x_1 = 0.07 - 0.77 = -0.70$$

$$Q_1 = 50(-1.23) + 50 = -11.50$$

$$Q_2 = 25(-0.70) = -17.50$$

de la ec.1 :

$$\ddot{x}_1 = -6.00 \neq 10.00$$

$$\ddot{x}_2 = 17.50 \neq 10.00$$

t	x_o	Q_1	Q_2	$\ddot{x}_1$	$\ddot{x}_2$	$\dot{x}_1$	x_1	$\dot{x}_2$	x_2	x_1-x_0	x_2-x_1	$\dot{x}_1-\dot{x}_0$	$\dot{x}_2-\dot{x}_1$	OBS
seg	cm	t	ton	cm/seg^2	cm/seg^2	cm/seg	cm	cm/seg	cm	cm	cm	cm/seg	cm/seg	
0.0	2.0	-50.00	0.00	50.00	0.00	0.00	0.00	0.00	0.00	-2.00	0.00	0.00	0.00	
0.1	2.0	-43.75	-6.25	37.50	6.25	4.38	0.23	0.31	0.01	-1.77	-0.22	4.38	-4.06	
		-38.54	-5.47	33.07	5.47	4.15	0.22	0.27	0.01	-1.78	-0.21	4.15	-3.88	
		-38.91	-5.32	33.59	5.32	4.18	0.22	0.27	0.01	-1.78	-0.21	4.18	-3.91	
		-38.87	-5.34	33.52	5.34	4.18	0.22	0.27	0.01	-1.78	-0.21	4.18	-3.91	
		-38.87	-5.34	33.53	5.34	4.18	0.22	0.27	0.01	-1.78	-0.21	4.18	-3.91	
		-38.87	-5.34	33.53	5.34	4.18	0.22	0.27	0.01	-1.78	-0.21	4.18	-3.91	
0.2	2.0	-20.00	-10.00	10.00	10.00	6.36	0.77	1.04	0.07	-1.23	-0.69	6.36	-5.32	
		-11.68	-17.37	- 5.70	17.37	5.57	0.74	1.41	0.08	-1.26	-0.66	5.57	-4.17	
		-12.99	-16.41	- 3.43	16.41	5.69	0.74	1.36	0.08	-1.26	-0.66	5.69	-4.33	
		-12.80	-16.55	- 3.75	16.55	5.67	0.74	1.36	0.08	-1.26	-0.66	5.67	-4.30	
		-12.82	-16.53	- 3.70	16.53	5.67	0.74	1.36	0.08	-1.26	-0.66	5.67	-4.31	
		-12.82	-16.53	- 3.71	16.53	5.67	0.74	1.36	0.08	-1.26	-0.66	5.67	-4.31	
		-12.82	-16.53	- 3.71	16.53	5.67	0.74	1.36	0.08	-1.26	-0.66	5.67	-4.31	
0.3	2.0	10.00	-25.00	-35.00	25.00	3.73	1.24	3.44	0.31	-0.76	-0.92	3.73	-0.30	
		11.82	-23.09	-34.90	23.09	3.74	1.24	3.34	0.31	-0.76	-0.93	3.74	-0.40	
		11.82	-23.17	-35.00	23.17	3.73	1.24	3.35	0.31	-0.76	-0.93	3.73	-0.39	
		11.82	-23.16	-34.98	23.16	3.74	1.24	3.34	0.31	-0.76	-0.93	3.74	-0.39	
		11.82	-23.17	-34.98	23.17	3.74	1.24	3.34	0.31	-0.76	-0.93	3.74	-0.39	
		11.82	-23.17	-34.98	23.17	3.74	1.24	3.34	0.31	-0.76	-0.93	3.74	-0.39	
0.4	2.0	25.00	-15.00	-40.00	15.00	-0.01	1.43	5.25	0.75	-0.57	-0.68	-0.01	5.26	
		21.54	-17.11	-38.65	17.11	0.06	1.43	5.35	0.75	-0.57	-0.68	0.06	5.30	
		21.65	-17.08	-38.73	17.08	0.05	1.43	5.35	0.75	-0.57	-0.68	0.05	5.30	
		21.64	-17.08	-38.72	17.08	0.05	1.43	5.35	0.75	-0.57	-0.68	0.05	5.30	
		21.64	-17.08	-38.72	17.08	0.05	1.43	5.35	0.75	-0.57	-0.68	0.05	5.30	*
0.5	2.0	15.00	-10.00	-25.00	10.00	-3.14	1.26	6.70	1.36	-0.74	0.09	-3.14	9.84	
		13.21	2.36	-10.86	- 2.36	-2.43	1.29	6.09	1.34	-0.71	0.05	-2.43	8.51	
		14.39	1.25	-13.14	- 1.25	-2.54	1.28	6.14	1.34	-0.72	0.06	-2.54	8.68	
		14.20	1.40	-12.81	- 1.40	-2.53	1.28	6.13	1.34	-0.72	0.06	-2.53	8.66	
		14.23	1.38	-12.85	- 1.38	-2.53	1.28	6.14	1.34	-0.72	0.06	-2.53	8.66	
		14.23	1.38	-12.85	- 1.38	-2.53	1.28	6.14	1.34	-0.72	0.06	-2.53	8.66	
0.6	2.0	0.00	15.00	15.00	-15.00	-2.42	1.01	5.32	1.92	-0.99	0.92	-2.42	7.74	
		0.46	22.88	22.42	-22.88	-2.05	1.02	4.93	1.91	-0.98	0.89	-2.05	6.98	
		1.08	22.24	21.17	-22.24	-2.11	1.02	4.96	1.91	-0.98	0.89	-2.11	7.07	
		0.97	22.32	21.35	-22.32	-2.11	1.02	4.95	1.91	-0.98	0.89	-2.11	7.06	
		0.99	22.31	21.32	-22.31	-2.11	1.02	4.96	1.91	-0.98	0.89	-2.11	7.06	
		0.99	22.31	21.33	-22.31	-2.11	1.02	4.96	1.91	-0.98	0.89	-2.11	7.06	
		0.99	22.31	21.33	-22.31	-2.11	1.02	4.96	1.91	-0.98	0.89	-2.11	7.06	

* $\dot{x}_1-\dot{x}_o$ SE HACE CASI CERO, CAMBIO DE NEGATIVO A POSITIVO . $|x_1|_{máx}=1.43$

t	x_o cm	Q_1 ton	Q_2 ton	$\ddot{x}_1$ cm/seg^2	$\ddot{x}_2$ cm/seg^2	$\dot{x}_1$ cm/seg	x_1 cm	$\dot{x}_2$ cm/seg	x_2 cm	x_1-x_0 cm	x_2-x_1 cm	$\dot{x}_1-\dot{x}_0$ cm/seg	$\dot{x}_1$ cm/seg	OBS
0.615	2.0	-3.00	25.00	28.00	-25.00	-1.74	0.99	4.61	1.98	-1.01	0.99	-1.74	6.35	
		-0.45	24.77	25.22	-24.77	-1.76	0.99	4.61	1.98	-1.01	0.99	-1.76	6.37	
		-0.46	24.77	25.23	-24.77	-1.76	0.99	4.61	1.98	-1.01	0.99	-1.76	6.37	
		-0.46	24.77	25.23	-24.77	-1.76	0.99	4.61	1.98	-1.01	0.99	-1.76	6.37	**
0.7	2.0	- 3.00	25.00	28.00	-25.00	0.36	0.93	2.59	2.29	-1.07	1.36	0.36	2.24	
		- 3.66	34.08	37.74	-34.08	0.84	0.94	2.14	2.27	-1.06	1.33	0.84	1.30	
		- 2.85	33.30	36.15	-33.30	0.76	0.94	2.18	2.28	-1.06	1.34	0.76	1.42	
		- 2.98	33.39	36.38	-33.39	0.78	0.94	2.17	2.28	-1.06	1.34	0.78	1.40	
		- 2.96	33.38	36.34	-33.38	0.77	0.94	2.18	2.28	-1.06	1.34	0.77	1.40	
		- 2.97	33.38	36.35	-33.38	0.77	0.94	2.18	2.28	-1.06	1.34	0.77	1.40	
		- 2.97	33.38	36.35	-33.38	0.77	0.94	2.18	2.28	-1.06	1.34	0.77	1.40	
.723	2.0	-1.00	25.00	26.00	-25.00	1.49	0.97	1.51	2.32	-1.03	1.36	1.49	0.02	
		-1.68	25.00	26.68	-25.00	1.49	0.97	1.51	2.32	-1.03	1.36	1.49	0.01	
		-1.68	25.00	26.68	-25.00	1.49	0.97	1.51	2.32	-1.03	1.36	1.49	0.01	***
.787	2.0	-1.00	25.00	26.00	-25.00	3.48	1.13	0.01	2.38	-0.87	1.24	3.48	-3.48	
		6.58	25.00	18.42	-25.00	3.15	1.12	0.01	2.38	-0.88	1.25	3.15	-3.15	
		6.10	25.00	18.90	-25.00	3.17	1.12	0.01	2.38	-0.88	1.25	3.17	-3.17	
		6.13	25.00	18.87	-25.00	3.17	1.12	0.01	2.38	-0.88	1.25	3.17	-3.17	
		6.13	25.00	18.87	-25.00	3.17	1.12	0.01	2.38	-0.88	1.25	3.17	-3.17	****
0.8	2.0	-10.00	25.00	35.00	-25.00	4.34	1.20	-0.74	2.35	-0.80	1.15	4.34	-5.08	
		9.83	25.00	15.18	-25.00	3.35	1.16	-0.74	2.35	-0.84	1.18	3.35	-4.09	
		8.17	25.00	16.83	-25.00	3.43	1.17	-0.74	2.35	-0.83	1.18	3.43	-4.17	
		8.31	25.00	16.69	-25.00	3.42	1.17	-0.74	7.35	-0.83	1.18	3.42	-4.16	
		8.30	25.00	16.70	-25.00	3.42	1.17	-0.74	2.35	-0.83	1.18	3.42	-4.16	
		8.30	25.00	16.70	-25.00	3.42	1.17	-0.74	2.35	-0.83	1.18	3.42	-4.16	
0.9	2.0	-1.00	25.00	26.00	-25.00	5.56	1.61	-3.24	2.15	-0.39	0.54	5.56	-8.80	
		30.55	25.00	- 5.55	-25.00	3.98	1.56	-3.24	2.15	-0.44	0.59	3.98	-7.22	
		27.92	25.00	- 2.92	-25.00	4.11	1.56	-3.24	2.15	-0.44	0.59	4.11	-7.35	
		28.14	25.00	- 3.14	-25.00	4.10	1.56	-3.24	2.15	-0.44	0.59	4.10	-7.34	
		28.12	25.00	- 3.12	-25.00	4.10	1.56	-3.24	2.15	-0.44	0.59	4.10	-7.34	
		28.12	25.00	- 3.12	-25.00	4.10	1.56	-3.24	2.15	-0.44	0.59	4.10	-7.34	

** Cambio de rigidez en el segundo entrepiso, $x_2-x_1 \triangleq 1$; $Q_2=25$.

*** $\dot{x}_2-\dot{x}_1 \doteq 0$

**** $\dot{x}_2 \doteq 0$, $|x_2|_{max} = 2.38$cm .

PROGRAMA PARA CALCULADORA DE BOLSILLO HP-41C

- Limpiar los registros con la instrucción XEQ CLRG
- Meter en las memorias que se indican los valores de;

M_1 - STO19

M_2 - STO20

x_0 - STO09

δ - STO21

α - STO22

Δt - STO23

- Para cada intervato (Δt), meter los valores que a continuación se indican:

Q_1 - STO15

Q_2 - STO16

$\dot{x}_{1,t}$ - STO00

$\dot{x}_{2,t}$ - STO03

$\ddot{x}_{1,t}$ - STO01

$\ddot{x}_{2,t}$ - STO04

$x_{1,t}$ - STO05

$x_{2,t}$ - STO08

- Se iniciará el programa con la tecla "restart-stop" (R/S) e irán apareciendo los valores para llenar la tabla en el orden que se indica en el programa.
- Cuando $\ddot{x}_{1,t+\Delta t}$ haya convergido, se oirá un "beep". Cuando $\ddot{x}_{2,t+\Delta t}$ haya convergido, se oirán dos "beep". En este momento se redefiniran en las memorias, los valores del tercer inciso para el intervalo siguiente.

El listado del programa es el que a continuación se indica.

01 LBL BETA	11 VEL1 STO 00	21 RCL 15	
02 LBL E	12 PROMPT	22 —	
03 Q1 EN STO15	13 VEL2 STO03	23 RCL 19	
04 PROMPT	14 PROMPT	24 /	
05 Q2 EN STO16	15 DESP1 STO05	25 FIX 2	
06 PROMPT	16 PROMPT	26 END	
07 AC 1 STO01	17 DESP 2 STO08	27 RCL 17	
08 PROMPT	18 PROMPT	28 X ≷ Y	
09 AC2 STO04	19 LBL A	29 X=Y ?	
10 PROMPT	20 RCL 16	30 GTO B	

31 STO 17	64 RCL 23	97 STOP → [8] $(\dot{X}_1 - \dot{X}_0)_{t+\Delta t}$
32 STOP → [1] $\ddot{X}_{1,t+\Delta t}$	65 *	98 0.5
33 RCL 16	66 RCL 03	99 RCL 22
34 CHS	67 +	100 −
35 RCL 20	68 STO 07	101 RCL 04
36 /	69 STOP → [5] $\dot{X}_{2,t+\Delta t}$	102 *
37 LBL D	70 RCL 02	103 RCL 22
38 STO 18	71 −	104 RCL 18
39 STOP → [2] $\ddot{X}_{2,t+\Delta t}$	72 STO 11	105 *
40 1	73 STOP → [6] $(\dot{X}_2 - \dot{X}_1)_{t+\Delta t}$	106 +
41 RCL 21	74 0.5	107 RCL 23
42 −	75 RCL 22	108 X↑2
43 RCL 01	76 −	109 *
44 *	77 RCL 01	110 RCL 23
45 RCL 21	78 *	111 RCL 03
46 RCL 17	79 RCL 22	112 *
47 *	80 RCL 17	113 +
48 +	81 *	114 RCL 08
49 RCL 23	82 +	115 +
50 *	83 RCL 23	116 STO 06
51 RCL 09	84 X↑2	117 STOP → [9] $\dot{X}_{2,t+\Delta t}$
52 +	85 *	118 RCL 13
53 STO 02	86 RCL 23	119 −
54 STOP → [3] $\dot{X}_{1,t+\Delta t}$	87 RCL 00	120 STO 14
55 1 [4] $(\dot{X}_1 - \dot{X}_0)_{t+\Delta t}$	88 *	121 STOP → [10] $(\dot{X}_2 - \dot{X}_1)_{t+\Delta t}$
56 RCL 21	89 +	122 RCL 10
57 −	90 RCL 05	123 50
58 RCL 04	91 +	124 *
59 *	92 STO 13	125 50
60 RCL 21	93 STOP → [7] $X_{1,t+\Delta t}$	126 +
61 RCL 18	94 RCL 09	127 STO 15
62 *	95 −	128 STOP → [11] Q_1
63 +	96 STO 10	129 RCL 14

130	25	140	CHS	150	LBL C
131	#	141	RCL 20	151	BEEP
132	GTO16	142	/	152	BEEP
133	STOP → (12) Q_2	143	FIX 2	153	STOP
134	GTO A	144	END	154	GTO E
136	LBL B	145	RCL 18	155	END
136	BEEP	146	$X \geq Y$		
137	STO 17	147	$X = Y$?		
138	STOP	148	GTO C		
139	RCL 16	149	GTO D		

NOTAS:

- Las condiciones iniciales del problema deben de ser nulas.
- El valor de x_0 debe ser continuo durante todo el tiempo.
- Los valores de Q_1 y Q_2 serán calculados de acuerdo a las gráficas que se proporcionas, en los pasos 122 a 128 y 129 a 134 respectivamente. Estos dependen de las diferencias x_1-x_0 y x_2-x_1 respectivamente (verificarlos en cada intervalo).
- Si no hubiera convergencia, esto se debe a errores por redondeo y en ese caso habrá que cambiarlo en las instrucciones 25 y 144 a una decimal más. Una vez terminada esta iteración se deberá regresar a la aproximación anterior.

DIRECTORIO DE ASISTENTES AL CURSO ANALISIS DE RIESGO SISMICO
(DEL 26 DE JULIO AL 4 DE AGOSTO DE 1983)

NOMBRE Y DIRECCION	EMPRESA Y DIRECCION
1. JOSE MANUEL CUATLAYOTL SARMIENTO Priv. 5 de Mayo "B" Ote. 3814 Col. Hidalgo Puebla, Pue. Tel: 46-04-62	UNIVERSIDAD POPULAR AUTONOMA DEL EDO. DE PUEBLA 21 Sur 1103 Col. Santiago Puebla, Pue. Tel: 41-21-38
2. MARCOS LUIS CHAVEZ MINEROS Barrio Abato Ave. Jerez-Casa No.236 Tegucigalpa de Honduras,C.A. Tel: 22-05-80	EMPRESA NACIONAL DE ENERGIA ELECTRICA Edificio Principal Antiguo Puente Nacional Tegucigalpa de Honduras, C.A. Tel: 22-85-10 Ext. 225
3. ROBERTO DAM LAU Urb. Las Mercedes Casa 110 C.P. 9000 Zona 6 Ciudad de Panama 60-79-57	UNIVERSIDAD NACIONAL DE PANAMA FACULTAD DE ARQUITECTURA Universidad Nacional de Panama Ciudad de Panama
4. CARLOS A. FERNANDEZ CORDOBA Apdo. Postal 318 Cartago, Costa Rica Tel: 51 46 75	INSTITUTO TECNOLOGICO DE C.R. Y MUNICIPALI- Cartago, Costa Rica - DAD DE CARTAGO Tel: 51 00 58
5. HUMBERTO GARCIA DIAZ Kra. 10 No. 17N-87 Popayan, Colombia Tel: 3864	UNIVERSIDAD DEL CAUCA Popayan, Colombia Tel: 3023
6. JOSE ANTONIO GRACIA-GARCIA SANCHEZ Calle G-5-1 Alianza Popular Revolucionaria Coyoacán, D. F. C.P. 04800 Tel: 6 77 45 89	COMISION FEDERAL DE ELECTRICIDAD Río Misissipi 71-12o. Piso Deleg. Cuauhtémoc C.P. 06000 México, D. F.
7. JOSE LUIS HERNANDEZ AVILA Rinc. Fauna Ed. Vicuña 104 Col. Villa Panamericana C.P. 04700 México, D. F.	FACULTAD DE INGENIERIA, UNAM Ciudad Universitaria Deleg. Coyoacán México, D. F. TEL: 5 50 57 11

DIRECTORIO DE ASISTENTES AL CURSO ANALISIS DE RIESGO SISMICO
(DEL 26 DE JULIO AL 4 DE AGOSTODE 1983)

NOMBRE Y DIRECCION	EMPRESA Y DIRECCION
8. BENJAMIN HERNANDEZ GALLARDO OTE. 4 Mz. 24 Lte. 35 Cuchilla del Tesoro Deleg. Gustavo A. Madero México, D. F.	SECRETARIA DE COMUNICACIONES Y TRANSPORTES Av. Fernando No. 247 Col. Narvarte Deleg. Benito Juárez C.P. 03028 México, D. F. TEL: 5 90 89 86
9. WILSON MESIAS MEDINA PAZMIÑO Las Acacias-Ficoa Calle Los Cumbie y Las Ubillas Las Acacias-Ficoa, Ambazo Ecuador TEL: 82-61-59	UNIVERSIDAD TECNICA DE AMBATO Av. Colombia-Ingahurco Ambazo Ecuador TEL" 82-42-05
10. GIANFRANCO OTTAZZI PASINO J. Basaare 1435-502 S. Isidro Lima, Peru Tel: 22-72-10	POTIFICIA UNIVERSIDAD CATOLICA DEL PERU Final AV. Bolivar s/n Fundo Pando-Pueblo Lima, Peru Tel: 62-25-40
11. OSCAR PALACIOS GOMEZ México, D. F.	EPYCSA, S. A. México, D. F.
12. ROGELIO BERNARDO PEREZ ANGON La Quemada No. 349 Col. Narvarte Deleg. Benito Juárez C.P. 03020 México, D. F. 5-79-30-08	COMISION FEDERAL DE ELECTRICIDAD Carretera San Rafael Sta. Cecilia No. 211 Col. San Rafael Tlalnepantla, Edo. de México Tel: 3-90-25-53
13. MIGUEL POZAS ESTRADA México, D. F.	FACULTAD DE INGENIERIA Ciudad Universitaria México, D. F.
14. ANGEL PUJALTE PIÑEIRO Piamonte No. 22 Col. Acoxpa-Miramontes Deleg. Coyoacán C.P. 14300 México, D. F. Tel: 6 84 55 47	

DIRECTORIO DE ASISTENTES AL CURSO DE ANALISIS DE RIESGO SISMICO
(DEL 26 DE JULIO AL 4 DE AGOSTO DE 1983)

NOMBRE Y DIRECCION	EMPRESA Y DIRECCION
15. RIGOBERTO RIVERA CONSTANTINO Gpe. Victoria No. 29 Chimalcoyotl Deleg. Tlalpan C.P. 14630 México, D. F. Tel: 5- 73 82 92	FACULTAD DE INGENIERIA, UNAM Ciudad Universitaria Coyoacán México, D. F. Tel: 5-50-52-15 Ext. 3733
16. JOSE RAUL ROSADO LORENZO Gardenias No. 4 Fracc. Los Robles México, D. F. Tel: 6 84 44 61	
17. DAVID SANCHEZ NAVARRO Retorno 809 No. 9 Col. Centinela Deleg. Coyoacán C.P. 04450 México, D. F. Tel: 5 44 59 72	INGENIERIA Y ARQUITECTURA ESPECIALIZADA, S. A. Baja California 284-702 Col. Hipódromo Condesa México, D. F. Tel: 5 64 51 28
18. ERNESTO SIENTIES ARZAMENDI Via Lactea No. 141 Col. Prado Churubusco Deleg. Coyoacán México, D. F. Tel: 5 82 26 43	COMISION FEDERAL DE ELECTRICIDAD DEPARTAMENTO DE ESTUDIOS EXPERIMENTALES Augusto Rodín 265 Col. Noche Buena Deleg. Benito Juárez México, D. F. Tel: 5 63 37 00
19. FERNANDO SPINEL GOMEZ Canera 35A No. 57-94 Bogota, Colombia Tel: 2110560	UNIVERSIDAD NACIONAL DE COLOMBIA Ciudad Universitaria Bogota, Colombia Tel: 2685791
20. MARIO ROBERTO VALDEAVELLANO MUÑOZ 6a. Ave. "A" 13-25 Zona 9 Guatemala, Guatemala, C.A. Tel: 61286	UNIVERSIDAD DE SAN CARLOS DE GUATEMALA Ciudad Universitaria Zona 12 Guatemala, Guatemala, C.A. Tel: 760790

DIRECTORIO DE ASISTENTES AL CURSO DE ANALISIS DE RIESGO SISMICO
(DEL 26 DE JULIO AL 4 DE AGOSTO DE 1983)

NOMBRE Y DIRECCION	EMPRESA Y DIRECCION
21. JUAN MANUEL VAZQUEZ BECERRA C.4 Lote 22 Manz. 12 Col. Ampl..Gundalupe Prolet. Deleg. Gustavo A. Madero México, D. F.	INSTITUTO MEXICANO DEL PETROLEO Ave. Eje Central Lazaro Cárdenas No. 152 Deleg. Gustavo A. Madero México, D. F. Tel: 5-67-66-00 Ext. 2504
22. ROBERTO G. VEGA GUZMAN Apdo. 159 Costa, Rica Tel: 51 70 24	INSTITUTO TECNOLOGICO DE COSTA RICA Apdo. Postal 159 Costa, Rica Tel: 51 53 33
23. MA. MARTHA VILLAR SALGADO Lago Silverio 275 Col. Anáhuac Deleg. Miguel Hidalgo C.P. 11320 México, D. F. Tel: 5 45 91 71	INSTITUTO MEXICANO DEL PETROLEO Av. de los Cien Metros No. 152 Deleg. Gustavo A. Madero México, D. F. Tel: 5-67-66-00 Ext. 2559
24. MARIO EDUARDO ZERMEÑO DE LEON Av. Universidad No. 1879-5 Col. Oxtopulco Deleg. Coyoacán C.P. 04510 México, D. F. Tel: 5-48-77-88	FACULTAD DE INGENIERIA, UNAM Ciudad Universitaria México, D. F.